NATIONAL AERONAUTICS AND SPACE ADMINISTRATION

Bibliography 39-14

Publications
of the
Jet Propulsion Laboratory:
January Through December 1972

Foreword

JPL Bibliography 39-14 describes and indexes the formalized technical reporting, released January through December 1972, that resulted from scientific and engineering work performed, or managed, by the Jet Propulsion Laboratory. Five classes of publications are included:

(1) Technical Reports (32-series), in which the information is complete for a specific accomplishment and is intended for a wide audience.

(2) Articles from the bimonthly *Deep Space Network (DSN) Progress Report* (Technical Report 32-1526). Each volume's collection of articles presents a periodical survey of current accomplishments by the Deep Space Network.

(3) Technical Memorandums (33-series), in which the information is complete for a specific accomplishment but is intended for a limited audience to satisfy unique requirements.

(4) Articles from the *JPL Quarterly Technical Review*. Each article summarizes a recent important development, interim or final results, or an advancement in the state of the art in a scientific or engineering endeavor.

(5) Articles published in the open literature.

The publications are indexed by: (1) author, (2) subject, and (3) publication type and number. A descriptive entry appears under the name of each author of each publication; an abstract is included with the entry for the primary (first-listed) author. Unless designated otherwise, all publications listed are unclassified.

JPL personnel can obtain loan copies of formal documents cited from the JPL Library. Personnel of outside organizations can obtain information copies of documents cited by addressing a written request to the Technical Information and Documentation Division Support Section, Attention: Mr. Leo R. Lunine, Jet Propulsion Laboratory, 4800 Oak Grove Drive, Pasadena, California 91103. If documents are out of print, an alternate source for the material will be given to the requester.

Contents

Author Index With Abstracts

ABREU, A.

A001 Transformation of Received Signal Polarization Angle to the Plane of the Ecliptic

C. T. Stelzried, T. Sato, and A. Abreu

J. Spacecraft Rockets, Vol. 9, No. 2, pp. 69–70, February 1972

For abstract, see Stelzried, C. T.

ACHESON, D.

A002 DSN Progress Report for September–October 1972: Improved RF Calibration Techniques: Commercial Precision IF Attenuator Evaluation

C. T. Stelzried, B. L. Seidel, M. Franco, and D. Acheson

Technical Report 32-1526, Vol. XII, pp. 74–82, December 15, 1972

For abstract, see Stelzried, C. T.

ADAMS, R. W.

A003 Ion Thruster Performance Calibration

E. V. Pawlik, R. Goldstein, D. J. Fitzgerald, and R. W. Adams

Preprint 72-475, AIAA Ninth Electric Propulsion Conference, Bethesda, Maryland, April 17–19, 1972

For abstract, see Pawlik, E. V.

AKLONIS, J. J.

A004 Viscoelastic Behavior of Polymers Undergoing Crosslinking Reactions

J. Moacanin and J. J. Aklonis (University of Southern California)

J. Polym. Sci., Pt. C: Polym. Sym., No. 35, pp. 71–76, 1971

For abstract, see Moacanin, J.

AKYUZ, F. A.

A005 VISCEL—A General-Purpose Computer Program for Analysis of Linear Viscoelastic Structures: User's Manual

K. K. Gupta, F. A. Akyuz, and E. Heer

Technical Memorandum 33-466, Vol. I, Rev. 1, October 1, 1972

For abstract, see Gupta, K. K.

A006 VISCEL—A General-Purpose Computer Program for Analysis of Linear Viscoelastic Structures: Program Manual

K. K. Gupta and F. A. Akyuz

Technical Memorandum 33-466, Vol. II, July 15, 1972

For abstract, see Gupta, K. K.

ALLEN, J. E.

A007 DSN Progress Report for March–April 1972: DSN Monitor Performance Program

J. E. Allen

Technical Report 32-1526, Vol. IX, pp. 5–11, June 15, 1972

This article provides: (1) a general description of the programs used by DSN monitor analysts in the generation of the weekly and monthly performance summary reports, and (2) the format guide used by the DSN real-time analyst to assist in interpreting the formatted data.

AMOROSE, R. J.

A008 DSN Progress Report for July–August 1972: Network Operations Control

R. J. Amorose

Technical Report 32-1526, Vol. XI, pp. 157–160, October 15, 1972

The DSN Operations Control Team controls and operates the DSN in real-time to support flight project operations. DSN Operational Control, a mission-independent organization, is headed by the DSN Operations Chief, who is supported by the Deep Space Instrumentation Facility Operations Chief, Ground Communications Facility Operations Chief, Network Operations Analysis

Chief, and Network Operations Support Chief. The real-time operation is supported by two non-real-time functions, with liaison provided by: (1) the DSN Operations Representative, who represents the DSN organization to the DSN Manager and flight project Chief of Mission Operations, and (2) the DSN Scheduling Representative, who schedules DSN resources for flight projects.

ANDERSON, J. D.

A009 Determination of Astrodynamic Constants and a Test of the General Relativistic Time Delay With S-Band Range and Doppler Data From Mariners 6 and 7

J. D. Anderson, P. B. Esposito, W. Martin, and D. O. Muhleman (California Institute of Technology)

Space Research XI, pp. 105–112, Akademie-Verlag, Berlin, 1971

Range and doppler tracking data from Mariners 6 and 7 have been used to obtain information on the ratio μ^{-1} of the mass of the Earth to the mass of the Moon and on the mass and ephemeris of Mars. Based on data from five Mariner and two Pioneer spacecraft, the best value for μ^{-1} is 81.3007 ± 0.0005. The best value of the ratio of the mass of the sun to the mass of Mars was obtained by Null from analyses of the Mariner 4 data. This value (3098714 ± 5) has been substantiated by the Mariner 6 data which give 3098697 ± 72. By combining the Mariner 6 range data with optical and radar data of the planets, it is possible to deduce that the mean equatorial radius of Mars is 3393.0 ± 1.7 km.

Range data around the time of solar superior conjunction have yielded a test of the general relativistic time delay to the level of ±10%. Additional post-conjunction data will significantly improve the accuracy of this test.

ANDERSON, T. O.

A010 DSN Progress Report for March–April 1972: Wide Range, Essentially Linear Control Circuit for Control of the Reference Frequency in Digital Phase-Locked Loops

T. O. Anderson

Technical Report 32-1526, Vol. IX, pp. 119–122, June 15, 1972

A simple all-digital control circuit intended for control of the frequency of the reference signal in all-digital phase-locked loops is presented. Such control circuits, of prior art, are often nonlinear and provide only narrow frequency range. The present control circuit, though very simple, provides essentially linear control for a wide frequency range. The circuit presented in this article is

intended for use in all-digital phase-locked loops and is described in this context.

A011 DSN Progress Report for March–April 1972: Efficient Implementation of a Multichannel High-Speed Correlator

T. O. Anderson

Technical Report 32-1526, Vol. IX, pp. 123–127, June 15, 1972

The correlator presented in this article is an all-digital or sampled real-time signal processing system. It is intended for applications requiring wide bandwidth and high resolution, such as measurement of spacecraft spectra or the close scrutiny of a wide bandwidth for interference to validate the performance of the new dual S/X-band DSN system. The detection of signals in noise upon reception of radio astronomy signals is yet another application for which the present instrumentation would be useful.

A012 DSN Progress Report for September–October 1972: Two-Station Interferometer Analog Input Channel

T. O. Anderson

Technical Report 32-1526, Vol. XII, pp. 112–123, December 15, 1972

A signal-sampling system, used for the DSN Venus two-station radar experiment, intended to demonstrate hydrogen maser compatibility in two-station spacecraft tracking with planetary round-trip times, has been implemented. This article describes in detail one sampling channel. Four such channels, one for the sine and one for the cosine signal from each of two antennas, are used in the demonstration interferometer system. Each channel contains two multiplexed subchannels, and each subchannel consists of an integrating circuit, a track-and-hold circuit, and an analog-to-digital converter. All components of the subchannels are multiplexed and the output is derived from a digital multiplexing circuit which puts out digital data in parallel to line drivers for computer connection. Part of the four-channel system, a special-purpose test and calibration system, is also described.

ANDRYCZYK, R. W.

A013 A Closely Regulated TWT Converter

D. J. Hopper and R. W. Andryczyk (General Electric Company)

IEEE Trans. Aerosp. Electron. Sys., Vol. AES-7, No. 6, pp. 1147–1150, November 1971

For abstract, see Hopper, D. J.

ANENBERG, G. L.

A014 Spacecraft Ion Beam Noise Effects

G. L. Anenberg

JPL Quarterly Technical Review, Vol. 2, No. 2,
pp. 61–71, July 1972

An estimate of the antenna noise temperature and the uplink signal-to-noise ratio (S/N) has been made for Bremsstrahlung radiation emitted by a spacecraft ion beam; a worst-case situation in which the spacecraft antenna is located in the exit plane of the ion beam and directed at varying angles into the ion beam is assumed. Numerical results of the antenna noise temperature versus antenna pointing angle are given for a typical set of ion-beam and antenna-pattern parameters. The uplink S/N due to the ion-beam noise alone is given in terms of a critical range in AU at which a typical ranging transmission is received with S/N = 0 dB. The effects of the ion-beam divergence angle and antenna distance on the ion beam are also presented. Results of the study show typical increases in the antenna noise temperature of about 0.2 K and critical ranges of the order of 3–5 AU. An ion engine thus generally introduces an undetectable level of noise into a spacecraft receiver.

ANNO, G. H.

A015 Nuclear Radiation Sources On-Board Outerplanet Spacecraft

E. L. Noon, G. H. Anno, and M. A. Dore

IEEE Trans. Nucl. Sci., Vol. NS-18, No. 5,
pp. 50–57, October 1971

For abstract, see Noon, E. L.

ANSPAUGH, B. E.

A016 ATS-5 Solar Cell Experiment Results After One Year in Synchronous Orbit

B. E. Anspaugh

Technical Memorandum 33-522, January 1, 1972

The results of the ATS-5 solar cell experiment after one year in synchronous orbit are reported. A partial failure in the experimental electronics package has caused a loss of data from half of the 80 experimental solar cells. Procedures for extracting data due to a partial spacecraft failure are described and discussed. Data from the remaining 40 solar cells, including 15 mounted on a thin flexible structure, are analyzed. Data are corrected to a solar intensity of 140 mW/cm^2 and a temperature of 25°C.

After one year in synchronous orbit: (1) cells with 1.52-mm-thick coverslides did not show a clear-cut advantage over those with 0.15-mm coverslides, (2) cells with solderless grid lines are degrading at the same rate as are cells with solder-dipped grid lines, (3) cells not quite completely covered with coverslides suffered a large power loss in comparison to cells fully covered, (4) no clear-cut advantage of 10-Ω-cm cells over 2-Ω-cm cells has yet been observed, (5) cells mounted on the flexible panel with relatively little backshielding did not degrade any faster than those with substantial backshielding, and (6) the flight data in large part confirms the adequacy of the ground-based techniques used in the preflight radiation test program.

ARMS, J. T.

A017 Heat-Sterilized Silver Oxide–Zinc Cells: Cycle Life Studies

J. T. Arms

Technical Memorandum 33-581, January 1, 1973

This memorandum presents the results of a JPL study to evaluate the cell design parameters that contribute to the cycle life of sealed, heat-sterilized silver-oxide–zinc cells. Test cells having a rated capacity of 4.2 A-h were fabricated using zinc-oxide electrodes prepared by the sintered Teflon process developed at JPL, silver electrodes purchased from ESB, Inc., and separators produced by Southwest Research Institute under NASA contract. Two separator variations were evaluated, one having acrylic acid and the other having methacrylic acid grafted to irradiated polyethylene film.

All cycle-life tests were conducted at ambient temperature on a 24-h cycle consisting of 3-h discharge through a fixed resistance and 21-h charge by modified constant potential having a current limit. Cells were tested as 6-cell batteries. The depth of cycle was approximately 50% of nominal. (The nominal rating was based on the value of 0.25 A-h/g of silver.)

Significant results of this study include the following: (1) Cycle life in excess of 300 cycles was attained; (2) a zinc-oxide–silver stoichiometric ratio of 1.5:1 resulted in a greater cycle life than a ratio of 1.1:1 and a cycle life similar to that for a ratio of 2:1; (3) cells having methacrylic-acid-grafted separators suffered somewhat less in capacity loss due to zinc-electrode shape change than cells having acrylic-acid-type separators; (4) acrylic-acid-grafted separators were slightly superior to methacrylic-acid-type separators with respect to silver penetration; and (5) the inclusion of a layer of potassium titanate paper adjacent to the zinc electrodes resulted in cells that achieved a higher cycle life before any failure than that reached by cells of any other construction.

ARNETT, J. C.

A018 Development of Automatic Through-Insulation Welding for Microelectronic Interconnections

J. C. Arnett

Technical Memorandum 33-544,
December 15, 1972

The capability of automatically route, remove insulation from, and weld small-diameter solid conductor (magnet) wire would facilitate the economical small-quantity production of complex, miniature electronic assemblies. JPL has developed and evaluated an engineering model of equipment having this capability. Whereas early work in the use of welded magnet-wire interconnections concentrated on opposed-electrode systems and generally used heat to melt the wire insulation, the present method is based on a concentric-electrode system (patented as "Through Insulation Welding System") and a wire feed system (patent on "Wire Feed System" pending) which splits the insulation by application of pressure prior to welding. (The "Through Insulation Welding System" is the subject of U.S. Patent 3,596,044, and the "Wire Feed System" is the subject of a pending U.S. patent application. Both are licensed exclusively under terms which require that sublicenses be granted. Information regarding these inventions may be obtained from: Patent Officer, 1201 East California Blvd., Pasadena, California 91109.)

The work described in this memorandum deals with the design, fabrication, and evaluation testing of an improved version of this concentric-electrode system. Two different approaches for feeding the wire to the concentric electrodes were investigated. It was concluded that the process described is feasible for the interconnection of complex, miniature electronic assemblies. Recommendations for further work are presented.

ATKINSON, G.

A019 Dissipation Mechanisms in a Pair of Solar-Wind Discontinuities

T. W. J. Unti, G. Atkinson (Communications Research Center), C.-S. Wu (University of Maryland), and M. Neugebauer

J. Geophys. Res., Space Physics, Vol. 77, No. 13, pp. 2250–2263, May 1, 1972

For abstract, see Unti, T. W. J.

AUE, D. H.

A020 Mechanisms of Ion–Molecule Reactions of Propene and Cyclopropane

M. T. Bowers (University of California, Santa Barbara), D. H. Aue (University of California, Santa Barbara), and D. D. Elleman

J. Am. Chem. Soc., Vol. 94, No. 12, pp. 4255–4261, June 14, 1972

For abstract, see Bowers, M. T.

AVIŽIENIS, A.

A021 The STAR (Self-Testing and Repairing) Computer: An Investigation of the Theory and Practice of Fault-Tolerant Computer Design

A. Avižienis, G. C. Gilley, F. P. Mathur, D. A. Rennels, J. A. Rohr, and D. K. Rubin

IEEE Trans. Computers, Vol. C-20, No. 11, pp. 1312–1321, November 1971

This article presents the results obtained in a continuing investigation of fault-tolerant computing being conducted at JPL. Initial studies led to the decision to design and construct an experimental computer with dynamic (standby) redundancy, including replaceable subsystems and a program rollback provision to eliminate transient errors. This system, called the STAR computer, began operation in 1969. The following aspects of the STAR system are described: architecture, reliability analysis, software, automatic maintenance of peripheral systems, and adaptation to serve as the central computer of an outer-planet spacecraft.

A022 Arithmetic Error Codes: Cost and Effectiveness Studies for Application in Digital System Design

A. Avižienis

IEEE Trans. Computers, Vol. C-20, No. 11, pp. 1322–1331, November 1971

The application of error-detecting or error-correcting codes in digital computer design requires studies of cost and effectiveness trade-offs to supplement the knowledge of their theoretical properties. General criteria for cost and effectiveness studies of error codes are developed, and results are presented for arithmetic error codes with the low-cost check modulus $2^a - 1$. Both separate (residue) and nonseparate (AN) codes are considered. The class of multiple arithmetic error codes is developed as an extension of low-cost single codes.

BACK, L. H.

B001 Viscous Slipstream Flow Downstream of a Centerline Mach Reflection

L. H. Back and R. F. Cuffel

4

AIAA J., Vol. 9, No. 10, pp. 2107-2109,
October 1971

An important aspect of supersonic flows with shock
waves is the reflections of these waves at boundaries
such as along centerlines, along surfaces, and along free
jet extremities. The first of these interactions is consid-
ered in this article for a situation where the reflection
from the centerline in an axisymmetric flow is through a
shock stem (Mach reflection). The purpose of this inves-
tigation was to determine the mean structure of the
viscous flowfield downstream of the intersection from
Pitot and static pressure probe measurements. There was
virtually no experimental information available on the
structure of such a shear flow and on the size of the
subsonic flow region that is imbedded in the supersonic
flow.

**B002   Very High Temperature Laminar Flow of a Gas
Through the Entrance Region of a Cooled Tube—
Numerical Calculations and Experimental Results**

L. H. Back

Int. J. Heat Mass Transfer, Vol. 15, No. 5,
pp. 1001-1021, May 1972

The laminar flow equations in differential form are
solved numerically on a digital computer for flow of a
very high temperature gas through the entrance region of
an externally cooled tube. The solution method is de-
scribed and calculations are carried out in conjunction
with experimental measurements. The agreement with
experiment is good, with the result indicating relatively
large energy and momentum losses in the highly cooled
flows considered where the pressure is nearly uniform
along the flow and the core flow becomes non-adiabatic
a few diameters downstream of the inlet. The effects of a
large range of Reynolds number and Mach number (vis-
cous dissipation) are also investigated.

**B003   Influence of Contraction Section Shape and Inlet
Flow Direction on Supersonic Nozzle Flow and
Performance**

L. H. Back, R. F. Cuffel, and P. F. Massier

J. Spacecraft Rockets, Vol. 9, No. 6, pp. 420-427,
June 1972

This article presents wall static pressure measurements
and performance parameters for axisymmetric supersonic
nozzles with relatively steep convergent sections and
comparatively small radius-of-curvature throats. The
nozzle walls were essentially adiabatic. These results are
compared with those obtained in other nozzles tested
previously to appraise the influence of contraction shape
on performance. Both the flow coefficient and the thrust
were less than the corresponding values for one-dimen-
sional, isentropic, plane flow for both the axial and radial

inflow nozzles considered; but the specific impules, the
most important performance parameter, was found to be
relatively unchanged. The thrust decrement for the axial
inflow nozzles was established primarily by the shape of
the contraction section and could be estimated reason-
ably well from a conical sink flow consideration. The
radial inflow nozzle has a potential advantage from a
cooling point of view if used in a rocket engine.

**B004   Turbulent Boundary Layer and Heat Transfer
Measurements Along a Convergent-Divergent Nozzle**

L. H. Back and R. F. Cuffel

Trans. ASME, Ser. C: J. Heat Transf., Vol. 93,
No. 4, pp. 397-407, November 1971

This article presents boundary layer and heat transfer
measurements along a cooled, conical nozzle with a
convergent and a divergent half-angle of 10 deg. Semi-
empirical analyses are considered in conjunction with the
measurements. The heat transfer is found to be describ-
able by using the integral form of the energy equation
once the relationship between the Stanton number and
energy thickness Reynolds number has been established
from the measurements. The friction coefficient, how-
ever, is not described accurately along the entire nozzle
by the existing formulations considered.

**B005   Partially Ionized Gas Flow and Heat Transfer in the
Separation, Reattachment, and Redevelopment
Regions Downstream of an Abrupt Circular Channel
Expansion**

L. H. Back, P. F. Massier, and E. J. Roschke

Trans. ASME, Ser. C: J. Heat Transf., Vol. 94,
No. 1, pp. 119-127, February 1972

Heat transfer and pressure measurements obtained in the
separation, reattachment, and redevelopment regions
along a tube and nozzle located downstream of an ab-
rupt channel expansion are presented for a very-high-
enthalpy flow of argon. The ionization energy fraction
extended up to 0.6 at the tube inlet just downstream of
the arc heater. Reattachment resulted from the growth of
an instability in the vortex sheet-like shear layer between
the central jet that discharged into the tube and the
reverse flow along the wall at the lower Reynolds num-
bers, as indicated by water flow visualization studies
which were found to dynamically model the high-tem-
perature gas flow. A reasonably good prediction of the
heat transfer in the reattachment region where the
highest heat transfer occurred and in the redevelopment
region downstream can be made by using existing lami-
nar-boundary-layer theory for a partially ionized gas. In
the experiments, as much as 90% of the inlet energy was
lost by heat transfer to the tube and the nozzle wall.

B006 Partially Ionized Gas Flow and Heat Transfer in the Separation, Reattachment, and Redevelopment Regions Downstream of an Abrupt Circular Channel Expansion

L. H. Back, P. F. Massier, and E. J. Roschke

Trans. ASME, Ser. C: J. Heat Transf., Vol. 94, No. 1, pp. 119–127, February 1972

Heat transfer and pressure measurements obtained in the separation, reattachment, and redevelopment regions along a tube and nozzle located downstream of an abrupt channel expansion are presented for a very high enthalpy flow of argon. The ionization energy fraction extended up to 0.6 at the tube inlet just downstream of the arc heater. Reattachment resulted from the growth of an instability in the vortex sheet-like shear layer between the central jet that discharged into the tube and the reverse flow along the wall at the lower Reynolds numbers, as indicated by water flow visualization studies which were found to dynamically model the high-temperature gas flow. A reasonably good prediction of the heat transfer in the reattachment region where the highest heat transfer occurred and in the redevelopment region downstream can be made by using existing laminar boundary layer theory for a partially ionized gas. In the experiments as much as 90% of the inlet energy was lost by heat transfer to the tube and the nozzle wall.

BAHM, E. J.

B007 Magnetic Tape Recorder for Long Operating Life in Space

E. J. Bahm and J. K. Hoffman

IEEE Trans. Magnetics, Vol. MAG-7, No. 3, pp. 517–520, September 1971

Magnetic tape recorders have long been used on satellites and spacecraft for onboard storage of large quantities of data. As satellites enter into commercial service, long operating life at high reliability becomes important. Also, the presently planned long-duration space flights to the outer planets require long-life tape recorders. Past satellite tape recorders have achieved a less-than-satisfactory performance record and the operating life of other spacecraft tape recorders has been relatively short and unpredictable. Most failures have resulted from malfunctions of the mechanical tape transport.

Recent advances in electric motors and static memories have allowed the development of the new tape recorder reported in this article. This recorder uses a very simple tape transport with few possible failure modes. It consists of only two brushless dc motors, two tape guides, and the recording heads. Relatively low tape tension, wide torque capability, and precise speed control facili-

tate design for mechanical reliability to match that of tape-recorder electronics.

BALL, J. E.

B008 A Summary of the Pioneer 10 Maneuver Strategy

R. B. Frauenholz and J. E. Ball

JPL Quarterly Technical Review, Vol. 2, No. 3, pp. 46–62, October 1972

For abstract, see Frauenholz, R. B.

BARBER, T. A.

B009 Basic Parameters for Low Thrust Mission and System Analysis

T. A. Barber, J. L. Horsewood (Analytical Mechanics Associates, Inc.), and H. Meissinger (TRW Systems, Inc.)

Preprint 72-426, AIAA Ninth Electric Propulsion Conference, Bethesda, Maryland, April 17–19, 1972

Any form of mission analysis has as its basis a large number of trajectories mapping out the parameter range of the mission under study. Low thrust mission analysis has long been hampered by this requirement to generate many optimized trajectories which frequently need to be rerun to explore the effect of changes in some vehicle or mission parameters, particularly launch vehicle changes. This paper proposes a basic set of normalized parameters to represent the low thrust system characteristics and derives the conditions which must be met to obtain trajectory and performance data which are invariant with the launch vehicle characteristics, the selected power, the specific mass of the low thrust vehicle, and the efficiency of the ion propulsion system. This normalized representation of mission characteristics frees the analyst from having to rerun the trajectories if any of the aforementioned parameters are varied. Examples pertaining to a low thrust Jupiter flyby and comet Encke rendezvous are given to demonstrate the utility of the method of presentation.

BARKER, B. J.

B010 Dynamic Measurement of Bulk Modulus of Dielectric Materials Using a Microwave Phase Shift Technique

B. J. Barker and L. D. Strand

Technical Memorandum 33-577, November 15, 1972

This memorandum discusses a microwave doppler-shift technique which has been developed for measuring the

dynamic bulk modulus of dielectric materials such as solid propellants. The system has a demonstrated time resolution on the order of milliseconds and a theoretical spatial resolution of a few microns. Accuracy of the technique is dependent on an accurate knowledge of the wavelength of the microwave in the sample being tested. Preliminary tests with two solid propellants, one non-aluminized and one containing 16% aluminum, yielded reasonable, reproducible results. It was concluded that, with refinements, the technique holds promise as a practical means for obtaining accurate dynamic-bulk-modulus data over a variety of transient conditions.

BARNES, G. D.

B011   DSN Progress Report for January–February 1972: Angle Tracking Analysis and Test Development for the Integrated Stations

G. D. Barnes

Technical Report 32-1526, Vol. VIII, pp. 131–140, April 15, 1972

Analysis and test development have been completed for the integrated tracking system. An antenna servo model was developed and its transfer function and gain constants are presented. The model was used to simulate the response of an antenna in the autotrack and program modes. These simulation results are compared with the data collected at the Pioneer Deep Space Station, and the differences between the two modes are shown. Antenna response data for the integrated servo system are compared with the Echo Deep Space Station response data and the Deep Space Instrumentation Facility servo specification curves. The servo specification curves are shown to be unrealistic for either the standard or integrated angle tracking systems.

BARNES, T. G.

B012   Jupiter: Observation of Deuterated Methane in the Atmosphere

R. Beer, C. B. Farmer, R. H. Norton,
J. V. Martonchik (University of Texas), and
T. G. Barnes (University of Texas)

Science, Vol. 175, No. 4028, pp. 1360–1361, March 24, 1972

For abstract, see Beer, R.

BARTH, C. A.

B013   Mariner 9 Science Experiments: Preliminary Results

R. H. Steinbacher, A. J. Kliore, J. Lorell,
H. Hipsher (National Aeronautics and Space Administration), C. A. Barth (University of Colorado), H. Masursky (U.S. Geological Survey), G. Münch (California Institute of Technology), J. C. Pearl (Goddard Space Flight Center), and B. A. Smith (New Mexico State University)

Science, Vol. 175, No. 4019, pp. 293–294, January 21, 1972

For abstract, see Steinbacher, R. H.

B014   Mariner 9 Ultraviolet Spectrometer Experiment: Initial Results

C. A. Barth (University of Colorado),
C. W. Hord (University of Colorado),
A. I. Stewart (University of Colorado), and
A. L. Lane

Science, Vol. 175, No. 4019, pp. 309–312, January 21, 1972

The ultraviolet airglow spectrum of Mars has been measured from an orbiting spacecraft during a 30-day period in November–December 1971. The emission rates of the carbon monoxide Cameron and fourth positive bands, the atomic oxygen 1304-Å line and the atomic hydrogen 1216-Å line have been measured as a function of altitude. Significant variations in the scale height of the CO Cameron band airglow have been observed during a period of variable solar activity; however, the atomic oxygen and hydrogen airglow lines are present during all the observations. Measurements of the reflectance of the lower atmosphere of Mars show the spectral characteristics of particle scattering and a magnitude that is about 50% of that measured during the Mariner 6 and 7 experiments in 1969. The variation of reflectance across the planet may be represented by a model in which the dominant scatterer is dust that absorbs in the ultraviolet and has an optical depth greater than 1. The atmosphere above the polar region is clearer than over the rest of the planet.

B015   Mariner 9 Ultraviolet Spectrometer Experiment: Stellar Observations

C. F. Lillie (University of Colorado),
R. C. Bohlin (University of Colorado),
M. R. Molnar (University of Colorado),
C. A. Barth (University of Colorado), and
A. L. Lane

Science, Vol. 175, No. 4019, pp. 321–322, January 21, 1972

For abstract, see Lillie, C. F.

BATELAAN, P. D.

B016 DSN Progress Report for March–April 1972: Radio Source Calibration Program (RASCAL)—Phase 1: Antenna Gain Calibration

P. D. Batelaan

Technical Report 32-1526, Vol. IX, pp. 137–140, June 15, 1972

A new program for measuring antenna gain of the large DSN antennas is described. The gain measurement procedure is outlined. Improvements over past techniques have resulted in better knowledge of gain-standard-horn calibrations, in more compact procedure, and in changes in the precision comparison attenuator. The gain accuracy goal of the primary station is ±0.05 dB, 1 σ.

BATHKER, D. A.

B017 DSN Progress Report for July–August 1972: Dual Carrier Preparations for Viking

D. A. Bathker and D. W. Brown

Technical Report 32-1526, Vol. XI, pp. 146–149, October 15, 1972

Multiple spacecraft vehicles for the Viking mission require simultaneous transmission of two S-band carriers from a single deep space station. Past experience in high-power diplexing, coupled with dual carriers, has shown that, in addition to controlled uplink-intermodulation products, a complex form of receive-band interference will be generated within the ground station. Recent efforts to define and minimize these effects are being supplemented with additional resources including reconfiguration of the Venus Deep Space Station (DSS 13) for dual-carrier diplexed operation with the objective of assuring DSN capability in the Viking mode.

BAUMAN, A. J.

B018 Isolation and Characterization of Keto-Carotenoids From the Neutral Extract of Algal Mat Communities of a Desert Soil

A. J. Bauman, H. G. Boettger, A. M. Kelly, R. E. Cameron, and H. Yokoyama (U.S. Department of Agriculture)

Eur. J. Biochem., Vol. 22, No. 2, pp. 287–293, September 1971

The carotenoid pigments of surficial algal mat communities of a California absolute subtropical desert were isolated and characterized principally by means of high resolution mass spectrometry. The pigments were all oxidized keto-types, predominantly canthaxanthin, its isomers, and echinone. The carotenoid pattern suggests that the mats represent an old climax ecosystem in which the algal cells at the time of collection were starved for nitrogen.

B019 Absence of Porphyrins in an Apollo 12 Lunar Surface Sample

J. H. Rho, A. J. Bauman, T. F. Yen (University of Southern California), and J. Bonner (California Institute of Technology)

Proceedings of the Second Lunar Science Conference, Houston, Texas, January 11–14, 1971, Vol. 2, pp. 1875–1877, The M.I.T. Press, Cambridge, 1971

For abstract, see Rho, J. H.

B020 A Simple Electrostatic Model for the Chromatographic Behavior of the Primary Dithizonates

A. J. Bauman and J. H. Richards

Separ. Sci., Vol. 6, No. 5, pp. 715–725, October 1971

A simple electrostatic model of the reactive sites of primary metal dithizonates which fits their published chromatographic behavior is described. Coordination with a metal ion tends to increase the formal charge on the hindered imino hydrogens in the molecule. This increase is a function of the individual metal's Sanderson electronegativity. Plots of R_m versus electronegativity are rectilinear, have the same form for all systems and adsorbents described, and place dithizonates of similar molecular geometry on separate curves. The results of this study suggest that the dithizonates are a heterogeneous group of compounds which differ in coordination configuration and geometry.

BAUMERT, L. D.

B021 DSN Progress Report for March–April 1972: A Note on the Griesmer Bound

L. D. Baumert and R. J. McEliece

Technical Report 32-1526, Vol. IX, pp. 49–52, June 15, 1972

Griesmer's lower bound for the word length n of a linear code of dimension k and minimum distance d is shown to be sharp for fixed k when d is sufficiently large. For $k < 6$ and all d, the minimum word length is determined.

B022 Weights of Irreducible Cyclic Codes

L. D. Baumert and R. J. McEliece

Inform. Control, Vol. 20, No. 2, pp. 158–175,
March 1972

With any fixed prime number p and positive integer N, not divisible by p, there is associated an infinite sequence of cyclic codes. In a previous article, it was shown that a theorem of Davenport–Hasse reduces the calculation of the weight distributions for this whole sequence of codes to a single calculation (essentially that of calculating the weight distribution for the simplest code of the sequence). The primary object of this paper is the development of machinery which simplifies this remaining calculation. Detailed examples are given. In addition, tables are presented which essentially solve the weight distribution problem for all such binary codes with $N < 100$ and, when the block length is less than one million, give the complete weight enumerator.

B023 A Combinatorial Packing Problem

L. D. Baumert

SIAM/AMS (Society for Industrial and Applied Mathematics/American Mathematical Society) Book Series, Vol. IV, pp. 97–108, 1970

This article is concerned with the efficient packing of squares of side two into the $p \times p$ torus. Of more general interest is the analogous n-dimensional problem: that of packing n-dimensional two-cubes efficiently into a $p \times p \times \ldots \times p$ torus. Of course, when p is even, the problem is trivial. (Then, the simplest possible alignment of the cubes completely fills the torus.) Thus, p here is restricted to be an odd integer. Further, it should be pointed out that the primary interest here is in determining the maximum number $[= \alpha(C_p{}^n)]$ of cubes which can be packed into the torus and of only secondary concern are the actual structural details of any particular maximal packing.

BECK, A. J.

B024 Jupiter Trapped Radiation Belts

A. J. Beck

JPL Quarterly Technical Review, Vol. 1, No. 4,
pp. 78–88, January 1972

Previously developed models for trapped electron radiation belts and trapped proton radiation belts in the Jovian magnetosphere are described. The spatial distribution of flux and the L-shell dependence of the characteristic energy are displayed for both models. Based on these models, the fluence accumulated by a Jupiter flyby spacecraft is given in terms of the equivalent 3-MeV fluence for electrons and the equivalent 20-MeV proton fluence for protons. Finally, some impacts of these fluences on outer-planet missions are described.

BEER, R.

B025 Astronomical Infrared Spectroscopy With a Connes-Type Interferometer: III. Alpha Orionis, 2600–3450 cm^{-1}

R. Beer, R. B. Hutchison, R. H. Norton, and
D. L. Lambert (University of Texas)

Astrophys. J., Vol. 172, No. 1, Pt. 1, pp. 89–115,
February 15, 1972

Recent spectra of α Ori in the 3–4-μ region at a resolving power of about 10,000 show clear evidence of the $\Delta v = 1$ sequence of the rotation-vibration bands of OH. A detailed investigation of the rotational and vibrational populations suggests that the OH is close to being in LTE at an apparent temperature of $4100 \pm 200°$K. We deduce an OH abundance of 1.2×10^{20} molecules cm^{-2} and upper limits for H_2O and $H^{35}Cl$ of 8×10^{18} and 8×10^{17} molecules cm^{-2}, respectively. We further deduce that the rms turbulence velocity in the region of OH line formation is 11.5 ± 2 km s^{-1}. The implications of these data on abundances in M supergiant atmospheres are discussed.

B026 Astronomical Infrared Spectroscopy With a Connes-Type Interferometer: I. Instrumental

R. Beer, R. H. Norton, and C. H. Seaman

Rev. Sci. Instr., Vol. 42, No. 10, pp. 1393–1403,
October 1971

Shortly after P. and J. Connes had completed the first model of their now well-known Fourier spectrometer, JPL undertook the construction of a similar instrument. The JPL instrument differs significantly from the original. In this article, the construction and operation of the JPL instrument are discussed in an astronomical context, and a sample is given of the type of spectra obtained with the system.

B027 Jupiter: Observation of Deuterated Methane in the Atmosphere

R. Beer, C. B. Farmer, R. H. Norton,
J. V. Martonchik (University of Texas), and
T. G. Barnes (University of Texas)

Science, Vol. 175, No. 4028, pp. 1360–1361,
March 24, 1972

During May 1971, the authors obtained a number of whole-planet spectra of Jupiter in the spectral region from 1800 to 2200 cm^{-1} at a resolution of 0.55 cm^{-1}. Singly deuterated methane was positively identified in the 4- to 5-μ spectrum of Jupiter.

BEJCZY, A. K.

B028 Switched-Mode Adaptive Terminal Control for Propulsive Landing of Nonlifting Spacecraft

A. K. Bejczy

Preprint 71-903, AIAA Guidance,
Control and Flight Mechanics Conference,
Hempstead, New York, August 16–18, 1971

A combined estimation and control scheme is described for propulsive landing of a nonlifting gravity-turn ballistic vehicle under uncertain atmospheric conditions. The core of the scheme is a dual integration algorithm. One algorithm acts as a sequential filter producing updated estimates on the *a priori* uncertain atmospheric parameters and the state variables, while the other algorithm acts in an iterative-logical mode to control the throttle setting. The filter inputs are on-board radar range and doppler velocity measurements and accelerometer data related to the vehicle's nongravitational longitudinal acceleration. Three different filter schemes are developed, utilizing different combinations of measurement inputs. The adaptive switched-mode landing control policy can handle a considerable number of errors in initial altitude and velocity, as well as 50–70% uncertainties in the atmospheric parameters, and performs the soft-landing task with a 20–35% reduction of the fuel consumption needed by a comparable control law.

B029 Analytical Methods for Performance Evaluation of Nonlinear Filters

A. K. Bejczy and R. Sridhar (University of California, Los Angeles)

J. Math. Anal. Appl., Vol. 36, No. 3, pp. 477–505, December 1971

The investigation described in this article is addressed to the question of developing analytical methods for evaluating the performance of suboptimal nonlinear filters such that the filters' structure is fixed by postulating a simple form for it. The filtering problem is considered in the continuous time domain. The postulated simple suboptimal nonlinear filter structure closely parallels the structure of the Kalman–Bucy optimal linear filter algorithm.

Two filter performance evaluation methods are developed based on the Kolmogorov equations for the transition density of Markov processes. The expansions in the approximations for the nonlinear system and observation functions are, in effect, carried out up to second-order terms in both methods. The difference between the methods is the sequencing of expansions and averaging. The description of the filters' performance is sought in terms of second-order statistics (mean and covariance) in both methods. The equations for the mean and covariance of the filtering error resulting from the two methods

are different. The resulting equations of both methods have, however, an important common feature: They are *deterministic* differential equations describing the time evolution of the mean and covariance of the filtering error process for the fixed filter structure in terms of the known (postulated) filter gain and system and noise parameters. The developed deterministic differential equations can also be utilized to determine appropriate (deterministic) filter gains for the fixed structure nonlinear filter. The salient features of the new performance evaluation (and filter gain construction) methods are illustrated with two examples.

B030 Approximate Nonlinear Filters and Deterministic Filter Gains

A. K. Bejczy and R. Sridhar (University of California, Los Angeles)

Trans. ASME, Ser. G: J. Dynam. Sys., Meas., Contr., Vol. 94, No. 1, pp. 57–63, March 1972

A simple nonlinear filter construction and performance evaluation method is described and illustrated on several examples by comparing it to more complex nonlinear filter schemes. In the new method, the filter gain is a precomputed, deterministic quantity (possibly a constant) and, the filter's performance is (approximately) described by deterministic differential equations which can be solved off-line.

BENSON, G. C.

B031 Integration of a Breadboard Power Conditioner With a 20-cm Ion Thruster

T. D. Masek, T. W. Macie, E. N. Costogue,
W. J. Muldoon (Hughes Aircraft Company),
D. R. Garth (Hughes Aircraft Company), and
G. C. Benson (Hughes Aircraft Company)

J. Spacecraft Rockets, Vol. 9, No. 2, pp. 71–78, February 1972

For abstract, see Masek, T. D.

BERLEKAMP, E. R.

B032 DSN Progress Report for July–August 1972: Decoding the Golay Code

E. R. Berlekamp

Technical Report 32-1526, Vol. XI, pp. 81–85, October 15, 1972

This article describes a procedure for correcting all patterns of three or fewer errors with the (23,12) or (24,12) Golay code. The procedure decodes any 24-bit word in about 26 "steps," each of which consists of only a few

simple operations such as counting the number of ones in a 12-bit word. The procedure is based on the circulant view-point introduced by Karlin (1969). In addition it is shown how the (24,12) Golay code can be used to correct certain patterns of more than three errors.

BERMAN, A. L.

B033 **DSN Progress Report for March–April 1972: Effects of the Pioneer 10 Antenna Polarization and Spacecraft Rotation as Seen in the Radio Metric Data**

A. L. Berman

Technical Report 32-1526, Vol. IX, pp. 201–206, June 15, 1972

The Pioneer 10 antenna polarization and spacecraft rotation introduce a signature into the radio metric doppler data, which, unless otherwise noted, might be confused with a degradation of the tracking system. This signature, especially in regard to effects as seen in doppler residuals and doppler noise, is analyzed in detail in this article.

BERMAN, P. A.

B034 **Considerations With Respect to the Design of Solar Photovoltaic Power Systems for Terrestrial Applications**

P. A. Berman

Technical Report 32-1558, June 15, 1972

The various factors involved in the development of solar photovoltaic power systems for terrestrial application are discussed. The trade-offs, compromises, and optimization studies which must be performed in order to develop a viable terrestrial solar array system are described. It is concluded that the technology now exists for the fabrication of terrestrial solar arrays, but that the costs would be prohibitive. Various approaches to cost reduction are presented, and the general requirements for materials and processes are delineated.

B035 **Solar Cell Contact Pull Strength as a Function of Pull-Test Temperature**

R. K. Yasui and P. A. Berman

Technical Report 32-1563, September 1, 1972

For abstract, see Yasui, R. K.

B036 **Photovoltaic Solar Array Technology Required for Three Wide-Scale Generating Systems for Terrestrial Applications: Rooftop, Solar Farm, and Satellite**

P. A. Berman

Technical Report 32-1573, October 15, 1972

This report presents three major options for wide-scale generation of photovoltaic energy for terrestrial use: (1) Rooftop Array, (2) Solar Farm, and (3) Satellite Station. The rooftop Array would use solar-cell arrays on the roofs of residential or commercial buildings; the Solar Farm would consist of large ground-based arrays, probably in arid areas with high insolation; and the Satellite Station would consist of an orbiting solar array, many square kilometers in area.

The Technology Advancement Requirements necessary for each option are discussed, including cost reduction of solar cells and arrays, weight reduction, resistance to environmental factors, reliability, and fabrication capability, including the availability of raw materials. The majority of the Technology Advancement Requirements are applicable to all three options, making possible a flexible basic approach regardless of the options that may eventually be chosen. No conclusions are drawn as to which option is most advantageous, since the feasibility of each option depends on the success achieved in the Technology Advancement Requirements specified.

B037 **Development of Lithium-Doped Radiation-Resistant Solar Cells**

P. A. Berman

Technical Report 32-1574, November 15, 1972

In the middle 1960s, it was discovered that the addition of lithium to n-base silicon solar cells resulted in what appeared to be annealing of radiation-induced defects. For the past five years, JPL has been involved in an effort to exploit this phenomenon in order to develop a highly-radiation-resistant, high-efficiency silicon solar cell. This paper discusses the results of the investigations which represent major achievements for attaining this goal. Lithium-doped solar cells have now been fabricated with initial lot efficiencies averaging 11.9% in an air-mass-zero solar simulator and a maximum observed efficiency of 12.8%. The best lithium-doped solar cells are approximately 15% higher in maximum power than state-of-the-art n–p cells after moderate-to-high fluences of 1-MeV electrons and after 6–7 months exposure to low-flux (approximately 10^{12}-electrons/cm^2/day) irradiation by a strontium-90 beta source, which approximates the electron spectrum and flux associated with near-Earth space. Furthermore, lithium-doped cells were found to degrade at a rate only one-tenth that of state-of-the-art n–p cells under 28-MeV electron irradiation.

Excellent progress has been made in quantitative predictions of post-irradiation current–voltage characteristics as a function of cell design by means of capacitance–voltage measurements, and this information has been used to achieve further improvements in lithium-doped cell design. Major improvements in cell processing have

also been achieved, resulting in higher cell efficiency and greater reproducibility.

B038 JPL Lithium-Doped Solar Cell Development Program

P. A. Berman

JPL Quarterly Technical Review, Vol. 2, No. 1, pp. 29–36, April 1972

One of the most significant problems encountered in the use of silicon solar cells in space has been their sensitivity to electron and proton radiation exposure. A major advancement was achieved when the P-diffused-into-N-base solar cells were replaced with the more radiation-tolerant N-diffused-into-P-base solar cells. Another advancement in achieving greater radiation tolerance was the discovery that the addition of lithium to N-base silicon resulted in what appeared to be annealing of radiation-induced defects. This phenomenon is being exploited to develop a high-efficiency, radiation-resistant, lithium-doped solar cell. In this investigation, lithium-doped solar cells fabricated from oxygen-lean and oxygen-rich silicon have been obtained with average initial efficiencies of 11.9% at air mass zero and 28°C, as compared to state-of-the-art N/P cells fabricated from 10-Ω-cm silicon with average efficiencies of 11.3% under similar conditions. Lithium-doped cells have demonstrated the ability to withstand three to five times the fluence of 1-MeV electrons before degrading to a power equivalent to that of state-of-the-art solar cells. This article discusses the principal investigations carried out with respect to fabrication of high-efficiency, radiation-resistant, lithium-doped cells, including starting material, P/N junction diffusion, lithium source introduction, and lithium diffusion.

BIERMAN, G. J.

B039 Power Series Evaluation of Transition and Covariance Matrices

G. J. Bierman (Litton Systems)

IEEE Trans. Automat. Contr., Vol. AC-17, No. 2, pp. 228–232, April 1972

Power series solutions to the matrix covariance differential equation

$$\dot{P} = AP + (AP)' + Q$$

and the transition differential equation

$$\dot{\Phi} = A\Phi$$

are re-examined. Truncation error bounds are derived which are computationally attractive and which extend previous results. Polynomial approximations are obtained

by exploiting the functional equations satisfied by the transition and covariance matrices. The series-functional equation propagation technique represents a fast and accurate alternative to the numerical integration of the time-invariant transition and covariance equations.

BILLINGSLEY, F. C.

B040 Computer-Generated Color Image Display of Lunar Spectral Reflectance Ratios

F. C. Billingsley

Photogr. Sci. Eng., Vol. 16, No. 1, pp. 51–57, January–February 1972

Color separation pictures were taken on Apollo 12 through red, green, and blue filters on black-and-white film. Computer processing has been utilized to extract quantitative color information from these pictures and to produce output color pictures. Four computer-generated output color separations are combined to give a color image in which small color reflectance differences on the lunar surface are represented by the computer-generated colors independent of the intensity of the light reflected from the lunar surface. Calibration step wedges have been carried through the entire process to provide total system calibration for the removal of film nonlinearities. The computer calculations map the red/green, blue/green combination at each image point onto the chromaticity diagram so that it is represented by a unique color, and then calculates the four color sources used to produce the desired color at this point in the output picture. These same methods can be used to represent other parameters occurring and sensed simultaneously over a spatial region.

B041 Apollo 12 Multispectral Photography Experiment

A. F. H. Goetz, F. C. Billingsley,
J. W. Head (Bellcomm, Inc.),
T. B. McCord (Massachusetts Institute of Technology), and E. Yost (Long Island University)

Proceedings of the Second Lunar Science Conference, Houston, Texas, January 11–14, 1971, Vol. 3, pp. 2301–2310, The M.I.T. Press, 1971

For abstract, see Goetz, A. F. H.

BJORKLUND, R. A.

B042 Trajectory Correction Propulsion for TOPS

H. R. Long and R. A. Bjorklund

Technical Report 32-1571, November 15, 1972

For abstract, see Long, H. R.

BLAIR, P. M.

B043 Discoloration and Lunar Dust Contamination of Surveyor III Surfaces

W. F. Carroll and P. M. Blair (Hughes Aircraft Corporation)

Proceedings of the Second Lunar Science Conference, Houston, Texas, January 11–14, 1971, Vol. 3, pp. 2735–2742, The M.I.T. Press, Cambridge, 1971

For abstract, see Carroll, W. F.

BLINN, J. C., III

B044 Microwave Emission From Geological Materials: Observations of Interference Effects

J. C. Blinn III, J. E. Conel, and J. G. Quade (University of Nevada)

J. Geophys. Res., Vol. 77, No. 23, pp. 4366–4378, August 10, 1972

Microwave radiometric field observations were conducted at wavelengths of 21, 2.8, and 0.95 cm to determine the microwave penetration depth of a number of sands and gravels as a function of particle size and moisture content. Observations of a reflecting plate covered with varying thicknesses of test material exhibit a pronounced oscillatory behavior that is consistent with established electromagnetic theory for plane-parallel layered mediums. Utilization of this interference effect is proposed as a microwave radiometric technique for determining the bulk electrical properties of geologic materials, snow, ice, and other materials readily adapted to layering experiments. Extension of the technique could lead to a method for remotely determining layer thickness in certain naturally layered systems such as sea ice.

BOETTGER, H. G.

B045 Isolation and Characterization of Keto-Carotenoids From the Neutral Extract of Algal Mat Communities of a Desert Soil

A. J. Bauman, H. G. Boettger, A. M. Kelly, R. E. Cameron, and H. Yokoyama (U.S. Department of Agriculture)

Eur. J. Biochem., Vol. 22, No. 2, pp. 287–293, September 1971

For abstract, see Bauman, A. J.

BOGGS, D. H.

B046 A Partial-Step Algorithm for the Nonlinear Estimation Problem

D. H. Boggs

AIAA J., Vol. 10, No. 5, pp. 675–679, May 1972

The "normal equations" solution to the weighted least-squares estimation problem is recast in terms of singular-value decomposition of the equations-of-condition matrix, A. The superior convergence properties of rank-deficient, pseudoinverse solutions in the presence of nonlinearities and ill-conditionedness of the normal matrix $A^T A$ are examined. An extension of this partial-step technique, which makes use of part of the information contained along "eigen-directions" associated with singular values previously ignored in the standard rank-deficient solution, is presented. Results are given showing the relative convergence powers of the methods in obtaining a solution to the orbit-determination problem for a simulated Martian orbiter trajectory. These results indicate that the extended partial-step method will be of value during the orbit phase of the Mariner Mars 1971 mission.

BOGNER, R. S.

B047 Development and Testing of a High Cycle Life 30 A-h Sealed AgO–Zn Battery

R. S. Bogner

Technical Memorandum 33-536, May 1, 1972

A two-phase program was initiated to investigate design parameters and new technology for the development of an improved AgO–Zn battery. The basic performance goal was 100 charge/discharge cycles (22 h/2 h) at 50% depth-of-discharge following a 6-mo period of charged stand at room temperature (25 ± 4°C). Phase I, cell evaluation, involved testing 70 cells in five-cell groups. The major design variables were active material ratios, electrolyte concentrations, separator systems, and negative plate shape. Phase I testing showed that cycle life could be improved 10 to 20% by using greater ratios of zinc to silver oxide and higher electrolyte concentrations. Wedge-shaped negatives increased cycle life by nearly 100%. The fibrous-sausage-casing separators proved superior to the RAI 2291 separators for cycle life; however, test results were complicated by the cell-pack tightness, a variable not originally planned to be introduced into the tests.

Phase II battery evaluation, which was initiated before the Phase I results were known completely, involved evaluation of six designs of 19-cell batteries. Phase II testing was done at the Naval Ammunition Depot, Crane, Indiana. Only one battery exceeded 100 cycles following a 9-mo charged stand. That battery, containing fibrous-sausage-casing separators, gave 204 cycles at 50% depth-of-discharge before the first cell failed. Unfortunately, the wedge-shaped negative was not evaluated in Phase II. Phase II and Phase I failures were due to loss of negative plate capacity caused by negative plate erosion.

BOHLIN, R. C.

B048 Mariner 9 Ultraviolet Spectrometer Experiment: Stellar Observations

C. F. Lillie (University of Colorado),
R. C. Bohlin (University of Colorado),
M. R. Molnar (University of Colorado),
C. A. Barth (University of Colorado), and
A. L. Lane

Science, Vol. 175, No. 4019, pp. 321–322, January 21, 1972

For abstract, see Lillie, C. F.

BONNER, J.

B049 Absence of Porphyrins in an Apollo 12 Lunar Surface Sample

J. H. Rho, A. J. Bauman, T. F. Yen (University of Southern California), and J. Bonner (California Institute of Technology)

Proceedings of the Second Lunar Science Conference, Houston, Texas, January 11–14, 1971, Vol. 2, pp. 1875–1877, The M.I.T. Press, Cambridge, 1971

For abstract, see Rho, J. H.

BOOTH, R. W. D.

B050 DSN Progress Report for July–August 1972: Preliminary Analysis of the Microwave Weather

M. S. Reid and R. W. D. Booth

Technical Report 32-1526, Vol. XI, pp. 111–120, October 15, 1972

For abstract, see Reid, M. S.

BORN, G. H.

B051 Mariner 9 Celestial Mechanics Experiment: Gravity Field and Pole Direction of Mars

J. Lorell, G. H. Born, E. J. Christensen,
J. F. Jordan, P. A. Laing, W. Martin,
W. L. Sjogren, I. I. Shapiro (Massachusetts Institute of Technology),
R. D. Reasenberg (Massachusetts Institute of Technology), and G. L. Slater (Massachusetts Institute of Technology)

Science, Vol. 175, No. 4019, pp. 317–320, January 21, 1972

For abstract, see Lorell, J.

BOSE, T. K.

B052 Cross-Flow Blowing of a Two-Dimensional Stationary Arc

T. K. Bose (Indian Institute of Technology)

AIAA J., Vol. 10, No. 1, pp. 80–86, January 1972

The effect of cross-flow blowing on a two-dimensional stationary arc between a pair of electrodes has been studied theoretically. It is demonstrated in the analysis that the electrons emitted from the cathode undergo collisions with the heavy particles and are deflected in the flow direction by the component of a collisional force associated with the relative difference in flow velocities between electrons and heavy particles. The resultant motion of the electrons describing the arc is thus caused by a combined action of the collisional force that results from the externally applied electric field. An expression is given which enables computation of the arc shape to be made provided the velocity distribution of the cross-flow and the distribution of the externally applied electric field are prescribed. The analysis has been applied for a case in which an analytical expression for the distribution of the externally applied electric field is available. An electrical discharge between two point electrodes was chosen with a uniform velocity distribution of the cross-flow. Numerical results are presented for the maximum deflection as a function of a blowing parameter. In addition, it is shown that the temperature distribution within the arc is asymmetric.

BOUDREAU, J. E.

B053 Closed-Loop Dynamics of In-Core Thermionic Reactor Systems

C. D. Sawyer and J. E. Boudreau

Technical Memorandum 33-546, May 15, 1972

For abstract, see Sawyer, C. D.

BOWERS, M. T.

B054 Mechanisms of Ion–Molecule Reactions of Propene and Cyclopropane

M. T. Bowers (University of California, Santa Barbara), D. H. Aue (University of California, Santa Barbara), and D. D. Elleman

J. Am. Chem. Soc., Vol. 94, No. 12, pp. 4255–4261, June 14, 1972

Ion–molecule reaction of the $C_3H_6.^+$ ion from propene proceeds via a "four-center" mechanism to a $C_6H_{12}.^+$ ion capable of 1,2- and 1,4-hydrogen migrations but not 1,3-hydrogen migration. The $C_6H_{12}.^+$ ion can rearrange via the various structures shown. Decomposition to eth-

ylene proceeds via a "four-center" cleavage of the dimethylcyclobutane ion. The $C_3H_6.^+$ ion from cyclopropane can be distinguished from that formed from propene. The $C_6H_{12}.^+$ ion formed on reaction of propene and cyclopropane is different from that formed from propene alone; it undergoes facile cleavage with loss of ethylene. By study of ion–molecule reactions of $CD_3CHCH_2.^+$ formed at energies below the appearance potential of fragment ions a small amount of isotopic scrambling has been observed in the $CD_3CHCH_2.^+$ ion in accord with predictions based on quasi-equilibrium theory. Part of the $C_3H_3^+$ ions formed from propene are unusually unreactive at high pressures with propene and may have the cyclopropenium ion structure.

B055 Dependence of the Rates on Ion Kinetic Energy for the Reactions $D_2^+ + D_2$ and $HD^+ + HD$

W. T. Huntress, Jr., D. D. Elleman, and
M. T. Bowers (University of California, Santa
Barbara)

J. Chem. Phys., Vol. 55, No. 11, pp. 5413–5414,
December 1, 1971

For abstract, see Huntress, W. T., Jr.

BRERETON, R. G.

B056 A View of the Moon

R. G. Brereton

JPL Quarterly Technical Review, Vol. 2, No. 1,
pp. 1–11, April 1972

Apollo information on lunar science is now voluminous, and NASA has recognized the need for a task that would collate and interpret Apollo results and provide a synthesized view of the Moon. The initial conclusions of such a task carried out at JPL are reviewed in this article. In summary, whereas most of the Earth's surface is highly mobile because of dynamic endogenic and exogenic processes, the lunar surface is old and stable and coexists with the ambient environment of space. The Moon is essentially quiet seismically, does not have a heavy solid or liquid core, and has a much cooler internal temperature than Earth. The lunar lithosphere is both old and strong and appears to have been little modified by volcanic or tectonic activity for more than three billion years.

BROKL, S. S.

B057 DSN Progress Report for March–April 1972: Computer Display and Entry Panel

S. S. Brokl

Technical Report 32-1526, Vol. IX, pp. 44–48,
June 15, 1972

The computer display and entry panel is a programmable high-speed numerical display and entry device for use with XDS 900-series computers. It contains additional sense-switch and sense-light capability along with a system interrupt. This type of device is expected to find application in troubleshooting Deep Space Instrumentation Facility minicomputers in the network repair facility, in developing minicomputer software, and as a status-display device for the DSN network operations control facility.

BROWN, D. W.

B058 DSN Progress Report for January–February 1972: Third-Order Phase-Locked Loop Perspectives

D. W. Brown

Technical Report 32-1526, Vol. VIII, pp. 103–114,
April 15, 1972

Compared with the development of a second-order phase-lock design, the analysis and practical application of a third-order phase-lock design have been sporadic in both the servomechanism and telecommunication fields. The attractiveness of minimal tracking errors resulting from near "perfect" third-order filtering (three true integrators) has been largely offset by undesirable acquisition properties and to some extent by a dearth of analysis of this configuration. A useful approach, both in viewpoint and in design, is to consider the prevalent "imperfect" second-order and third-order configurations for what they are—namely, loops with one integrator augmented by one or two lag time constants, so proportioned with respect to loop gain as to approximate the closed-loop response of true second- and third-order configurations, while manifesting a controlled (but not infinite) improvement in tracking performance over the first-order loop. This article seeks to apply this approach to the existing work in third-order analysis, and to emphasize the principal effects, both positive and negative, of the relative proportioning of loop gain and time constants, with a view toward practical exploitation of the best features of these loop configurations.

B059 DSN Progress Report for July–August 1972: Dual Carrier Preparations for Viking

D. A. Bathker and D. W. Brown

Technical Report 32-1526, Vol. XI, pp. 146–149,
October 15, 1972

For abstract, see Bathker, D. A.

BROWN, W. E., JR.

B060 Lunar Subsurface Exploration With Coherent Radar

W. E. Brown, Jr.

The Moon, Vol. 4, pp. 113–127, April 1972

The Apollo Lunar Sounder Experiment that is scheduled to orbit the Moon on Apollo 17 consists of a three-frequency coherent radar system and an optical recorder. The coherent radar can be used to measure both phase and amplitude characteristics of the radar echo. Measurement methods that are related to the phase and amplitude will be used to determine the surface profile, locate subsurface features, and ascertain near-surface electrical properties of the lunar surface. The key to the coherent radar measurement is a highly stable oscillator that preserves an accurate phase reference (2 or 3 electrical degrees) over a long period of time. This reference provides a means for reducing surface clutter so that subsurface features are more easily detected and also provides a means of measuring range to the surface to within a fraction of a wavelength.

BUCHANAN, H. R.

B061 DSN Progress Report for September–October 1972: X-Band Uplink Microwave Components

H. R. Buchanan

Technical Report 32-1526, Vol. XII, pp. 22–25, December 15, 1972

Waveguide components for use in the 400-kW X-band radar system will be electrically stressed to a considerably greater extent than previous Deep Space Instrumentation Facility equipment. The electrical characteristics of several possible waveguide sizes have been investigated. A size has been selected which offers an adequate safety margin for X-band radar and other possible X-band uplink applications.

BUECHLER, G.

B062 A Surface-Layer Representation of the Lunar Gravitational Field

L. Wong (Aerospace Corporation),
G. Buechler (Aerospace Corporation),
W. Downs (Aerospace Corporation), W. L. Sjogren,
P. M. Muller, and P. Gottlieb

J. Geophys. Res., Vol. 76, No. 26, pp. 6220–6236, September 10, 1971

For abstract, see Wong, L.

BURKE, E. S.

B063 DSN Progress Report for May–June 1972: DSN Telemetry Predicts Generation and Distribution

C. W. Harris and E. S. Burke

Technical Report 32-1526, Vol. X, pp. 210–212, August 15, 1972

For abstract, see Harris, C. W.

BUTMAN, S.

B064 DSN Progress Report for March–April 1972: On a Communications Strategy for Channels With Unknown Capacity

S. Butman

Technical Report 32-1526, Vol. IX, pp. 53–58, June 15, 1972

When the capacity of a channel cannot be determined in advance, or if it can change unpredictably, there is a problem in selecting the rate of transmission. On the one hand, a design for the worst case prevents recovery of large amounts of data when the situation is better than anticipated. On the other hand, a design based on optimistic assumptions is threatened by total failure when the conditions are bad. This article discusses a strategy that covers the in-between range of possibilities, and its implementation on Mariner-type telemetry systems. It is shown that large increases in expected data rate can be obtained at the cost of small reductions in the minimum rate. Final decisions are made on the ground after all the data are received.

B065 Interplex—An Efficient Multichannel PSK/PM Telemetry System

S. Butman and U. Timor

IEEE Trans. Commun., Vol. COM-20, No. 3, pp. 415–419, June 1972

This article describes a new phase-shift-keyed/phase-modulation (PSK/PM) scheme, called Interplex, which improves the performance of multichannel telemetry systems by reducing the cross-modulation loss. In the case of two-channel systems, the improvement in data power efficiency relative to a conventional system can be as much as 3 dB. A major feature of Interplex is that it can be implemented with very minor modification of existing conventional PSK/PM systems.

CAIN, D. L.

C001 Mariner 9 S-Band Martian Occultation Experiment: Initial Results on the Atmosphere and Topography of Mars

A. J. Kliore, D. L. Cain, G. Fjeldbo,
B. L. Seidel, and S. I. Rasool (National
Aeronautics and Space Administration)

Science, Vol. 175, No. 4019, pp. 313–317,
January 21, 1972

For abstract, see Kliore, A. J.

CAMERON, R. E.

C002   Surface Distribution of Microorganisms in Antarctic Dry-Valley Soils: A Martian Analog

R. E. Cameron, H. P. Conrow, D. R. Gensel,
G. H. Lacy, and F. A. Morelli

Antarctic J. U.S., Vol. VI, No. 5, pp. 211–213,
September–October 1971

Planners for future soft landings on Mars need to know whether a single soil sample taken near the point of landing is likely to be adequate for analysis and life detection or whether several samples taken at various locations would be better. A JPL project in the barren dry valleys of Antarctica is helping to resolve that problem and others related to Martian exploration.

Two Antarctic dry valleys, McKelvey Valley and Pearse Valley, were selected for systematic sampling of the surface 2 cm of soil to determine if a sterile soil could be found in a specified area of the dry valleys and to determine the distribution, abundance, and kinds of microorganisms present within a given area. This article presents the results of analyses performed on the soil samples.

C003   Isolation and Characterization of Keto-Carotenoids From the Neutral Extract of Algal Mat Communities of a Desert Soil

A. J. Bauman, H. G. Boettger, A. M. Kelly,
R. E. Cameron, and H. Yokoyama (U.S.
Department of Agriculture)

Eur. J. Biochem., Vol. 22, No. 2, pp. 287–293,
September 1971

For abstract, see Bauman, A. J.

C004   Farthest South Algae and Associated Bacteria

R. E. Cameron

Phycologia, Vol. 11, No. 2, pp. 133–139,
June 1972

A new record is reported for algae collected from the highest latitude, a frozen pond in the La Gorce Mountains, Antarctica (86°45'S, 146°00'W). Culturable algae included *Neochloris aquatica* Starr and *Schizothrix calcicola* (Ag.) Gom. *Porphyrosiphon Notarisii* (Menegh.) Kütz. was not recoverable in culture. Associated bacteria

were soil diphtheroids of the genus *Arthrobacter*. The occurrence of high latitude photosynthetic organisms is important in the search for possible extra-terrestrial life because environmental conditions, in some aspects, approach those of Mars.

C005   Microbiology of the Dry Valleys of Antarctica

N. H. Horowitz (California Institute of Technology),
R. E. Cameron, and J. S. Hubbard

Science, Vol. 176, No. 4032, pp. 242–245,
April 21, 1972

For abstract, see Horowitz, N. H.

CAMPBELL, J. D.

C006   DSN Progress Report for January–February 1972: Antenna Drive System Performance Evaluation Using PN Codes

R. M. Gosline, E. B. Jackson, and J. D. Campbell

Technical Report 32-1526, Vol. VIII, pp. 74–79,
April 15, 1972

For abstract, see Gosline, R. M.

CANNON, W. A.

C007   Fixation of Virgin Lunar Surface Soil

J. M. Conley, R. Frazer, and W. A. Cannon

Technical Memorandum 33-521, February 1, 1972

For abstract, see Conley, J. M.

C008   Physical Adsorption of Rare Gas on Terrigenous Sediments

F. P. Fanale and W. A. Cannon

Earth Planet. Sci. Lett., Vol. 11, No. 5,
pp. 362–368, August 1971

For abstract, see Fanale, F. P.

C009   Origin of Planetary Primordial Rare Gas: The Possible Role of Adsorption

F. P. Fanale and W. A. Cannon

Geochim. Cosmochim. Acta, Vol. 36, No. 3,
pp. 319–328, March 1972

For abstract, see Fanale, F. P.

CANNOVA, R. D.

C010   Development and Testing of the Propulsion Subsystem for the Mariner Mars 1971 Spacecraft

R. D. Cannova, et al.

Technical Memorandum 33-552, August 1, 1972

In November 1971, the Mariner 9 spacecraft was injected into Mars orbit by a 574-kg (1265-lbm) propulsion system. Design of that system provided for a directed impulse, upon command, to accomplish in-transit trajectory corrections, an orbit-insertion maneuver at encounter to transfer from a flyby to an orbital trajectory about Mars, and a subsequent trim maneuver.

The propulsion system is an integrated, pressure-fed, multi-start, fixed-thrust, storable bipropellant system. The primary subassemblies are a propellant feed system, a 1334-N (300-lbf) thrust rocket engine assembly, and the propulsion module structure. The subsystem was capable of being fueled, pressurized, and monitored before installation on the spacecraft.

This document describes the design, testing, fabrication, and problems associated with the development of the Mariner 9 propulsion system. Also covered are the design and operation of the associated ground support equipment used to test and service the propulsion system.

C011 Development and In-Flight Performance of the Mariner 9 Spacecraft Propulsion System

D. D. Evans, R. D. Cannova, and M. J. Cork

Technical Memorandum 33-574, November 1, 1972

For abstract, see Evans, D. D.

CARON, L. G.

C012 Bernal Model: A Simple Equilibrium Theory of Close-Packed Liquids

L. G. Caron

J. Chem. Phys., Vol. 55, No. 11, pp. 5227–5232, December 1, 1971

The Bernal model of a hard-sphere liquid is used in conjunction with an extension of the cell method to predict the behavior of liquid argon near melting. The entropy of disorder associated with the Bernal state is deduced. The model is found to be applicable to liquid metals.

C013 Electron Correlations at Large Densities

L. G. Caron

Phys. Rev., Pt. B: Solid State, Vol. 5, No. 1, pp. 238–240, January 1, 1972

In two papers, Singwi, et al., presented a self-consistent scheme to calculate the dielectric function of an electron gas at metallic densities. An improvement made to obtain results that better satisfied the compressibility sum

rules was presented in the second paper; this improvement, however, led to a great increase in computational time. In an attempt to reduce this time and yet retain the improved features of the dielectric function, an approximate scheme for numerical calculation of the dielectric function of an electron gas in the theory of Singwi, et al., was formulated. This scheme and the numerical results of its application are presented in this article.

C014 Quantum Crystals in the Single-Particle Picture

L. G. Caron

Phys. Rev., Pt. B: Solid State, Vol. 6, No. 4, pp. 1081–1090, August 15, 1972

This article presents a low-temperature formalism for quantum crystals based on the localized-single-particle picture. A proposed transcription to a quasiparticle space provides the basis for an easily accessible thermal analysis and yields correlation and lifetime information. The excitations are shown to be the same as Werthamer's. The effect of wave-function overlap and its impact on magnetism are discussed and the defect crystal is examined.

CARRAWAY, J. B.

C015 Miniature Biotelemeter Gives Multichannel Wideband Biomedical Data

J. B. Carraway

JPL Quarterly Technical Review, Vol. 2, No. 1, pp. 152–166, April 1972

Doctors and biologists have expressed a need for the capability to monitor vital physiological functions from human and animal subjects unrestrained by wires. JPL has responded under NASA Technology Applications Office sponsorship by developing an advanced device suitable for a wide variety of medical and biological research applications. The design of this miniature, 12-cm^3, 10-channel, wideband (5-kHz/channel), pulse-amplitude-modulation/frequency-modulation biotelemeter takes advantage of modern device technology (e.g., integrated-circuit operational amplifiers, complementary-symmetry metal oxide semiconductor logic, and solid-state switches) and hybrid packaging techniques. The telemeter is currently being used for monitoring 10 channels of neuron firings from specific regions of the brains in rats implanted with chronic electrodes. Possible follow-on applications include multichannel telemetry of electroencephalograms, electrocardiograms, electromyograms, state functions, and dynamic processes such as blood flow and body chemistry. The design, fabrication, and testing of an engineering-model biotelemeter are described in this article.

CARROLL, W. F.

C016 Discoloration and Lunar Dust Contamination of Surveyor III Surfaces

W. F. Carroll and P. M. Blair (Hughes Aircraft Corporation)

Proceedings of the Second Lunar Science Conference, Houston, Texas, January 11–14, 1971, Vol. 3, pp. 2735–2742, The M.I.T. Press, Cambridge, 1971

As discussed in this article, the discoloration of Surveyor 3 surfaces observed by the Apollo 12 astronauts during their examination of the spacecraft on the Moon and clearly evident on the returned hardware has been analyzed and shown to be due to expected radiation darkening and a heavier-than-expected layer of lunar fines. Lunar surface material disturbed by the Apollo 12 lunar module (LM) landing 155 m away reached the Surveyor spacecraft and produced significant changes in its surfaces.

CASSON, D.

C017 Solution Properties of Novel Polyelectrolytes

D. Casson and A. Rembaum

Macromolecules, Vol. 5, No. 1, pp. 75–81, January–February 1972

A series of polyelectrolytes, of different molecular weights, with the unit segment structure

$$\left[\begin{array}{c} CH_3 Z^- \\ | \\ -N^+ \!\!-\!\!-\!\!-(CH_2)_x\!\!-\!\!N^+ \!\!-\!\!-\!\!-(CH_2)_y\!\!-\!\! \\ | \\ CH_3 \end{array} \begin{array}{c} CH_3 Z^- \\ | \\ \\ | \\ CH_3 \end{array} \right]_n$$
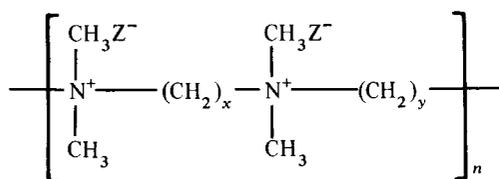
were synthesized through the Menschutkin reaction and are referred to as ionene polymers. The solution properties of a high-charge-density ionene polymer (3,4 Br, $x = 3$, $y = 4$, $Z = Br$) were compared with those of an ionene polymer in which the positive charges are separated by six CH_2 groups (6,6 Br, $x = 6$, $y = 6$, $Z = Br$). These polyelectrolytes, when dissolved in aqueous 0.4 M KBr, were found to approximate the behavior of conventional polymers. The intrinsic viscosity–molecular weight relationship in aqueous 0.4 M KBr was determined for 3,4 Br and 6,6 Br by means of the light-scattering technique and can be expressed by

$$[\eta]_{3,4\ Br} = (2.94 \times 10^{-4}) M^{0.61}$$

$$[\eta]_{6,6\ Br} = (6.22 \times 10^{-4}) M^{0.58}$$

A viscosity study as a function of concentration of a number of potassium salts in water revealed that the reduced viscosity of a 6,6 Br increases as the anions change in the following order: $CNS^- < I^- < NO_3^- < Br^- < Cl^- < F^-$. This trend is attributed to a parallel decrease of counterion site binding. In the absence of added salts, the viscosity behavior is adequately represented by the Fuoss equation.

CHADWICK, H. D.

C018 A Markov Chain Technique for Determining the Acquisition Behavior of a Digital Tracking Loop

H. D. Chadwick

JPL Quarterly Technical Review, Vol. 1, No. 4, pp. 49–57, January 1972

Tracking loops have two characteristic modes of operation: acquisition and steady-state tracking. The steady-state behavior of such nonlinear tracking loops as the phase-locked loop has been the subject of considerable analysis. The acquisition behavior of a loop, the transition period between turning the loop on and the steady state, has resisted analysis for all but the simplest configurations. An iterative procedure is presented for determining the acquisition behavior of discrete or digital implementations of the tracking loop. The technique is based on the theory of Markov chains and provides the cumulative probability of acquisition in the loop as a function of time in the presence of noise and a given set of initial condition probabilities. A digital second-order tracking loop to be used in the Viking command receiver for continuous tracking of the command subcarrier phase has been analyzed using this technique, and the results agree closely with experimental data.

C019 The Error Probability of a Wide-Band FSK Receiver in the Presence of Multipath Fading

H. D. Chadwick

IEEE Trans. Commun., Vol. COM-19, No. 5, pp. 699–707, October 1971

Calculations are made for the probability of error of a wide-band FSK (frequency-shift-keyed) receiver of the type used in space telemetry when multipath reflections off the planetary surface cause signal fading. The error probability is found for both low and high fading bandwidths and for small or large reflected path delays.

C020 Binary Single-Sideband Phase-Modulated Communication Systems

H. D. Chadwick

IEEE Trans. Inform. Theor., Vol. IT-18, No. 1, pp. 214–215, January 1972

Single-sideband phase modulation, in which a signal is simultaneously phase- and amplitude-modulated by a signal and its Hilbert transform, is shown to be suboptimum for binary signaling in white gaussian noise. An alternative single-sideband technique based on the properties of binary suppressed-carrier phase modulation is proposed and shown to give performance equivalent to the double-sideband version.

CHAHINE, M. T.

C021 A General Relaxation Method for Inverse Solution of the Full Radiative Transfer Equation

M. T. Chahine

J. Atmos. Sci., Vol. 29, No. 4, pp. 741–747, May 1972

The relaxation method for the inverse solution of the full radiative transfer equation is generalized to solve for all atmospheric parameters which appear in the integrand as functions or functionals, without any *a priori* information related to the expected solution. The method is illustrated by examples in the Earth's atmosphere for the determination of water vapor mixing ratio profiles from observations in the 6.3-μ band.

CHAN, S. I.

C022 Ferromagnetic Resonance of Lunar Samples

F.-D. Tsay (California Institute of Technology), S. I. Chan (California Institute of Technology), and S. L. Manatt

Geochim. Cosmochim. Acta, Vol. 35, No. 9, pp. 865–875, September 1971

For abstract, see Tsay, F.-D.

C023 Electron Paramagnetic Resonance of Radiation Damage in a Lunar Rock

F.-D. Tsay, S. I. Chan, and S. L. Manatt

Nature Phys. Sci., Vol. 237, No. 77, pp. 121–122, June 19, 1972

For abstract, see Tsay, F.-D.

C024 Magnetic Resonance Studies of Apollo 11 and Apollo 12 Samples

F.-D. Tsay (California Institute of Technology), S. I. Chan (California Institute of Technology), and S. L. Manatt

Proceedings of the Second Lunar Science Conference, Houston, Texas, January 11–14, 1971, Vol. 3, pp. 2515–2528, The M.I.T. Press, Cambridge, 1971

For abstract, see Tsay, F.-D.

CHANEY, W. D.

C025 DSN Progress Report for January–February 1972: DSN Tracking System: Operation With the Mutual Stations

W. D. Chaney and H. E. Nance

Technical Report 32-1526, Vol. VIII, pp. 5–7, April 15, 1972

Two types of 26-m-antenna tracking stations are available to the DSN for spacecraft tracking. Pioneer F will be supported primarily by the Mutual stations (combined DSN and Spaceflight Tracking and Data Network equipment). This article describes in some detail the various functions performed by the Mutual station tracking system and compares the system equipment and functions with those of the standard DSN tracking station. The operational capabilities and interfaces between the modules within the station are presented in a logical sequence, with the final output interfacing with the Ground Communications Facility and the Space Flight Operations Facility.

CHAPMAN, A. K.

C026 DSN Progress Report for November–December 1971: Apollo Bistatic Radar Investigation

A. K. Chapman

Technical Report 32-1526, Vol. VII, pp. 190–194, February 15, 1972

The first bistatic Moon radar experiments were conducted by the Stanford Center for Radar Astronomy, using Lunar Orbiter spacecraft. Apollo not only provides stronger signals, but provides for conduct of the experiment on two frequency bands. The JPL 64-m-diameter tracking antenna at Goldstone is uniquely suited to the reception of the S-band signals involved, and has been used on both Apollo 14 and Apollo 15 for the bistatic investigation.

CHASE, S. C., JR.

C027 **Mariner 1969 Infrared Radiometer Results: Temperatures and Thermal Properties of the Martian Surface**

G. Neugebauer (California Institute of Technology),
G. Münch (California Institute of Technology),
H. Kieffer (University of California, Los Angeles),
S. C. Chase, Jr. (Santa Barbara Research Center),
and E. Miner

Astron. J., Vol. 76, No. 8, pp. 719–749,
October 1971

For abstract, see Neugebauer, G.

C028 **Infrared Radiometry Experiment on Mariner 9**

S. C. Chase, Jr. (Santa Barbara Research Center),
H. Hatzenbeler (Santa Barbara Research Center),
H. Kieffer (University of California, Los Angeles),
E. Miner, G. Münch (California Institute of
Technology), and G. Neugebauer (California
Institute of Technology)

Science, Vol. 175, No. 4019, pp. 308–309,
January 21, 1972

The brightness temperatures at 10 and 20 μm measured by the Mariner 9 infrared radiometer differ substantially from those predicted by the radiometer results of Mariners 6 and 7. The results indicate a significant latitude-dependent contribution of the atmospheric dust to the observed thermal emission.

CHELSON, P. O.

C029 **Failure-Rate Computations Based on Mariner Mars 1969 Spacecraft Data**

P. O. Chelson

Technical Report 32-1544, December 1, 1971

This report describes an analysis of in-flight spacecraft part hours and failure data from the Mariner Mars 1969 Project. It contains failure rates computed from these data for all electronic and electromagnetic parts on the Mariner 6 and 7 spacecraft. Also included are failure rates based on combining flight data from Mariners 4 through 7.

CHEN, C. J.

C030 **Raman Scattering Cross Section for N_2O_4**

C. J. Chen and F. Wu (State University of New York, Buffalo)

Appl. Phys. Lett., Vol. 19, No. 11, pp. 452–453,
December 1, 1971

As reported in this article, the Raman scattering cross section for N_2O_4 at a Raman shift of 1360 cm^{-1} has been measured by using a Q-switched ruby laser as an excitation source. The cross section for N_2 at a Raman shift of 2330 cm^{-1} has also been measured. The latter measurement is compared with a previous measurement reported elsewhere, and the result is normalized to the wavelength.

CHEUNG, C. S.

C031 **Calculations of Geometries of Organic Molecules Using the CNDO/2 Method: I. Empirical Correlations Between Observed and Calculated Bond Lengths in Simple Acyclics, Strained Cycloalkenes and Some Polycyclic Molecules**

C. S. Cheung, M. A. Cooper, and S. L. Manatt

Tetrahedron, Vol. 27, No. 4, pp. 689–700,
February 1971

In this article, it is shown that calculations of C—C and C—H bond lengths in hydrocarbons using the CNDO/2 semi-empirical MO method exhibit systematic deviations from the observed values. An empirical correlation relating the observed and calculated bond lengths with the number of substituents attached to the bond may be devised. This correlation is capable of providing theoretical bond lengths within 0.008 Å of the experimental for a wide range of simple acyclic molecules. Furthermore, calculations of molecular geometries for some strained cycloalkenes and also some larger molecules, e.g., naphthalene, biphenylene, and azulene, are similarly found to be in good agreement with experiment.

C032 **Calculations of Geometries of Organic Molecules Using the CNDO/2 Molecular Orbital Method: II. Structural Predictions for the Benzocycloalkenes, and a Theoretical Rationalization of Their Proton–Proton Spin–Spin Coupling Constants**

C. S. Cheung, M. A. Cooper, and S. L. Manatt

Tetrahedron, Vol. 27, No. 4, pp. 701–709,
February 1971

In this article, the CNDO/2 semiempirical MO method is applied to calculations of the geometries of some strained benzocycloalkenes. The strain-induced bond-length distortions predicted are in disagreement with earlier work, although the lack of accurate experimental data precludes a decision as to the validity of either treatment. The CNDO/2 wavefunctions are examined for features which may throw light on previous qualitative descriptions which have been proposed to account for recent experimental data on this series, such as nu-

clear-magnetic-resonance and electron-spin-resonance spectra, and rates of electrophilic substitution. In particular, trends in the proton–proton spin–spin coupling constants in the benzocycloalkenes and also benzene, naphthalene, and biphenylene are well-accounted-for by the CNDO/2 wavefunctions.

CHIRIVELLA, J. E.

C033 Small Rocket Exhaust Plume Data

J. E. Chirivella, P. I. Moynihan, and W. Simon

JPL Quarterly Technical Review, Vol. 2, No. 2, pp. 90–99, July 1972

During recent cryodeposit tests with an 0.18-N (0.04-lbf) thruster in the JPL Molsink facility, the mass flux in the plume back field was measured for the first time for nitrogen, carbon dioxide, and a mixture of nitrogen, hydrogen, and ammonia at various inlet pressures. This mixture simulated gases that would be generated by a hydrazine-plenum attitude propulsion system. The measurements furnish a base upon which to build a mathematical model of plume back flow that will be used in predicting the mass distribution in the boundary region of other plumes. The results are analyzed and compared with existing analytical predictions.

CHITTY, W. H.

C034 Development and Testing of the Flight Command Subsystem for the Mariner Mars 1971 Spacecraft

W. H. Chitty

Technical Memorandum 33-531, March 15, 1972

The flight command subsystem for the Mariner Mars 1971 spacecraft is of the same basic design and construction as that for the Mariner Mars 1969 spacecraft, except for its expanded capability. Its primary purpose is to provide remote control for the spacecraft. This memorandum briefly describes the design changes, fabrication, and significant problems associated with the development of the Mariner Mars 1971 flight command subsystem.

CHRISTENSEN, E. J.

C035 Mariner 9 Celestial Mechanics Experiment: Gravity Field and Pole Direction of Mars

J. Lorell, G. H. Born, E. J. Christensen, J. F. Jordan, P. A. Laing, W. Martin, W. L. Sjogren, I. I. Shapiro (Massachusetts Institute of Technology), R. D. Reasenberg (Massachusetts Institute of Technology), and G. L. Slater (Massachusetts Institute of Technology)

Science, Vol. 175, No. 4019, pp. 317–320, January 21, 1972

For abstract, see Lorell, J.

CLAUSS, R. C.

C036 DSN Progress Report for March–April 1972: Low Noise Receivers: Microwave Maser Development

R. C. Clauss and R. B. Quinn

Technical Report 32-1526, Vol. IX, pp. 128–136, June 15, 1972

Microwave maser amplifiers have been used by JPL in the DSN for 12 yr. Pump-frequency requirements have been met mainly with reflex klystron oscillators. Other microwave-power sources have been tested for use as maser pump sources. Successful performance tests have been achieved with backward-wave oscillators, crystal-controlled oscillators using solid-state multipliers, impatt oscillators, and an impatt noise generator. Current maser pump source requirements have a frequency range of 12.5 to 45 GHz. Power required is approximately 150 mW. Cost, availability, reliability, frequency and power stability, tunability, and power-requirement considerations have resulted in the use of klystrons as pump sources for all maser amplifiers now operating in the DSN.

C037 DSN Progress Report for July–August 1972: Low Noise Receivers: Microwave Maser Development

R. C. Clauss, E. Wiebe, and R. B. Quinn

Technical Report 32-1526, Vol. XI, pp. 71–80, October 15, 1972

A traveling-wave maser, tunable from 7750 to 8750 MHz, has been completed and tested in the laboratory. The maser is ready for installation on the 64-m-diameter antenna at the Deep Space Communications Complex at Goldstone, California. Gain, phase, and group-delay stability were measured as a function of magnetic field, refrigerator temperature, power-supply voltages, and large interfering signals. Several features have been included in this maser to improve the stability performance. A superconducting magnet provides a very stable magnetic field. Push–push pumping results in complete pump saturation and reduced pump frequency-stability

requirements. Low-pass filters at a temperature of 4.5 K reduce pump power radiation in signal waveguides.

The maser has a 45-dB net gain and a 17-MHz, 3-dB bandwidth with an equivalent input noise temperature of 6.5 K at 8415 MHz and 8.5 K at 7850 MHz. Simultaneous operation at two frequencies, separated by up to 500 MHz, is available at reduced gain.

C038 **DSN Progress Report for September–October 1972: Improved RF Calibration Techniques—A Practical Technique for Accurate Determination of Microwave Surface Resistivity**

R. C. Clauss and P. D. Potter

Technical Report 32-1526, Vol. XII, pp. 59–67, December 15, 1972

This article describes a surface-loss measurement technique using a TE_{011}-mode circular-waveguide cavity resonator. A novel feature of this technique is the use of a standard cavity, with a test sample (a flat plate) forming one of the end walls of the cavity. The unique properties of this cavity eliminate the need for intimate contact between the test surface and the rest of the cavity; a surface contact problem is thereby avoided.

Precision Q-measurement equipment is required for this technique. Formulas for the surface resistivity of the sample as a function of the measured cavity Q are derived. Preliminary test data are presented and compared with predicted values, where available. The method described in this article appears to have a wide range of applicability.

CLAYTON, R. M.

C039 **Stability Evaluation of a Rocket Engine for Gaseous Oxygen Difluoride (OF_2) and Gaseous Diborane (B_2H_6) Propellants**

R. M. Clayton

Technical Report 32-1561, August 15, 1972

Results of an experimental evaluation of the dynamic stability of a candidate combustor for the space-storable propellants gaseous OF_2/B_2H_6 show that the combustor is unstable without supplementary damping. An analysis using a JPL computer program (TRDL) indicated that the uninhibited engine could be unstable. The experiments, conducted with O_2/C_2H_4 substitute propellants and with 70-30 FLOX/B_2H_6 (OF_2 simulated with FLOX), show that the uninhibited combustor has a low stability margin to starting-transient perturbations, but that it is relatively insensitive to bomb disturbances. Damping cavities are shown to provide stability.

CLEMENTS, P. A.

C040 **DSN Progress Report for November–December 1971: Electrical Length Stability of Coaxial Cable in a Field Environment**

P. A. Clements

Technical Report 32-1526, Vol. VII, pp. 97–100, February 15, 1972

Various environmental conditions will cause a coaxial cable to change electrical length. In the past, the effects of these changes were not important; however, recent requirements for future DSS accuracies have forced their consideration. Preliminary studies on the effects due to temperature changes and mechanical stress have been made. Results to date indicate some problem areas.

COFFIN, R. C.

C041 **DSN Progress Report for March–April 1972: Firmware Control of Block IV Ranging Demodulator Assembly**

R. C. Coffin

Technical Report 32-1526, Vol. IX, pp. 188–195, June 15, 1972

The Mark III Data System Development Plan is encouraging engineers designing equipment for use in the DSN to utilize computer control and monitoring. It is becoming apparent that the difficulty of development and the cost of software are prohibitive. A concept called firmware is proposed. Firmware is a design concept which directs the engineer to employ special-purpose digital and/or analog circuitry whenever possible to reduce software or interface requirements. The ranging demodulator assembly (RDA) is being developed under the firmware concept. By employing firmware, the RDA interface and software requirements have been kept to a minimum. The phase calibration of the RDA is achieved with a single switch or one-line command from the computer. Monitoring is handled by the firmware, which supplies one line to the computer indicating the operability of the RDA.

CONEL, J. E.

C042 **Microwave Emission From Geological Materials: Observations of Interference Effects**

J. C. Blinn III, J. E. Conel, and J. G. Quade (University of Nevada)

J. Geophys. Res., Vol. 77, No. 23, pp. 4366–4378, August 10, 1972

For abstract, see Blinn, J. C., III

C043 **Luminescence and Reflectance of Apollo 12 Samples**

D. B. Nash and J. E. Conel

*Proceedings of the Second Lunar Science
Conference, Houston, Texas, January 11–14, 1971,*
Vol. 3, pp. 2235–2244, The M.I.T. Press,
Cambridge, 1971

For abstract, see Nash, D. B.

C044 **Objectives and Requirements of Unmanned Rover
Exploration of the Moon**

D. B. Nash, J. E. Conel, and F. P. Fanale

The Moon, Vol. 3, No. 2, pp. 221–230,
August 1971

For abstract, see Nash, D. B.

CONLEY, J. M.

C045 **Fixation of Virgin Lunar Surface Soil**

J. M. Conley, R. Frazer, and W. A. Cannon

Technical Memorandum 33-521, February 1, 1972

Two systems have been shown to be suitable for fixing
loose particulate soils with a polymer film without visu-
ally detectable disturbance of the soil particle spatial
relationships. A two-component system uses a gas mono-
mer condensible at the soil temperature and a gas-phase
catalyst acting to polymerize the monomer. A one-com-
ponent system uses a monomer which polymerizes spon-
taneously on and within the top few millimeters of the
soil.

The two-component system may result in a simpler appa-
ratus, but has been demonstrated to operate over a
narrower temperature range, i.e., approximately −40 to
−10°C. Other two-component polymer systems have
been identified which may operate at soil temperatures
as high as +100°C, but still over relatively narrow
temperature ranges of approximately 30°C. The one-
component system has been demonstrated to operate
successfully with initial soil temperatures from −70°C or
lower to +150°C.

CONNES, J.

C046 **Fourier Spectroscopy With a One-Million-Point
Transformation (Translation From the Original
Published in the Nouvelle Revue d'Optique
Appliquée, Vol. 1, pp. 3–22, 1970)**

J. Connes (National Center for Scientific Research,
Orsay, France), H. Delouis (National Center for
Scientific Research, Orsay, France),
P. Connes (National Center for Scientific Research,
Orsay, France), G. Guelachvili (National Center for
Scientific Research, Orsay, France),
J.-P. Maillard (National Center for Scientific
Research, Orsay, France), and G. Michel (National
Center for Scientific Research, Orsay, France)

Technical Memorandum 33-525, March 15, 1972

A new type of interferometer for use in Fourier spectros-
copy has been devised at the Aimé Cotton Laboratory of
the National Center for Scientific Research (CNRS), Or-
say, France. With this interferometer and with computa-
tional techniques developed by the Regional Interdisci-
plinary Center for Electronic Calculation (CIRCE) at the
CNRS, interferograms comprising as many as 10^6 sam-
ples can now be transformed. The techniques are de-
scribed, and examples of spectra of thorium and hol-
mium, derived from 10^6-point interferograms, are pre-
sented in this paper, which was translated by R. Beer of
JPL.

CONNES, P.

C047 **Fourier Spectroscopy With a One-Million-Point
Transformation (Translation From the Original
Published in the Nouvelle Revue d'Optique
Appliquée, Vol. 1, pp. 3–22, 1970)**

J. Connes (National Center for Scientific Research,
Orsay, France), H. Delouis (National Center for
Scientific Research, Orsay, France),
P. Connes (National Center for Scientific Research,
Orsay, France), G. Guelachvili (National Center for
Scientific Research, Orsay, France),
J.-P. Maillard (National Center for Scientific
Research, Orsay, France), and G. Michel (National
Center for Scientific Research, Orsay, France)

Technical Memorandum 33-525, March 15, 1972

For abstract, see Connes, J.

CONRATH, B. J.

C048 **Infrared Spectroscopy Experiment on the Mariner 9
Mission: Preliminary Results**

R. A. Hanel (Goddard Space Flight Center),
B. J. Conrath (Goddard Space Flight Center),
W. A. Hovis (Goddard Space Flight Center),
V. G. Kunde (Goddard Space Flight Center),
P. D. Lowman (Goddard Space Flight Center),
J. C. Pearl (Goddard Space Flight Center),
C. Prabhakara (Goddard Space Flight Center),
B. Schlachman (Goddard Space Flight Center), and
G. V. Levin (Biospherics Incorporated)

Science, Vol. 175, No. 4019, pp. 305–308,
January 21, 1972

For abstract, see Hanel, R. A.

CONROW, H. P.

C049 **Surface Distribution of Microorganisms in Antarctic Dry-Valley Soils: A Martian Analog**

R. E. Cameron, H. P. Conrow, D. R. Gensel,
G. H. Lacy, and F. A. Morelli

Antarctic J. U.S., Vol. VI, No. 5, pp. 211–213,
September–October 1971

For abstract, see Cameron, R. E.

CONSTENLA, L. C.

C050 **DSN Progress Report for September–October 1972: Complex Mixer System**

L. C. Constenla

Technical Report 32-1526, Vol. XII, pp. 189–194,
December 15, 1972

The complex-mixer system is a signal preconditioner for a Fast-Fourier-Transform power-spectrum analyzer. It generates a complex time-series output of the real-valued time series fed to its input. Two complex mixers have been constructed and installed at the Mars Deep Space Station (DSS 14). They have processed signals received from the Mariner 1971 spacecraft to investigate induced cross polarization of signals passing close to the solar corona.

COOPER, B. M.

C051 **DSN Progress Report for July–August 1972: NASTRAN Data Generation and Management Using Interactive Graphics**

M. S. Katow and B. M. Cooper

Technical Report 32-1526, Vol. XI, pp. 104–110,
October 15, 1972

For abstract, see Katow, M. S.

COOPER, M. A.

C052 **Calculations of Geometries of Organic Molecules Using the CNDO/2 Method: I. Empirical Correlations Between Observed and Calculated Bond Lengths in Simple Acyclics, Strained Cycloalkenes and Some Polycyclic Molecules**

C. S. Cheung, M. A. Cooper, and S. L. Manatt

Tetrahedron, Vol. 27, No. 4, pp. 689–700,
February 1971

For abstract, see Cheung, C. S.

C053 **Calculations of Geometries of Organic Molecules Using the CNDO/2 Molecular Orbital Method: II. Structural Predictions for the Benzocycloalkenes, and a Theoretical Rationalization of Their Proton–Proton Spin–Spin Coupling Constants**

C. S. Cheung, M. A. Cooper, and S. L. Manatt

Tetrahedron, Vol. 27, No. 4, pp. 701–709,
February 1971

For abstract, see Cheung, C. S.

CORK, M. J.

C054 **Development and In-Flight Performance of the Mariner 9 Spacecraft Propulsion System**

D. D. Evans, R. D. Cannova, and M. J. Cork

Technical Memorandum 33-574, November 1, 1972

For abstract, see Evans, D. D.

C055 **Mariner 9 Propulsion Subsystem Performance During Interplanetary Cruise and Mars Orbit Insertion**

M. J. Cork, R. L. French, C. J. Leising, and
D. D. Schmit

JPL Quarterly Technical Review, Vol. 2, No. 1,
pp. 113–122, April 1972

On November 14, 1971, the Mariner 9 1334-N (300-lbf) thrust rocket engine was fired for just over 15 min to place a man-made satellite into orbit about another planet for the first time. Propulsion subsystem data gathered during the 5-mo interplanetary cruise and the orbit insertion are of significance to future missions of this type. Specific results related to performance predictability; zero-g heat transfer; and nitrogen permeation, diffusion, and solubility values are presented.

COSTOGUE, E. N.

CO56 Integration of a Breadboard Power Conditioner With a 20-cm Ion Thruster

T. D. Masek, T. W. Macie, E. N. Costogue,
W. J. Muldoon (Hughes Aircraft Company),
D. R. Garth (Hughes Aircraft Company), and
G. C. Benson (Hughes Aircraft Company)

J. Spacecraft Rockets, Vol. 9, No. 2, pp. 71–78,
February 1972

For abstract, see Masek, T. D.

COULBERT, C. D.

CO57 Survey of Materials for Hydrazine Propulsion Systems in Multicycle Extended Life Applications

C. D. Coulbert and G. Yankura

Technical Memorandum 33-561,
September 15, 1972

This report presents an assessment of materials-compatibility data for hydrazine monopropellant propulsion systems applicable to the Space Shuttle vehicle missions. Materials were evaluated for application over a 10-yr/ 100-mission operational lifetime with minimum refurbishment. A general materials-compatibility rating for a broad range of materials and several propellants based primarily on static liquid propellant immersion testing and an in-depth evaluation of hydrazine decomposition as a function of purity, temperature, material, surface conditions, etc., are presented.

The most promising polymeric material candidates for propellant diaphragms and seals appear to have little effect on increasing hydrazine decomposition rates, but the materials themselves do undergo changes in physical properties which can affect their 10-yr performance in multicycle applications. The available data on these physical properties of elastomeric materials such as EPT-10 and AF-E-332 as affected by exposure to hydrazine or related environments is presented.

The data in this report provides a basis for the preliminary selection of propulsion-system materials. The results of system and component long-term compatibility studies currently being conducted by the Air Force, Martin-Marietta, JPL, and others plus the completion of studies recommended in this report will enable the prediction of 10-yr multicycle performance of the selected materials.

CRAWFORD, W. E.

CO58 Digital Canopus Tracker Digital Electronics

W. E. Crawford

Technical Report 32-1559, July 1, 1972

Circuitry has been developed for digital control of the Canopus tracker. A feasibility and demonstration breadboard has been constructed using microelectronic integrated circuits. The breadboard contains the digital circuits necessary for closed-loop electro-optical control of the tracker. Also included in the breadboard is the digital logic necessary for star acquisition, particle rejection, programmable gate selection, cone angle selection, and routing of the digital roll error signal.

CROW, R. B.

CO59 DSN Progress Report for May–June 1972: S-Band Receiver Third-Order Loop Demonstration

R. B. Crow

Technical Report 32-1526, Vol. X, pp. 168–171,
August 15, 1972

In mid-April 1972, the Mariner Mars 1971 spacecraft began encountering high doppler rates under weak signal conditions. The Block III receiver was dropping lock, resulting in lost data. This article describes a third-order tracking filter which was designed for the Block III receiver and successfully demonstrated at the Mars Deep Space Station (DSS 14).

CUDDIHY, E. F.

CO60 Lifetime Estimates for Sterilizable Silver–Zinc Battery Separators

E. F. Cuddihy, D. E. Walmsley, and J. Moacanin

JPL Quarterly Technical Review, Vol. 2, No. 1,
pp. 72–81, April 1972

The lifetime of the current separator membrane in the electrolyte environment of JPL silver–zinc batteries has been estimated at 3 to 5 yr. The separator membranes are crosslinked polyethylene film containing grafted poly(potassium acrylate) (PKA), the latter being the hydrophilic agent which promotes electrolyte ion transport. The lifetime was estimated by monitoring the rate of loss of PKA from the separators, caused by chemical attack of the electrolyte, and relating this loss rate to a known relationship between battery performance and PKA concentration in the separators.

CO61 Analysis of the Failure of a Polyester Peripheral Drive Belt on the Mariner Mars 1971 Flight Tape Recorder

E. F. Cuddihy

JPL Quarterly Technical Review, Vol. 2, No. 1,
pp. 82–99, April 1972

A polyester peripheral drive belt on the Mariner Mars 1971 flight tape recorder failed when a thin longitudinal strip separated off along one edge. Analysis showed that the most probable cause of failure occurred from flexural fatigue initiating in mechanically weak locations introduced into the belt during fabrication. Also, methyl ethyl ketone (MEK), which is employed as a cleaning solvent during fabrication, was found to cause permanent degradation of engineering properties of polyester and could have contributed to the reduction of the fatigue resistance. This article reviews fatigue properties of the polyester drive belt for the specific operating condition, as well as the sensitivity of polyester to cleaning solvents and the origin of the mechanically weak locations introduced during fabrication.

C062   **Fatigue of Teflon Bladder Materials**

E. F. Cuddihy

J. Appl. Polym. Sci., Vol. 15, No. 12,
pp. 3101–3108, December 1971

The fatigue properties of Teflon laminates employed in the fabrication of liquid propellant expulsion bladders were studied by cyclically stretching specimens to constant load in order to achieve a correlation of cycles to failure versus the maximum stress amplitude. This approach provides a useful technique for evaluating the resistance of bladder materials to fatigue failure which could be caused by vibration-induced cyclic loadings during ground testing and launch. Further, the data provides for a direct comparison of the relative fatigue properties of Teflon laminates and, in particular for those which were studied, the relative fatigue properties correlated with their ultimate breaking stresses. This observation, which suggests a simple and rapid method for evaluating relative fatigue behavior of candidate Teflon laminates, is discussed along with the effect of delamination on the fatigue properties observed for one laminate.

CUFFEL, R. F.

C063   **Viscous Slipstream Flow Downstream of a Centerline Mach Reflection**

L. H. Back and R. F. Cuffel

AIAA J., Vol. 9, No. 10, pp. 2107–2109,
October 1971

For abstract, see Back, L. H.

C064   **Influence of Contraction Section Shape and Inlet Flow Direction on Supersonic Nozzle Flow and Performance**

L. H. Back, R. F. Cuffel, and P. F. Massier

J. Spacecraft Rockets, Vol. 9, No. 6, pp. 420–427,
June 1972

For abstract, see Back, L. H.

C065   **Turbulent Boundary Layer and Heat Transfer Measurements Along a Convergent-Divergent Nozzle**

L. H. Back and R. F. Cuffel

Trans. ASME, Ser. C: J. Heat Transf., Vol. 93,
No. 4, pp. 397–407, November 1971

For abstract, see Back, L. H.

CURKENDALL, D. W.

C066   **DSN Progress Report for January–February 1972: On Modeling Continuous Accelerations as Piecewise Constant Functions**

R. K. Russell and D. W. Curkendall

Technical Report 32-1526, Vol. VIII, pp. 45–52,
April 15, 1972

For abstract, see Russell, R. K.

CURTRIGHT, J.

C067   **DSN Progress Report for January–February 1972: DSN Frequency and Time Scale Change From UTC to IAT or New UTC**

J. Curtright

Technical Report 32-1526, Vol. VIII, pp. 127–130,
April 15, 1972

By international agreement, the Universal Time, Coordinated (UTC) time scale was changed to parallel that of the atomic (A.1) scale. The new time scale is called New UTC 1972 or International Atomic Time (IAT). This change in time scale made it necessary to change the frequency and time standards at all Deep Space Instrumentation Facility stations. The existing offset of UTC from A.1 time was removed from the oscillators, and all clocks were retarded approximately 107,600 μsec. This article covers the background material leading to the change, problems dealt with during the planning for it, and the procedures used to implement the change.

DALLAS, S. S.

D001   **DSN Progress Report for November–December 1971: A Comparison of Cowell's Method and a Variation-of-Parameters Method for the Computation of Precision Satellite Orbits: Addendum 1**

S. S. Dallas and E. A. Rinderle

Technical Report 32-1526, Vol. VII, pp. 32–36,
February 15, 1972

Additional test cases using a precision special perturbations program employing either Cowell's method or a variation-of-parameters method to compute an elliptical orbit are analyzed to determine which method is more efficient. The results obtained indicate that the variation-of-parameters method with a predict-only integrator and Cowell's method with a predict-partial-correct integrator are equally efficient and both are significantly more efficient than Cowell's method with a predict-correct integrator. Either of these two methods for computing precision satellite orbits offers the potential for reducing the total costs of computations during orbit design and computer execution time during real-time mission operations for future orbiter projects.

D002 DSN Progress Report for July–August 1972: A Comparison of Cowell's Method and a Variation-of-Parameters Method for the Computation of Precision Satellite Orbits: Phase Three Results

S. S. Dallas and E. A. Rinderle

Technical Report 32-1526, Vol. XI, pp. 30–35,
October 15, 1972

Additional test cases were run using a precision special-perturbations program employing either Cowell's method or a variation-of-parameters method to compute a nearly circular, nearly equatorial orbit using two different perturbative accelerations. The results obtained again indicate that the variation-of-parameters method with a predict-only integrator and Cowell's method with a predict-partial-correct integrator are equally efficient, and both are significantly more efficient than Cowell's method with a predict-correct integrator.

DAVIS, D. P.

D003 Initiation System for Low Thrust Motor Igniter

L. D. Strand, D. P. Davis, and J. I. Shafer

Technical Memorandum 33-520, January 1, 1972

For abstract, see Strand, L. D.

DAVIS, E. K.

D004 DSN Progress Report for September–October 1972: Mariner Venus–Mercury 1973 Mission Support

E. K. Davis

Technical Report 32-1526, Vol. XII, pp. 10–13,
December 15, 1972

Major planning and design activities and associated reviews and documentation have been completed for the Mariner Venus–Mercury 1973 Project. This article summarizes achievements of the past year as the DSN fully enters the implementation and test phase.

DE WINTER, F.

D005 Xenon-Filled Silicon Germanium Thermoelectric Generators

F. de Winter

JPL Quarterly Technical Review, Vol. 2, No. 3,
pp. 22–31, October 1972

This article presents an analysis that shows the desirability and feasibility of using a xenon fill in the initial stages of operation of a silicon–germanium radioisotope thermoelectric generator to be used in outer-planetary exploration. The xenon cover gas offers protection against oxidation and against material sublimation, and allows the generator to deliver required power throughout the prelaunch and launch phases. The protective mechanisms afforded by the xenon cover gas and the mechanization of a xenon supply system are also discussed.

DECKER, D. K.

D006 Methods for Utilizing Maximum Power From a Solar Array

D. K. Decker

JPL Quarterly Technical Review, Vol. 2, No. 1,
pp. 37–48, April 1972

Ion thrusters are being considered for outer-planet spacecraft propulsion. In a typical mission, the spacecraft primary energy source may be required to deliver as high as 16 kW of power to the thruster system. This power level is quite high compared to system power levels developed in the past. It is therefore very important to utilize the maximum available power from the energy source at all times.

A preliminary study of maximum power utilization methods was performed for an outer-planet spacecraft using an ion thruster propulsion system and a solar array as the primary energy source. The problems which arise from operating the array at or near the maximum power point of its current–voltage characteristic are discussed. Two closed-loop system configurations which use extremum regulators to track the array maximum power point are presented. Also, three open-loop systems are presented that either: (1) measure the maximum power of each array section and compute the total array power, (2)

utilize a reference array to predict the characteristics of the solar array, or (3) utilize impedance measurements to predict the maximum power utilization. The advantages and disadvantages of each system are discussed, and recommendations for further development are made.

DeGENNARO, L. I.

D007 DSN Progress Report for November–December 1971: Occultation Recording Assembly Implementation

L. I. DeGennaro

Technical Report 32-1526, Vol. VII, pp. 175–181, February 15, 1972

The Mariner Mars 1971 occultation experiment, in order to expedite data reduction and analysis, required real-time digital tape recordings of the Mars Deep Space Station (DSS) open loop receiver signal and nonreal-time digital tape conversion of the analog tapes (of the open loop receivers) produced by the Woomera DSS (Australia) and the Cebreros DSS (Spain). This article presents a description of the implementation of the two occultation recording assemblies, which were used to satisfy these requirements.

D008 DSN Progress Report for May–June 1972: Post-Detection Subcarrier Recording Subsystem

L. I. DeGennaro and G. Hamilton

Technical Report 32-1526, Vol. X, pp. 161–163, August 15, 1972

The Post-Detection Subcarrier Recording Subsystem for the 64-m-diameter antenna stations will be revised from the present configuration at the Mars Deep Space Station (DSS 14). The reasons for the change are to provide for future computer control of the pre/post-calibration process at the new 64-m-diameter antenna stations and to reduce the number of cabinets required to perform the essential functions of the Analog Instrumentation/Recording Subsystems. This article describes changes from the present configuration, including patching functions, test equipment, and semi-automatic and automatic computer control.

DELOUIS, H.

D009 Fourier Spectroscopy With a One-Million-Point Transformation (Translation From the Original Published in the Nouvelle Revue d'Optique Appliquée, Vol. 1, pp. 3–22, 1970)

J. Connes (National Center for Scientific Research, Orsay, France), H. Delouis (National Center for Scientific Research, Orsay, France), P. Connes (National Center for Scientific Research, Orsay, France), G. Guelachvili (National Center for Scientific Research, Orsay, France), J.-P. Maillard (National Center for Scientific Research, Orsay, France), and G. Michel (National Center for Scientific Research, Orsay, France)

Technical Memorandum 33-525, March 15, 1972

For abstract, see Connes, J.

DeMORE, W. B.

D010 Photolysis of CO_2 at 1849 Å

W. B. DeMore and M. M. Mosesman

J. Atmos. Sci., Vol. 28, No. 6, pp. 842–846, September 1971

Photolysis of CO_2 at 1849 Å (Hg lamp) has been studied at pressures in the range 65–800 psi at room temperature. The primary dissociation quantum yield is 1.0, as determined by experiments in which the atomic oxygen product was scavenged in the form of O_3. At high pressures (~400 psi), O_3 photolysis at 2537 Å gave appreciable CO_3 formation by the reaction

$$O(^1D) + CO_2 + M \rightarrow CO_3 + M$$
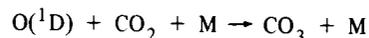
as evidenced by loss of O_3. To observe quantitative O_3 production, it was therefore necessary to filter out the 2537-Å light. The products CO and O_2 could not be recovered in 100% yield in most of the experiments. No satisfactory mechanism can be given for the product losses, although a number of possibilities can be ruled out. In particular, CO_3 did not oxidize CO to CO_2. The CO yield could be increased to nearly 100% by coating the cell walls with Kel-F grease, whereas the O_2 yield simultaneously dropped to zero. The quantum yield results at 1849 Å suggest that CO_2 dissociates at all wavelengths where absorption is appreciable.

DEVLIN, J. D.

D011 Dry-Heat Resistance of Bacillus Subtilis Var. Niger Spores on Mated Surfaces

G. J. Simko, J. D. Devlin, and M. D. Wardle

Appl. Microbiol., Vol. 22, No. 4, pp. 491–495, October 1971

For abstract, see Simko, G. J.

DIAZ, A. F.

D012 Carbon-to-Metal Chlorine Exchange: IV. Mercuric Salt Promoted Acetolysis of exo-Norbornyl Chloride

J. P. Hardy, A. F. Diaz, and S. Winstein

J. Am. Chem. Soc., Vol. 94, No. 7, pp. 2363–2370, April 5, 1972

For abstract, see Hardy, J. P.

DIVINE, N.

D013 Models for the Atmospheres of Jupiter and Saturn

N. Divine and F. D. Palluconi

JPL Quarterly Technical Review, Vol. 2, No. 2, pp. 1–8, July 1972

Numerical models of the atmospheres of Jupiter and Saturn have been created for use in the development of design criteria for space vehicles intended to investigate these planets. These models contribute to spacecraft design by providing a basis for the assessment of entry heating, the transmission and emission of radiation, and structural and aerodynamic interactions. The model atmospheres are based on data and analyses published in the literature through 1970. The composition is discussed, and the relative amounts of each molecular species are tabulated for nominal and extreme cases. The structure of the atmospheric regions is discussed, and the principal features of one nominal and two limiting models for each planet are indicated. The models are illustrated by pressure–temperature profiles which also display the major cloud layers. Reference is made to complete descriptions of altitude, pressure, temperature, density, scale height, and cloud relationships for these models which are specified in appropriate NASA publications.

DONNELLY, H.

D014 DSN Progress Report for May–June 1972: Programmed Oscillator Development

H. Donnelly and M. R. Wick

Technical Report 32-1526, Vol. X, pp. 180–185, August 15, 1972

This article describes the addition of programmed oscillators in the Block III receiver/exciter subsystems at the Mars and Ballima Deep Space Stations (DSSs 14 and 43) for Pioneer 10 support during Jupiter flyby. A brief description of the tracking requirements of the mission and the subsystem modifications to incorporate the programmed oscillators is given.

DORE, M. A.

D015 Nuclear Radiation Sources On-Board Outerplanet Spacecraft

E. L. Noon, G. H. Anno, and M. A. Dore

IEEE Trans. Nucl. Sci., Vol. NS-18, No. 5, pp. 50–57, October 1971

For abstract, see Noon, E. L.

DORMAN, J.

D016 DSN Progress Report for March–April 1972: Overseas 64-m-Diameter Antenna Power Configuration

J. Dorman

Technical Report 32-1526, Vol. IX, pp. 218–226, June 15, 1972

The construction of the two new 64-m-diameter antennas at Deep Space Stations 63 (Madrid) and 43 (Tidbinbilla) required additional power generating equipment at these sites. As the new sites were in close proximity to the existing Deep Space Stations 61 (Madrid) and 42 (Tidbinbilla), the new equipment was designed to integrate with the existing power generating and distribution systems. This integration will enable the new and existing generators to be combined into a single generating system and provide total site power for both 64-m and 26-m antenna station requirements. Studies are being made to determine the economic and technical advantages of using commercial power. If proved favorable, the equipment presently being installed is designed to provide parallel operation of the generating system with commercially produced power.

The new equipment is equipped with automatic generator starting and stopping features and power demand sensing monitors. The monitors automatically start, synchronize, and connect, generators to share load demand equally between running generators as power demand increases. Conversely, if the demand decreases, unnecessary generators are removed from the generating system. This article describes the techniques developed and incorporated into the design of the new generation and distribution equipment and the proposed future development of the power generating systems.

DOWNS, G. S.

D017 The Distribution of Linear Polarization in Cassiopeia A at Wavelengths of 9.8 and 11.1 cm

G. S. Downs and A. R. Thompson (Stanford University)

Two series of observations of the brightness distribution of the linearly polarized component of the radiation of Cassiopeia A are described. The first was made at a wavelength of 9.8 cm using a two-element interferometer at Stanford University which provided a synthesized beamwidth of 1.6×2.7. The second set of observations was made with the three-element interferometer of the National Radio Astronomy Observatory (NRAO) at a wavelength of 11.1 cm and a beamwidth of $8''1 \times 9''3$ was obtained. Because the increments in the antenna spacing of the NRAO interferometer are greater than the critical interval for Cassiopeia A, part of the brightness distribution is missing from the synthesized map at 11.1 cm. This missing component is estimated to contain only 5% of the polarized flux density. The polarized radiation is concentrated in the main bright ring of the source and at a 11.1-cm wavelength the maxima in the polarized brightness correspond to $\approx 5\%$ of the unpolarized radiation. A comparison of the observations with published results at other wavelengths shows that Faraday depolarization reduces the polarized radiation to half the intrinsic value at a wavelength of approximately 7.5 cm. The mean values of the rotation of the position angle of the polarization at a number of points indicate a greater rate of rotation as a function of λ^2 at wavelengths shorter than 6 cm than at longer ones.

These data are hardly detailed enough to rule out the possibility of linear rotation with λ^2 but appear to be best interpreted in terms of a nonlinear rotation within the source, together with a linear rotation of about –35 rad-m^{-2} which may be attributed to the interstellar medium. The internal rotation can be explained by a model of the source with a radial magnetic field and a thermal electron density of 2 cm^{-3}. The Appendix discusses the effect on synthesis observations of the use of increments in the antenna spacing which are too large. Such undersampling results in the presence of grating lobes, the responses of which can only be separated from the main-beam responses for components of the source of dimensions less than the spacing of the grating lobes. Broader components of the source are lost, and to estimate the flux density of the unconfused main-beam responses it is necessary to correct the brightness scale by a factor derived from the beam pattern.

D018 Second Decrease in the Period of the Vela Pulsar

P. E. Reichley and G. S. Downs

Nature Phys. Sci., Vol. 234, No. 46, p. 48, November 15, 1971

For abstract, see Reichley, P. E.

D019 Mars Radar Observations, a Preliminary Report

G. S. Downs, R. M. Goldstein, R. R. Green, and G. A. Morris

Science, Vol. 174, No. 4016, pp. 1324–1327, December 24, 1971

Radar observations of narrow belt of the surface of Mars, centered at 16° south latitude, show a very rugged terrain, with elevation differences greater than 13 km from peak to valley. For nearby points, the relative altitude is measured to 40 m at best; the precision is worse for points at different latitudes, or widely separated in longitude, because of orbital uncertainties. Some of the larger craters have been resolved, and their depth and, in some cases, the height of the raised rim have been measured. Where high-resolution photographs are available, the correlation is excellent.

DOWNS, W.

D020 A Surface-Layer Representation of the Lunar Gravitational Field

L. Wong (Aerospace Corporation),
G. Buechler (Aerospace Corporation),
W. Downs (Aerospace Corporation), W. L. Sjogren,
P. M. Muller, and P. Gottlieb

J. Geophys. Res., Vol. 76, No. 26, pp. 6220–6236, September 10, 1971

For abstract, see Wong, L.

DUXBURY, T. C.

D021 In-Flight Calibration of an Interplanetary Navigation Instrument

T. C. Duxbury and H. Ohtakay

J. Spacecraft Rockets, Vol. 8, No. 10, pp. 1038–1042, October 1971

This article presents the results of an analytical investigation that demonstrates the feasibility of geometrically calibrating a navigation instrument during interplanetary flight to arc-sec accuracy. The instrument, similar to a television camera, would view selected natural satellites and reference stars simultaneously for navigating to the outer planets. An 11×11 reseau grid, etched onto the target raster of a vidicon tube, would be used to remove electromagnetic distortion from the satellite and reference star data to less than 1.2 arc-sec (1σ) in each and every data frame, independent of reseau data from any other data frame. Taking advantage of expected optical distortion stability, 50 star images obtained from many data frames would be used to determine optical distortion to less than 4.3 arc-sec (1σ). Therefore, the use of the reseau grid and star images could enable the naviga-

tion measurements to be geometrically calibrated to an accuracy of 5 arc-sec (1σ).

DWIVEDI, N. P.

D022 Aiming Strategies for Quarantined Multi-Planet Missions

N. P. Dwivedi

JPL Quarterly Technical Review, Vol. 2, No. 2, pp. 9–17, July 1972

An important flight-path constraint for current and future interplanetary missions arises from planetary quarantine restrictions. Each planet is assigned a maximum allowable probability of contamination which must not be exceeded. A portion of this probability is suballocated among the trajectory correction maneuvers. The remaining portion is allocated to the small ejecta/efflux sources released from the spacecraft that could possibly reach the planetary atmosphere and surface. For each maneuver, the suballocation is translated into an allowable probability of planetary impact. At the time of making a maneuver, the allowable probability of impact may dictate biasing the aim point. This study describes the technique of determining preferred biased aim points, given the suballocated probability of contamination for each maneuver.

DYER, P.

D023 A Computational Algorithm for Sequential Estimation

R. J. Hanson and P. Dyer (Imperial Chemical Industries Ltd.)

Comput. J., Vol. 14, No. 3, pp. 285–290, August 1971

For abstract, see Hanson, R. J.

EASTON, R. A.

E001 Centralized Data Handling for Grand Tour Missions

R. A. Easton

Advan. Astronaut. Sci., Vol. 29, No. II, pp. 367–376, 1971

This article describes an adaptive self-testing and repairing centralized data system incorporating the flexibility and reliability necessary for the Grand Tour class of deep-space missions. It was developed as part of the Thermoelectric Outer-Planet Spacecraft (TOPS) effort at JPL. The data system consists of a programmable adaptive computer-aided telemetry system (CATS) called the measurement processor, a 2×10^9-bit data storage sys-

tem consisting of a buffer plus single-speed tape recorders, science instrument interface units customized to each instrument, a ground command decoder, a central timing source, and a self-testing and repairing (STAR) control computer that coordinates the operations of the other parts of the system and of the spacecraft.

This data system is organized such that the measurement processor performs all repetitive high-speed data gathering and reduction functions, alerting the STAR computer through a shared two-port memory if any abnormal readings are noted. It also routes compressed spacecraft data to data storage for periodic data dump transmissions to the ground while some data are transmitted to the ground in real time. Meanwhile, the STAR computer performs non-routine data handling functions and issues commands to the spacecraft as needed. It can also back-up failed portions of the data system at a reduced capability. If the STAR computer is the spacecraft's brain, then CATS is its nervous system. This division of labor allows a substantial reduction in the power, weight, and complexity of the overall system as opposed to using one general-purpose computer for all functions. The CATS and STAR computer have been breadboarded at JPL.

EDELSON, R. E.

E002 Telecommunications Systems Design Techniques Handbook

R. E. Edelson

Technical Memorandum 33-571, July 15, 1972

The DSN, managed by JPL for NASA, increasingly supports deep space missions sponsored and managed by organizations without long experience in DSN design and operation. This memorandum is intended as a textbook for those DSN users inexperienced in the design and specification of a DSN-compatible spacecraft telecommunications system. For experienced DSN users, the memorandum provides a reference source of telecommunication information which summarizes knowledge previously available only in a multitude of sources. Extensive references are quoted for those who wish to explore specific areas more deeply.

EISENBERGER, I.

E003 DSN Progress Report for March–April 1972: An Inventory Policy for the Deep Space Network

I. Eisenberger, F. R. Maiocco, and G. Lorden (California Institute of Technology)

Technical Report 32-1526, Vol. IX, pp. 84–87, June 15, 1972

This article describes a proposed inventory and procurement policy for optimal procedures in ordering and

allocating for the DSN network supply depot (NSD). The policy defined differs from conventional inventory stockage and resupply systems in that it takes into consideration the inventory status not only of NSD but also of each of the complex supply facilities.

E004 DSN Progress Report for September–October 1972: An Inventory and Procurement Policy for the Deep Space Network

I. Eisenberger, F. R. Maiocco, and
G. Lorden (California Institute of Technology)

Technical Report 32-1526, Vol. XII, pp. 131–148, December 15, 1972

This article presents a technical description of a proposed inventory and procurement policy for ordering and allocating maintenance and operating supplies throughout the DSN. This policy differs from the conventional economic lot-size procurement policy in that the reorder point for the Network Supply Depot (NSD) depends upon the stockage levels at all area, station, or Complex Supply Facilities (CSF), as well as on the level at the NSD. Thus, by basing reorder decisions upon the state of the inventory supplies throughout the entire DSN, an efficient cost-minimizing policy is possible. Safe minimum inventory levels are established for each CSF by means of statistical decision-theory techniques which require NSD to reorder whenever one or more of the CSFs reaches its prescribed minimum. Some results of a statistical study of the effect of this policy are included.

ELACHI, C.

E005 Dipole Antenna in Space–Time Periodic Media

C. Elachi

IEEE Trans. Anten. Prop., Vol. AP-20, No. 3, pp. 280–287, May 1972

The problem of dipole radiation in sinusoidally space–time periodic media is studied and solved. The space–time periodicity can be considered as due to a strong pump wave and is expressed as a traveling-wave type change in the dielectric constant or the plasma density, i.e.,

$$\epsilon(z,t) = \epsilon_0 \epsilon_r [1 + \epsilon_1 \cos(Kz - \Omega t)]$$

$$N(z,t) = N_0 [1 + N_1 \cos(Kz - \Omega t)]$$

The solution also covers the limit case of a sinusoidally stratified medium ($\Omega = 0$). The solution is formulated in a matrix form, such that the basic results and diagrams apply, with minor changes, to the different cases studied: electric and magnetic dipole in a dielectric, plasma, and uniaxial plasma. The wave-vector diagram is used exten-

sively in studying and presenting the different properties of the solution: caustics, effect of the disturbance (pump wave) motion, harmonics, radiation outside the allowed cone in a uniaxial plasma. Many dipole radiation patterns are given and their features explained physically. Finally, the solution and results are extended to the generally space–time periodic media where $\epsilon(z,t)$ and $N(z,t)$ behave as

$$\eta(z,t) = \eta_0 [1 + \eta_1 f(Kz - \Omega t)]$$

where $f(\xi)$ is any periodic function.

E006 Electromagnetic Wave Propagation and Wave-Vector Diagram in Space–Time Periodic Media

C. Elachi

IEEE Trans. Anten. Prop., Vol. AP-20, No. 4, pp. 534–536, July 1972

The electromagnetic wave propagation and wave-vector diagram in generally space–time periodic dielectric, plasma, and uniaxial plasma are studied for transverse electric and transverse magnetic waves. The case of a sinusoidal periodicity is solved numerically. Special properties due to the inhomogeneity are presented.

E007 Cerenkov and Transition Radiation in Space–Time Periodic Media

C. Elachi

J. Appl. Phys., Vol. 43, No. 9, pp. 3719–3723, September 1972

The solution to the problem of determining the radiation emitted by a uniformly moving charged particle in a sinusoidally space–time periodic medium is obtained. The space–time periodicity can be considered as due to a strong pump wave and is expressed as a traveling-wave-type change in the dielectric constant or the plasma density. The solution covers also the limiting case of sinusoidally stratified media. The expression and spectrum of the radiated electromagnetic field are determined for different media: dielectric, isotropic and uniaxial plasma. Depending on the nature of the medium and the velocity of the particle, the radiated field is of the Cerenkov and/or transition type. The Brillouin diagram is used extensively in understanding and determining the nature, extent, and spectrum of the different modes of radiation, and a focusing effect is also studied.

ELLEMAN, D. D.

E008 Mechanisms of Ion–Molecule Reactions of Propene and Cyclopropane

M. T. Bowers (University of California, Santa Barbara), D. H. Aue (University of California, Santa Barbara), and D. D. Elleman

J. Am. Chem. Soc., Vol. 94, No. 12, pp. 4255–4261, June 14, 1972

For abstract, see Bowers, M. T.

E009 Dependence of the Rates on Ion Kinetic Energy for the Reactions D_2^+ + D_2 and HD^+ + HD

W. T. Huntress, Jr., D. D. Elleman, and M. T. Bowers (University of California, Santa Barbara)

J. Chem. Phys., Vol. 55, No. 11, pp. 5413–5414, December 1, 1971

For abstract, see Huntress, W. T., Jr.

ERICKSON, D. E.

E010 DSN Progress Report for November–December 1971: The SAPDP Program Set for Sigma 5 Assembly

D. E. Erickson

Technical Report 32-1526, Vol. VII, pp. 91–96, February 15, 1972

This article describes a set of programs that have been written to enable the Sigma 5 computer to assemble programs for the PDP-11 minicomputer. It consists of two parts: a system procedure deck, which allows SIGMA METASYMBOL to assemble a source language similar to PDP's own PAL-11; and a secondary loader, which reformats the Sigma 5 load module into PDP-11 absolute binary format and punches it onto paper tape. The syntactic differences between this assembler and PAL-11 are described, as well as the process of generating a PDP-11 program using this program set on the Sigma 5.

ERPENBACH, H.

E011 DSN Progress Report for November–December 1971: High Output Power for Hydrogen Maser Frequency Standards

H. Erpenbach and C. Finnie

Technical Report 32-1526, Vol. VII, pp. 106–108, February 15, 1972

This article describes the use of an FEP and TFE Teflon mixture to form duplicable storage bulb wall coatings for hydrogen maser frequency standards. The use of this mixture has resulted in wall coatings more efficient than previous coatings fabricated at this facility. A hydrogen

maser has been optimized for high-power operation using these new storage bulbs, and a power output level of –80 dBmW has been achieved.

E012 DSN Progress Report for September–October 1972: Frequency Generation and Control: Atomic Hydrogen Dissociator

H. Erpenbach and D. Norris

Technical Report 32-1526, Vol. XII, pp. 56–58, December 15, 1972

This article describes a long-life hydrogen gas discharge source for the JPL hydrogen maser. The lifetime of this source has been extended from approximately 6 months to 2 years or more by changing the geometry of the RF power coupling mechanism. Other improvements over the older type source are: (1) the gas discharge may be started without increasing hydrogen pressure, and (2) an acceptable impedance match to the RF power generator can be achieved over a broader range of operating hydrogen pressures.

ESCOBAL, P. R.

E013 3-D Multilateration: A Precision Geodetic Measurement System

P. R. Escobal, H. F. Fliegel, R. M. Jaffe, P. M. Muller, K. M. Ong, O. H. von Roos, and M. S. Shumate

JPL Quarterly Technical Review, Vol. 2, No. 3, pp. 1–11, October 1972

The assessment of earthquake hazards, indication of probable locations for earthquakes, and the eventual possibility of earthquake prediction or premonitory warning have become an important part of the NASA Earth Physics Applications Program. The key to moving toward these goals is believed to be precision monitoring of the near- and far-field strain buildup and release within a few hundred kilometers of active fault zones such as the San Andreas. A system with the capability of determining station positions in three dimensions with 1-cm accuracy has been designed using pulsed-laser Earth-satellite tracking stations coupled with strictly geometric data reduction.

ESPOSITO, P. B.

E014 Geocentric Gravitational Constant Determined From Mariner 9 Radio Tracking Data

P. B. Esposito and S. K. Wong

Preprint of paper presented at International Symposium on Earth Gravity Models and Related Problems (Sponsored by the American Geophysical Union, NASA), St. Louis, Missouri, August 16–18, 1972

Several days of the Mariner 9 near-Earth radio tracking data have been analyzed to determine the Earth's gravitational constant. The doppler data distribution is essentially continuous as five deep space network stations have been receiving data. All basic forces influencing the spacecraft's motion have been modeled and a typical analysis of the data yields doppler residuals within ±0.004 Hz which amounts to ±0.3 mm s^{-1} in range-rate. During this interval, the spacecraft's range-rate varied from 5.6 to 3.2 km s^{-1}.

The value of the Earth's gravitational constant and associated standard deviation deduced from this preliminary analysis is GM $= 398600.8 \pm 0.4$ km^3 s^{-2}. Additional analysis, which includes refining the model for the attitude-control perturbations, incorporating an ionospheric model, and extending the data arc, should improve both the value and uncertainty of this constant. The major source of error is due to perturbative accelerations caused by the attitude-control subsystem on the spacecraft. A comparison of this result with independent determinations deduced from analyses of previous spacecraft data is also presented.

E015   Determination of Astrodynamic Constants and a Test of the General Relativistic Time Delay With S-Band Range and Doppler Data From Mariners 6 and 7

J. D. Anderson, P. B. Esposito, W. Martin, and D. O. Muhleman (California Institute of Technology)

Space Research XI, pp. 105–112, Akademie-Verlag, Berlin, 1971

For abstract, see Anderson, J. D.

EVANS, D. D.

E016   Development and In-Flight Performance of the Mariner 9 Spacecraft Propulsion System

D. D. Evans, R. D. Cannova, and M. J. Cork

Technical Memorandum 33-574, November 1, 1972

On November 14, 1971, Mariner 9 was decelerated into orbit about Mars by a 1334-N (300-lbf) liquid-bipropellant propulsion system. This memorandum describes and summarizes the development and in-flight performance of this pressure-fed, nitrogen tetroxide/monomethyl hydrazine bipropellant system. The design of all Mariner propulsion subsystems has been predicated upon the

premise that simplicity of approach, coupled with thorough qualification and margin-limits testing, is the key to cost-effective reliability. The Mariner 9 subsystem design illustrates this approach in that little functional redundancy is employed. This memorandum summarizes the design and test rationale employed in the Mariner 9 design and development program.

The qualification test program and analytical modeling are also discussed. Since the propulsion subsystem is modular in nature, it was completely checked, serviced, and tested independent of the spacecraft. Proper prediction of in-flight performance required the development of three significant modeling tools to predict and account for nitrogen saturation of the propellant during the 6-month coast period and to predict and statistically analyze in-flight data. The flight performance of the subsystem was excellent, as were the performance-prediction correlations, which are presented.

FANALE, F. P.

F001   Physical Adsorption of Rare Gas on Terrigenous Sediments

F. P. Fanale and W. A. Cannon

Earth Planet. Sci. Lett., Vol. 11, No. 5, pp. 362–368, August 1971

A physical–chemical explanation is offered for the paucity of Xe in the Earth's atmosphere and for the recently reported enrichments of heavy rare gases in shales. Brunauer–Emmett–Teller (BET) plots for N_2 adsorption at $-195°C$ and Freundlich plots for Kr and Xe adsorption at 25 and 0°C were determined for shale samples. The results, together with geological considerations, suggest that Xe has been significantly depleted from the Earth's atmosphere, relative to other rare gases, by physical adsorption on terrigenous sediments.

F002   Origin of Planetary Primordial Rare Gas: The Possible Role of Adsorption

F. P. Fanale and W. A. Cannon

Geochim. Cosmochim. Acta, Vol. 36, No. 3, pp. 319–328, March 1972

The degree of physical adsorption of Ne, Ar, Kr, and Xe on pulverized samples of the Allende meteorite at 113°K has been measured. The observed pattern of equilibrium enrichment of heavy rare gases over light on the pulverized meteorite surfaces relative to the gas phase is similar to the enrichment pattern (Xe > Kr > Ar $\gg$ Ne, He) exhibited by "planetary primordial" rare gas when compared with the composition of solar rare gas. Results indicate that at 113°K a total nebular pressure of from 10^{-2} to 10^{-3} atm would be required to explain the Ar, Kr, and Xe abundances in carbonaceous chondrites with

an adsorption mechanism. This pressure estimate is compatible with the range of possible nebular pressures (10^{-2} to 10^{-6} atm), suggested by astrophysical arguments. However, the subsequent mechanism by which initially adsorbed gas might have been transferred into the interiors of grains cannot be identified at present. The hypothesis that the presence of "planetary primordial" Ar, Kr, and Xe in carbonaceous chondrites is due to their adsorption from the gaseous portion of the pre-planetary cloud is offered as an alternative to the hypothesis that these gases were incorporated as the result of attainment of solubility equilibrium between dust and gas.

F003   History of Martian Volatiles: Implications for Organic Synthesis

F. P. Fanale

Icarus, Vol. 15, No. 2, pp. 279–303, October 1971

As described in this article, a theoretical reconstruction of the history of Martian volatiles indicates that Mars probably possessed a substantial reducing atmosphere at the outset of its history and that its present tenuous and more oxidized atmosphere is the result of extensive chemical evolution. As a consequence, it is probable that Martian atmospheric chemical conditions, now hostile with respect to abiotic organic synthesis in the gas phase, were initially favorable. Evidence indicating the chronology and degradational history of Martian surface features, surface mineralogy, bulk volatile content, internal mass distribution, and thermal history suggests that Mars catastrophically developed a substantial reducing atmosphere as the result of rapid accretion. This atmosphere probably persisted—despite the direct and indirect effects of hydrogen escape—for a geologically short time interval during, and immediately following, Martian accretion. That was the *only* portion of Martian history when the atmospheric environment could have been chemically suited for organic synthesis in the gas phase. Subsequent gradual degassing of the Martian interior throughout Martian history could not sustain a reducing atmosphere due to the low intensity of planet-wide orogenic activity and the short atmospheric mean residence time of hydrogen on Mars. During the post-accretion history of Mars, the combined effects of planetary hydrogen escape, solar-wind sweeping, and reincorporation of volatiles into the Martian surface produced and maintained the present atmosphere.

F004   Objectives and Requirements of Unmanned Rover Exploration of the Moon

D. B. Nash, J. E. Conel, and F. P. Fanale

The Moon, Vol. 3, No. 2, pp. 221–230, August 1971

For abstract, see Nash, D. B.

FARMER, C. B.

F005   Global Studies of Atmospheric Pollutants and Trace Constituents

R. A. Toth (California Institute of Technology) and C. B. Farmer (California Institute of Technology)

AIAA Preprint 71-1109, ACS (American Chemical Society)/AIAA (American Institute of Aeronautics and Astronautics)/EPA (Environmental Protection Agency)/IEEE (Institute of Electrical and Electronic Engineers)/ISA (Instrument Society of America)/NASA (National Aeronautics and Space Administration)/NOAA (National Oceanographic and Atmospheric Administration) Joint Conference on Sensing of Environmental Pollutants, Palo Alto, California, November 8–10, 1971

For abstract, see Toth, R. A.

F006   The Infrared Investigations on the Outer Planets Grand Tour

C. B. Farmer

Advan. Astronaut. Sci., Vol. 29, No. I, pp. 589–599, 1971

The infrared experiments being planned for the outer-planet Grand Tour include fundamental investigations in planetary radiation balance, atmospheric composition, structures and dynamics, and compositional and physical properties of the satellites. The multiple-planet missions to the outer solar system provide significant advantages to infrared experiments in terms of spatial resolution and planetary phase angle coverage over the limitations to Earth-based observations. The experiment and instrument design are based on the requirements of those investigations which can best exploit these advantages in a multiple-planet opportunity, as opposed to single-planet missions. The infrared instrument is a combined multi-channel radiometer and low-resolution spectrometer, covering the range from visible wavelengths out to 100 μ.

F007   The Strengths of H_2O Lines in the 8200 Å Region and Their Application to High Dispersion Spectra of Mars

C. B. Farmer

Icarus, Vol. 15, No. 2, pp. 190–196, October 1971

The improvement in the quality of spectroscopic plates taken in recent years in the search for water vapor in the atmosphere of Mars has dictated the need for improved laboratory data with which to interpret the spectra. This article presents the results of measurements of the strengths of 41 lines of the 8200-Å (211) water vapor band. The measured values show evidence of vibration–rotation interactions on the line intensities beyond the

principal stretching effect. The value of the vibrational band strength derived from the results is 9.46 ± 0.5 × 10^{-22} cm^{-1}-mol^{-1}-cm^2.

F008 The Detection and Mapping of Water Vapor in the Martian Atmosphere

C. B. Farmer and D. D. LaPorte

Icarus, Vol. 16, No. 1, pp. 34–46, February 1972

The objectives of the water vapor investigations, to be carried out during the Viking missions, are described in the light of our current knowledge of Martian atmospheric conditions and the diurnal and seasonal variations of the water abundance. A discussion is given of the relative merits of the different experimental approaches which can be adopted for this purpose, followed by a summary of the detection limits achievable in the available spectral regions.

These considerations led to the choice of a spectrometer operating in the 7300-cm^{-1} (1.4-μ) region, with a spectral resolution of approximately 1 cm^{-1} and a surface spatial resolution at periapsis of 3 × 24 km. The design of the spectrometer and the results of laboratory simulation tests which have been carried out to verify the expected instrumental performance are described.

F009 Jupiter: Observation of Deuterated Methane in the Atmosphere

R. Beer, C. B. Farmer, R. H. Norton, J. V. Martonchik (University of Texas), and T. G. Barnes (University of Texas)

Science, Vol. 175, No. 4028, pp. 1360–1361, March 24, 1972

For abstract, see Beer, R.

FARRAR, J. W.

F010 Development and Testing of the Ultraviolet Spectrometer for the Mariner Mars 1971 Spacecraft

J. W. Farrar

Technical Memorandum 33-569, October 15, 1972

The Mariner Mars 1971 ultraviolet spectrometer is an Ebert–Fastie type of the same basic design as the Mariner Mars 1969 instrument. Light enters the instrument and is split into component wavelengths by a scanning reflection diffraction grating. Two monochrometer exit slits allow the use of two independent photomultiplier-tube sensors. Channel 1 has a spectral range of 1100 to 1692 Å with a fixed gain, while Channel 2 has a spectral range of 1450 to 3528 Å with an automatic step gain control, providing a dynamic range over the expected atmosphere and surface brightness of Mars.

This memorandum describes the scientific objectives, basic operation, design, testing, and calibration for the Mariner Mars 1971 ultraviolet spectrometer. The design discussion includes those modifications that were necessary to extend the lifetime of the instrument in order to accomplish the Mariner Mars 1971 mission objectives.

FAVERO, M. S.

F011 Microbiological Sampling of Returned Surveyor III Electrical Cabling

M. D. Knittel, R. H. Green, and M. S. Favero (U.S. Public Health Department)

Proceedings of the Second Lunar Science Conference, Houston, Texas, January 11–14, 1971, Vol. 3, pp. 2715–2719, The M.I.T. Press, 1971

For abstract, see Knittel, M. D.

FEDORS, R. F.

F012 A Molecular Theory of Elastomer Deformation and Rupture

R. F. Landel and R. F. Fedors

Mechanical Behavior of Materials: Proceedings of the 1971 International Conference on Mechanical Behavior of Materials (Sponsored by the Society of Materials Science), Kyoto, Japan, August 1971, Vol. III, pp. 496–507

For abstract, see Landel, R. F.

FERRERA, J. D.

F013 A Mechanism for Three-Axis Control of an Ion Thruster Array

G. S. Perkins, K. G. Johnson, J. D. Ferrera, and T. D. Masek

J. Spacecraft Rockets, Vol. 9, No. 3, pp. 218–220, March 1972

For abstract, see Perkins, G. S.

FINNEGAN, E. J.

F014 DSN Progress Report for November–December 1971: A New Crowbar Logic Unit

E. J. Finnegan

Technical Report 32-1526, Vol. VII, pp. 136–138, February 15, 1972

A new crowbar logic unit has been designed and installed for the Mars Deep Space Station 400-kW transmitter

utilizing integrated circuits and plug-in modular construction. The logic unit of the crowbar consists of four detecting channels that generate and shape a new pulse which is used to trigger the crowbar. The crowbar is a device that short-circuits the power supply when a high-voltage arc threatens to destroy the output klystron.

F015   DSN Progress Report for September–October 1972: A Dual-Ignitron Crowbar

E. J. Finnegan

Technical Report 32-1526, Vol. XII, pp. 205–208, December 15, 1972

This article describes a high-voltage protective device (crowbar) that is capable of operating at 100,000 V. This device has two ignitrons in series, with the appropriate electronics to trigger the tubes to a conducting state when desired. The crowbar is needed to increase the reliability of the transmitter, as the present tubes have difficulty operating at over 60,000 V. A new photon generator was designed and tested using light-emitting diodes and infrared-detecting pin diodes in conjunction with fiber optics for transmitting a pulse to the high-voltage deck and triggering the ignitron crowbar.

FINNIE, C.

F016   DSN Progress Report for November–December 1971: High Output Power for Hydrogen Maser Frequency Standards

H. Erpenbach and C. Finnie

Technical Report 32-1526, Vol. VII, pp. 106–108, February 15, 1972

For abstract, see Erpenbach, H.

F017   DSN Progress Report for May–June 1972: Tracking and Ground Based Navigation: Performance of Hydrogen Maser Cavity Tuning Servo

S. Petty and C. Finnie

Technical Report 32-1526, Vol. X, pp. 113–115, August 15, 1972

For abstract, see Petty, S.

FITZGERALD, D. J.

F018   Ion Thruster Performance Calibration

E. V. Pawlik, R. Goldstein, D. J. Fitzgerald, and R. W. Adams

Preprint 72-475, AIAA Ninth Electric Propulsion Conference, Bethesda, Maryland, April 17–19, 1972

For abstract, see Pawlik, E. V.

FJELDBO, G.

F019   Bistatic Radar Measurements of the Surface of Mars With Mariner 1969

G. Fjeldbo, A. J. Kliore, and B. L. Seidel

Icarus, Vol. 16, No. 3, pp. 502–508, June 1972

This article describes the detection of echoes produced by oblique reflection of the radio frequency (2300 MHz) spacecraft carrier from the Martian surface as Mariners 6 and 7 flew behind Mars in 1969. Changes in echo center frequency and bandwidth are utilized to study the radius and roughness of the surface along a quasi-specular radar track that led from an optically dark and densely cratered region of Meridiani Sinus over into a smoother and brighter looking area of Thymiamata. A 3 to 1 decrease in surface roughness of large size compared to the wavelength (13 cm) was observed as the reflecting zone moved across the boundary between these two regions. The average radius obtained along the track was 3393 ± 3 km. Due to large angles of incidence (86 to 90°), and surface shadowing, the data are not suitable for mapping the reflection coefficient of the surface material.

F020   Mariner 9 S-Band Martian Occultation Experiment: Initial Results on the Atmosphere and Topography of Mars

A. J. Kliore, D. L. Cain, G. Fjeldbo, B. L. Seidel, and S. I. Rasool (National Aeronautics and Space Administration)

Science, Vol. 175, No. 4019, pp. 313–317, January 21, 1972

For abstract, see Kliore, A. J.

F021   Summary of Mariner 6 and 7 Radio Occultation Results on the Atmosphere of Mars

A. J. Kliore, G. Fjeldbo, and B. L. Seidel

Space Research XI, pp. 165–175, Akademie-Verlag, Berlin, 1971

For abstract, see Kliore, A. J.

FLEISCHER, G. E.

F022   Large-Deformation Modal Coordinates for Nonrigid Vehicle Dynamics

P. W. Likins and G. E. Fleischer

Technical Report 32-1565, November 1, 1972

For abstract, see Likins, P. W.

FLIEGEL, H. F.

F023 DSN Progress Report for July–August 1972: Use of Doppler Determinations of Polar Motion Using Artificial Satellites to Support JPL Planetary Missions

H. F. Fliegel

Technical Report 32-1526, Vol. XI, pp. 36–41, October 15, 1972

Standard deviations and systematic differences are calculated between the U.S. Navy Weapons Laboratory (USNWL) determination of the X and Y coordinates of the pole using artificial satellites, and the smoothed 5-day means published by the Bureau International de l'Heure (BIH). The results indicate slowly varying errors of about 1 m in the conventionally obtained optical data of the BIH, which are presently used by JPL. Although current values of polar coordinates should be based upon the BIH Rapid Service, values for previous months might be improved with the help of USNWL doppler data.

F024 3-D Multilateration: A Precision Geodetic Measurement System

P. R. Escobal, H. F. Fliegel, R. M. Jaffe, P. M. Muller, K. M. Ong, O. H. von Roos, and M. S. Shumate

JPL Quarterly Technical Review, Vol. 2, No. 3, pp. 1–11, October 1972

For abstract, see Escobal, P. R.

FORNEY, P. B.

F025 Mariner Mars 1969 Infrared Spectrometer

K. C. Herr (University of California, Berkeley), P. B. Forney (University of California, Berkeley), and G. C. Pimentel (University of California, Berkeley)

Appl. Opt., Vol. 11, No. 3, pp. 493–501, March 1972

For abstract, see Herr, K. C.

FOSTER, C. F.

F026 DSN Progress Report for July–August 1972: Wideband Distribution Amplifier for Coherent Reference Generator

C. F. Foster

Technical Report 32-1526, Vol. XI, pp. 140–145, October 15, 1972

A wideband (0.1- to 100-MHz) frequency-distribution module has been designed to have high output-to-output isolation, low phase shift with temperature, no RF tuning, and internal means to detect module performance that can be monitored by a computer. The amplifier and its use with a coherent reference generator are described in this article.

FRANCO, M.

F027 DSN Progress Report for September–October 1972: Improved RF Calibration Techniques: Commercial Precision IF Attenuator Evaluation

C. T. Stelzried, B. L. Seidel, M. Franco, and D. Acheson

Technical Report 32-1526, Vol. XII, pp. 74–82, December 15, 1972

For abstract, see Stelzried, C. T.

FRANK, J.

F028 A Study on Heavy/Light Atom Discrimination in Bright-Field Electron Microscopy Using the Computer

J. Frank (Cornell University)

Biophys. J., Vol. 12, No. 5, pp. 484–511, May 1972

The Z dependence of the phase angle of the complex atomic scattering amplitude can be used to separate the image due to the heavy atoms from that due to the light atoms of the object structure. The linear theory of image formation applied to a focus series of bright-field images leads to Schiske's formula for the calculation of the structure factor. A program system is described which uses this algorithm for computing both images from a set of digitized electron micrographs of a focus series of uranyl-stained DNA on a thin carbon film.

FRANZGROTE, E. J.

F029 Use of a Solid-State Detector for the Analysis of X-Rays Excited in Silicate Rocks by Alpha-Particle Bombardment

E. J. Franzgrote

Advances in X-Ray Analysis, Vol. 15, pp. 388–406, Plenum Publishing Corporation, New York, 1972

The analysis of alpha-excited X-rays has been studied as a possible addition to the alpha-scattering technique used on the Surveyor spacecraft for the first *in situ* chemical

analyses of the lunar surface. Targets of pure elements, simple compounds, and silicate rocks have been exposed to alpha particles and other radiation from a curium-244 source and the resulting X-ray spectra measured by means of a cooled lithium-drifted silicon detector and pulse-height analysis.

The study shows that the addition of an X-ray mode to the alpha-scattering analysis technique would result in a significant improvement in analytical capability for the elements. In particular, important indicators of geochemical differentiation between certain elements (that are only marginally separated in an alpha-scattering and alpha-proton analysis) may be determined quantitatively by measuring the alpha-excited X-rays. An X-ray detector is under consideration as an addition to an alpha-scattering instrument now under development for possible use on a Mars-lander mission.

FRASER, S. J.

F030 **A Re-evaluation of Material Effects on Microbial Release From Solids**

D. M. Taylor, S. J. Fraser (The Boeing Company), E. A. Gustan (The Boeing Company), R. L. Olson (The Boeing Company), and R. H. Green

Life Sciences and Space Research X, pp. 23–28, Akademie-Verlag, Berlin, 1972

For abstract, see Taylor, D. M.

FRAUENHOLZ, R. B.

F031 **A Summary of the Pioneer 10 Maneuver Strategy**

R. B. Frauenholz and J. E. Ball

JPL Quarterly Technical Review, Vol. 2, No. 3, pp. 46–62, October 1972

The Pioneer Project placed a number of interesting and precise requirements on the navigation of the Pioneer 10 flyby mission to Jupiter during 1972–1973. To satisfy these requirements the Pioneer Navigation Team employed a number of versatile computer programs to evaluate the strategies and maneuver sequences required to execute midcourse corrections. This article summarizes the Pioneer 10 mission objectives and the midcourse strategies used to satisfy these objectives.

FRAZER, R.

F032 **Fixation of Virgin Lunar Surface Soil**

J. M. Conley, R. Frazer, and W. A. Cannon

Technical Memorandum 33-521, February 1, 1972

For abstract, see Conley, J. M.

FRENCH, R. L.

F033 **Mariner 9 Propulsion Subsystem Performance During Interplanetary Cruise and Mars Orbit Insertion**

M. J. Cork, R. L. French, C. J. Leising, and D. D. Schmit

JPL Quarterly Technical Review, Vol. 2, No. 1, pp. 113–122, April 1972

For abstract, see Cork, M. J.

FYMAT, A. L.

F034 **Jones's Matrix Representation of Optical Instruments: 2. Fourier Interferometers (Spectrometers and Spectropolarimeters)**

A. L. Fymat

Appl. Opt., Vol. 10, No. 12, pp. 2711–2716, December 1971

The author's method of matrix synthesis of optical components and instruments is applied to the derivation of Jones's matrices appropriate for Fourier interferometers (spectrometers and spectropolarimeters). These matrices are obtained for both the source beam and the detector beam. In the course of synthesis, Jones's matrices of the various reflectors (plane mirrors; retroreflectors: roofed mirror, trihedral and prism cube corner, cat's eye) used by these interferometers are also obtained.

F035 **Polarization Effects in Fourier Spectroscopy: |I. |Coherency Matrix Representation**

A. L. Fymat

Appl. Opt., Vol. 11, No. 1, pp. 160–173, January 1972

A general analytical method using the formalisms of polarization coherency and Jones's matrices is provided for the evaluation of all polarization effects in fourier spectroscopy. The method applies to any incident state of arbitrary (complete, random, or partial) polarization. Inversely, it may also be used for determining the intensity and state of polarization of the source of light. TE- and TM-mode reflectivity and transmissivity for beam splitters and the dependence of these quantities on the incident polarization are obtained. It is demonstrated that three different efficiencies for these optical components must be introduced. Interferometer efficiency expressions for the source beam and the detector beam are also derived and shown to be essentially different from

the previous efficiencies. Polarization effects of beam splitters, reflectors, and their composite combinations (interferometers) are investigated in detail. General conditions for complete or restricted polarization compensation are derived. Theoretical signal-to-noise ratio expressions for both the source beam and the detector beam are also obtained; these formulas specifically account for the incident state of polarization, the polarization effects of the interferometer, and make use of the exact expressions for the appropriate interferometer efficiency. In an appendix, a brief comparison is made between some usual representations of the state of wave polarization.

GALE, G.

G001 DSN Progress Report for November–December 1971: Overseas 64-m Hydrostatic Bearing Performance

G. Gale

Technical Report 32-1526, Vol. VII, pp. 154–158, February 15, 1972

The first azimuth rotation of the 64-m antenna under construction at the Ballima Deep Space Station (Australia) was made June 12, 1971. Film height records, profile records, and a bull gear reference level survey were made during this and subsequent rotations. This article includes the summary of data collected during these rotations.

GALLILY, I.

G002 On the Orientation of Nonspherical Particles at Solid Surfaces: A Method of Analysis

I. Gallily

J. Colloid Interface Sci., Vol. 37, No. 2, pp. 403–409, October 1971

The relation between the projected and true linear measures of nonspherical particles at solid surfaces is discussed in terms of an orientation distribution function. It is shown that this function can be determined by a geometric method, which is tested on spheroidal bacterial spores.

GARDNER, J. A.

G003 Solar Electric Propulsion System Integration Technology (SEPSIT) Final Report: Encke Rendezvous Mission and Space Vehicle Functional Description

J. A. Gardner

Technical Memorandum 33-583, Vol. II, November 15, 1972

This memorandum is the final report on the Solar Electric Propulsion System Integration Technology study conducted at JPL. This volume describes in detail the solar electric propulsion (SEP) space vehicle and the mission to which it is applied. It includes a detailed functional description of the SEP thrust subsystem along with its technical specifications and requirements as are known at this time.

Detailed analyses that were performed in support of the SEP module thrust subsystem functional description are contained in Volume III of this memorandum series. Volume I contains a technical summary of the work documented in Volumes II and III.

G004 Solar Electric Propulsion System Integration Technology (SEPSIT) Final Report: Supporting Analyses

J. A. Gardner

Technical Memorandum 33-583, Vol. III, November 15, 1972

This memorandum is the final report on the Solar Electric Propulsion System Integration Technology study conducted at JPL. This volume contains detailed analyses that were performed in support of the solar electric propulsion (SEP) module thrust subsystem functional description that is presented in Volume II of this memorandum series.

Volume II describes in detail the SEP space vehicle and the mission to which it is applied. A technical summary of the work documented in Volumes II and III is presented in Volume I.

GARRISON, G. W.

G005 Telecommunications System Design for the Mariner Mars 1971 Spacecraft

F. J. Taylor and G. W. Garrison

Technical Memorandum 33-535, May 1, 1972

For abstract, see Taylor, F. J.

GARTH, D. R.

G006 Integration of a Breadboard Power Conditioner With a 20-cm Ion Thruster

T. D. Masek, T. W. Macie, E. N. Costogue, W. J. Muldoon (Hughes Aircraft Company), D. R. Garth (Hughes Aircraft Company), and G. C. Benson (Hughes Aircraft Company)

J. Spacecraft Rockets, Vol. 9, No. 2, pp. 71–78, February 1972

For abstract, see Masek, T. D.

GELLER, E. N.

G007 Nature of Two-Particle Correlations in Atoms

E. N. Geller and M. Geller

J. Chem. Phys., Vol. 57, No. 4, p. 1814, August 15, 1972

This article presents an analytical evaluation of radial integrals of the form

$$I_n(Z') = \int_0^\infty \int_0^\infty \exp\left[-2Z'(r_1 + r_2)\right]$$

$$\times \frac{r_1^{n+1} r_2^{n+1}}{(r_1^2 + r_2^2)^{n-0.5}} dr_1\, dr_2$$

The first few integrals are given as well as a recurrence relation for successive integrals.

GELLER, M.

G008 The James Wavefunction for the Ground State of H_2^+

M. Geller and O. Ludwig (Villanova University)

Chem. Phys. Lett., Vol. 12, No. 2, p. 403, December 15, 1971

A recent article in *Chem. Phys. Lett.* by Jackson, McEachran, and Cohen on the James wavefunction for the ground state of H_2^+ duplicates and thereby confirms previous calculations by the present authors (published in *J. Chem. Phys.*, 1962).

G009 Nature of Two-Particle Correlations in Atoms

E. N. Geller and M. Geller

J. Chem. Phys., Vol. 57, No. 4, p. 1814, August 15, 1972

For abstract, see Geller, E. N.

GENSEL, D. R.

G010 Surface Distribution of Microorganisms in Antarctic Dry-Valley Soils: A Martian Analog

R. E. Cameron, H. P. Conrow, D. R. Gensel, G. H. Lacy, and F. A. Morelli

Antarctic J. U.S., Vol. VI, No. 5, pp. 211–213, September–October 1971

For abstract, see Cameron, R. E.

GEORGEVIC, R. M.

G011 The Solar Radiation Pressure on the Mariner 9 Mars Orbiter

R. M. Georgevic

Technical Memorandum 33-582, December 15, 1972

The refined mathematical model of the force created by the light pressure of the Sun has been used to compute the solar-radiation pressure force acting on the Mariner 9 (Mariner Mars 1971) spacecraft, taking into account the reflectivity characteristics of all its components. As demonstrated in this memorandum, the results have been compared with values obtained from Mariner 9 observations during the cruise phase and found to be in agreement within 0.1% of the experimental values.

GILLESPIE, A. R.

G012 An Orthographic Photomap of the South Pole of Mars From Mariners 6 and 7

A. R. Gillespie and J. M. Soha

Icarus, Vol. 16, No. 3, pp. 522–527, June 1972

Television pictures of the south polar regions of Mars obtained by the Mariner 6 and 7 spacecraft in 1969 are rectified to a standard mapping projection using computer image processing techniques. Mosaicking of these pictures produces the first photomap of the entire south polar cap.

GILLEY, G. C.

G013 The STAR (Self-Testing and Repairing) Computer: An Investigation of the Theory and Practice of Fault-Tolerant Computer Design

A. Aviẑienis, G. C. Gilley, F. P. Mathur, D. A. Rennels, J. A. Rohr, and D. K. Rubin

IEEE Trans. Computers, Vol. C-20, No. 11, pp. 1312–1321, November 1971

For abstract, see Aviẑienis, A.

GINGO, P. J.

G014 Neutron Radiation Characteristics of Plutonium Dioxide Fuel

M. Taherzadeh and P. J. Gingo (Akron State University)

Nucl. Technol., Vol. 15, No. 3, pp. 396–410, September 1972

For abstract, see Taherzadeh, M.

GODFREY, J. F.

G015 The Effect of Temperature on the Survival of Microorganisms in a Deep Space Vacuum

C. A. Hagen, J. F. Godfrey, and R. H. Green

Space Life Sci., Vol. 3, No. 2, pp. 108–117, December 1971

For abstract, see Hagen, C. A.

GOETZ, A. F. H.

G016 Apollo 12 Multispectral Photography Experiment

A. F. H. Goetz, F. C. Billingsley,
J. W. Head (Bellcomm, Inc.),
T. B. McCord (Massachusetts Institute of Technology), and E. Yost (Long Island University)

Proceedings of the Second Lunar Science Conference, Houston, Texas, January 11–14, 1971, Vol. 3, pp. 2301–2310, The M.I.T. Press, 1971

Apollo 12 carried a four-band camera system for orbital lunar surface photography. New image processing techniques were developed to delineate accurately subtle spectral reflectivity differences, independent of brightness differences within selected areas of the lunar surface. Ground-based photoelectric photometry was used to verify large area color differences.

In general, the highlands areas covered are quite uniform in normalized spectral reflectivity on a 200-m scale. Differences were detected in the Descartes region, which can be attributed to exposed rock in the ejecta blanket of Dollond E. No color difference was detected across the mare-highland boundary at Fra Mauro. With few exceptions, the highlands areas studied are extremely uniform and the variation in spectral reflectivity in the wavelength region covered seen in any frame is less than that found in some Apollo 12 core samples.

GOLDER, J.

G017 Thermal Noise in Space-Charge-Limited Hole Current in Silicon

A. Shumka, J. Golder, and M.-A. Nicolet

JPL Quarterly Technical Review, Vol. 2, No. 2, pp. 72–76, July 1972

For abstract, see Shumka, A.

GOLDSTEIN, R.

G018 Ion Thruster Performance Calibration

E. V. Pawlik, R. Goldstein, D. J. Fitzgerald, and R. W. Adams

Preprint 72-475,
AIAA Ninth Electric Propulsion Conference, Bethesda, Maryland, April 17–19, 1972

For abstract, see Pawlik, E. V.

GOLDSTEIN, R. M.

G019 Radar Observations of Mercury

R. M. Goldstein

Astron. J., Vol. 76, No. 10, pp. 1152–1154, December 1971

Radar scattering properties of the planet Mercury at 12.5-cm wavelength are presented. Data from two inferior conjunctions show that backscattering anomalies can be attributed to specific regions on the planetary surface. The rotation period of Mercury is measured to better than 0.4%.

G020 Mars Radar Observations, a Preliminary Report

G. S. Downs, R. M. Goldstein, R. R. Green, and G. A. Morris

Science, Vol. 174, No. 4016, pp. 1324–1327, December 24, 1971

For abstract, see Downs, G. S.

GOODWIN, P. S.

G021 DSN Progress Report for November–December 1971: Helios Mission Support

P. S. Goodwin

Technical Report 32-1526, Vol. VII, pp. 17–24, February 15, 1972

Project Helios is a joint Deep Space Project between the Federal Republic of West Germany and the United States. Two solar orbiting spacecraft are planned: the first to be launched in mid-1974 and the second in late 1975. The spacecraft will have a perihelion of approximately 0.25 AU and an aphelion of 1.0 AU. These highly

elliptical orbits will come closer to the Sun than any known or presently planned deep space venture to date. Prior volumes of this report have provided the reader with an overview of the division of responsibilities between West Germany and the United States, the Project management organization, and the spacecraft design—including a functional description of its radio system and the latter's interface with the Deep Space Network. This article highlights the supporting activities of the TDS organization during the Fifth Helios Joint Working Group meeting, which was held October 20–27, 1971 at Oberpfaffenhofen, West Germany.

G022   DSN Progress Report for January–February 1972: Helios Mission Support

P. S. Goodwin

Technical Report 32-1526, Vol. VIII, pp. 16–19, April 15, 1972

Project Helios is a cooperative U.S./West German space effort. Two unmanned solar-orbiting spacecraft are planned for launching: the first in mid-1974, and the second in late 1975. These spacecraft will follow a trajectory that brings them closer to the Sun (under 0.3 AU) than any known spacecraft to date. Using specially designed instruments, the Helios spacecraft will enter unexplored regions near the Sun in an attempt to expand mankind's knowledge of how the Sun influences life on Earth.

In addition to the scientific goals, Project Helios presents many challenging technological problems—none the least of which is to design a spacecraft which will endure 16 times the amount of heat from the Sun (at 0.25 AU) than is normally received on Earth. In addition, the spacecraft will reach its closest approach to the Sun (perihelion) only 90 days after launch. These and other facets of this unique mission were described in Volumes II through VI of this series. Volume VII treated the JPL/Tracking and Data System activities during the Sixth Helios Joint Working Group Meeting held at Oberpfaffenhofen, West Germany, October 20 to 27, 1971. This article covers the DSN Helios activities since that date.

G023   DSN Progress Report for March–April 1972: Helios Mission Support

P. S. Goodwin

Technical Report 32-1526, Vol. IX, pp. 33–34, June 15, 1972

Project Helios is a joint space endeavor between the United States and West Germany, the objective of which is to place two unmanned spacecraft into heliocentric orbits whose perihelion will be closer to the Sun than any previously or presently planned free-world deep space undertaking. The West German government is designing and fabricating the spacecraft and will conduct mission operations. NASA will provide the launch vehicle, the launch facilities, and the major portion of the tracking. The launch of the first spacecraft is planned for mid-1974 and the second in late-1975. This article deals with the DSN support to Project Helios during March and April 1972.

G024   DSN Progress Report for May–June 1972: Helios Mission Support

P. S. Goodwin

Technical Report 32-1526, Vol. X, pp. 14–19, August 15, 1972

Project Helios, named after the ancient Greek God of the Sun, is a joint undertaking by the Federal Republic of West Germany and the United States of America, who divide the project responsibilities. Each country has a Project Manager who is responsible for his own country's contribution as determined by the International Agreement. In addition, the two Project Managers act as co-Chairmen of the internationally structured Helios Joint Working Group Meetings which are held semi-annually and alternate between the two countries. The project objective is to launch into heliocentric orbits two unmanned scientific spacecraft that will come closer to the Sun than any known or planned spacecraft to date for the purpose of obtaining further knowledge about the Sun and its influence upon life on Earth. The plan is to launch the first spacecraft in mid-1974 and the second in late 1975.

Prior articles of this series described the history and organization of this program, the spacecraft configuration and trajectory, its telecommunications system, and the results of Joint Working Group Meetings. This article deals with the activities and highlights of the Sixth Helios Joint Working Group Meeting which was held at JPL in April–May 1972.

G025   DSN Progress Report for September–October 1972: Helios Mission Support

P. S. Goodwin

Technical Report 32-1526, Vol. XII, pp. 5–9, December 15, 1972

Project Helios is a joint deep space project of the Federal Republic of West Germany and the United States. Two solar orbiting spacecraft are planned, the first to be launched in mid-1974 and the second in late 1975. The spacecraft will have a perihelion of approximately 0.25 AU and an aphelion of 1.0 AU. These spacecraft with their highly elliptical orbits will come closer to the Sun than any previous or planned spacecraft.

Prior articles of this series described the history and organization of this program, the spacecraft configura-

tion and trajectory, its telecommunications system, and the results of the semi-annual Helios Joint Working Group Meetings which are held alternately in the United States and the Federal Republic of West Germany. This article deals with DSN activities since the Sixth Helios Joint Working Group Meeting, which was held at JPL in April–May 1972.

GOSLINE, R. M.

G026 DSN Progress Report for January–February 1972: Antenna Drive System Performance Evaluation Using PN Codes

R. M. Gosline, E. B. Jackson, and J. D. Campbell

Technical Report 32-1526, Vol. VIII, pp. 74–79, April 15, 1972

A maintenance tool for quick and easy evaluation of the performance of an antenna drive system is described and preliminary results are given. The technique uses a pseudo-noise (PN) code as a system input signal and correlates the system output with all possible states of the input pseudo-noise code. The resulting correlation function has the same shape as the system response to an impulse input and can be considered in the same way. A program description, block diagrams, and some system response curves are given.

G027 DSN Progress Report for July–August 1972: DSN Research and Technology Support

R. M. Gosline

Technical Report 32-1526, Vol. XI, pp. 132–134, October 15, 1972

This article summarizes the activities of the Development Support Group for the 2-month period ending August 15, 1972. The activities are arranged according to whether they were performed at the Venus Deep Space Station (DSS 13) or at the Microwave Test Facility, and are further subdivided as to the section receiving support. Activities include operational clock synchronization, precision antenna-gain measurements, weak-source observations, pulsar observations, planetary radar, and Mars Deep Space Station (DSS 14) 400-kW transmitter support.

GOTTLIEB, P.

G028 A Surface-Layer Representation of the Lunar Gravitational Field

L. Wong (Aerospace Corporation),
G. Buechler (Aerospace Corporation),
W. Downs (Aerospace Corporation), W. L. Sjogren,
P. M. Muller, and P. Gottlieb

J. Geophys. Res., Vol. 76, No. 26, pp. 6220–6236, September 10, 1971

For abstract, see Wong, L.

G029 Lunar Gravity via Apollo 14 Doppler Radio Tracking

W. L. Sjogren, P. Gottlieb, P. M. Muller, and W. Wollenhaupt (Manned Spacecraft Center)

Science, Vol. 175, No. 4018, pp. 165–168, January 14, 1972

For abstract, see Sjogren, W. L.

GRAULING, C. R.

G030 DSN Progress Report for May–June 1972: Performance Capabilities of the Data Decoder Assembly Through the Viking Era

C. R. Grauling and N. J. Jones

Technical Report 32-1526, Vol. X, pp. 164–167, August 15, 1972

The Data Decoder Assembly will be performing several different telemetry processing functions at various antenna sites through the Mariner Venus–Mercury 1973, Helios, and Viking eras. These include sequential decoding, block decoding, and high-rate formatting of telemetry data. This article describes how these functions have been implemented by either test or operational software.

GREEN, R. H.

G031 A Re-evaluation of Material Effects on Microbial Release From Solids

D. M. Taylor, S. J. Fraser (The Boeing Company),
E. A. Gustan (The Boeing Company),
R. L. Olson (The Boeing Company), and
R. H. Green

Life Sciences and Space Research X, pp. 23–28, Akademie-Verlag, Berlin, 1972

For abstract, see Taylor, D. M.

G032 Microbiological Sampling of Returned Surveyor III Electrical Cabling

M. D. Knittel, R. H. Green, and
M. S. Favero (U.S. Public Health Department)

Proceedings of the Second Lunar Science Conference, Houston, Texas, January 11–14, 1971, Vol. 3, pp. 2715–2719, The M.I.T. Press, 1971

For abstract, see Knittel, M. D.

G033 The Effect of Temperature on the Survival of Microorganisms in a Deep Space Vacuum

C. A. Hagen, J. F. Godfrey, and R. H. Green

Space Life Sci., Vol. 3, No. 2, pp. 108–117, December 1971

For abstract, see Hagen, C. A.

GREEN, R. R.

G034 Mars Radar Observations, a Preliminary Report

G. S. Downs, R. M. Goldstein, R. R. Green, and G. A. Morris

Science, Vol. 174, No. 4016, pp. 1324–1327, December 24, 1971

For abstract, see Downs, G. S.

GREEN, W. B.

G035 Recent Developments in Digital Image Processing at the Image Processing Laboratory at the Jet Propulsion Laboratory

D. A. O'Handley and W. B. Green

Proc. IEEE, Vol. 60, No. 7, pp. 821–828, July 1972

For abstract, see O'Handley, D. A.

GREENWOOD, R. F.

G036 Results of the 1970 Balloon Flight Solar Cell Standardization Program

R. F. Greenwood and R. L. Mueller

Technical Report 32-1575, December 1, 1972

For the eighth consecutive year, high-altitude calibration of solar cells was accomplished with the aid of free-flight balloons. Flights were conducted to an altitude of 36,576 m (120,000 ft), which is above 99.5% of the Earth's atmosphere where all water vapor and significant ozone bands are absent. Solar cells calibrated in this manner are recovered and used as intensity references in solar simulators and in terrestrial sunlight. Balloon-calibrated solar cells were made available by JPL to NASA centers and other government agencies through a cooperative effort. An attempt to fly radiometers to measure the solar constant was aborted because of a balloon failure at launch. This report discusses the method employed for high-altitude balloon flight solar-cell calibration. Also presented are the data collected on 52 standard solar cells on two flights conducted during July and August 1970.

Solar cells flown repeatedly on successive flights have shown correlation of better than ±1.0%.

GRUMM, R.

G037 Mariner Mars 1971 Data Storage Subsystem Final Report

R. Grumm

Technical Memorandum 33-554, September 15, 1972

A digital tape recorder was used on the Mariner Mars 1971 spacecraft to record television and scientific data. Data was recorded at 132 kbits/s and reproduced at one of five available rates (16.2, 8.1, 4.05, 2.025, or 1.0125 kbits/s) selected by ground command to be congruous with the spacecraft-to-Earth communications link performance. The transport mechanism contained 167 m of 1.2-cm magnetic recording tape. A single motor was used to drive the peripheral drive transport.

During development of the design, "stick–slip" problems were encountered and the selection of 3M 20250 tape, made by Minnesota Mining and Manufacturing, was an important part of the solution to this problem. The design life of 2400 tape passes was achieved during the mission.

GUELACHVILI, G.

G038 Fourier Spectroscopy With a One-Million-Point Transformation (Translation From the Original Published in the Nouvelle Revue d'Optique Appliquée, Vol. 1, pp. 3–22, 1970)

J. Connes (National Center for Scientific Research, Orsay, France), H. Delouis (National Center for Scientific Research, Orsay, France), P. Connes (National Center for Scientific Research, Orsay, France), G. Guelachvili (National Center for Scientific Research, Orsay, France), J.-P. Maillard (National Center for Scientific Research, Orsay, France), and G. Michel (National Center for Scientific Research, Orsay, France)

Technical Memorandum 33-525, March 15, 1972

For abstract, see Connes, J.

GULKIS, S.

G039 Radio Emission From the Major Planets—The Thermal Component

S. Gulkis

Measurements of the radio emission from all the major planets have been reported at millimeter and centimeter wavelengths, and from Jupiter and Saturn at decimeter wavelengths as well. This achievement has become possible with the development of low-noise receivers and large aperture radiotelescopes. The measured brightness temperatures deduced from these measurements exceed the expected effective temperatures calculated from solar heating, and the observed spectra of the individual planets do not follow the classical blackbody spectral form. Nevertheless, the observed radiation is believed to be of thermal origin, except for the planet Jupiter, where a non-thermal component is known to contribute to its spectrum. The observed spectra are believed to depart from the simple blackbody form because of the dependence of the atmospheric emissivity on wavelength. The gross features of the major planet radio spectra can be explained in terms of thermal emission by an atmosphere whose temperature increases with depth and in which ammonia is assumed to be the principal source of opacity.

G040 Jupiter: New Evidence of Long-Term Variations of Its Decimeter Flux Density

M. J. Klein, S. Gulkis, and C. T. Stelzried

Astrophys. J., Vol. 176, No. 2, Pt. 2, pp. L85–L88, September 1, 1972

For abstract, see Klein, M. J.

GUPTA, K. K.

G041 VISCEL—A General-Purpose Computer Program for Analysis of Linear Viscoelastic Structures: User's Manual

K. K. Gupta, F. A. Akyuz, and E. Heer

Technical Memorandum 33-466, Vol. I, Rev. 1, October 1, 1972

This revised user's manual describes the details of a general-purpose computer program VISCEL (VISCoE-Lastic analysis) which has been developed for an analysis of equilibrium problems of linear thermoviscoelastic structures. The program, an extension of the linear equilibrium problem solver ELAS, is an updated and extended version of its earlier form (written in FORTRAN II for the IBM 7094 computer). A synchronized material property concept utilizing incremental time steps and the finite-element matrix displacement approach has been adopted for the current analysis. Resulting recursive equations incorporating memory of material properties are solved at the end of each time step of the general step-by-step procedure in the time domain. A special

option enables employment of constant time steps in the logarithmic scale, thereby reducing computational efforts resulting from accumulative material memory effects. A wide variety of structures with elastic or viscoelastic material properties can be analyzed by VISCEL.

The program is written in FORTRAN V language for the UNIVAC 1108 computer operating under the EXEC 8 system. Dynamic storage allocation is automatically effected by the program, and the user may request up to 195K core memory in a 260K UNIVAC 1108/EXEC 8 machine. The physical program VISCEL, consisting of about 7200 instructions, has four distinct links (segments), and the compiled program occupies a maximum of about 11711-word decimal core storage. VISCEL is stored on magnetic tape and is available from the Computer Software Management and Information Center (COSMIC).

G042 VISCEL—A General-Purpose Computer Program for Analysis of Linear Viscoelastic Structures: Program Manual

K. K. Gupta and F. A. Akyuz

Technical Memorandum 33-466, Vol. II, July 15, 1972

VISCEL is a general-purpose computer program developed for the equilibrium analysis of linear viscoelastic structures. The program is written in FORTRAN V language to operate on the UNIVAC 1108 computer under the EXEC 8 operating system. VISCEL, an extension of the linear equilibrium problem solver ELAS, is an updated and extended version of its earlier form written for the IBM 7094 computer. The users may change the size of labeled COMMON to accommodate the particular problem to be solved without recompilation; it is possible to utilize up to 195K core memory in a 260K UNIVAC 1108/EXEC 8 machine. The physical program, consisting of approximately 7200 instructions, is stored on magnetic tape and is available from the Computer Software Management and Information Center (COSMIC), the NASA agency for the distribution of computer programs.

Finite-element matrix displacement approach coupled with the synchronized material property concept, utilizing incremental time steps, has been adopted for the present solution. The step-by-step procedure involves solution of recursive equations in the time domain, which takes into account the memory of material properties. Incremental and accumulative displacements and stresses are obtained at the end of each such time step. In order to minimize the extent of computations resulting from accumulative effects of material memory, the program provides an option which enables the employment of constant time steps in the logarithmic scale. Vol. I, Rev. 1, of this memorandum describes the user's man-

ual, whereas the present volume is concerned with program documentation.

G043 Dynamic Response Analysis of Geometrically Non-linear Structures Subjected to High Impact

K. K. Gupta

Int. J. Numer. Methods Eng., Vol. 4, No. 2, pp. 163-174, March-April 1972

This article presents an efficient digital computer method for the determination of propagation of elastic stresses and deformations in certain geometrically non-linear structures subjected to high-impact loading. The finite-element matrix displacement approach utilizing curved quadrilateral shell elements in conjunction with a nodewise predictor-corrector method employing Runge-Kutta extrapolation techniques has been adopted for the present solution.

The related computer program written in FORTRAN V for the UNIVAC 1108 computer has proved to be effective for the solution of a range of practical problems including rectangular and cylindrical panels. Numerical results are presented for a relevant structure, the cell container and the negative electrode of an impact-resistant battery subjected to high impact, simulating its free landing on a planetary surface.

G044 Solution of Eigenvalue Problems by Sturm Sequence Method

K. K. Gupta

Int. J. Numer. Methods Eng., Vol. 4, No. 3, pp. 379-404, May-June 1972

This article presents a generalized eigenvalue algorithm along with the complete listing of the associated computer program which may be conveniently utilized for the efficient solution of certain broad classes of eigenvalue problems. Extensive applications of the procedure are envisaged in the analysis of many important engineering problems, such as stability and natural frequency analysis of practical discrete structural systems, idealized by the finite-element technique. The procedure based on the Sturm sequence method is accurate and fast, possessing several significant advantages over other known methods of such analysis. Numerical results are also presented for two representative structural engineering problems.

GUSTAN, E. A.

G045 A Re-evaluation of Material Effects on Microbial Release From Solids

D. M. Taylor, S. J. Fraser (The Boeing Company),
E. A. Gustan (The Boeing Company),
R. L. Olson (The Boeing Company), and
R. H. Green

Life Sciences and Space Research X, pp. 23-28, Akademie-Verlag, Berlin, 1972

For abstract, see Taylor, D. M.

HADEK, V.

H001 Superconductivity in the Alkali Metal Intercalates of Molybdenum Disulphide

R. B. Somoano, V. Hadek, and A. Rembaum

JPL Quarterly Technical Review, Vol. 2, No. 2, pp. 83-89, July 1972

For abstract, see Somoano, R. B.

HAGEN, C. A.

H002 The Effect of Temperature on the Survival of Microorganisms in a Deep Space Vacuum

C. A. Hagen, J. F. Godfrey, and R. H. Green

Space Life Sci., Vol. 3, No. 2, pp. 108-117, December 1971

A Space Molecular Sink Research Facility (Molsink) was used to evaluate the ability of microorganisms to survive the vacuum of outer space. This facility could be programmed to simulate flight spacecraft vacuum environments at pressures in the 10^{-10}-torr range and thermal gradients (30 to 60°C) closely associated to surface temperatures of inflight spacecraft.

Initial populations of *Staphylococcus epidermidis* and a *Micrococcus* sp. were reduced approximately 1 log while exposed to -105 and 34°C, and approximately 2 logs while exposed to 59°C for 14 days in the vacuum environment. Spores of *Bacillus subtilis* var. *niger* were less affected by the environment. Initial spore populations were reduced 0.2, 0.3, and 0.8 log during the 14-day vacuum exposure at -124, 34, and 59°C, respectively.

HAINES, E. L.

H003 Precise Coordinate Control in Fission Track Uranium Mapping

E. L. Haines

Nucl. Instr. Methods, Vol. 98, No. 1, pp. 183-184, January 1, 1972

An important problem in fission track uranium mapping is coordinate control; it is hard to relate locations of

track concentrations on the detector to the locations of the uranium-rich minerals on the polished section. This article presents a method for precisely locating mineral grains related to uranium concentrations revealed by the track detector. The method uses a congruent transformation of the coordinate system of the detector to the coordinate system of the polished rock section.

HALL, J. R.

H004 DSN Progress Report for July–August 1972: Network Control System

J. R. Hall

Technical Report 32-1526, Vol. XI, pp. 5–11, October 15, 1972

This article provides: (1) background material describing the philosophy leading to a Network Control System (NCS) function using data-processing equipment separate from that used by flight projects, (2) key characteristics of the NCS, (3) a listing of the functional requirements for each NCS subsystem, (4) a generic subsystem data-flow description, and (5) an overall NCS data-flow description.

HAMILTON, G.

H005 DSN Progress Report for November–December 1971: Post-Detection Subcarrier Recording Equipment Implementation for Analog Recording Playback

G. Hamilton

Technical Report 32-1526, Vol. VII, pp. 182–184, February 15, 1972

The post-detection subcarrier recording reproduce capability has been implemented at the playback facility for playback of analog tapes recorded at stations in the Deep Space Instrumentation Facility. The primary purpose for this facility is to reproduce the analog tape data (which could not be played back at the stations) if a failure in the station subcarrier demodulator assembly or on the spacecraft occurs. The analog data is used to produce digital data tapes and to generate data for input to the Space Flight Operations Facility. Reproduce modes of baseband playback and telemetry data bit stream playback are discussed.

H006 DSN Progress Report for May–June 1972: Post-Detection Subcarrier Recording Subsystem

L. I. DeGennaro and G. Hamilton

Technical Report 32-1526, Vol. X, pp. 161–163, August 15, 1972

For abstract, see DeGennaro, L. I.

HANEL, R. A.

H007 Infrared Spectroscopy Experiment on the Mariner 9 Mission: Preliminary Results

R. A. Hanel (Goddard Space Flight Center),
B. J. Conrath (Goddard Space Flight Center),
W. A. Hovis (Goddard Space Flight Center),
V. G. Kunde (Goddard Space Flight Center),
P. D. Lowman (Goddard Space Flight Center),
J. C. Pearl (Goddard Space Flight Center),
C. Prabhakara (Goddard Space Flight Center),
B. Schlachman (Goddard Space Flight Center), and
G. V. Levin (Biospherics Incorporated)

Science, Vol. 175, No. 4019, pp. 305–308, January 21, 1972

The Mariner 9 infrared spectroscopy experiment has provided good-quality spectra of many areas of Mars, predominantly in the southern hemisphere. Large portions of the thermal emission spectra are significantly affected by dust with a silicon oxide content approximately corresponding to that of an intermediate igneous rock, thus implying that Mars has undergone substantial geochemical differentiation. Derived temperature profiles indicate a warm daytime upper atmosphere with a strong warming over the south polar cap. Atmospheric water vapor is clearly observed over the south polar area and less strongly over other regions.

HANSON, R. J.

H008 A Computational Algorithm for Sequential Estimation

R. J. Hanson and P. Dyer (Imperial Chemical Industries Ltd.)

Comput. J., Vol. 14, No. 3, pp. 285–290, August 1971

This article details a highly reliable computational algorithm for sequential least-squares estimation (filtering) with process noise. The various modular components of the algorithm are described in detail so that their conversion to computer code is straightforward. These components can also be used to solve any least-squares problem with possibly rank-deficient coefficient matrices.

HARDY, J.

H009 Gain Calibration of a Horn Antenna Using Pattern Integration

A. C. Ludwig, J. Hardy, and R. Norman

Technical Report 32-1572, October 1, 1972

For abstract, see Ludwig, A. C.

HARDY, J. P.

H010 Rapid Determination of Twenty Amino Acids by Gas Chromatography

J. P. Hardy and S. L. Kerrin

Anal. Chem., Vol. 44, No. 8, pp. 1497–1499, July 1972

Determination of amino acids by gas chromatographic separation of appropriate volatile derivatives has been described in numerous literature reports. For all methods, the limiting step in analyses of multiple samples is the gas chromatographic determination time, since preparation of volatile derivatives of several samples may be carried along in parallel, but each gas chromatographic analysis must be performed sequentially.

This article presents a method for the preparation of volatile *N*-trimethylsilyl-*O*-*n*-butyl ester (TMSi-butyl) derivatives of 20 amino acids and the conditions under which they can be separated, in less than 35 minutes, on a lightly-loaded textured-glass-bead gas chromatographic column.

H011 Carbon-to-Metal Chlorine Exchange: IV. Mercuric Salt Promoted Acetolysis of exo-Norbornyl Chloride

J. P. Hardy, A. F. Diaz, and S. Winstein

J. Am. Chem. Soc., Vol. 94, No. 7, pp. 2363–2370, April 5, 1972

Mercuric salts enhance the rate of acetolysis of *exo*-norbornyl chloride, I-Cl. Rate constants have been measured for solvolysis, k_t, exchange of radiolabeled chlorine between mercuric chloride and I-Cl, k_e, and loss of optical activity, k_α. Relative solvolytic rate constants for mercuric acetate, chloromercuric acetate, and mercuric chloride-promoted reactions at 75°C are 1820, 89, and 1, respectively. Since the rate enhancements are much greater than expected for normal salt effects, the mercuric salts must be intimately involved in the ionization process. For the mercuric chloride-promoted reaction,

$$\frac{k_\alpha}{k_t} = 9.6$$

indicating that some 90% of the ion pairs return to covalent I-Cl in the poorly dissociating acetic acid solvent. The ratio

$$\frac{k_{rac}}{k_e} = \frac{k_\alpha - k_t}{k_e} = 2.0$$

for mercuric chloride can be interpreted in terms of one or more ion-pair intermediates $I^+HgCl_3^-$ of differing structure. In a manner similar to $HgCl_2$, $Hg(OAc)_2$ facilitates C—Cl bond heterolysis, and carries the solvent anion, OAc^-, into intimate contact with the incipient carbonium ion, which makes the chloromercuric diacetate anion a unique "leaving group."

HARPER, L. H.

H012 DSN Progress Report for July–August 1972: Reducing the Complexity of Calculating Syndromes for Error-Correcting Codes

L. H. Harper and J. E. Savage

Technical Report 32-1526, Vol. XI, pp. 89–91, October 15, 1972

The calculation of the syndrome—the first step performed by all decoders of linear codes—can require a number of logical operations which grows faster than the square of block length. This article shows that the complexity of syndrome calculation can be reduced for many linear codes by a factor of log of the code block length and that Hamming codes can be decoded with combinational machines having a number of logic elements which is linear with block length.

HARRIS, C. W.

H013 DSN Progress Report for May–June 1972: DSN Telemetry Predicts Generation and Distribution

C. W. Harris and E. S. Burke

Technical Report 32-1526, Vol. X, pp. 210–212, August 15, 1972

The DSN Telemetry System Analysis Group is responsible for generating and/or disseminating the predicted uplink signal levels at the spacecraft, and the predicted downlink signal levels at the deep space stations. Also included in the predictions are the telemetry signal-to-noise ratios. Two different Univac 1108 programs are used to generate these data. The JPL spacecraft-oriented predicts are generated by the Telecommunications Prediction and Analysis Program. The non-JPL spacecraft-oriented predicts are generated by the DSN Telecommunications Prediction Program which is operated by the Telemetry Group of the Network Analysis Team. These predicts are distributed throughout the DSN and to specified project personnel.

HARSTAD, K. G.

H014 One Dimensional Line Radiative Transfer

K. G. Harstad

Technical Memorandum 33-538, April 1, 1972

Integrations over solid angle and frequency are performed in the expressions for the radiant heat flux and local energy loss of a line in a region of strong variation of the source function in one direction. Approximations are given for the coefficients and kernels in the resulting forms, which involve integrals over the physical coordinate.

H015 Review of Laser–Solid Interaction and Its Possibilities for Space Propulsion

K. G. Harstad

Technical Memorandum 33-578,
November 15, 1972

This memorandum surveys the literature on laser–solid-matter interaction and delineates the important regimes of this process. This information is used to discuss the possibility of a laser-induced ablation thruster. It is concluded that such a thruster may be feasible if a sufficiently high-intensity, high-frequency laser beam is available and that further study of laser–solid-matter interaction is needed.

H016 Rational Approximation for the Voigt Line Profile

K. G. Harstad

J. Opt. Soc. Am., Vol. 62, No. 6, pp. 827–828,
June 1972

For many problems of calculating radiative transfer or curves of growth for a line, the Voigt profile is used. This article presents an accurate approximation for this profile in cases where the ratio of the Lorentz semi-half-width to doppler width is not small.

HARTLEY, R. B.

H017 DSN Progress Report for May–June 1972: Apollo Mission Support

R. B. Hartley

Technical Report 32-1526, Vol. X, pp. 41–48,
August 15, 1972

This article describes the support provided by the DSN to the Spaceflight Tracking and Data Network during the Apollo 16 mission. Support was provided by three 26-m- (85-ft-) antenna deep space stations, the 64-m- (210-ft-) antenna Mars Deep Space Station (DSS 14), the Ground Communications Facility, and the Space Flight Operations Facility. Pre-mission and mission activities of the DSN are discussed, and the mission is described.

HASBACH, W. A.

H018 Summary Report on the Development, Design and Test of a 66-W/kg (30-W/lb) Roll-Up Solar Array

W. A. Hasbach and R. G. Ross, Jr.

Technical Report 32-1562, September 15, 1972

This report summarizes the results of a program to develop a 23-m² (250-ft²) roll-up solar array with a power-to-weight ratio exceeding 66 W/kg (30 W/lb). Descriptions of the system design and fabrication of a full-scale engineering development unit are included, the system and development test program results are described, and conclusions are drawn. Special test equipment and test procedures are included, together with comparisons of experimental and analytical results.

HATZENBELER, H.

H019 Infrared Radiometry Experiment on Mariner 9

S. C. Chase, Jr. (Santa Barbara Research Center),
H. Hatzenbeler (Santa Barbara Research Center),
H. Kieffer (University of California, Los Angeles),
E. Miner, G. Münch (California Institute of Technology), and G. Neugebauer (California Institute of Technology)

Science, Vol. 175, No. 4019, pp. 308–309,
January 21, 1972

For abstract, see Chase, S. C., Jr.

HAVENS, W. F.

H020 Scan Pointing Calibration for the Mariner Mars 1971 Spacecraft

W. F. Havens, G. I. Jaivin, G. D. Pace, and R. A. Virzi

Technical Memorandum 33-556, August 1, 1972

This report describes the methods used to calibrate the pointing direction of the Mariner Mars 1971 spacecraft scan platform. Accurate calibration was required to meet the pointing accuracy requirements of the scientific instruments mounted on the platform. A detailed ground calibration was combined with an in-flight calibration utilizing narrow-angle television pictures of stars. Results of these calibrations are summarized.

HEAD, J. W.

H021 Apollo 12 Multispectral Photography Experiment

A. F. H. Goetz, F. C. Billingsley,
J. W. Head (Bellcomm, Inc.),
T. B. McCord (Massachusetts Institute of
Technology), and E. Yost (Long Island University)

*Proceedings of the Second Lunar Science
Conference, Houston, Texas, January 11–14, 1971,*
Vol. 3, pp. 2301–2310, The M.I.T. Press, 1971

For abstract, see Goetz, A. F. H.

HEER, E.

H022 VISCEL—A General-Purpose Computer Program for Analysis of Linear Viscoelastic Structures: User's Manual

K. K. Gupta, F. A. Akyuz, and E. Heer

Technical Memorandum 33-466, Vol. I, Rev. 1,
October 1, 1972

For abstract, see Gupta, K. K.

HELTON, M. R.

H023 Mariner Mars 1971 Television Picture Catalog: Sequence Design and Picture Coverage

P. E. Koskela, M. R. Helton, L. N. Seeley, and
S. J. Zawacki

Technical Memorandum 33-585, Vol. II,
December 15, 1972

For abstract, see Koskela, P. E.

HERR, K. C.

H024 Mariner Mars 1969 Infrared Spectrometer

K. C. Herr (University of California, Berkeley),
P. B. Forney (University of California, Berkeley),
and G. C. Pimentel (University of California,
Berkeley)

Appl. Opt., Vol. 11, No. 3, pp. 493–501,
March 1972

The infrared spectrometer that recorded spectra of the atmosphere and surface of Mars during the Mariner 6 and 7 flyby missions is described. The instrument continuously scanned the 1.9- to 14.4-μ spectral region at 10 s per scan. Approximately 1% spectral resolution was furnished by two rotating, circular, variable interference filters. The spectral region 1.9–6.0 μ was recorded with a PbSe detector cooled to 175 K by radiation to deep space. The spectral region 3.9–14.4 μ was modulated by a cold (175-K) tuning fork chopper and recorded with a mercury-doped germanium detector cooled to 22 K by a Joule–Thomson two-stage (N_2 and H_2) cryostat. The

total weight of the instrument was 17.4 kg (monochromator plus electronics, 11.5 kg; gas delivery system, 5.9 kg), and it consumed 11 W of power.

HERRIN, P. D.

H025 DSN Progress Report for March–April 1972: The Development of a Dual-In-Line Package Microcircuit Card and Card Cage Assembly

P. D. Herrin

Technical Report 32-1526, Vol. IX, pp. 103–114,
June 15, 1972

An improved dual-in-line package microcircuit card and card-cage assembly have been developed. The external dimensions and the basic configuration of a previously-developed card have been essentially maintained. However, the number of microcircuit socket locations has been increased from 106 to 126 by compressing dimensions, and the number of interface plug connections has been raised from 82 to 240 by using a new high-density connector. Also, the physical size of the filtering capacitors has been reduced by selecting a miniaturized version. All wire-wrap terminals have been placed on 2.5-mm (0.100-in.) centers, with the exception of the capacitor terminals, to allow the card to be wired on an automated wire-wrap machine for potential savings of time, effort, and cost.

HIGA, W. H.

H026 Time Synchronization via Lunar Radar

W. H. Higa

Proc. IEEE, Vol. 60, No. 5, pp. 552–557,
May 1972

The advent of round-trip radar measurements has permitted the determination of the ranges to the nearby planets with greater precision than was previously possible. When the distances to the planets are known with high precision, the propagation delay for electromagnetic waves reflected by the planets may be calculated and used to synchronize remotely located clocks. Details basic to the operation of a lunar radar indicate a capability for clock synchronization to ± 20 μs. One of the design goals for this system was to achieve a simple semiautomatic receiver for remotely located tracking stations.

The lunar radar system is in operational use for deep space tracking at JPL and synchronizes five world-wide tracking stations with a master clock at Goldstone, Calif. Computers are programmed to correct the Goldstone transmissions for transit time delay and doppler shifts so as to be received on time at the tracking stations; this dictates that only one station can be synchronized at a

given time period and that the moon must be simultaneously visible to both the transmitter and receiver for a minimum time of 10 min. Both advantages and limitations of the system are given. Finally, an experiment is described which has detected the effects of lunar topography and libration on radar results; a monthly cyclic effect in time synchronization of about ±6 μs is shown.

HILDEBRAND, C. E.

H027   DSN Progress Report for May–June 1972: Preliminary Evaluation of Radio Data Orbit Determination Capabilities for the Saturn Portion of a Jupiter–Saturn–Pluto 1977 Mission

V. J. Ondrasik, C. E. Hildebrand, and G. A. Ransford

Technical Report 32-1526, Vol. X, pp. 59–75, August 15, 1972

For abstract, see Ondrasik, V. J.

H028   DSN Progress Report for May–June 1972: Determining the Mass and Ephemeris of Saturn by Radio Tracking of a Jupiter–Saturn–Pluto 1977 Spacecraft

V. J. Ondrasik, C. E. Hildebrand, and G. A. Ransford

Technical Report 32-1526, Vol. X, pp. 76–81, August 15, 1972

For abstract, see Ondrasik, V. J.

HIPSHER, H.

H029   Mariner 9 Science Experiments: Preliminary Results

R. H. Steinbacher, A. J. Kliore, J. Lorell, H. Hipsher (National Aeronautics and Space Administration), C. A. Barth (University of Colorado), H. Masursky (U.S. Geological Survey), G. Münch (California Institute of Technology), J. C. Pearl (Goddard Space Flight Center), and B. A. Smith (New Mexico State University)

Science, Vol. 175, No. 4019, pp. 293–294, January 21, 1972

For abstract, see Steinbacher, R. H.

HOBBY, G. L.

H030   The Carbon-Assimilation Experiment: The Viking Mars Lander

N. H. Horowitz, J. S. Hubbard, and G. L. Hobby

Icarus, Vol. 16, No. 1, pp. 147–152, February 1972

For abstract, see Horowitz, N. H.

HOEHN, F. W.

H031   Liquid-Phase Mixing of Bipropellant Doublets

F. W. Hoehn, J. H. Rupe, and J. G. Sotter

Technical Report 32-1546, February 15, 1972

Comparisons of cold-flow mixing efficiency for sprays formed by unlike impinging doublet injector elements comprising circular and noncircular orifices have recently been reported by other investigators. It was concluded that noncircular elements produce significantly better mixing efficiencies than a circular unlike doublet at equivalent design conditions. The fact that the mixing efficiency for the circular-orifice unlike doublet was significantly lower than typical values for a number of other circular-orifice doublets suggested that factors other than orifice shape might have been present in the comparisons.

Experimental results of unlike doublet mixing obtained at JPL are correlated with an analytically derived equation predicting fluid cavitation. The correlation relates the minimum orifice pressure drop required to initiate cavitation to the system back pressure, cold-flow simulant vapor pressure, and orifice flow discharge and contraction coefficients. Stream flow instabilities are also visually correlated with cavitation and orifice discharge coefficient measurements.

In addition, the influence of cavitation on the characteristic phenomenon of hydraulic flip is observed for both circular and noncircular orifices. For particular orifice lengths, some noncircular shapes are shown to produce more fully developed flows (shorter recovery lengths) and therefore provide slightly higher cold-flow mixing uniformities than circular orifices of equal length. The particular noncircular elements evaluated, however, are shown to be more sensitive to liquid-stream misimpingement than the corresponding circular orifices.

HOFFMAN, J. K.

H032   A Study of the Frictional and Stick–Slip Behavior of Magnetic Recording Tapes

S. H. Kalfayan, R. H. Silver, and J. K. Hoffman

Technical Report 32-1548, April 1, 1972

For abstract, see Kalfayan, S. H.

H033   Studies on the Frictional Behavior of Magnetic Recording Tapes

S. H. Kalfayan, R. H. Silver, and J. K. Hoffman

JPL Quarterly Technical Review, Vol. 2, No. 1,
pp. 100–106, April 1972

For abstract, see Kalfayan, S. H.

H034 Magnetic Tape Recorder for Long Operating Life in Space

E. J. Bahm and J. K. Hoffman

IEEE Trans. Magnetics, Vol. MAG-7, No. 3,
pp. 517–520, September 1971

For abstract, see Bahm, E. J.

HOGGAN, H. R.

H035 DSN Progress Report for March–April 1972: Prototype S- and X-Band Feed System Hardware

M. S. Katow and H. R. Hoggan

Technical Report 32-1526, Vol. IX, pp. 185–187,
June 15, 1972

For abstract, see Katow, M. S.

H036 DSN Progress Report for May–June 1972: Experimental S- and X-Band Feed System Ellipsoid Reflector

H. R. Hoggan and W. Kissane

Technical Report 32-1526, Vol. X, pp. 186–190,
August 15, 1972

To support the Mariner Venus–Mercury 1973 X-band experiment, the S/X feed system has been designed and is currently under fabrication for installation on the Mars Deep Space Station (DSS 14) 64-m-diameter antenna. The system will allow both S- and X-band signals to be received along the same bore-sight direction. Basic elements of the system are the ellipsoid reflector over the S-band horn and a dichroic reflector plate over the X-band cone. The first parts to be manufactured are the ellipsoid reflector and its backup structure. This article describes the ellipsoid reflector, the method used to form it, the measured accuracy of the finished part, and its connection to the backup structure.

HOLCOMB, L. B.

H037 Satellite Auxiliary-Propulsion Selection Techniques: Application of Selection Techniques to the ATS-H Satellite

L. B. Holcomb

Technical Report 32-1505, Suppl. 1,
October 1, 1972

JPL Technical Report 32-1505 and the addendum thereto described auxiliary-propulsion systems applicable to unmanned satellites and documented an approach for satellite designers to use in selecting systems that are the most effective for their mission. This supplement discusses the analysis required to estimate auxiliary-propulsion system requirements for a mission. These requirements include tipoff rate reduction, acquisitions, disturbance torques, orbital disturbances, and spacecraft-commanded maneuvers. A comparison of several candidate auxiliary-propulsion systems and system combinations for an Advanced Applications Technology Satellite (ATS-H) is presented. A generalized auxiliary propulsion system tradeoff, based on mission cost effectiveness criteria, is described. The specific mission assumptions for the ATS-H spacecraft are included, along with a discussion of the sensitivity of the final selection to these assumptions.

H038 European Auxiliary Propulsion—1972

L. B. Holcomb

Technical Memorandum 33-555,
September 1, 1972

During the last half decade, low-thrust auxiliary-propulsion technology has experienced rapid growth in Europe due to the development of new and more complex satellites. To gain insight into the auxiliary-propulsion technology state-of-the-art in Europe, the survey presented in this report was undertaken. The chemical and electric auxiliary-propulsion technology of the United Kingdom, France, and West Germany is discussed in detail, and the propulsion technology achievements of Italy, India, Japan, and Russia are reviewed. A comparison of Shell 405 catalyst and a European spontaneous hydrazine catalyst called CNESRO I is also presented. Finally, conclusions are drawn regarding future trends in European auxiliary-propulsion technology development.

HOLDRIDGE, D. B.

H039 Simultaneous Solution for the Masses of the Principal Planets From Analysis of Optical, Radar, and Radio Tracking Data

J. H. Lieske, W. G. Melbourne, D. A. O'Handley,
D. B. Holdridge, D. E. Johnson, and
W. S. Sinclair

Celest. Mech., Vol. 4, No. 2, pp. 233–245,
October 1971

For abstract, see Lieske, J. H.

HOLMES, J. K.

H040 DSN Progress Report for September–October 1972: Optimum Noncoherent Receiver at Low Signal-to-Noise Ratio for Unknown Doppler Shifted Signals

J. K. Holmes

Technical Report 32-1526, Vol. XII, pp. 88–91, December 15, 1972

This article derives an optimum, low-signal-to-noise-ratio receiver for the case when the received signal has unknown phase and an unknown doppler shift. This receiver appears to be new and is quite similar in form to the wideband frequency-shift-keyed receiver.

H041 Performance of a First-Order Transition Sampling Digital Phase-Locked Loop Using Random-Walk Models

J. K. Holmes

IEEE Trans. Commun., Vol. COM-20, No. 2, pp. 119–131, April 1972

A new mechanization of a first-order all digital phase-locked loop is discussed and analyzed. The purpose of the loop is to provide continuous tracking of the incoming waveform corrupted by the presence of white gaussian noise. Based on a random-walk model, solutions are obtained for the steady-state timing-error variance and mean time to slip a cycle. As a result of the mean first-time-to-slip analysis, a difference equation and its solution are obtained that generalize a previously derived equation. Using a procedure that appears new, an upper bound on the timing-error bias due to a doppler shift of the synchronized waveform is also derived. An example, for which the results presented here are applicable, is considered in some detail.

HOLTZE, R. F.

H042 Properties of Conductive Thick-Film Inks

R. F. Holtze

Technical Memorandum 33-532, April 15, 1972

Ten different conductive inks used in the fabrication of thick-film circuits were evaluated for their physical and handling properties. Viscosity, solid contents, and spectrographic characteristics of the unfired inks were determined. Inks were screened on ceramic substrates and fired for varying times at specified temperatures. Selected substrates were given additional firings to simulate the heat exposure that would be received if thick-film resistors were added to the substrate.

Data are presented covering: (1) printing characteristics, (2) solderability using Sn-63 and a 4% silver solder, (3) leach resistance, (4) solder adhesion, and (5) wire bonding

properties. The results obtained using different firing schedules are compared, and the general results obtained for each ink are given. The changes in firing time or the application of a simulated-resistor firing had little effect on the properties of most inks.

HOPPER, D. J.

H043 A Closely Regulated TWT Converter

D. J. Hopper and R. W. Andryczyk (General Electric Company)

IEEE Trans. Aerosp. Electron. Sys., Vol. AES-7, No. 6, pp. 1147–1150, November 1971

The design concept for the traveling wave tube amplifier converter for possible use in the Thermoelectric Outer-Planet Spacecraft (TOPS) is presented. An unusual combination of semiconductors and magnetics was utilized to achieve very stable voltage regulation on a number of separate outputs to satisfy the requirements of a high-power traveling wave tube (TWT), and at the same time operate at an efficiency of better than 90% from a 30-V source. The circuitry consists of an output filter, an auxiliary Jensen oscillator driving a high-reactance transformer to provide current limiting to the heater, a variable time delay, a main Jensen oscillator driving the power transformer with a maximum step-up ratio of 120 to 1, and series transistorized post regulators to provide precise voltage adjustment and low output impedance.

This paper discusses the design of the high-reactance transformer and the high step-up ratio transformer, as well as the high-voltage series regulators that are limited in range and operate at the top of the unregulated output voltage. Test data is presented, and details of current transients caused by charging the filter circuits, input current ripple, and output voltage ripples are considered. The circuit provides better than 0.5% regulation against load change, input voltage change, and over-operating temperature range of from –20 to 80°C, with output ripple voltage of less than 2 V peak-to-peak on top of the 3600-Vdc output. The measured efficiency was typically 87%, and recommendations are included to improve this to in excess of 90%.

HORD, C. W.

H044 Mariner 9 Ultraviolet Spectrometer Experiment: Initial Results

C. A. Barth (University of Colorado),
C. W. Hord (University of Colorado),
A. I. Stewart (University of Colorado), and
A. L. Lane

Science, Vol. 175, No. 4019, pp. 309–312,
January 21, 1972

For abstract, see Barth, C. A.

HOROWITZ, N. H.

H045 The Carbon-Assimilation Experiment: The Viking Mars Lander

N. H. Horowitz, J. S. Hubbard, and G. L. Hobby

Icarus, Vol. 16, No. 1, pp. 147–152,
February 1972

The carbon-assimilation experiment detects life in soils by measuring the incorporation of carbon from ^{14}CO and $^{14}CO_2$ into organic matter. It is based on the premise that Martian life, if it exists, is carbonaceous and exchanges carbon with the atmosphere, as do all terrestrial organisms. It is especially sensitive for photosynthesizing cells, but it detects heterotrophs also. The experiment has the particular advantage that it can be carried out under essentially Martian conditions of temperature, pressure, atmospheric composition, and water abundance.

H046 Microbiology of the Dry Valleys of Antarctica

N. H. Horowitz (California Institute of Technology), R. E. Cameron, and J. S. Hubbard

Science, Vol. 176, No. 4032, pp. 242–245,
April 21, 1972

The dry valleys of South Victoria Land, Antarctica, together with a few other ice-free areas on the perimeter of the Antarctic continent, form what is generally considered to be the most extreme cold-desert region of the Earth. During the past 5 years, the dry valleys have served as a model environment for investigating questions connected with the biological exploration of Mars. The extraordinary aridity of the region, its low temperature, and its geographical isolation give it a quasi-Martian character, although it is to be understood that the actual Martian environment is still more hostile than that of the valleys.

The kinds, numbers, and distribution of soil microorganisms in the valleys have been investigated in order to gain insight into the practical problems of searching for life in an extreme environment. Detailed results of these studies have been reported elsewhere. This article reviews the major findings in this region, especially as they apply to Martian exploration.

HORSEWOOD, J. L.

H047 Basic Parameters for Low Thrust Mission and System Analysis

T. A. Barber, J. L. Horsewood (Analytical Mechanics Associates, Inc.), and
H. Meissinger (TRW Systems, Inc.)

Preprint 72-426,
AIAA Ninth Electric Propulsion Conference,
Bethesda, Maryland, April 17–19, 1972

For abstract, see Barber, T. A.

HOVIS, W. A.

H048 Infrared Spectroscopy Experiment on the Mariner 9 Mission: Preliminary Results

R. A. Hanel (Goddard Space Flight Center),
B. J. Conrath (Goddard Space Flight Center),
W. A. Hovis (Goddard Space Flight Center),
V. G. Kunde (Goddard Space Flight Center),
P. D. Lowman (Goddard Space Flight Center),
J. C. Pearl (Goddard Space Flight Center),
C. Prabhakara (Goddard Space Flight Center),
B. Schlachman (Goddard Space Flight Center), and
G. V. Levin (Biospherics Incorporated)

Science, Vol. 175, No. 4019, pp. 305–308,
January 21, 1972

For abstract, see Hanel, R. A.

HUBBARD, J. S.

H049 The Carbon-Assimilation Experiment: The Viking Mars Lander

N. H. Horowitz, J. S. Hubbard, and G. L. Hobby

Icarus, Vol. 16, No. 1, pp. 147–152,
February 1972

For abstract, see Horowitz, N. H.

H050 Microbiology of the Dry Valleys of Antarctica

N. H. Horowitz (California Institute of Technology), R. E. Cameron, and J. S. Hubbard

Science, Vol. 176, No. 4032, pp. 242–245,
April 21, 1972

For abstract, see Horowitz, N. H.

HUGHES, R. S.

H051 The Mariner Mars 1971 Radio Frequency Subsystem

R. S. Hughes

Technical Memorandum 33-573, December 1, 1972

This memorandum describes the radio frequency subsystem (RFS) for the Mariner Mars 1971 spacecraft. The

Mariner Mars 1969 RFS was used as the baseline design for the Mariner Mars 1971 RFS, and the memorandum describes design changes made to the Mariner Mars 1969 RFS for use on Mariner Mars 1971. The memorandum also notes various problems encountered during the fabrication and testing of the RFS as well as the types of tests the RFS was subjected to. In areas where significant problems were encountered, a detailed description of the problem and its solution is presented. In addition, the memorandum recommends some modifications to the RFS and to the test techniques for future programs.

H052 Spacecraft S-Band 10–100 W RF Amplifier Tubes

R. S. Hughes

Progr. Astronaut. Aeronaut., Vol. 25, pp. 19–41, 1971

The results of electrical, environmental, and life tests on several S-band power amplifier tubes operated under saturated conditions are presented. These amplifiers operate in the 2.3-GHz region and are intended for spacecraft applications. The amplifiers tested include the amplitron, Raytheon Model QKS 1300; several traveling wave tubes, Hughes Aircraft Co. Models 216H and 242H; Watkins–Johnson Models 274-1, 274-6, and 395-3; and an electrostatically focused amplifier, Eimac Model X-3064. Overall efficiencies of 25 to 50% are exhibited; the Watkins–Johnson 395-3 and Eimac X-3064 100-W tubes exhibit overall efficiencies of 47 and 39%, respectively. The Eimac X-3064 tube employs a unique radiation-cooled collector which radiates heat through a sapphire window. Three 25-W amplitrons tested exhibited an average life of about 2350 h. Life tests on several 10- to 20-W traveling wave tubes have shown these tubes to have excellent life characteristics, which at present range up to 40,000 h.

HUNT, G. E.

H053 Laboratory Simulation of Diffuse Reflectivity From a Cloudy Planetary Atmosphere

J. S. Margolis, D. J. McCleese, and G. E. Hunt

Appl. Opt., Vol. 11, No. 5, pp. 1212–1216, May 1972

For abstract, see Margolis, J. S.

H054 Formation of Spectral Lines in Planetary Atmospheres: I. Theory for Cloudy Atmospheres; Application to Venus

G. E. Hunt

J. Quant. Spectrosc. Radiat. Transfer, Vol. 12, No. 3, pp. 387–404, March 1972

The theory of the formation of spectral lines in a cloudy planetary atmosphere is studied in detail. It is shown that models based upon homogeneous, isotropically scattering atmospheres cannot be used to reproduce observed spectroscopic features of phase effect and the shape of spectral lines for weak *and* strong bands. The theory must, therefore, be developed using an inhomogeneous (gravitational) model of a planetary atmosphere, accurately incorporating all the physical processes of radiative transfer.

Such a model of the lower Venus atmosphere, consistent with our present knowledge, is constructed. The results discussed in this article demonstrate the effects of the parameters that describe the atmospheric model on the spectroscopic features of spectral line profile and phase effect, at visible and near infrared wavelengths. This information enables us to develop a comprehensive theory of line formation in a Venus atmosphere.

H055 Formation of Spectral Lines in a Planetary Atmosphere: II. Spectroscopic Evidence for the Structure of the Visible Venus Clouds

G. E. Hunt

J. Quant. Spectrosc. Radiat. Transfer, Vol. 12, No. 3, pp. 405–419, March 1972

This article demonstrates that there is spectroscopic evidence for the structure of the visible Venus cloud layers. From physically realistic models of the lower Venus atmosphere, we have shown that only observations of the phase variations of the CO_2 bands in the Venus spectrum can provide the information for a unique identification of the structure of the cloud layers. It is proved that Venus cannot have a single dense cloud layer, but must have two scattering layers; a thin aerosol layer is situated in the lower stratosphere, overlying a dense cloud deck.

The aerosol plays an important role in the scattering of radiation, so that its identification provides an explanation of the reflecting layer-scattering model controversy for the interpretation of spectra formed in a cloudy planetary atmosphere.

H056 Formation of Spectral Lines in Planetary Atmospheres: III. The Use of Analytic Scattering Diagrams in Computations of Synthetic Spectra for Cloudy Atmospheres

G. E. Hunt

J. Quant. Spectrosc. Radiat. Transfer, Vol. 12, No. 6, pp. 1023–1028, June 1972

In order to interpret planetary spectra formed in a cloudy atmosphere in a meaningful way, it is necessary to compute synthetic spectra from realistic models where the physical processes are accurately taken into account. Anisotropic scattering diagrams for the cloud particles must be used. This article presents the results of some comparisons that have been made of line profiles and equivalent widths computed from atmospheric models where the scattering has been represented by the Mie theory and a simple analytic expression, the Heyney–Greenstein function. These results show that the spectroscopic features for these models are indistinguishable and demonstrate the value of using this simple analytic function in terms of the enormous saving in computer time, when computing synthetic spectra for any cloudy planetary atmosphere.

H057 Laboratory Simulation of Absorption Spectra in Cloudy Atmospheres

D. J. McCleese, J. S. Margolis, and G. E. Hunt

Nature Phys. Sci., Vol. 233, No. 40, pp. 102–103, October 4, 1971

For abstract, see McCleese, D. J.

H058 The Infrared Spectrum of Jupiter: Structure and Radiative Properties of the Clouds

F. W. Taylor and G. E. Hunt

Proceedings of the Conference on Atmospheric Radiation, Fort Collins, Colorado, August 7–9, 1972, pp. 100–102

For abstract, see Taylor, F. W.

HUNTRESS, W. T., JR.

H059 An ESCA Study of Lunar and Terrestrial Materials

W. T. Huntress, Jr., and L. Wilson (Varian Associates)

Earth Planet. Sci. Lett., Vol. 15, pp. 59–64, May 1972

The electron spectroscopy for chemical analysis (ESCA) technique is used to obtain rapid, nondestructive, elemental analysis of selected lunar samples. The chemical shift of the $Fe(2p)$ line in lunar material is found characteristic of iron in the Fe^{2+} state. A difference in binding energy of approximately 0.5 eV is observed between the $O(1s)$ levels of the terrestrial minerals fayalite and quartz, and effects due to surface oxidation and adsorption are also observed in terrestrial materials.

H060 Dependence of the Rates on Ion Kinetic Energy for the Reactions $D_2^+ + D_2$ and $HD^+ + HD$

W. T. Huntress, Jr., D. D. Elleman, and M. T. Bowers (University of California, Santa Barbara)

J. Chem. Phys., Vol. 55, No. 11, pp. 5413–5414, December 1, 1971

The kinetic energy dependence of the reactions of H_2^+, D_2^+, and HD^+ ions with most of the isotopic variants of the hydrogen molecule has been studied, and several interesting dynamic features have been noted. There still remains some disagreement, however, on the kinetic energy dependence of the rates for some of the isotopic reactions. It is the purpose of this article to report some preliminary work which helps to alleviate some of this controversy.

H061 Hydrogen Atom Scrambling in Ion–Molecule Reactions of Methane and Ethylene

W. T. Huntress, Jr.

J. Chem. Phys., Vol. 56, No. 10, pp. 5111–5120, May 15, 1972

The product distribution for the reactions $CH_4^+ + CD_4$, $CH_3^+ + CD_4$, $C_2H_4^+ + C_2D_4$, and their isotopic complements are determined as a function of reactant-ion kinetic energy over the range from thermal energies to 10 eV. The reaction of CH_4^+ with the parent neutral proceeds both via proton transfer and hydrogen atom abstraction accompanied by approximately 10% hydrogen atom exchange during reaction. The reactions $CH_3^+ + CD_4$ and $C_2H_4^+ + C_2D_4$ are shown to proceed with isotopic scrambling of the hydrogen atoms over the entire kinetic energy range from thermal energies to 10 eV. Several endothermic channels are observed at high kinetic energies for the reaction $C_2H_4^+ + C_2H_4$ including the production of $C_2H_2^+$, $C_2H_3^+$, $C_2H_5^+$, and $C_3H_3^+$ ions.

HURD, W. J.

H062 DSN Progress Report for May–June 1972: DSN Station Clock Synchronization by Maximum Likelihood VLBI

W. J. Hurd

Technical Report 32-1526, Vol. X, pp. 82–95, August 15, 1972

The clocks at the deep space stations can be accurately synchronized by very-long-baseline interferometry (VLBI) at lower operational cost than by the existing Moon bounce system. More than an order of magnitude improvement in accuracy can be attained using existing DSN hardware, and ultimate accuracies on the order of

10 ns are possible. The purpose of the analysis described in this article is to optimize the acquisition and processing of the VLBI data subject to hardware constraints, in order to achieve the best possible time synchronization estimate for a given amount of data and the most efficient usage of the DSN facilities.

H063 DSN Progress Report for July–August 1972: Efficient Generation of Statistically Good Pseudonoise by Linearly Interconnected Shift Registers

W. J. Hurd

Technical Report 32-1526, Vol. XI, pp. 92–103, October 15, 1972

This article presents some new algorithms for generating pseudorandom noise utilizing binary maximal-length recursive sequences of high degree and with many nonzero terms. The ability to efficiently implement high-degree recursions is important because the number of consecutive bits which can be guaranteed to be both linearly and statistically independent is equal to the degree of the recursion. The implementations are by interconnection of several short shift registers in a linear manner in such a way that different widely spaced phase shifts of the same pseudonoise sequence appear in the stages of the several registers. This is efficient both in hardware and in software. Several specific algorithms are subjected to extensive statistical evaluation, with no evidence found to distinguish the sequences from purely random binary sequences.

H064 DSN Progress Report for September–October 1972: A Demonstration of DSN Clock Synchronization by VLBI

W. J. Hurd

Technical Report 32-1526, Vol. XII, pp. 149–160, December 15, 1972

A prototype of a semi-real-time system for synchronizing the DSN station clocks by radio interferometry was successfully demonstrated on August 30, 1972. Synchronization accuracies as good as 100 ns rms were achieved between the Pioneer Deep Space Station (DSS 11) and the Echo Deep Space Station (DSS 12), both at Goldstone. The accuracy can be improved by increasing the system bandwidth until the fundamental limitations due to baseline and source-position uncertainties and atmospheric effects are reached. These limitations are about 10 ns for transcontinental baselines.

HUTCHISON, R. B.

H065 Automated Analysis of Astronomical Spectra

R. B. Hutchison

Astron. J., Vol. 76, No. 8, pp. 711–718, October 1971

A description is given of a computer program that automates the analysis of high-resolution, infrared astronomical spectra. Procedures for the detection of spectral features and for the determination of accurate line frequencies, line depths, and equivalent widths are presented. Line profile analysis, identification, and other specialized operations are discussed.

H066 Turbulence Velocities in the Atmosphere of Alpha Orionis

R. B. Hutchison

Astrophys. J., Vol. 170, No. 3, Pt. 1, pp. 551–555, December 15, 1971

The curve of line-width correlation has been applied to OH lines in the spectrum of α Orionis, characteristic microturbulence, macroturbulence, and thermal velocities in the atmosphere of this star have been determined to be 9.9 ± 2.0, ≤ 3, and $\cong 1.8$ km/s, respectively. Implications of these results are discussed in this article.

H067 Astronomical Infrared Spectroscopy With a Connes-Type Interferometer: III. Alpha Orionis, 2600–3450 cm^{-1}

R. Beer, R. B. Hutchison, R. H. Norton, and D. L. Lambert (University of Texas)

Astrophys. J., Vol. 172, No. 1, Pt. 1, pp. 89–115, February 15, 1972

For abstract, see Beer, R.

INGHAM, J. D.

I001 New Polymer Systems: Chain Extension By Dianhydrides

R. A. Rhein and J. D. Ingham

JPL Quarterly Technical Review, Vol. 1, No. 4, pp. 97–103, January 1972

For abstract, see Rhein, R. A.

JACKSON, E. B.

J001 DSN Progress Report for November–December 1971: DSN Research and Technology Support

E. B. Jackson

Technical Report 32-1526, Vol. VII, pp. 124–125, February 15, 1972

The major current activities of the Development Support Group at both the Venus Deep Space Station and the

Microwave Test Facility are presented, and accomplishments and progress are described. Activities include pulsar measurements, tri-cone implementation, precision antenna gain measurement (26-m antenna), weak source observations, Faraday rotation measurements on Applications Technology Satellite 1 (ATS-1), clock synchronization transmissions, and Block IV receiver/exciter testing and demonstration.

J002 DSN Progress Report for January–February 1972: DSN Research and Technology Support

E. B. Jackson

Technical Report 32-1526, Vol. VIII, pp. 68–73, April 15, 1972

Major activities in support of the DSN research and technology program performed at both the Venus Deep Space Station and the Microwave Test Facility during the last two months are presented. Progress and performance summaries are given in the following areas: pulsar reception, mu ranging from the Mars Deep Space Station, tricone assembly and testing, precision antenna gain measurements on the 26-m antenna weak-source observations of various radio sources, very long baseline interferometry in cooperation with National Radio Astronomy Observatory, dual carrier measurements, noise and intermodulation experiments, clock synchronization transmissions, and various maintenance activities.

J003 DSN Progress Report for January–February 1972: Antenna Drive System Performance Evaluation Using PN Codes

R. M. Gosline, E. B. Jackson, and J. D. Campbell

Technical Report 32-1526, Vol. VIII, pp. 74–79, April 15, 1972

For abstract, see Gosline, R. M.

J004 DSN Progress Report for March–April 1972: DSN Research and Technology Support

E. B. Jackson and R. B. Kolbly

Technical Report 32-1526, Vol. IX, pp. 147–151, June 15, 1972

The activities of the development support group, including the Microwave Test Facility, during the two-month period ending April 15, 1972, are summarized. Activities include operational clock synchronization, precision antenna-gain measurement, weak-source observation, pulsar observation, tricone-support-structure testing, and planetary-radar preparation and execution. Activities at the Microwave Test Facility include special klystron testing and tuning for the Manned Spaceflight Tracking and Data Network, special part fabrication for the tricone support structure, and design and fabrication of the

flow panel and crowbar subassemblies for the clock-synchronization transmitting system. Significant maintenance items include replacement of the azimuth drive gear reducer on the 26-m-diameter antenna and modification of the power-distribution system associated with the 100-kW clock synchronization transmitter.

J005 DSN Progress Report for May–June 1972: DSN Research and Technology Support

E. B. Jackson

Technical Report 32-1526, Vol. X, pp. 149–152, August 15, 1972

This article summarizes the activities of the Development Support Group, including the Microwave Test Facility, during the two-month period ending June 15, 1972. Activities include operational clock synchronization, precision antenna gain measurements, weak source observations, pulsar observations, demonstration of the Scan and Correct Using Receiver computer program for automatic antenna tracking, planetary radar experiments, dual-carrier measurements, and shipment of the tricone support structure. Activities at the Microwave Test Facility include DSN klystron testing and general machine shop and other support for the Venus Deep Space Station. Significant maintenance activities include replacement of an azimuth drive gear reducer and rework of the elevation ball screw nuts on the 26-m-diameter antenna.

J006 DSN Progress Report for September–October 1972: DSN Research and Technology Support

E. B. Jackson and R. B. Kolbly

Technical Report 32-1526, Vol. XII, pp. 124–130, December 15, 1972

This article presents the activities of the Development Support Group in operating the Venus Deep Space Station (DSS 13) and the Microwave Test Facility for the period August 16–October 15, 1972, categorized by the JPL technical section supported. Major activities include a strong planetary-radar and pulsar-observation program for the Communications Systems Research Section, extensive precision-antenna-gain measurements for the Communications Elements Research Section, and a major installation and modification effort for dual-carrier experimentation for the RF Systems Development Section. Preliminary activity in measuring the side-lobe patterns of the 26-m-diameter antenna at the Venus Deep Space Station is described, and the cessation of clock synchronization transmissions (due to nonavailability of polynomial predicts) is noted.

JAFFE, L. D.

J007 Cracking of Lunar Mare Soil

L. D. Jaffe

Nature, Vol. 234, No. 5329, pp. 402–403,
December 17, 1971

Some of the early photographs of the disturbed lunar mare soil seemed to suggest that the soil layer consists of a thin, flat, rather rigid crust over a softer substrate. As described in this article, more recent photographs give evidence that the former impression of flatness and crusting is an illusion and that the lunar soil deforms and cracks in the same manner as homogeneous isotropic terrestrial soils of moderate bulk density, having a small amount of cohesion.

J008 Results of Recent Manned and Unmanned Lunar Exploration

L. D. Jaffe

Space Research XI, pp. 31–49, Akademie-Verlag,
Berlin, 1971

Important data about the Moon obtained from spacecraft during the past year include the age-dating and chemical analyses of samples returned by Apollos 11 and 12. The material of the surface fragmental layer was differentiated 4.6×10^9 yr ago. The surfaces of Mare Tranquillitatis and Oceanus Procellarum solidified 3.7×10^9 and about 3×10^9 yr ago from lava of very low viscosity which had undergone extensive chemical fractionation. The lunar interior is of different composition from these surfaces. The Moon is tectonically rather quiet. The rate impact of moderate-sized objects was much greater before the mare formation than since. Micrometeorite impact has produced rock erosion, pitting, shock, melting, vitrification, and induration in the surface layer. Pictures, taken by Apollo astronauts, of the lunar surface disturbed by Surveyor 3 show that little change has occurred in 31 mo.

J009 Bearing Strength of Lunar Soil

L. D. Jaffe

The Moon, Vol. 3, No. 3, pp. 337–345,
December 1971

Bearing load versus penetration curves have been obtained using a 1.3-g sample of lunar soil from the scoop of the Surveyor 3 soil mechanics surface sampler and a circular indentor 2 mm in diameter. Measurements were made in an Earth laboratory, in air. This sample provided a unique opportunity to evaluate earlier, remotely controlled, in-situ measurements of lunar surface bearing properties. Bearing capacity, measured at a penetration equal to the indentor diameter, varied from 0.02–0.04 $N\text{-}cm^{-2}$ at bulk densities of 1.15 $g\text{-}cm^{-3}$ to 30–100 $N\text{-}cm^{-2}$ at 1.9 $g\text{-}cm^{-3}$. Deformation was by compression directly below the indentor at bulk densities below 1.61 $g\text{-}cm^{-3}$, by outward displacement at bulk densities over

1.62 $g\text{-}cm^{-3}$. Preliminary comparison of in-situ remote measurements with those on returned material indicates good agreement if the lunar regolith at Surveyor 3 has a bulk density of 1.6 $g\text{-}cm^{-3}$ at a depth of 2.5 cm. Definitive comparison awaits both better data on bulk density of the undisturbed lunar soil and additional mechanical-property measurements on returned material.

JAFFE, R. M.

J010 3-D Multilateration: A Precision Geodetic Measurement System

P. R. Escobal, H. F. Fliegel, R. M. Jaffe,
P. M. Muller, K. M. Ong, O. H. von Roos, and
M. S. Shumate

JPL Quarterly Technical Review, Vol. 2, No. 3,
pp. 1–11, October 1972

For abstract, see Escobal, P. R.

JAIVIN, G. I.

J011 Scan Pointing Calibration for the Mariner Mars 1971 Spacecraft

W. F. Havens, G. I. Jaivin, G. D. Pace, and
R. A. Virzi

Technical Memorandum 33-556, August 1, 1972

For abstract, see Havens, W. F.

J012 A General Purpose Maneuver Turns Computer Program

G. I. Jaivin

Technical Memorandum 33-558, August 15, 1972

This report presents the theory, functional description, and operating instructions of a general purpose maneuver analysis program. The program computes the maneuver turns required to point a given spacecraft-fixed vector in the direction of a given inertially-fixed vector. Any two-turn maneuver sequence may be arbitrarily chosen. If it is not possible to accomplish the desired orientation with a two-turn sequence, a three-turn sequence can be specified. In addition, the coordinates of an arbitrarily selected inertially-fixed reference vector are computed before and after each turn that is performed. Two program options provide, if desired, the reference vector coordinates at selected points throughout each turn and the reference vector positions before and after each turn of an arbitrarily prescribed set of maneuver turns.

J013 Mariner Mars 1971 Scan Platform Pointing Calibration

G. D. Pace, G. I. Jaivin, and R. A. Virzi

JPL Quarterly Technical Review, Vol. 2, No. 1, pp. 49–57, April 1972

For abstract, see Pace, G. D.

JENSEN, W. M.

J014   Development of Boron Epoxy Rocket Motor Chambers

W. M. Jensen, A. C. Knoell, and C. Zweben (Materials Sciences Corporation)

Proceedings of the Twenty-Seventh Annual Technical Conference of the Reinforced Plastics/Composites Institute, Washington, D.C., February 8–11, 1972, sponsored by the Society of the Plastics Industry, Inc., Sect. 17-C, pp. 1–10

A 71-cm-diameter 74-cm-long boron/epoxy composite rocket motor chamber was designed based on the geometric configuration of the JPL Applications Technology Satellite titanium alloy apogee motor chamber. Because analyses showed large stress concentrations in the domes, the configuration was modified using the same basic constraints for openings and attachments. The rocket motor chamber was then fabricated by filament winding with boron/epoxy tape and hydrostatically tested to failure at 264 N/cm^2, 57.2 N/cm^2 above the design value. Two more rocket motor chambers were fabricated with the same basic constraints, but shortened to 57.6 cm for a smaller propellant load. The first of these short chambers failed in proof because of filament winding fabrication difficulties. The second chamber was successfully fabricated and passed the hydrostatic proof test.

JET PROPULSION LABORATORY

J015   Proceedings of the Jupiter Radiation Belt Workshop (Held at the Jet Propulsion Laboratory, Pasadena, California, July 13–15, 1971)

Jet Propulsion Laboratory

Technical Memorandum 33-543, July 1, 1972

Outer-planet mission studies emphasized the need to reduce the uncertainty in Jupiter trapped radiation belt models and the requirement to establish the best models from which spacecraft design requirements should be derived. The best models should be conservative enough that spacecraft designed to the models have an acceptable risk associated with the models, but not so overly conservative that a large design penalty is required for a small reduction in risk.

Because of the highly specialized nature of this topic, questions could best be addressed by a group of specialists who actually were working in the fields involved. Consequently, the Jupiter Radiation Belt Workshop was

sponsored by JPL to provide a forum to review the current state of Jupiter radiation belt knowledge and to recommend a best set of models for the determination of spacecraft design requirements. The 22 formal presentations of the workshop, the conclusions, and some post-workshop models of Jupiter radiation belts are presented in these proceedings, which were edited by A. J. Beck of JPL.

JOHNS, C. E.

J016   DSN Progress Report for May–June 1972: Block IV Receiver Development

C. E. Johns

Technical Report 32-1526, Vol. X, pp. 175–179, August 15, 1972

This article describes a digital control assembly developed for use in controlling the frequency of a Dana Laboratory Digiphase synthesizer, Model 7010-S-179. The control assembly allows the synthesizer to be used as the oscillator within a phase-locked loop. A brief analysis using the synthesizer control assembly in a third-order loop is included.

JOHNSON, D. E.

J017   Simultaneous Solution for the Masses of the Principal Planets From Analysis of Optical, Radar, and Radio Tracking Data

J. H. Lieske, W. G. Melbourne, D. A. O'Handley, D. B. Holdridge, D. E. Johnson, and W. S. Sinclair

Celest. Mech., Vol. 4, No. 2, pp. 233–245, October 1971

For abstract, see Lieske, J. H.

JOHNSON, K. G.

J018   A Mechanism for Three-Axis Control of an Ion Thruster Array

G. S. Perkins, K. G. Johnson, J. D. Ferrera, and T. D. Masek

J. Spacecraft Rockets, Vol. 9, No. 3, pp. 218–220, March 1972

For abstract, see Perkins, G. S.

JOHNSTON, A. R.

J019   Stark-Effect Modulation of a CO_2 Laser by NH_2D

A. R. Johnston and R. D. S. Melville, Jr.

Appl. Phys. Lett., Vol. 19, No. 12, pp. 503–506, December 15, 1971

The molecular Stark effect in NH_2D was used to modulate the 10.6-μ $P(20)$ line of a CO_2 laser, yielding a modulation depth of 40% from a 200-V-cm^{-1} rms signal applied to a 19.7-cm gas cell external to the laser. NH_2D was prepared by mixing ND_3 and NH_3. The absorption coefficient of the $M = 4$ Stark-split line was measured as a function of mixing ratio and pressure. The observed pressure-broadening coefficient was 32.5 MHz/torr.

JONES, N. J.

J020 DSN Progress Report for May–June 1972: Performance Capabilities of the Data Decoder Assembly Through the Viking Era

C. R. Grauling and N. J. Jones

Technical Report 32-1526, Vol. X, pp. 164–167, August 15, 1972

For abstract, see Grauling, C. R.

JORDAN, J. F.

J021 Mariner 9 Celestial Mechanics Experiment: Gravity Field and Pole Direction of Mars

J. Lorell, G. H. Born, E. J. Christensen,
J. F. Jordan, P. A. Laing, W. Martin,
W. L. Sjogren, I. I. Shapiro (Massachusetts Institute of Technology),
R. D. Reasenberg (Massachusetts Institute of Technology), and G. L. Slater (Massachusetts Institute of Technology)

Science, Vol. 175, No. 4019, pp. 317–320, January 21, 1972

For abstract, see Lorell, J.

JUSTISS, J.

J022 DSN Progress Report for January–February 1972: Manufacturing Engineering of Surface Panels for the 64-m Antennas

J. Justiss, W. Kissane, and M. S. Katow

Technical Report 32-1526, Vol. VIII, pp. 89–97, April 15, 1972

The procurement of two 26-m antennas for the overseas deep space stations was authorized with new vendors. These changes engendered new procedures to insure quality manufacturing of the surface panels for maximum RF performance. The new checking procedures are described including the mathematical formulations and functional aspects of the checking fixtures. A computer program was developed to solve for the parameters. Notes on the computing of arc lengths along the parabolic curve are included.

JUVINALL, G. L.

J023 Gravitational Effects on Electrochemical Batteries

R. E. Meredith (Oregon State University),
G. L. Juvinall, and A. A. Uchiyama

Technical Report 32-1570, November 15, 1972

For abstract, see Meredith, R. E.

KALFAYAN, S. H.

K001 A Study of the Frictional and Stick–Slip Behavior of Magnetic Recording Tapes

S. H. Kalfayan, R. H. Silver, and J. K. Hoffman

Technical Report 32-1548, April 1, 1972

Methods were developed to determine the coefficient of friction and the extent of stick–slip of magnetic recording tapes. After a preliminary phase during which experimental procedures were established and screening of candidate tapes was carried out, the frictional and stick–slip behavior of four selected tapes, using four different kinds of magnetic heads, was studied at various temperatures, under dry and humid conditions, and in various gaseous atmospheres such as argon, helium, nitrogen, and air. The effects of tape speed and outgassing on the drag properties of the tapes were also studied.

A rank was assigned to each tape and magnetic head as a result of these tests. This study helped in the selection of a magnetic tape for a flight project and will be useful in the consideration of tapes and magnetic heads for future spacecraft applications.

K002 Studies on the Frictional Behavior of Magnetic Recording Tapes

S. H. Kalfayan, R. H. Silver, and J. K. Hoffman

JPL Quarterly Technical Review, Vol. 2, No. 1, pp. 100–106, April 1972

Magnetic tape recorders exhibit various failure modes. Those ascribable to friction between tape and magnetic head cause phenomena such as seizure (stick) and seizure and release (stick–slip). Methods have been developed at JPL for the measurement of frictional forces acting on the tape while in motion or at rest, as well as the extent of stick–slip. The effects of factors such as temperature, humidity, kind of gaseous atmosphere, and tape speed on the frictional interaction between various tapes and heads have been investigated. The results were instrumental in the selection of a tape for the Mariner Mars

1971 spacecraft. This article discusses recent studies on the stick–slip behavior of tapes, as well as the performance of a metallic tape compared to that of the usual plastic tapes.

K003 Long-Term Aging of Elastomers: Chemorheology of Viton B Fluorocarbon Elastomer

S. H. Kalfayan, R. H. Silver, A. A. Mazzeo, and S. T. Liu

JPL Quarterly Technical Review, Vol. 2, No. 3, pp. 32–39, October 1972

Elastomers have extensive aerospace applications. They are used as bladder materials for liquid-propellant expulsion systems, propellant binders, and fuel-tank sealants for high-speed aircraft. Predicting the long-term behavior of these materials is of primary importance. This article is a continuation of a study to ascertain the nature, extent, and rate of chemical changes that take place in certain selected elastomers. Under discussion is Viton B, regarded as a temperature- and fuel-resistant fluorocarbon rubber. The kinetic analysis of the chemical stress relaxation, and infrared and gel-permeation chromatography analysis results are discussed.

KATOW, M. S.

K004 DSN Progress Report for January–February 1972: Manufacturing Engineering of Surface Panels for the 64-m Antennas

J. Justiss, W. Kissane, and M. S. Katow

Technical Report 32-1526, Vol. VIII, pp. 89–97, April 15, 1972

For abstract, see Justiss, J.

K005 DSN Progress Report for March–April 1972: Prototype S- and X-Band Feed System Hardware

M. S. Katow and H. R. Hoggan

Technical Report 32-1526, Vol. IX, pp. 185–187, June 15, 1972

The hardware for supporting the prototype S- and X-band feed system on the 64-m-diameter antenna is described. The S-band ellipsoid reflector is supported on flextures which provide for thermal expansion. The X-band-dichroic/S-band-flat reflector assembly consists of a welded assembly of aluminum plates with provisions for mounting the X-band transparent sheet.

K006 DSN Progress Report for July–August 1972: NASTRAN Data Generation and Management Using Interactive Graphics

M. S. Katow and B. M. Cooper

Technical Report 32-1526, Vol. XI, pp. 104–110, October 15, 1972

For effective use of the NASA Structural Analysis computer system, the input bulk data must accurately model the structure to be analyzed with a minimum expenditure of time and money. This article describes a method of using an interactive graphics device to generate a large portion of the input bulk data with visual checks of the structure and the card images. The generation starts from GRID and PBAR cards. The visual checks result from a three-dimensional display of the model in any rotated position. By detailing the steps, the time saving and cost effectiveness of this method may be judged, and its potential as a useful tool for the structural analyst may be established.

KELLY, A. M.

K007 Isolation and Characterization of Keto-Carotenoids From the Neutral Extract of Algal Mat Communities of a Desert Soil

A. J. Bauman, H. G. Boettger, A. M. Kelly, R. E. Cameron, and H. Yokoyama (U.S. Department of Agriculture)

Eur. J. Biochem., Vol. 22, No. 2, pp. 287–293, September 1971

For abstract, see Bauman, A. J.

KELLY, L. B.

K008 Tracking and Data System Support for the Mariner Mars 1971 Mission: First Trajectory Correction Maneuver Through Orbit Insertion

G. P. Textor, L. B. Kelly, and M. Kelly

Technical Memorandum 33-523, Vol. II, June 15, 1972

For abstract, see Textor, G. P.

KELLY, M.

K009 Tracking and Data System Support for the Mariner Mars 1971 Mission: First Trajectory Correction Maneuver Through Orbit Insertion

G. P. Textor, L. B. Kelly, and M. Kelly

Technical Memorandum 33-523, Vol. II, June 15, 1972

For abstract, see Textor, G. P.

KERRIN, S. L.

K010 Rapid Determination of Twenty Amino Acids by Gas Chromatography

J. P. Hardy and S. L. Kerrin

Anal. Chem., Vol. 44, No. 8, pp. 1497–1499, July 1972

For abstract, see Hardy, J. P.

KIEFFER, H.

K011 Mariner 1969 Infrared Radiometer Results: Temperatures and Thermal Properties of the Martian Surface

G. Neugebauer (California Institute of Technology),
G. Münch (California Institute of Technology),
H. Kieffer (University of California, Los Angeles),
S. C. Chase, Jr. (Santa Barbara Research Center),
and E. Miner

Astron. J., Vol. 76, No. 8, pp. 719–749, October 1971

For abstract, see Neugebauer, G.

K012 Infrared Radiometry Experiment on Mariner 9

S. C. Chase, Jr. (Santa Barbara Research Center),
H. Hatzenbeler (Santa Barbara Research Center),
H. Kieffer (University of California, Los Angeles),
E. Miner, G. Munch (California Institute of Technology), and G. Neugebauer (California Institute of Technology)

Science, Vol. 175, No. 4019, pp. 308–309, January 21, 1972

For abstract, see Chase, S. C., Jr.

KIKIN, G. M.

K013 Completely Modular Thermionic Reactor Ion Propulsion System (TRIPS)

M. L. Peelgren, G. M. Kikin, and C. D. Sawyer

Technical Memorandum 33-550, May 15, 1972

For abstract, see Peelgren, M. L.

KINDER, W. J.

K014 DSN Progress Report for May–June 1972: End-to-End Medium Rate Telemetry System Test

W. J. Kinder

Technical Report 32-1526, Vol. X, pp. 5–9, August 15, 1972

An end-to-end test of the operational medium-rate telemetry system was conducted on May 23, 1972. The errors recorded seem to group themselves around three patterns: those errors associated with 360-computer time corrections, those errors concerned with Ground Communications Facility (GCF) transmission, and those errors originating in the GCF/synchronizer/360 interface. Noise on the data-block-detected signal from the GCF decoder to the Space Flight Operations Facility (SFOF) synchronizers is suspected. A recommendation is made for a facility test between the GCF and SFOF to be undertaken to validate the quality of the data-block-detected signal per transfer agreement and assembly specifications.

KISSANE, W.

K015 DSN Progress Report for January–February 1972: Manufacturing Engineering of Surface Panels for the 64-m Antennas

J. Justiss, W. Kissane, and M. S. Katow

Technical Report 32-1526, Vol. VIII, pp. 89–97, April 15, 1972

For abstract, see Justiss, J.

K016 DSN Progress Report for May–June 1972: Experimental S- and X-Band Feed System Ellipsoid Reflector

H. R. Hoggan and W. Kissane

Technical Report 32-1526, Vol. X, pp. 186–190, August 15, 1972

For abstract, see Hoggan, H. R.

KLASCIUS, A. F.

K017 Microwave Radiation Protective Suit

A. F. Klascius

Am. Ind. Hygiene Assoc. J., Vol. 32, No. 11, pp. 771–774, November 1971

The use of a Navy-developed microwave radiation protective suit in a JPL project is described. The composition of the suit material is analyzed, and the amount of radiation absorbed by the various parts of the suit is measured. The effects of microwave radiation on the human body are considered, and the degree of protection provided by the suit during actual entry into a microwave field is evaluated.

KLEIN, M. J.

K018 Jupiter: New Evidence of Long-Term Variations of Its Decimeter Flux Density

M. J. Klein, S. Gulkis, and C. T. Stelzried

Astrophys. J., Vol. 176, No. 2, Pt. 2, pp. L85–L88, September 1, 1972

Jupiter's flux density at 12.6 cm was measured at weekly intervals from May through October 1971. When compared with previous decimetric measurements, these data indicate that Jupiter's total flux density has decreased approximately 20% since 1964. No short-term variations greater than a few percent were observed.

KLIMASAUSKAS, C. C.

K019 DSN Progress Report for November–December 1971: The X930 Program Set for Sigma 5 Assembly

C. C. Klimasauskas

Technical Report 32-1526, Vol. VII, pp. 86–90, February 15, 1972

This article describes a set of programs that have been written to enable the Sigma 5 computer to assemble programs for the XDS 920/930 computers. It consists of two parts: a system procedure deck which allows SIGMA METASYMBOL to assemble a source language similar to the XDS 900-series METASYMBOL, and a secondary loader which reformats the Sigma 5 load module into the Universal Binary Language of the 900-series machines and writes it to cards or magnetic tape. The syntactic differences between this assembler and the 900-series METASYMBOL are described, as well as the process of generating a 920 program using this program set and the Sigma 5.

K020 DSN Progress Report for September–October 1972: An Execution Analyzer for the Sigma 5 Computer

C. C. Klimasauskas

Technical Report 32-1526, Vol. XII, pp. 176–188, December 15, 1972

Since many different computers on the market today claim to perform the same class of tasks, and no uniform criterion has been established to aid the decision-making process, the problem of how to select the "best" computer for a particular job mix becomes almost a matter of personal preference and chance. One technique for evaluating the performance of a central processing unit is based on the frequency of usage of the various machine instructions. This technique is particularly applicable to machines used in a dedicated process-control activity such as those of the deep space stations. This article describes a program which has been written for the Sigma 5 computer to gather data on the dynamic usage of computer instructions in various tasks.

KLIORE, A. J.

K021 Bistatic Radar Measurements of the Surface of Mars With Mariner 1969

G. Fjeldbo, A. J. Kliore, and B. L. Seidel

Icarus, Vol. 16, No. 3, pp. 502–508, June 1972

For abstract, see Fjeldbo, G.

K022 Mariner 9 Science Experiments: Preliminary Results

R. H. Steinbacher, A. J. Kliore, J. Lorell, H. Hipsher (National Aeronautics and Space Administration), C. A. Barth (University of Colorado), H. Masursky (U.S. Geological Survey), G. Münch (California Institute of Technology), J. C. Pearl (Goddard Space Flight Center), and B. A. Smith (New Mexico State University)

Science, Vol. 175, No. 4019, pp. 293–294, January 21, 1972

For abstract, see Steinbacher, R. H.

K023 Mariner 9 S-Band Martian Occultation Experiment: Initial Results on the Atmosphere and Topography of Mars

A. J. Kliore, D. L. Cain, G. Fjeldbo, B. L. Seidel, and S. I. Rasool (National Aeronautics and Space Administration)

Science, Vol. 175, No. 4019, pp. 313–317, January 21, 1972

A preliminary analysis of 15 radio occultation measurements taken on the day side of Mars between 40°S and 33°S has revealed that the temperature in the lower 15 to 20 km of the atmosphere of Mars is essentially isothermal and warmer than expected. This result, which is also confirmed by the increased altitude of the ionization peak of the ionosphere, can possibly be caused by the absorption of solar radiation by fine particles of dust suspended in the lower atmosphere. The measurements also revealed elevation differences of 13 km and a range of surface pressures between 2.9 and 8.3 mbars. The floor of the classical bright area of Hellas was found to be about 6 km below its western rim and 4 km below the mean radius of Mars at that latitude. The region between Mare Sirenum and Solis Lacus was found to be relatively high, lying 5 to 8 km above the mean radius. The maximum electron density in the ionosphere (about 1.5×10^5 electrons per cm^3), which was found to be remarkably constant, was somewhat lower than that observed in 1969 but higher than that observed in 1965.

K024 Summary of Mariner 6 and 7 Radio Occultation Results on the Atmosphere of Mars

A. J. Kliore, G. Fjeldbo, and B. L. Seidel

Space Research XI, pp. 165–175, Akademie-Verlag, Berlin, 1971

During the close flyby of Mars by Mariners 6 and 7 in the summer of 1969, their S-band radio beams were used to probe the atmosphere of Mars at four locations. These measurements indicate surface pressures ranging from a high of 7.3 mb in the Amazonis/Arcadia area to a low of 4.2 mb near the southern end of Hellespontus, indicating a range of local elevation differences of about 6 km. The surface temperatures range from about 250°K, measured near the equator in the afternoon, to about 173°K, in the north polar region at night. The temperature profiles suggest that condensation of CO_2 is probable at an altitude of about 15 km near the north pole and at altitudes ranging from 27 to 38 km in equatorial and temperate latitudes. The daytime measurements also show the existence of an ionosphere with a primary layer of about 1.7×10^5 el cm^{-3} at an altitude of about 135 km. The topside scale height indicates a plasma temperature of about 400–500°K if CO_2^+ is assumed to be the dominant ion.

KNITTEL, M. D.

K025 Microbiological Sampling of Returned Surveyor III Electrical Cabling

M. D. Knittel, R. H. Green, and M. S. Favero (U.S. Public Health Department)

Proceedings of the Second Lunar Science Conference, Houston, Texas, January 11–14, 1971, Vol. 3, pp. 2715–2719, The M.I.T. Press, 1971

A piece of electrical cabling was retrieved from the Surveyor 3 spacecraft by the crew of Apollo 12 and subjected to microbiological analysis for surviving terrestrial microorganisms. The experiment was done in a sealed environmental chamber to protect against contamination. No viable microorganisms were found on the wiring bundle samples.

KNOELL, A. C.

K026 Vibration and Buckling Analysis of Composite Plates and Shells

J. A. McElman (Lowell Technological Institute) and A. C. Knoell

J. Compos. Mater., Vol. 5, pp. 529–532, October 1971

For abstract, see McElman, J. A.

K027 Development of Boron Epoxy Rocket Motor Chambers

W. M. Jensen, A. C. Knoell, and C. Zweben (Materials Sciences Corporation)

Proceedings of the Twenty-Seventh Annual Technical Conference of the Reinforced Plastics/Composites Institute, Washington, D.C., February 8–11, 1972, sponsored by the Society of the Plastics Industry, Inc., Sect. 17-C, pp. 1–10

For abstract, see Jensen, W. M.

KOLBLY, R. B.

K028 DSN Progress Report for March–April 1972: DSN Research and Technology Support

E. B. Jackson and R. B. Kolbly

Technical Report 32-1526, Vol. IX, pp. 147–151, June 15, 1972

For abstract, see Jackson, E. B.

K029 DSN Progress Report for September–October 1972: DSN Research and Technology Support

E. B. Jackson and R. B. Kolbly

Technical Report 32-1526, Vol. XII, pp. 124–130, December 15, 1972

For abstract, see Jackson, E. B.

KOSKELA, P. E.

K030 Mariner Mars 1971 Television Picture Catalog: Sequence Design and Picture Coverage

P. E. Koskela, M. R. Helton, L. N. Seeley, and S. J. Zawacki

Technical Memorandum 33-585, Vol. II, December 15, 1972

This memorandum contains a collection of data relating to the Mariner 9 television pictures. The data are arranged to offer speedy identification of what took place during entire science cycles, on individual revolutions, and during individual science links or sequences.

Summary tables present the nominal design for each of the major picture-taking cycles, along with the sequences actually taken on each revolution. These tables enable one to identify, at a glance, all television sequences and the corresponding individual pictures for the first 262 revolutions (the primary mission). A list of television pictures, categorized according to their latitude and longitude, is also provided. The bulk of the memorandum consists of orthographic and/or mercator plots for all

pictures, along with pertinent numerical data for their center points. Other tables and plots of interest are also included. This memorandum is based upon data contained in the Supplementary Experiment Data Record (SEDR) files as of August 21, 1972.

KROLL, G. G.

K031 DSN Progress Report for November–December 1971: Fire Protection and Safety Activities Throughout the Deep Space Network

G. G. Kroll

Technical Report 32-1526, Vol. VII, pp. 213-216, February 15, 1972

Comprehensive fire and safety studies have been initiated to determine the effort required to protect the tracking network from loss of life, property, and operational continuity due to fire. The studies recommend the installation of water storage tanks, new water mains and fire hydrants, fire hose cabinets, automatic early fire warning devices, automatic smoke detectors, and manual alarm stations. The protection offered to the Deep Space Network with the installation of this equipment will be equal to the highly protective risk category used by private industry to describe maximum installed protection against loss of life and property. This article describes the scope of the initial surveys, the follow-on preliminary engineering reports, and the design/construction efforts.

KRUGER, G. W.

K032 Experimental Evaluation of High-Thrust, Throttleable, Monopropellant Hydrazine Reactors

R. W. Riebling and G. W. Kruger

Technical Report 32-1551, March 1, 1972

For abstract, see Riebling, R. W.

KUNDE, V. G.

K033 Infrared Spectroscopy Experiment on the Mariner 9 Mission: Preliminary Results

R. A. Hanel (Goddard Space Flight Center),
B. J. Conrath (Goddard Space Flight Center),
W. A. Hovis (Goddard Space Flight Center),
V. G. Kunde (Goddard Space Flight Center),
P. D. Lowman (Goddard Space Flight Center),
J. C. Pearl (Goddard Space Flight Center),
C. Prabhakara (Goddard Space Flight Center),
B. Schlachman (Goddard Space Flight Center), and
G. V. Levin (Biospherics Incorporated)

Science, Vol. 175, No. 4019, pp. 305-308, January 21, 1972

For abstract, see Hanel, R. A.

KUSHIDA, R.

K034 Effect on Supersonic Jet Noise of Nozzle Plenum Pressure Fluctuations

R. Kushida and J. H. Rupe

AIAA J., Vol. 10, No. 7, pp. 946-948, July 1972

The proportion of the total engine noise which is attributable to the jet plume in a jet propulsion device increases markedly as the exhaust velocity increases. When the jet velocity is nearly sonic or supersonic, then the jet noise can overwhelm other noise sources. In this preliminary study it is found that the interaction of upstream disturbance with a supersonic jet plume causes an increase in the total noise. It is expected that this added insight into jet noise sources will be useful in devising improved methods of noise reduction in future jet engines.

LACY, G. H.

L001 Surface Distribution of Microorganisms in Antarctic Dry-Valley Soils: A Martian Analog

R. E. Cameron, H. P. Conrow, D. R. Gensel,
G. H. Lacy, and F. A. Morelli

Antarctic J. U.S., Vol. VI, No. 5, pp. 211-213, September–October 1971

For abstract, see Cameron, R. E.

LAESER, R. P.

L002 DSN Progress Report for November–December 1971: Mariner Mars 1971 Mission Support

R. P. Laeser

Technical Report 32-1526, Vol. VII, pp. 25-28, February 15, 1972

At the start of the Mariner 9 orbit operations, some confusion existed over the varying number of bit errors observed in the picture transmissions. This article presents a summary of observations made in an attempt to clarify the situation.

LAING, P. A.

L003 Lunar Gravity Analysis From Long-Term Effects

A. S. Liu and P. A. Laing

Science, Vol. 173, No. 4001, pp. 1017–1020,
September 10, 1971

For abstract, see Liu, A. S.

**L004   Mariner 9 Celestial Mechanics Experiment: Gravity
Field and Pole Direction of Mars**

J. Lorell, G. H. Born, E. J. Christensen,
J. F. Jordan, P. A. Laing, W. Martin,
W. L. Sjogren, I. I. Shapiro (Massachusetts
Institute of Technology),
R. D. Reasenberg (Massachusetts Institute of
Technology), and G. L. Slater (Massachusetts
Institute of Technology)

Science, Vol. 175, No. 4019, pp. 317–320,
January 21, 1972

For abstract, see Lorell, J.

LAM, C.

**L005   DSN Progress Report for September–October 1972:
On the Weight Enumerators of Quadratic Residue
Codes**

J. Mykkeltveit (California Institute of Technology),
C. Lam (California Institute of Technology), and
R. J. McEliece

Technical Report 32-1526, Vol. XII, pp. 161–166,
December 15, 1972

For abstract, see Mykkeltveit, J.

LAMBERT, D. L.

**L006   Astronomical Infrared Spectroscopy With a Connes-
Type Interferometer: III. Alpha Orionis, 2600–3450
cm⁻¹**

R. Beer, R. B. Hutchison, R. H. Norton, and
D. L. Lambert (University of Texas)

Astrophys. J., Vol. 172, No. 1, Pt. 1, pp. 89–115,
February 15, 1972

For abstract, see Beer, R.

LANDEL, R. F.

**L007   Stored Energy Function of Rubberlike Materials
Derived From Simple Tensile Data**

T. J. Peng and R. F. Landel

J. Appl. Phys., Vol. 43, No. 7, pp. 3064–3067,
July 1972

For abstract, see Peng, T. J.

**L008   A Molecular Theory of Elastomer Deformation and
Rupture**

R. F. Landel and R. F. Fedors

*Mechanical Behavior of Materials: Proceedings of
the 1971 International Conference on Mechanical
Behavior of Materials (Sponsored by the Society of
Materials Science), Kyoto, Japan, August 1971,*
Vol. III, pp. 496–507

The mechanical properties of elastomers, including rupture and its time dependence, can be semi-quantitatively predicted from nine molecular parameters which are characteristic for a given species, from the initial molecular weight of a sample before crosslinking, and from the effective chain concentration (which must still be determined for each vulcanizate). Only two empirical quantities are involved—the Plazek retardation function $\psi(a_x)$ for entanglement slippage and a related constant which serves to locate $\psi(a_x)$ on the time scale. The theory leads to a new method of estimating fatigue lifetimes from short-time data.

LANE, A. L.

**L009   Mariner 9 Ultraviolet Spectrometer Experiment:
Initial Results**

C. A. Barth (University of Colorado),
C. W. Hord (University of Colorado),
A. I. Stewart (University of Colorado), and
A. L. Lane

Science, Vol. 175, No. 4019, pp. 309–312,
January 21, 1972

For abstract, see Barth, C. A.

**L010   Mariner 9 Ultraviolet Spectrometer Experiment:
Stellar Observations**

C. F. Lillie (University of Colorado),
R. C. Bohlin (University of Colorado),
M. R. Molnar (University of Colorado),
C. A. Barth (University of Colorado), and
A. L. Lane

Science, Vol. 175, No. 4019, pp. 321–322,
January 21, 1972

For abstract, see Lillie, C. F.

LANE, F. L.

**L011   Investigation of Gold Embrittlement in Connector
Solder Joints**

F. L. Lane

Technical Memorandum 33-533, April 1, 1972

An investigation was performed to determine to what extent, if any, typical flight connector solder joints may be embrittled by the presence of gold. In addition to mappings of gold content in connector solder joints by an electron microprobe analyzer, metallographic examinations and mechanical tests (thermal shock, vibration, impact, and tensile strength) were also conducted. This memorandum presents a description of the specimens and tests, a discussion of the data, and some conclusions.

LaPORTE, D. D.

L012   The Detection and Mapping of Water Vapor in the Martian Atmosphere

C. B. Farmer and D. D. LaPorte

Icarus, Vol. 16, No. 1, pp. 34–46, February 1972

For abstract, see Farmer, C. B.

LAYLAND, J. W.

L013   DSN Progress Report for November–December 1971: An Introduction to Minicomputer Software Support

J. W. Layland

Technical Report 32-1526, Vol. VII, pp. 84–85, February 15, 1972

This article discusses some problems associated with generating software for a possible deep space station configuration with a multiplicity of computers, and briefly describes an effort underway to help reduce those problems. It is a general introduction to "The X930 Program Set for Sigma 5 Assembly," and "The SAPDP Program Set for Sigma 5 Assembly," which describe specific results from the development effort.

L014   DSN Progress Report for March–April 1972: Performance of an Optimum Buffer Management Strategy for Sequential Decoding

J. W. Layland

Technical Report 32-1526, Vol. IX, pp. 88–96, June 15, 1972

Sequential decoding has been found to be an efficient means of communicating at low undetected error rates from deep space probes, but a failure mechanism known as erasure or computational overflow remains a significant problem. The erasure of a block occurs when the decoder has not finished decoding that block at the time that it must be output.

A recent article developed a technique for scheduling the operations of a sequential decoder that has the potential for significant reduction in erasure probability relative to a decoder with the same parameters and using the conventional method of scheduling. Performance results reported previously depend upon the accuracy of an accepted model for the number of computations needed to decode a block of data. This article presents a re-evaluation of decoder performance, using actual sequential decoding data. Results are generally unchanged: a decoder with a 10-block buffer will achieve less than a 10^{-4} erasure probability with the new scheduling technique whenever a similar decoder had achieved less than a 10^{-2} erasure probability in conventional operation.

L015   DSN Progress Report for March–April 1972: Variable Length Short Constraint-Length Convolutional Codes: A Comparison of Maximum Likelihood and Sequential Decoding

J. W. Layland

Technical Report 32-1526, Vol. IX, pp. 97–102, June 15, 1972

Maximum-likelihood decoding of short-constraint-length convolutional codes is one of the likely candidates for implementing high-performance telemetry systems for future deep-space missions. It has, in fact, been considered to be the best choice for video missions, providing better performance at the design point of 5×10^{-3} than other systems of comparable complexity. Recent advances in knowledge of sequential decoding have posed the question as to whether sequential decoding might, in fact, be preferable to maximum-likelihood decoding. The answer, developed here in terms of a hypothesized maximum-likelihood decoder built technologically similar to the JPL high-speed multi-mission sequential decoder, is that maximum-likelihood decoding is preferable to sequential decoding at a 5×10^{-3} bit error rate. The reverse is true at 10^{-3} and below.

Two code families of variable constraint length are also developed which permit easy implementation of encoders for this hypothesized maximum-likelihood decoder.

L016   DSN Progress Report for September–October 1972: Sequential Decoding With a Noisy Carrier Reference

J. W. Layland

Technical Report 32-1526, Vol. XII, pp. 167–175, December 15, 1972

This article presents an approximate analysis of the effect of a noisy carrier reference on the performance of sequential decoding. The limitations of the analysis are discussed, and steps that could be taken to extend the performance region over which the model used produces

accurate, rather than merely bounding, results are described.

L017   DSN Progress Report for September–October 1972: A Multicomputer Communications System

J. W. Layland and W. A. Lushbaugh

Technical Report 32-1526, Vol. XII, pp. 195–199, December 15, 1972

This article gives a general description of the requirements for, and one proposal for the provision of, the multicomputer communications facility needed in a multiple-minicomputer system, such as the anticipated tracking-station computer network of the DSN. The main features are: (1) a basically high-speed point-to-point link whose rate adapts without data loss to the capabilities of the computers with which it interfaces; and (2) a very-wide-bandwidth transmission control unit (TCU) which provides a functional path from each computer to every other computer, while requiring only one physical link between each computer and the TCU.

L018   A Flexible High-Speed Sequential Decoder for Deep Space Channels

J. W. Layland and W. A. Lushbaugh

IEEE Trans. Commun., Vol. COM-19, No. 5, pp. 813–820, October 1971

This article describes a sequential decoding machine, built at JPL, which uses a 3-bit quantization of the code symbols and achieves a computation rate of MHz. This machine is flexible and can be programmed to decode any complementary convolutional code with rates down to 1/4 and constraint lengths up to 32. In addition, metric programmability is provided for optimization of decoder performance with respect to channel parameter variations.

LEAVITT, R. K.

L019   The Least-Squares Process of MEDIA for Computing DRVID Calibration Polynomials

R. K. Leavitt

Technical Memorandum 33-542, May 15, 1972

This document describes and evaluates a process for computing a least-squares polynomial approximation of data points in which the optimum degree of the polynomial is automatically determined. An iterative smoothing technique is used to replace every point with the value taken on by a moving least-squares polynomial computed from a subset of points centered at the point being replaced. The optimum degree of the resulting polynomial approximation is determined by analyzing the finite differences of each successive set of smoothed points. To

evaluate the process, this document uses both artificially constructed data and actual Mariner Mars 1971 tracking data.

This process has been incorporated into the Transmission Media Calibration computer program (MEDIA), which calibrates radiometric data to overcome the effects on the tracking signal of charged-particle media. MEDIA was used in support of the Mariner Mars 1971 Project.

LEFLANG, J. G.

L020   DSN Progress Report for May–June 1972: Novel 70-MHz Limiting Amplifier

J. G. Leflang and R. N. MacClellan

Technical Report 32-1526, Vol. X, pp. 172–174, August 15, 1972

A high-speed digital differential comparator has been successfully utilized as the limiting element in an RF module operating in the VHF region. The device exhibits good amplitude and phase characteristics. This article describes the design and test results of the device, which uses emitter-coupled logic as a limiting amplifier.

LEIBOWITZ, L. P.

L021   Measurements of the Structure of an Ionizing Shock Wave in a Hydrogen–Helium Mixture

L. P. Leibowitz

Technical Memorandum 33-563, September 1, 1972

Shock structure during ionization of a hydrogen–helium mixture has been studied using hydrogen line and continuum emission measurements. A reaction scheme is proposed which includes hydrogen dissociation and a two-step excitation–ionization mechanism for hydrogen ionization by atom–atom and atom–electron collisions. Agreement has been achieved between numerical calculations and measurements of emission intensity as a function of time for shock velocities from 13 to 20 km/sec in a $0.208\ H_2 - 0.792\ He$ mixture. The electron temperature was found to be significantly different from the heavy-particle temperature during much of the ionization process. Similar time-histories for $H\beta$ and continuum emission indicate upper level populations of hydrogen in equilibrium with the electron concentration during the relaxation process. The expression for the rate constant for excitation of hydrogen by atom–atom collisions, that best fit the data was

$$k_{AA} = 4.0 \times 10^{-17} \left(\frac{8kT}{\pi\mu} \right)^{1/2} \exp{(-10/kT)} \, \text{cm}^3 \, \text{sec}^{-1},$$

where it has been assumed that the excitation cross section is the same for hydrogen and helium collision partners. The electron–atom excitation rate constant,

$$k_3 = 7.5 \times 10^{-16} \left(\frac{8kT_e}{\pi\mu_e} \right)^{1/2} \exp{(-10/kT_e)} \, \text{cm}^3 \, \text{sec}^{-1},$$

determined from this investigation, was in agreement with recent electron-beam cross section measurements.

L022 Nonequilibrium Ionization Measurements in Hydrogen–Helium Mixtures

L. P. Leibowitz

JPL Quarterly Technical Review, Vol. 1, No. 4, pp. 13–18, January 1972

Time-resolved emission measurements of several atomic line and continuum radiation channels have been made behind the incident shock wave of the JPL electric arc shock tube. Test times and nonequilibrium ionization times were obtained for shock velocities up to 2.5 × 10⁴ m/s in a 0.2 H₂–0.8 He gas mixture. The shock-heated test gas was found to be free from driver gas contamination, and the test times were adequate to achieve steady-state conditions. An activation energy of 4 eV was obtained from the nonequilibrium ionization time measurements. Modifications to experimental technique to determine the effect of test gas impurity level on ionization time measurements are discussed.

LEISING, C. J.

L023 Mariner 9 Propulsion Subsystem Performance During Interplanetary Cruise and Mars Orbit Insertion

M. J. Cork, R. L. French, C. J. Leising, and D. D. Schmit

JPL Quarterly Technical Review, Vol. 2, No. 1, pp. 113–122, April 1972

For abstract, see Cork, M. J.

LESH, J. R.

L024 DSN Progress Report for November–December 1971: Correlated Sampling With Application to Carrier Power Estimation Accuracy

J. R. Lesh

Technical Report 32-1526, Vol. VII, pp. 195–206, February 15, 1972

In this article the total sampling time and number of samples required to produce a sample mean having a specified variance is evaluated for various sampling intervals. The samples are assumed to be the correlated outputs of either a first- or second-order system having a white gaussian noise input. It is found that a reduction in both the total time and the number of samples can often be obtained for a given variance and sampling interval if the sampling is performed at the output of a second order system. These results are then applied to the automatic gain control sampling presently being used for carrier power estimation to show how its accuracy can be improved.

L025 DSN Progress Report for March–April 1972: Carrier Power Estimation Accuracy

J. R. Lesh

Technical Report 32-1526, Vol. IX, pp. 207–217, June 15, 1972

In this article, estimation theoretic techniques are used to derive expressions for the accuracy of the digital instrumentation subsystem (DIS) and telemetry and command processor (TCP) computer methods of carrier power estimation. Evaluation of these expressions shows that the TCP method is presently far more accurate than the DIS method. A procedure by which the DIS accuracy can be greatly improved is also presented.

L026 DSN Progress Report for May–June 1972: Accuracy of the Signal-to-Noise Ratio Estimator

J. R. Lesh

Technical Report 32-1526, Vol. X, pp. 217–235, August 15, 1972

In this article the effects of external and internal noise, finite sample size, and transition estimation errors are included in an analysis of the signal-to-noise ratio estimator used in the symbol-synchronizer assembly. Expressions for the estimator mean and variance are developed, from which their dependence on the above effects are determined. The results of this study show that the estimator mean depends almost entirely on the external and internal signal-to-noise ratios while the estimator variance depends almost exclusively on the sample size.

L027 DSN Progress Report for July–August 1972: Accuracy of the Signal-to-Noise Ratio Estimator: A Comment on the Derivation of the Estimator Mean

J. R. Lesh

Technical Report 32-1526, Vol. XI, pp. 164–166, October 15, 1972

The mean of the signal-to-noise ratio estimator used with the symbol-synchronizer assembly is derived without assuming independence of the sample mean and sample variance errors. The resulting expression is found to differ only slightly from a previous expression determined by assuming independence.

L028 DSN Progress Report for September–October 1972: Spectrum of an Asynchronously Biphase Modulated Square Wave

J. R. Lesh

Technical Report 32-1526, Vol. XII, pp. 226–230, December 15, 1972

This article presents an exact closed-form expression for the power spectrum of a square-wave carrier (or subcarrier) which is biphase modulated by a random binary data stream. The resulting expression is valid for any carrier frequency and data bit rate, provided that the two sources are not phase-coherently related. Also presented is an approximate expression which can be used to alleviate some computational difficulties of the exact expression at low spectral frequencies.

LEU, R. L.

L029 DSN Progress Report for November–December 1971: 400-kW Harmonic Filter

R. L. Leu

Technical Report 32-1526, Vol. VII, pp. 131–135, February 15, 1972

The low-power test data on the new 400-kW harmonic filter design shows that the new filter meets or exceeds the performance of the existing filters. This will not insure that the fourth harmonic from the 400-kW transmitter will not affect the X-band receiver performance. Additional fourth harmonic filters may be required.

LEVIN, G. V.

L030 Infrared Spectroscopy Experiment on the Mariner 9 Mission: Preliminary Results

R. A. Hanel (Goddard Space Flight Center),
B. J. Conrath (Goddard Space Flight Center),
W. A. Hovis (Goddard Space Flight Center),
V. G. Kunde (Goddard Space Flight Center),
P. D. Lowman (Goddard Space Flight Center),
J. C. Pearl (Goddard Space Flight Center),
C. Prabhakara (Goddard Space Flight Center),
B. Schlachman (Goddard Space Flight Center), and
G. V. Levin (Biospherics Incorporated)

Science, Vol. 175, No. 4019, pp. 305–308, January 21, 1972

For abstract, see Hanel, R. A.

LEVITT, B. K.

L031 DSN Progress Report for September–October 1972: Optimum Frame Sync Acquisition for Biorthogonally Coded Telemetry

B. K. Levitt

Technical Report 32-1526, Vol. XII, pp. 92–99, December 15, 1972

This article describes an optimum frame-sync algorithm for biorthogonally coded telemetry. This algorithm takes the coding into account and therefore performs significantly better than algorithms derived for uncoded telemetry, with only a slight increase in implementation complexity.

L032 Interplex: An Analysis of Optimized Power Allocations for Two- and Three-Channel PSK/PM Telecommunications Systems

B. K. Levitt

JPL Quarterly Technical Review, Vol. 2, No. 1, pp. 143–151, April 1972

Under certain conditions, interplex modulation techniques can significantly improve the performance of a multichannel phase-shift-keyed/phase-modulated (PSK/PM) telemetry system by increasing the useful available power relative to that of conventional PSK/PM systems. However, previous efforts to compare the two modulation schemes and provide a measure of this improvement have occasionally fostered the false impression that the total average signal power and the channel modulation indices were common to both systems. In practice, in designing either modulation system for a deep-space telecommunications link, optimal modulation indices are selected to minimize the total average signal power subject to certain minimum requirements on the average telemetry channel and carrier powers. This article illustrates these optimal design concepts for two- and three-channel telemetry modes in the context of the Mariner Venus–Mercury 1973 mission and provides a more realistic measure of the usefulness of interplex. These ideas are then applied as an example to a particular Mariner Venus–Mercury 1973 telemetry mode to demonstrate that interplex can reduce the required total average power by more than 2 dB in some cases.

LEVY, R.

L033 DSN Progress Report for November–December 1971: Improved Condensation Methods for Eigenvalue Problems

R. Levy

Technical Report 32-1526, Vol. VII, pp. 142–153, February 15, 1972

The conventional procedure used to condense the solution of eigenvalue problems for recovery of the lowest modes is tested by application to practical example structures. Evaluations are made of eigenvalue accuracy with respect to numbers of retained solution vectors. It is shown that solutions are likely to be inaccurate except in the special case of when prior knowledge of the mode shapes is available. One improvement for recovering the lowest modes is to supplement the retained vectors with static loading displacement functions. A further remedy is to perform iterative repetitions of the solution procedure. Great improvements in accuracy can be achieved with only a few iterative cycles. These improvements are effective in the typical case of when only a few valid lowest-mode solutions are required and the order of the problem is large so that it becomes important to minimize the computational time by means of solution condensation.

L034 DSN Progress Report for May–June 1972: Repositioning of Parabolic Antenna Panels Onto a Shaped Surface

R. Levy

Technical Report 32-1526, Vol. X, pp. 199–206, August 15, 1972

Optimal parameters for shifting existing parabolic-reflector surface panels for re-use within shaped antenna configurations are determined from theory and equations given in this article. The panels are reset to minimize the rms half-pathlength differences between their surface and the ideal, shaped surface. Input, output, and results are described for a computer program that implements the equations. Results for typical 26- and 64-m-diameter antennas indicate that, if all or most of the existing parabolic panels are re-used and repositioned according to the procedure, the consequent rms differences will be small.

L035 DSN Progress Report for September–October 1972: PARADES Structural Design System Capabilities

R. Levy and R. Melosh (Virginia Polytechnic Institute and State University)

Technical Report 32-1526, Vol. XII, pp. 68–73, December 15, 1972

This article outlines design approaches, program capabilities, problem formulation, and user options for the Parabolic Reflector Analysis and Design Subsystem (PARADES) program. PARADES is a new computer program for the analysis and design of parabolic antenna-reflector structures.

L036 DSN Progress Report for September–October 1972: Iterative Design of Antenna Structures

R. Levy

Technical Report 32-1526, Vol. XII, pp. 100–111, December 15, 1972

This article describes a new procedure for the design of antenna-reflector structures for improved performance when subjected to operational gravity loading. The design objective is to reduce the difference in pathlength of the RF energy beam that is reflected from the deformed surface with respect to the pathlength of the beam from a perfect paraboloidal surface. A virtual-work formulation is used to state this objective in terms of the bar areas that compose the structure. These bar areas become the design variables. A special application of the Lagrange-multiplier technique defines preferential redistributions of the design variables to improve performance. Improvements are developed subject to a primary constraint on total structure weight and additional practical side constraints. Design examples show efficient and effective applications of the described procedure.

LEWICKI, G.

L037 Barrier Energies in MIM Structures From Photoresponse: Effect of Scattering in the Insulating Film

G. Lewicki, J. Maserjian, and
C. A. Mead (California Institute of Technology)

J. Appl. Phys., Vol. 43, No. 4, pp. 1764–1767, April 1972

Scattering of electrons photoexcited into the insulator conduction band prevents photoresponse from following the Fowler relation in metal–insulator–metal (MIM) structures. However, barrier energies can be obtained without specific knowledge of the scattering process either by measuring the threshold for photoresponse directly, or by applying sufficiently large voltages across the insulator.

LIESKE, J. H.

L038   Simultaneous Solution for the Masses of the Principal Planets From Analysis of Optical, Radar, and Radio Tracking Data

J. H. Lieske, W. G. Melbourne, D. A. O'Handley, D. B. Holdridge, D. E. Johnson, and W. S. Sinclair

Celest. Mech., Vol. 4, No. 2, pp. 233–245, October 1971

JPL has developed a set of computer programs known as the Solar System Data Processing System (SSDPS) which is employed in improving the ephemerides of the major planets and for improving the values of several associated astronomical constants. A group of solutions for the masses of the major planets, together with the AU and radii of Mercury, Venus, and Mars, is presented. These solutions based upon optical, radar, and spacecraft radio tracking data are preliminary. The relative power of radar and radio tracking data vis-à-vis purely optical data in a solution is shown. The problems which could arise by adopting solutions based upon a single data type are demonstrated.

LIKINS, P. W.

L039   Large-Deformation Modal Coordinates for Nonrigid Vehicle Dynamics

P. W. Likins and G. E. Fleischer

Technical Report 32-1565, November 1, 1972

This report documents the derivation of minimum-dimension sets of discrete-coordinate and hybrid-coordinate equations of motion for a system consisting of an arbitrary number of hinge-connected rigid bodies assembled in tree topology. These equations are useful for the simulation of dynamic systems that can be idealized as tree-like arrangements of substructures, with each substructure consisting of either a rigid body or a collection of elastically interconnected rigid bodies restricted to small relative rotations at each connection. Thus, some of the substructures represent elastic bodies subjected to small strains or local deformations, but possibly large gross deformations; in the hybrid formulation, distributed coordinates, herein referred to as large-deformation modal coordinates, are used for the deformations of these substructures. The equations are in a form suitable for incorporation into one or more computer programs for use as multipurpose tools in the simulation of spacecraft and other complex electromechanical systems.

LILLIE, C. F.

L040   Mariner 9 Ultraviolet Spectrometer Experiment: Stellar Observations

C. F. Lillie (University of Colorado),
R. C. Bohlin (University of Colorado),
M. R. Molnar (University of Colorado),
C. A. Barth (University of Colorado), and
A. L. Lane

Science, Vol. 175, No. 4019, pp. 321–322, January 21, 1972

Photoelectric spectra have been obtained for a number of early-type stars in the 1100- to 2000-Å region with the Mariner 9 ultraviolet spectrometer. The resonance lines of H-I, Si-IV, and C-IV are easily identified, as are features due to C-II, C-III, Si-III, Fe-II, and N-IV. The absolute energy distribution derived from the data lie about 20% below those of OAO-2 in the 1200- to 2000-Å region.

LIN, H. S.

L041   Analysis of Morgantown Vehicle Steering Control

H. S. Lin and E. L. Marsh

JPL Quarterly Technical Review, Vol. 2, No. 1, pp. 58–71, April 1972

The proposed Morgantown public transportation system will use a fleet of computer-controlled vehicles operating on a separate dedicated network of roadways called a "guideway." An automatic steering system on each vehicle will enable the traversal of the proposed route of various guideway sections.

This article describes a preliminary study made at JPL to analyze the steering control for the Morgantown vehicles. The primary requirement was to design an automatic steering system that would achieve a smooth ride and simultaneously eliminate the need for excess margin in the guideway width, a significant factor in overall system cost. Front- and rear-wheel steering and front and rear sensing capabilities were assumed in the analysis. The system finally adopted—front- and rear-wheel steering and front sensing—was shown by computer simulations and by Boeing Company vehicle steering experiments to be adequate.

LINDLEY, P. L.

L042   DSN Progress Report for November–December 1971: DSIF Tracking and Monitor and Control Subsystem: Prototype Implementation

P. L. Lindley

Technical Report 32-1526, Vol. VII, pp. 159–167, February 15, 1972

A developmental model Deep Space Instrumentation Facility Tracking and Monitor and Control Subsystem has been installed and used in the support of the Mariner

Mars 1971 mission. The hardware and software necessary to support doppler measurements, including the ability to record the data locally as well as send it to the Space Flight Operations Facility both in real-time and recall (replay) modes, are operating. Checkout of other functions is in process.

LINDSEY, W. C.

L043 **Carrier Synchronization and Detection of Polyphase Signals**

W. C. Lindsey (University of Southern California) and M. K. Simon

IEEE Trans. Commun., Vol. COM-20, No. 3, pp. 441–454, June 1972

Digital communication networks used for the distribution of high-speed digital information are currently the subject of design studies for many civil and military applications. This article presents results that are useful in such studies as well as in network planning. In particular, the article is concerned with the problems of carrier synchronization and noisy reference detection of polyphase signals. Reconstruction of coherent references for the detection of polyphase (N-ary phase-shift-keyed) signals is considered and analyzed for three carrier reconstruction loops, namely, Nth power (multiply-and-divide) loops, generalized Costas (I–Q) loops, and extensions of data-aided (modulation wipeoff) loops. General expressions for the error probability are developed when the reconstructed reference signals are noisy. These expressions are evaluated numerically for cases of practical interest and compared with differentially coherent reception.

LINNES, K. W.

L044 **DSN Progress Report for November–December 1971: Radio Science Support**

K. W. Linnes

Technical Report 32-1526, Vol. VII, pp. 29–31, February 15, 1972

Since 1967, radio scientists have used the Deep Space Network 26- and 64-m antenna stations to investigate pulsars, to study the effect of solar corona on radio signals, and to observe radio emissions from X-ray sources. More recently, very long baseline interferometry (VLBI) techniques have been used for high-resolution studies of quasars. During the reporting period, VLBI observations were made in support of investigations of quasars. Support was also provided from the 64-m antenna for the mapping of nearby spiral galaxies.

L045 **DSN Progress Report for January–February 1972: Radio Science Support**

K. W. Linnes

Technical Report 32-1526, Vol. VIII, pp. 24–28, April 15, 1972

Since 1967, radio scientists have used the DSN 26- and 64-m-diameter antenna stations to investigate pulsars, to study the effect of solar corona on radio signals, and to observe radio emissions from X-ray sources. More recently, very long baseline interferometry (VLBI) techniques have been used for high-resolution studies of quasars. During the reporting period, VLBI observations were made of quasars and also of the Mariner 9 spacecraft. Support was also provided by the 64-m-diameter antenna for the measurement of cosmic background noise.

L046 **DSN Progress Report for May–June 1972: Radio Science Support**

K. W. Linnes

Technical Report 32-1526, Vol. X, pp. 52–58, August 15, 1972

Since 1967, radio scientists have used the DSN 26- and 64-m-diameter antenna stations to investigate pulsars, to study the effect of solar corona on radio signals, and to observe radio emissions from X-ray sources. More recently, very-long-baseline interferometry (VLBI) techniques have been used for high-resolution studies of quasars. During the reporting period, VLBI observations were made of quasars and pulsars. Support was also provided by the 64-m-diameter antenna for the measurement of cosmic background noise, mapping of nearby spiral galaxies, searching for ionized hydrogen in interstellar globular clusters, searching for interstellar molecules, and observing radiation from Jupiter.

L047 **DSN Progress Report for July–August 1972: Radio Science Support**

K. W. Linnes

Technical Report 32-1526, Vol. XI, pp. 26–29, October 15, 1972

Since 1967, radio scientists have used the DSN 26- and 64-m-diameter antenna stations to investigate pulsars, to study the effect of solar corona on radio signals, and to observe radio emissions from X-ray sources. More recently, very-long-baseline interferometry (VLBI) techniques have been used for high-resolution studies of quasars. During the reporting period, VLBI observations were made of quasars and pulsars. Support was also provided by the 64-m-diameter antenna for the measurement of cosmic background noise and weak radio sources

to search for interstellar molecules and for the observation of radiation from Jupiter.

LIPSIUS, P.

L048 DSN Progress Report for July–August 1972: Performance of the 64-Meter-Diameter Antenna Servo

P. Lipsius

Technical Report 32-1526, Vol. XI, pp. 153–156, October 15, 1972

A 64-m-diameter antenna has been installed and tested at the Tidbinbilla Deep Space Station in Australia. Part of the final acceptance testing was demonstration of antenna servo performance. This report summarizes the major tests and the resulting data.

LIU, A. S.

L049 Lunar Gravity Analysis From Long-Term Effects

A. S. Liu and P. A. Laing

Science, Vol. 173, No. 4001, pp. 1017–1020, September 10, 1971

As described in this article, the global lunar gravity field was determined from a weighted least-squares analysis of the averaged classical element of the five Lunar Orbiter spacecraft. The observed-minus-computed residuals have been reduced by a factor of 10 from a previously derived gravity field. The values of the second-degree zonal and sectorial harmonics are compatible with those derived from libration data.

LIU, S. T.

L050 Long-Term Aging of Elastomers: Chemorheology of Viton B Fluorocarbon Elastomer

S. H. Kalfayan, R. H. Silver, A. A. Mazzeo, and S. T. Liu

JPL Quarterly Technical Review, Vol. 2, No. 3, pp. 32–39, October 1972

For abstract, see Kalfayan, S. H.

LIVERMORE, R. W.

L051 DSN Progress Report for July–August 1972: High-Speed Data Communication: A Description of Software Techniques

R. W. Livermore

Technical Report 32-1526, Vol. XI, pp. 161–163, October 15, 1972

This article describes some methods of using the high-speed data assembly of the Ground Communications Facility operating at 4.8 kbps and the Xerox Data Systems 920 computers for keeping the deep space stations supplied with up-to-date programs and documentation. The present method for transmitting this information employs magnetic tapes, punched tapes, and hardcopy documentation transmitted by mail or air freight.

LONG, H. R.

L052 Trajectory Correction Propulsion for TOPS

H. R. Long and R. A. Bjorklund

Technical Report 32-1571, November 15, 1972

A blowdown-pressurized hydrazine propulsion subsystem was selected to provide trajectory-correction impulse for outer-planet flyby spacecraft as the result of cost/mass/reliability tradeoff analyses. Present hydrazine component and system technology and component designs were evaluated for application to the Thermoelectric Outer-Planet Spacecraft (TOPS). While general hydrazine technology was adequate, component design changes were deemed necessary for TOPS-type missions. A prototype hydrazine propulsion subsystem was fabricated and fired nine times for a total of 1600 s to demonstrate the operation and performance of the TOPS propulsion subsystem configuration. A flight-weight trajectory-correction propulsion subsystem was designed for the TOPS based on actual and estimated advanced components.

LORDEN, G.

L053 DSN Progress Report for March–April 1972: An Inventory Policy for the Deep Space Network

I. Eisenberger, F. R. Maiocco, and G. Lorden (California Institute of Technology)

Technical Report 32-1526, Vol. IX, pp. 84–87, June 15, 1972

For abstract, see Eisenberger, I.

L054 DSN Progress Report for September–October 1972: An Inventory and Procurement Policy for the Deep Space Network

I. Eisenberger, F. R. Maiocco, and G. Lorden (California Institute of Technology)

Technical Report 32-1526, Vol. XII, pp. 131–148, December 15, 1972

For abstract, see Eisenberger, I.

LORELL, J.

L055 Mariner 9 Science Experiments: Preliminary Results

R. H. Steinbacher, A. J. Kliore, J. Lorell,
H. Hipsher (National Aeronautics and Space
Administration), C. A. Barth (University of
Colorado), H. Masursky (U.S. Geological Survey),
G. Münch (California Institute of Technology),
J. C. Pearl (Goddard Space Flight Center), and
B. A. Smith (New Mexico State University)

Science, Vol. 175, No. 4019, pp. 293–294,
January 21, 1972

For abstract, see Steinbacher, R. H.

L056 Mariner 9 Celestial Mechanics Experiment: Gravity Field and Pole Direction of Mars

J. Lorell, G. H. Born, E. J. Christensen,
J. F. Jordan, P. A. Laing, W. Martin,
W. L. Sjogren, I. I. Shapiro (Massachusetts
Institute of Technology),
R. D. Reasenberg (Massachusetts Institute of
Technology), and G. L. Slater (Massachusetts
Institute of Technology)

Science, Vol. 175, No. 4019, pp. 317–320,
January 21, 1972

Analysis of the Mariner 9 radio-tracking data shows that the Martian gravity field is rougher than that of Earth or the Moon, and that the accepted direction of Mars rotation axis is in error by about 0.5 deg. The new value for the pole direction for the epoch 1971.9, referred to the mean equatorial system of 1950.0, is right ascension = 317.3 ± 0.3 deg, declination = 52.6 ± 0.2 deg. The values found for the coefficients of the low-order harmonics of Mars gravity field are as follows:

$$J_2 = (1.96 \pm 0.01) \times 10^{-3}$$

$$C_{22} = -(5 \pm 1) \times 10^{-5}$$

$$S_{22} = (3 \pm 1) \times 10^{-5}$$

where J_2 is referred to an equatorial radius of 3394 km. The value for J_2 is in excellent agreement with the result from Wilkins' analysis of the observations of Phobos. The other two coefficients imply a value of $(2.5 \pm 0.5) \times 10^{-4}$ for the fractional difference in the principal equatorial moments of inertia; the axis of the minimum moment passes near 105°W.

LOVELOCK, J. E.

L057 Rare Gases of the Atmosphere: Gas Chromatography Using a Thermal Conductivity Detector and a Palladium Transmodulator

J. E. Lovelock, P. G. Simmonds, and
G. R. Shoemake

Anal. Chem., Vol. 43, No. 14, pp. 1958–1961,
December 1971

This article reports on the application of the palladium transmodulator combined with a small-volume thermal conductivity detector to the determination of the rare gases in air. The analysis was performed directly on a 10-ml sample of air using a single column operated at room temperature. A gain in sensitivity of 10^3 is demonstrated. The system described was developed for planetary atmospheric analysis, but is of general use wherever gas analysis at high sensitivity is required.

LOWMAN, P. D.

L058 Infrared Spectroscopy Experiment on the Mariner 9 Mission: Preliminary Results

R. A. Hanel (Goddard Space Flight Center),
B. J. Conrath (Goddard Space Flight Center),
W. A. Hovis (Goddard Space Flight Center),
V. G. Kunde (Goddard Space Flight Center),
P. D. Lowman (Goddard Space Flight Center),
J. C. Pearl (Goddard Space Flight Center),
C. Prabhakara (Goddard Space Flight Center),
B. Schlachman (Goddard Space Flight Center), and
G. V. Levin (Biospherics Incorporated)

Science, Vol. 175, No. 4019, pp. 305–308,
January 21, 1972

For abstract, see Hanel, R. A.

LUDWIG, A. C.

L059 Gain Calibration of a Horn Antenna Using Pattern Integration

A. C. Ludwig, J. Hardy, and R. Norman

Technical Report 32-1572, October 1, 1972

A cooperative program between JPL and the National Bureau of Standards will result in the gain measurement of a horn antenna using three different techniques: a two-antenna insertion loss measurement, a pattern-integration method, and a near-field measurement method. This article describes the application of the pattern-integration method and the evaluation of the near-field gain correction factors for the horn, which are determined by a new method based directly on measured data. This method involves a spherical-wave expansion of the experimental

radiation pattern of the specific antenna being tested, rather than evaluation of an assumed analytical model. The spherical-wave expansion is compared to experimental near-field pattern data.

The gain of the antenna is determined by the pattern-integration method to be 22.02 dB within a 3σ tolerance (or 99.7% confidence interval) of ± 0.1 dB. It is concluded that the pattern-integration method is a valuable technique with a potential of even better accuracies with further development.

L060 Conical-Reflector Antennas

A. C. Ludwig

IEEE Trans. Anten. Prop., Vol. AP-20, No. 2, pp. 146–152, March 1972

The mechanical advantages of a singly curved conical reflector are demonstrated by the experimental test of a furlable 1.83-m conical-Gregorian antenna at 16.33 GHz. The measured gain of 47.5 dB corresponds to a net efficiency of over 57%. A ray-optics analysis of conical-reflector antennas is presented, and data useful in the design of conical antennas is given. The conical-Gregorian antenna, in which a subreflector is used in conjunction with a conventional horn feed, is considered in detail. A physical-optics analysis of the conical-Gregorian antenna is used to investigate diffraction and other effects, and to analytically confirm the high performance of the antenna. It is concluded that conical antennas are a valuable addition to available antenna-design concepts.

LUDWIG, O.

L061 The James Wavefunction for the Ground State of H_2^+

M. Geller and O. Ludwig (Villanova University)

Chem. Phys. Lett., Vol. 12, No. 2, p. 403, December 15, 1971

For abstract, see Geller, M.

LUNDY, C. C.

L062 DSN Progress Report for May–June 1972: New Probes for Tracing Electrical Noise

C. C. Lundy

Technical Report 32-1526, Vol. X, pp. 194–198, August 15, 1972

Stations of the DSN are vulnerable to many kinds of noise. This article describes three new designs of probes to discover and measure potentially harmful noise. The article also suggests design practices that defend the station against noise.

LUSHBAUGH, W. A.

L063 DSN Progress Report for September–October 1972: A Multicomputer Communications System

J. W. Layland and W. A. Lushbaugh

Technical Report 32-1526, Vol. XII, pp. 195–199, December 15, 1972

For abstract, see Layland, J. W.

L064 A Flexible High-Speed Sequential Decoder for Deep Space Channels

J. W. Layland and W. A. Lushbaugh

IEEE Trans. Commun., Vol. COM-19, No. 5, pp. 813–820, October 1971

For abstract, see Layland, J. W.

LUTES, G.

L065 DSN Progress Report for November–December 1971: Hydrogen Maser: Low Phase Noise, L-Band Frequency Multiplier

G. Lutes, J. MacConnell, and R. Meyer

Technical Report 32-1526, Vol. VII, pp. 81–83, February 15, 1972

A 100- to 1400-MHz discrete component $\times 14$ frequency multiplier was developed to determine the lowest phase noise achievable with present technology. The $1/f$ phase noise spectrum of the multiplier measured 11 dB lower than the hydrogen maser frequency standard and 13 dB better than a high-quality step recovery diode multiplier.

L066 DSN Progress Report for September–October 1972: Phase-Stable, Low-Phase-Noise Filters for Reference Signals

G. Lutes

Technical Report 32-1526, Vol. XII, pp. 44–46, December 15, 1972

This article describes a phase-locking filter which filters reference signals by locking the phase of the output signal to the phase of the input signal. A very small phase drift may be achieved over a large temperature range without the use of temperature-controlled ovens, which are bulky and costly.

LYTTLETON, R. A.

L067 Does a Continuous Solid Nucleus Exist in Comets?

R. A. Lyttleton

Astrophys. Space Sci., Vol. 15, No. 2,
pp. 175–184, February 1972

The implication of actual cometary observations for the physical nature of comets is briefly reviewed and brings out the complete conflict with observation of the ice-dust solid nucleus model put forward in recent years as representing the fundamental structure of comets. That under increasing solar heat the nucleus develops an expanding atmosphere is inconsistent with the well-established phenomenon that the coma *contracts* with decreasing distance from the Sun. Several comets remaining always beyond Mars have nevertheless been strongly active and produced fine tails. That some comets show at times a star-like point of light is readily explicable on the dust-cloud structure and by no means establishes that a solid nucleus exists. With the nucleus-area corresponding not to a small solid mass but to an optical phenomenon, there would be no reason to expect that it would describe a precise dynamical orbit. On the hypothesis of a nucleus, it is necessary to postulate further some internal jet-propulsion mechanism to account for the orbital deviations.

In planning a space-mission to a comet, and if search for a nucleus is included, it will be of the highest importance for its success to ensure beforehand that the equipment carried will not fail to discover a kilometric-sized body if one is present; otherwise a null result could be interpreted simply as a failure of this part of the mission and not as proving the absence of any nucleus.

MacCLELLAN, R. N.

M001 DSN Progress Report for May–June 1972: Novel 70-MHz Limiting Amplifier

J. G. Leflang and R. N. MacClellan

Technical Report 32-1526, Vol. X, pp. 172–174, August 15, 1972

For abstract, see Leflang, J. G.

M002 DSN Progress Report for September–October 1972: Digital Frequency Shifter

R. N. MacClellan

Technical Report 32-1526, Vol. XII, pp. 209–213, December 15, 1972

Digital techniques applied to the development of frequency shifters yield a circuit that exhibits both wide bandwidth and exceptionally low phase noise while requiring no alignment.

MacCONNELL, J.

M003 DSN Progress Report for November–December 1971: Hydrogen Maser: Low Phase Noise, L-Band Frequency Multiplier

G. Lutes, J. MacConnell, and R. Meyer

Technical Report 32-1526, Vol. VII, pp. 81–83, February 15, 1972

For abstract, see Lutes, G.

M004 DSN Progress Report for May–June 1972: L-Band Frequency Multipliers: Phase Noise, Stability, and Group Delay

J. MacConnell and R. Meyer

Technical Report 32-1526, Vol. X, pp. 104–109, August 15, 1972

In this article, three 100- to 1400-MHz frequency multipliers are evaluated for use in the hydrogen-maser receiver–synthesizer, with the conclusion that significant advancements have been made in the design of step-recovery diode multipliers. In addition, while it appears that the group delay performance in multipliers can be quite good, there are substantial problems that prevent resolving group delays of <1 ns in frequency multipliers.

MacDORAN, P. F.

M005 DSN Progress Report for September–October 1972: Very Long Baseline Interferometry (VLBI) Possibilities for Lunar Study

M. A. Slade, P. F. MacDoran, and J. B. Thomas

Technical Report 32-1526, Vol. XII, pp. 35–39, December 15, 1972

For abstract, see Slade, M. A.

MACIE, T. W.

M006 Integration of a Breadboard Power Conditioner With a 20-cm Ion Thruster

T. D. Masek, T. W. Macie, E. N. Costogue,
W. J. Muldoon (Hughes Aircraft Company),
D. R. Garth (Hughes Aircraft Company), and
G. C. Benson (Hughes Aircraft Company)

J. Spacecraft Rockets, Vol. 9, No. 2, pp. 71–78, February 1972

For abstract, see Masek, T. D.

MACLAY, J. E.

M007 **DSN Progress Report for March–April 1972: DSN Monitor and DSN Operations Control System Testing**

J. E. Maclay

Technical Report 32-1526, Vol. IX, pp. 12–14, June 15, 1972

In preparation for Mariner Mars 1971 support, the DSN Monitor System and Operations Control System were individually tested, after which they provided support for combined system tests. These tests provided valuable test preparation and execution practice.

MAILLARD, J.-P.

M008 **Fourier Spectroscopy With a One-Million-Point Transformation (Translation From the Original Published in the Nouvelle Revue d'Optique Appliquée, Vol. 1, pp. 3–22, 1970)**

J. Connes (National Center for Scientific Research, Orsay, France), H. Delouis (National Center for Scientific Research, Orsay, France), P. Connes (National Center for Scientific Research, Orsay, France), G. Guelachvili (National Center for Scientific Research, Orsay, France), J.-P. Maillard (National Center for Scientific Research, Orsay, France), and G. Michel (National Center for Scientific Research, Orsay, France)

Technical Memorandum 33-525, March 15, 1972

For abstract, see Connes, J.

MAIOCCO, F. R.

M009 **DSN Progress Report for March–April 1972: An Inventory Policy for the Deep Space Network**

I. Eisenberger, F. R. Maiocco, and G. Lorden (California Institute of Technology)

Technical Report 32-1526, Vol. IX, pp. 84–87, June 15, 1972

For abstract, see Eisenberger, I.

M010 **DSN Progress Report for September–October 1972: An Inventory and Procurement Policy for the Deep Space Network**

I. Eisenberger, F. R. Maiocco, and G. Lorden (California Institute of Technology)

Technical Report 32-1526, Vol. XII, pp. 131–148, December 15, 1972

For abstract, see Eisenberger, I.

MANATT, S. L.

M011 **Ferromagnetic Resonance of Lunar Samples**

F.-D. Tsay (California Institute of Technology), S. I. Chan (California Institute of Technology), and S. L. Manatt

Geochim. Cosmochim. Acta, Vol. 35, No. 9, pp. 865–875, September 1971

For abstract, see Tsay, F.-D.

M012 **Electron Paramagnetic Resonance of Radiation Damage in a Lunar Rock**

F.-D. Tsay, S. I. Chan, and S. L. Manatt

Nature Phys. Sci., Vol. 237, No. 77, pp. 121–122, June 19, 1972

For abstract, see Tsay, F.-D.

M013 **Magnetic Resonance Studies of Apollo 11 and Apollo 12 Samples**

F.-D. Tsay (California Institute of Technology), S. I. Chan (California Institute of Technology), and S. L. Manatt

Proceedings of the Second Lunar Science Conference, Houston, Texas, January 11–14, 1971, Vol. 3, pp. 2515–2528, The M.I.T. Press, Cambridge, 1971

For abstract, see Tsay, F.-D.

M014 **Calculations of Geometries of Organic Molecules Using the CNDO/2 Method: I. Empirical Correlations Between Observed and Calculated Bond Lengths in Simple Acyclics, Strained Cycloalkenes and Some Polycyclic Molecules**

C. S. Cheung, M. A. Cooper, and S. L. Manatt

Tetrahedron, Vol. 27, No. 4, pp. 689–700, February 1971

For abstract, see Cheung, C. S.

M015 **Calculations of Geometries of Organic Molecules Using the CNDO/2 Molecular Orbital Method: II. Structural Predictions for the Benzocycloalkenes, and a Theoretical Rationalization of Their Proton-Proton Spin–Spin Coupling Constants**

C. S. Cheung, M. A. Cooper, and S. L. Manatt

Tetrahedron, Vol. 27, No. 4, pp. 701–709, February 1971

For abstract, see Cheung, C. S.

MANCINI, R. A.

M016 DSN Progress Report for November–December 1971: Data Decoder Assembly Implementation Status

R. A. Mancini

Technical Report 32-1526, Vol. VII, pp. 168–174, February 15, 1972

Twelve data decoder assemblies have been acceptance-tested, delivered to the Deep Space Network stations, and are undergoing installation/testing and incorporation of field modifications in preparation for the Pioneer F mission. Eight additional data decoder assemblies are in different stages of testing and implementation. This article describes their present status.

MARGOLIS, J. S.

M017 A Compilation of Laboratory Spectra

J. S. Margolis

Technical Memorandum 33-541, May 15, 1972

This memorandum contains an up-to-date listing of the spectra obtained in the spectroscopy laboratory and a complete description of the experimental conditions.

M018 Laboratory Simulation of Diffuse Reflectivity From a Cloudy Planetary Atmosphere

J. S. Margolis, D. J. McCleese, and G. E. Hunt

Appl. Opt., Vol. 11, No. 5, pp. 1212–1216, May 1972

For the first time measurements in the multiple scattering regime of the diffuse reflectivity as a function of single scattering albedo have been made in a geometry that may be simulated by a plane parallel atmosphere of large optical depth. A comparison between the measurements and a theoretical computation of the diffuse reflectivity is presented. The measurements are within 1% agreement with the theoretical calculations for two different sizes of scattering particles which are larger than and smaller than the wavelength of the incident light, corresponding to the Mie and Rayleigh regimes, respectively.

M019 High Dispersion Spectroscopic Studies of Mars: V. A Search for Oxygen in the Atmosphere of Mars

J. S. Margolis, R. A. J. Schorn, and L. D. G. Young

Icarus, Vol. 15, No. 2, pp. 197–203, October 1971

In order to set a new upper limit on the amount of oxygen in the atmosphere of Mars, a number of high-dispersion spectra of the 7620-Å band of oxygen ob-tained during the 1969 apparition of Mars have been reduced by the authors. The new upper limit is $w = 15$ cm-atm (STP) for the Martian abundance in a single vertical path. This result confirms and lowers the 1963 upper limit of $w = 70$ cm-atm (STP) by Kaplan, Münch, and Spinrad. The features reported by Hunten and Belton do not appear in the authors' spectra. Furthermore, by measuring the pressure shift of the A band in the labora-tory, the authors found that the shift required by Hun-ten's and Belton's tentative identification of oxygen in the Martian atmosphere does not exist.

M020 Intensity and Half Width Measurements of the $(00^0 2-00^0 0)$ Band of N_2O

J. S. Margolis

J. Quant. Spectrosc. Radiat. Transfer, Vol. 12, No. 4, pp. 751–757, April 1972

Measurements of the intensities and half-widths of the lines of the $(00^0 2-00^0 0)$ band of N_2O have been made with a spectral resolution <0.06 cm^{-1}. The band inten-sity has been determined to be 1.29 cm^{-2} atm^{-1} at 296°K. The half-widths have been measured for both N_2- and self-broadened lines.

M021 Laboratory Simulation of Absorption Spectra in Cloudy Atmospheres

D. J. McCleese, J. S. Margolis, and G. E. Hunt

Nature Phys. Sci., Vol. 233, No. 40, pp. 102–103, October 4, 1971

For abstract, see McCleese, D. J.

MARINER MARS 1971 SCIENCE EXPERIMENTER TEAMS

M022 Mariner Mars 1971 Project Final Report: Preliminary Science Results

Mariner Mars 1971 Science Experimenter Teams

Technical Report 32-1550, Vol. II, February 1, 1972

This volume is the second of four volumes comprising the Mariner Mars 1971 Project Final Report. Presented in this volume are the preliminary science results for the Mariner 9 television, infrared spectroscopy, infrared ra-diometry, ultraviolet spectrometer, S-band occultation, and celestial mechanics experiments. These results, de-rived from data evaluation to December 14, 1971 (30 days after orbit insertion), have also been published in *Science*, Vol. 175, January 1972.

Volume I of this series describes project development through launch and the trajectory-correction maneuver; Volume III describes flight operations after the trajec-tory-correction maneuver and during the basic 90-day

orbital mission; and Volume IV describes the science results derived from the basic 90-day orbital mission and the experimenters' interpretations of the data.

MARSH, E. L.

M023 Analysis of Morgantown Vehicle Steering Control

H. S. Lin and E. L. Marsh

JPL Quarterly Technical Review, Vol. 2, No. 1, pp. 58–71, April 1972

For abstract, see Lin, H. S.

MARTIN, D. P.

M024 A Combined Radar–Radiometer With Variable Polarization

D. P. Martin

Technical Memorandum 33-570, October 15, 1972

This memorandum describes an instrument that provides both radar and radiometer data at the same time. The antenna and receiver are time shared for the two sensor functions. The antenna polarization can be electronically scanned at rates up to 5000 changes/s for both the transmit and receive signal paths. The purpose of the equipment is to investigate target signatures for remote sensing applications. The function of the equipment is described, and the results for observations of asphalt, grass, and gravel surfaces are presented.

MARTIN, W.

M025 Mariner 9 Celestial Mechanics Experiment: Gravity Field and Pole Direction of Mars

J. Lorell, G. H. Born, E. J. Christensen, J. F. Jordan, P. A. Laing, W. Martin, W. L. Sjogren, I. I. Shapiro (Massachusetts Institute of Technology), R. D. Reasenberg (Massachusetts Institute of Technology), and G. L. Slater (Massachusetts Institute of Technology)

Science, Vol. 175, No. 4019, pp. 317–320, January 21, 1972

For abstract, see Lorell, J.

M026 Determination of Astrodynamic Constants and a Test of the General Relativistic Time Delay With S-Band Range and Doppler Data From Mariners 6 and 7

J. D. Anderson, P. B. Esposito, W. Martin, and D. O. Muhleman (California Institute of Technology)

Space Research XI, pp. 105–112, Akademie-Verlag, Berlin, 1971

For abstract, see Anderson, J. D.

MARTONCHIK, J. V.

M027 Jupiter: Observation of Deuterated Methane in the Atmosphere

R. Beer, C. B. Farmer, R. H. Norton, J. V. Martonchik (University of Texas), and T. G. Barnes (University of Texas)

Science, Vol. 175, No. 4028, pp. 1360–1361, March 24, 1972

For abstract, see Beer, R.

MASEK, T. D.

M028 Solar–Electric Propulsion Breadboard Thrust Subsystem

T. D. Masek

JPL Quarterly Technical Review, Vol. 2, No. 2, pp. 100–112, July 1972

A solar–electric propulsion, breadboard, thrust subsystem has been designed, built, and tested. A 1500-h test was performed to demonstrate the functional capabilities of the subsystem. This report describes the subsystem functions and testing process. The results show that the ground work has been established for development of an engineering model of the thrust subsystem.

M029 Integration of a Breadboard Power Conditioner With a 20-cm Ion Thruster

T. D. Masek, T. W. Macie, E. N. Costogue, W. J. Muldoon (Hughes Aircraft Company), D. R. Garth (Hughes Aircraft Company), and G. C. Benson (Hughes Aircraft Company)

J. Spacecraft Rockets, Vol. 9, No. 2, pp. 71–78, February 1972

A breadboard of a lightweight 2.5-kW power conditioner was developed and integrated with an oxide ion thruster. The power conditioner was subsequently modified and integrated with a hollow cathode thruster. The problems of integration with each type of thruster are reviewed. Work leading to optimization of the closed-loop system performance during startup and recycling after thruster arcing is described. Electrical efficiency, weight, reliability, and other critical parameters are evaluated. The

integration program has shown that the system satisfies the requirements of solar electric spacecraft.

M030 A Mechanism for Three-Axis Control of an Ion Thruster Array

G. S. Perkins, K. G. Johnson, J. D. Ferrera, and T. D. Masek

J. Spacecraft Rockets, Vol. 9, No. 3, pp. 218–220, March 1972

For abstract, see Perkins, G. S.

MASERJIAN, J.

M031 Barrier Energies in MIM Structures From Photoresponse: Effect of Scattering in the Insulating Film

G. Lewicki, J. Maserjian, and C. A. Mead (California Institute of Technology)

J. Appl. Phys., Vol. 43, No. 4, pp. 1764–1767, April 1972

For abstract, see Lewicki, G.

MASSIER, P. F.

M032 An Anechoic Chamber Facility for Investigating Aerodynamic Noise

P. F. Massier and S. P. Parthasarathy

Technical Report 32-1564, September 15, 1972

The aerodynamic-noise facility at JPL was designed to be used primarily for investigating the noise-generating mechanisms of high-temperature supersonic and subsonic jets. It can, however, be used for investigating other sources of noise as well. The facility consists of an anechoic chamber, an exhaust-jet silencer, instrumentation equipment, and an air heater with associated fuel and cooling systems. Compressed air, when needed for jet-noise studies, is provided by the wind tunnel compressor facility on a continuous basis.

The chamber is 8.1 m long, 5.0 m wide, and 3.0 m high. Provisions have been made for allowing outside air to be drawn into the anechoic chamber in order to replenish the air that is entrained by the jet as it flows through the chamber. Also, openings are provided in the walls and in the ceiling for the purpose of acquiring optical measurements. The chamber was calibrated for noise reflections from the wall in octave bands between 31.2 Hz and 32 kHz.

M033 Influence of Contraction Section Shape and Inlet Flow Direction on Supersonic Nozzle Flow and Performance

L. H. Back, R. F. Cuffel, and P. F. Massier

J. Spacecraft Rockets, Vol. 9, No. 6, pp. 420–427, June 1972

For abstract, see Back, L. H.

M034 Partially Ionized Gas Flow and Heat Transfer in the Separation, Reattachment, and Redevelopment Regions Downstream of an Abrupt Circular Channel Expansion

L. H. Back, P. F. Massier, and E. J. Roschke

Trans. ASME, Ser. C: J. Heat Transf., Vol. 94, No. 1, pp. 119–127, February 1972

For abstract, see Back, L. H.

M035 Partially Ionized Gas Flow and Heat Transfer in the Separation, Reattachment, and Redevelopment Regions Downstream of an Abrupt Circular Channel Expansion

L. H. Back, P. F. Massier, and E. J. Roschke

Trans. ASME, Ser. C: J. Heat Transf., Vol. 94, No. 1, pp. 119–127, February 1972

For abstract, see Back, L. H.

MASURSKY, H.

M036 Mariner 9 Science Experiments: Preliminary Results

R. H. Steinbacher, A. J. Kliore, J. Lorell, H. Hipsher (National Aeronautics and Space Administration), C. A. Barth (University of Colorado), H. Masursky (U.S. Geological Survey), G. Münch (California Institute of Technology), J. C. Pearl (Goddard Space Flight Center), and B. A. Smith (New Mexico State University)

Science, Vol. 175, No. 4019, pp. 293–294, January 21, 1972

For abstract, see Steinbacher, R. H.

M037 Mariner 9 Television Reconnaissance of Mars and Its Satellites: Preliminary Results

H. Masursky, et al.

Science, Vol. 175, No. 4019, pp. 294–305, January 21, 1972

At orbit insertion on November 14, 1971, the Martian surface was largely obscured by a dust haze with an extinction optical depth that ranged from near unity in the south polar region to probably greater than 2 over most of the planet. The only features clearly visible were the south polar cap, one dark spot in Nix Olympica, and three dark spots in the Tharsis region. During the third

week the atmosphere began to clear and surface visibility improved, but contrasts remained a fraction of their normal value. Each of the dark spots that apparently protrude through most of the dust-filled atmosphere has a crater or crater complex in its center. The craters are rimless and have featureless floors that, in the crater complexes, are at different levels. The largest crater within the southernmost spot is approximately 100 km wide. The craters apparently were formed by subsidence and resemble terrestrial calderas. The south polar cap has a regular margin, suggesting very flat topography. Two craters outside the cap have frost on their floors; an apparent crater rim within the cap is frost free, indicating preferential loss of frost from elevated ground. If this is so, then the curvilinear streaks, which were frost covered in 1969 and are now clear of frost, may be low-relief ridges. Closeup pictures of Phobos and Deimos show that Phobos is about 25 ± 5 by 21 ± 1 km and Deimos is about 13.5 ± 2 by 12.0 ± 0.5 km. Both have irregular shapes and are highly cratered, with some craters showing raised rims. The satellites are dark objects with geometric albedos of 0.05.

Contributors to this article include:

U.S. Geological Survey: H. Masursky, R. M. Batson, J. F. McCauley, L. A. Soderblom, R. L. Wildey, M. H. Carr, D. J. Milton, and D. E. Wilhelms

New Mexico State University: B. A. Smith, T. B. Kirby, and J. C. Robinson

University of Washington: C. B. Leovy

Jet Propulsion Laboratory: G. A. Briggs, T. C. Duxbury, and C. H. Acton, Jr.

California Institute of Technology: B. C. Murray, J. A. Cutts, R. P. Sharp, S. Smith, and R. B. Leighton

Cornell University: C. Sagan, J. Veverka, and M. Noland

Stanford University: J. Lederberg and E. Levinthal

Ames Research Center: J. B. Pollack and J. T. Moore, Jr.

IIT Research Institute: W. K. Hartmann

Bellcomm, Inc.: E. N. Shipley

University of Texas: G. de Vaucouleurs

Rand Corporation: M. E. Davies

MATHUR, F. P.

M038   A Brief Description and Comparison of Programming Languages FORTRAN, ALGOL, COBOL, PL/I, and LISP 1.5 From a Critical Standpoint

F. P. Mathur

Technical Memorandum 33-566, September 15, 1972

This report describes and compares several common higher-level programming languages, FORTRAN, ALGOL, COBOL, PL/I, and LISP 1.5. FORTRAN is the most widely used scientific programming language, however ALGOL is a more powerful language. COBOL is used for most commercial programming applications, and LISP 1.5 is primarily a list-processing language. PL/I attempts to combine the desirable features of FORTRAN, ALGOL, and COBOL into a single language.

M039   A Survey of and an Introduction to Fault Diagnosis Algorithms

F. P. Mathur

Technical Memorandum 33-567, October 1, 1972

This memorandum surveys the field of fault diagnosis and introduces the reader to some of the key algorithms and heuristics currently in use. Fault diagnosis is an important and rapidly growing discipline. This is important to JPL's research efforts in the design of self-repairable computers because the present diagnosis resolution of its fault-tolerant computer is limited to a functional unit or processor. Better resolution is necessary before failed units can become partially reuseable. The approach that holds the greatest promise is that of resident microdiagnostics; however, that presupposes a microprogrammable architecture for the computer being self-diagnosed. The presentation here is tutorial and contains examples. An extensive bibliography of some 220 entries is included.

M040   Phase 1 Report on a Cognitive Operating System (COGNOSYS) for JPL's Robot

F. P. Mathur

Technical Memorandum 33-568, September 15, 1972

The most important software requirement for any robot development is the COGNitive Operating SYStem (COGNOSYS). This memorandum describes the Stanford University Artificial Intelligence Laboratory's Hand/Eye software system from the point of view of developing a cognitive operating system for JPL's Robot. In this Phase I report of the JPL robot COGNOSYS task, the installation of a SAIL compiler and a FAIL assembler on Caltech's PDP-10 are described, and guidelines are given for the implementation of a Stanford-University-type Hand/Eye software system in JPL-Caltech's computing facility. The alternatives offered by using RAND-USC's PDP-10 Tenex operating system are also considered.

M041 The STAR (Self-Testing and Repairing) Computer: An Investigation of the Theory and Practice of Fault-Tolerant Computer Design

A. Avižienis, G. C. Gilley, F. P. Mathur, D. A. Rennels, J. A. Rohr, and D. K. Rubin

IEEE Trans. Computers, Vol. C-20, No. 11, pp. 1312–1321, November 1971

For abstract, see Avižienis, A.

M042 On Reliability Modeling and Analysis of Ultrareliable Fault-Tolerant Digital Systems

F. P. Mathur

IEEE Trans. Computers, Vol. C-20, No. 11, pp. 1376–1382, November 1971

The processes of protective redundancy, namely, standby replacement redundancy and hybrid redundancy (a combination of standby replacement and multiple-line voting redundancy), find application in the architecture of fault-tolerant digital computers and enable them to be ultrareliable and self-repairing. The claims to ultrareliability lead to the challenge of quantitatively evaluating and assigning a value to the probability of survival as a function of the mission durations intended. This article presents various mathematical models and derives and displays quantitative evaluations of system reliability as a function of various mission parameters of interest to the system designer.

MAXWORTHY, T.

M043 Comments on "A Mechanism for Jupiter's Equatorial Acceleration"

T. Maxworthy

J. Atmos. Sci., Vol. 29, No. 5, pp. 1007–1008, July 1972

The mechanism proposed by Gierasch and Stone (1968) to account for the equatorial jet found high in the Jovian atmosphere has recently been criticized by Hide (1969, 1970). This article presents one more comment which casts further doubt on the validity of the Gierasch–Stone picture. It is based more directly on the fluid dynamical processes invoked by Gierasch and Stone and less on general considerations, as presented by Hide.

MAZZEO, A. A.

M044 Long-Term Aging of Elastomers: Chemorheology of Viton B Fluorocarbon Elastomer

S. H. Kalfayan, R. H. Silver, A. A. Mazzeo, and S. T. Liu

JPL Quarterly Technical Review, Vol. 2, No. 3, pp. 32–39, October 1972

For abstract, see Kalfayan, S. H.

McCLEESE, D. J.

M045 Laboratory Simulation of Diffuse Reflectivity From a Cloudy Planetary Atmosphere

J. S. Margolis, D. J. McCleese, and G. E. Hunt

Appl. Opt., Vol. 11, No. 5, pp. 1212–1216, May 1972

For abstract, see Margolis, J. S.

M046 Laboratory Simulation of Absorption Spectra in Cloudy Atmospheres

D. J. McCleese, J. S. Margolis, and G. E. Hunt

Nature Phys. Sci., Vol. 233, No. 40, pp. 102–103, October 4, 1971

This article describes a laboratory investigation of diffuse reflectivity from a suspension of polymer latex spheres in a medium of variable absorption. This investigation was carried out in order to simulate the formation of absorption lines in cloudy planetary atmospheres. The experimental techniques derived may be generalized to situations which are too complicated for present computational techniques (for example, atmospheres which contain non-spherical scatterers, where the distribution of scatterers is inhomogeneous, or atmospheres with a complete structure).

McCLURE, J. P.

M047 DSN Progress Report for March–April 1972: Madrid-to-JPL 50-kbit/s Wideband Error Statistics

J. P. McClure

Technical Report 32-1526, Vol. IX, pp. 177–184, June 15, 1972

Detailed analysis of the results of wideband data tests conducted at 50 kbit/s in June 1971 between Madrid and the Space Flight Operations Facility confirms the burst nature of the transmission errors. Measured burst length depends critically on the definition of a burst. A typical burst length of 200 bits was determined for the error model and method of measurement employed. During good circuit conditions, the block error rate varies directly with block length; however, this proportionality does not hold during poor circuit conditions. The average number of error bits in an error block holds reasonably constant even as the error rate changes by several orders of magnitude.

M048 DSN Progress Report for July–August 1972: Ground Communications Facility Functional Design for 1973–1974

J. P. McClure

Technical Report 32-1526, Vol. XI, pp. 124–131, October 15, 1972

This article describes the Ground Communications Facility (GCF) 1973–1974 capability that will be used to support Pioneer, Mariner Venus–Mercury 1973, and Helios operations, plus the early development and testing associated with the 1975 Viking Project. The design includes a full spectrum of GCF capabilities for the overseas 64-m-diameter antenna stations. The wideband data system will be enlarged to cover all 64-m-diameter antenna stations, plus the Compatibility Test Area (CTA 21) at JPL and the Compatibility Test Station (DSS 71) at Cape Kennedy. The standard wide-band rate will be 28.5 kbps with limited use of 50 and 230 kbps for special purposes. The wide-band block length will be increased to 2400 bits after Mariner Venus–Mercury 1973 operations. The number of teletype circuits will be reduced in keeping with the DSN policy of eliminating this medium for computer-to-computer data transfer.

McCORD, T. B.

M049 Apollo 12 Multispectral Photography Experiment

A. F. H. Goetz, F. C. Billingsley, J. W. Head (Bellcomm, Inc.), T. B. McCord (Massachusetts Institute of Technology), and E. Yost (Long Island University)

Proceedings of the Second Lunar Science Conference, Houston, Texas, January 11–14, 1971, Vol. 3, pp. 2301–2310, The M.I.T. Press, 1971

For abstract, see Goetz, A. F. H.

McELIECE, R. J.

M050 DSN Progress Report for November–December 1971: Hiding and Covering in a Compact Metric Space

R. J. McEliece and E. C. Posner

Technical Report 32-1526, Vol. VII, pp. 101–105, February 15, 1972

This article investigates the relationship between games of search on a compact metric space X and the absolute epsilon entropy $I(X)$ of X. The main result is that

$$I(X) = -\log v_L^*.$$

v_L^* being the lower value of a game on X we call "restricted hide and seek."

M051 DSN Progress Report for March–April 1972: A Note on the Griesmer Bound

L. D. Baumert and R. J. McEliece

Technical Report 32-1526, Vol. IX, pp. 49–52, June 15, 1972

For abstract, see Baumert, L. D.

M052 DSN Progress Report for July–August 1972: Weights Modulo 8 in Binary Cyclic Codes

R. J. McEliece

Technical Report 32-1526, Vol. XI, pp. 86–88, October 15, 1972

This article presents a new technique for computing the weights modulo 8 in binary cyclic codes. These codes have proved to be the most important ones for Ground Communications Facility error detection/correction, and the method described will frequently aid in the detailed analysis of such codes.

M053 DSN Progress Report for September–October 1972: On the Weight Enumerators of Quadratic Residue Codes

J. Mykkeltveit (California Institute of Technology), C. Lam (California Institute of Technology), and R. J. McEliece

Technical Report 32-1526, Vol. XII, pp. 161–166, December 15, 1972

For abstract, see Mykkeltveit, J.

M054 Hide and Seek, Data Storage, and Entropy

R. J. McEliece and E. C. Posner

Ann. Math. Statist., Vol. 42, No. 5, pp. 1706–1716, October 1971

This article discusses the relationship between games of search and the optimum storage of information. The presentation centers primarily around (1) the case of finite sets, and (2) a generalization to compact metric spaces. The result is a synthesis of the epsilon entropy theory of approximation with the theory of data transmission and compression.

M055 Weights of Irreducible Cyclic Codes

L. D. Baumert and R. J. McEliece

Inform. Control, Vol. 20, No. 2, pp. 158–175, March 1972

For abstract, see Baumert, L. D.

McELMAN, J. A.

**M056 Vibration and Buckling Analysis of Composite
Plates and Shells**

J. A. McElman (Lowell Technological Institute) and
A. C. Knoell

J. Compos. Mater., Vol. 5, pp. 529–532,
October 1971

In the analysis of laminated composites, it is known that
a coupling exists between extension and bending if the
plies are not balanced in number and fiber orientation.
This effect for the bending, vibration, and buckling of
two-, four-, and six-ply laminates was examined else-
where in the literature. The purpose of this article is to
investigate the magnitude of this effect for buckling and
vibration of doubly curved monocoque plates and shells
of positive and negative gaussian curvature. In addition,
the effect of stacking sequence (the order in which indi-
vidual plies are laid up) is examined. This effect is
considered since it is analogous to that of eccentric
stiffening of isotropic cylinders. Solutions are presented
which provide a means of simply and economically as-
sessing the magnitude of the coupling and stacking ef-
fects for various composite materials and geometric con-
figurations.

McGINNESS, H.

**M057 DSN Progress Report for July–August 1972:
Salvaging an Expensive Shaft by Brush
Electroplating**

H. McGinness

Technical Report 32-1526, Vol. XI, pp. 150–152,
October 15, 1972

An expensive shaft was salvaged by depositing nickel on
an undersized bearing journal. The shaft is a component
in the Master Equatorial instrument, required for the 64-
m-diameter antenna of the DSN. In special cases, this
electroplating process could be considered part of the
fabrication method rather than a salvage process.

**M058 DSN Progress Report for September–October 1972:
Excessive Shaft Friction Variation Corrected by
Lubricant Change**

H. McGinness

Technical Report 32-1526, Vol. XII, pp. 51–55,
December 15, 1972

During testing of the Master Equatorial for the 64-
m-diameter antenna under construction in Australia, a
drag-torque variation ratio as large as 5:1 was observed
on a shaft supported by two angular-contact ball bear-

ings. A change in the grease lubricant reduced the ratio
to 1.1:1.0.

McINNIS, J. H., JR.

**M059 DSN Progress Report for May–June 1972: DSN/
MSFN Antenna-Pointing and Tracking
Implementation**

J. H. McInnis, Jr.

Technical Report 32-1526, Vol. X, pp. 153–156,
August 15, 1972

The antenna-pointing and tracking-data processing func-
tions at the three DSN/Manned Space Flight Network
joint-usage ("wing") tracking stations have been altered
to implement a commonality between the two networks.
The changes affect both hardware and software and pro-
duce station configurations that differ from those of other
DSN stations.

McKINLEY, E. L.

**M060 Mariner Venus–Mercury 1973 Midcourse Velocity
Requirements and Delivery Accuracy**

E. L. McKinley

JPL Quarterly Technical Review, Vol. 1, No. 4,
pp. 104–115, January 1972

The Mariner Venus–Mercury 1973 mission represents the
first attempt to navigate a single spacecraft to more than
one planet. The primary mission consists of encounters
with Venus and Mercury (with a second encounter with
Mercury also possible). In this study, the expected navi-
gation sequences are simulated with a Monte Carlo com-
puter program for the purpose of determining midcourse
correction velocity requirements and delivery accuracies.
These simulations provide the sensitivity of the velocity
requirements and delivery accuracies to the error sources
affecting the navigation process. The orbit determination
capability at the final pre-Venus maneuver is shown to
be the dominant contributor to the velocity requirements
for the primary mission. Similarly, the orbit determina-
tion capability at the final pre-Mercury maneuver is
shown to be the dominant contributor to the delivery
accuracy at Mercury.

McRONALD, A. D.

**M061 On the Possibility of Earth Re-entry Simulation of
Shallow Angle Jupiter Entry**

A. D. McRonald

JPL Quarterly Technical Review, Vol. 1, No. 4,
pp. 19–29, January 1972

Possible Earth re-entry simulation of shallow angle (3- to 30-deg) Jupiter entry has been investigated in terms of four parameters of the bow shock layer ahead of a blunt vehicle: peak (equilibrium) temperature, peak pressure, peak inward radiative flux, and time-integrated radiative flux. The comparison shows that simulation ranging from fair to good can be achieved, generally the easiest (lowest Earth re-entry speed) at steep Earth re-entry, in the Earth entry speed range of 15–22 km/s for both the Jupiter "nominal" and "cool" atmospheres. Increasing Earth speed is required, generally, for increasing Jupiter entry angle, and for temperature, radiative flux, time-integrated flux, and pressure, in that order. It appears that a meaningful simulation test could be done using a launch vehicle with the speed and payload capability of the Titan IIID/Centaur/BII.

MEAD, C. A.

M062 Barrier Energies in MIM Structures From Photoresponse: Effect of Scattering in the Insulating Film

G. Lewicki, J. Maserjian, and
C. A. Mead (California Institute of Technology)

J. Appl. Phys., Vol. 43, No. 4, pp. 1764–1767, April 1972

For abstract, see Lewicki, G.

MEEKS, W. G.

M063 DSN Progress Report for May–June 1972: Initial Acquisition Planning

W. G. Meeks

Technical Report 32-1526, Vol. X, pp. 236–242, August 15, 1972

Each spacecraft supported by the DSN must be acquired and tracked by a deep space station. The first acquisition, generally referred to as initial acquisition, is unique for each spacecraft and presents problems that must be recognized and resolved long before a launch actually takes place. This article describes how plans are developed and implemented to ensure the successful beginning of DSN tracking support.

MEISSINGER, H.

M064 Basic Parameters for Low Thrust Mission and System Analysis

T. A. Barber, J. L. Horsewood (Analytical Mechanics Associates, Inc.), and
H. Meissinger (TRW Systems, Inc.)

Preprint 72-426,
AIAA Ninth Electric Propulsion Conference, Bethesda, Maryland, April 17–19, 1972

For abstract, see Barber, T. A.

MELBOURNE, W. G.

M065 Simultaneous Solution for the Masses of the Principal Planets From Analysis of Optical, Radar, and Radio Tracking Data

J. H. Lieske, W. G. Melbourne, D. A. O'Handley,
D. B. Holdridge, D. E. Johnson, and
W. S. Sinclair

Celest. Mech., Vol. 4, No. 2, pp. 233–245, October 1971

For abstract, see Lieske, J. H.

MELOSH, R.

M066 DSN Progress Report for September–October 1972: PARADES Structural Design System Capabilities

R. Levy and R. Melosh (Virginia Polytechnic Institute and State University)

Technical Report 32-1526, Vol. XII, pp. 68–73, December 15, 1972

For abstract, see Levy, R.

MELVILLE, R. D. S., JR.

M067 Stark-Effect Modulation of a CO_2 Laser by NH_2D

A. R. Johnston and R. D. S. Melville, Jr.

Appl. Phys. Lett., Vol. 19, No. 12, pp. 503–506, December 15, 1971

For abstract, see Johnston, A. R.

MENARD, W. A.

M068 A Higher Performance Electric-Arc-Driven Shock Tube

W. A. Menard

AIAA J., Vol. 9, No. 10, pp. 2096–2098, October 1971

Simulation of Jupiter and Saturn atmospheric entry has been difficult because entry velocities range from 25 to 48 km/s. Shock tube velocities have been limited to

about 15 km/s. The purpose of this article is to report the development of an electric arc-driven shock tube which has increased shock velocity by a factor of three. The new driver has a conical internal design of small volume and uses lightweight diaphragms. Data obtained from a 15.2-cm-diam driven tube show little shock wave attenuation. Shock velocities of 45 km/s with test times in excess of 4 μs have been attained.

MENICHELLI, V. J.

M069 Electrothermal Follow Display Apparatus for Electroexplosive Device Testing

L. A. Rosenthal (Rutgers University) and V. J. Menichelli

Technical Report 32-1554, March 15, 1972

For abstract, see Rosenthal, L. A.

M070 Fault Determinations in Electroexplosive Devices by Nondestructive Techniques

V. J. Menichelli and L. A. Rosenthal (Rutgers University)

Technical Report 32-1553, March 15, 1972

Several nondestructive test techniques have been developed for electroexplosive devices. The bridgewire responds, when pulsed with a safe-level current, by generating a characteristic heating curve. The response is indicative of the electrothermal behavior of the bridgewire–explosive interface. Bridgewires that deviate from the characteristic heating curve have been dissected and examined to determine the cause for the abnormality. Deliberate faults have been fabricated into squibs. The relationship of the specific abnormality and the fault associated with it is demonstrated.

M071 Evaluation of Electroexplosive Devices by Nondestructive Test Techniques and Impulsive Waveform Firings

V. J. Menichelli

Technical Report 32-1556, June 15, 1972

Special requirements of the aerospace industry necessitate more detailed knowledge of the quality and reliability of each electroexplosive device selected for use on spacecraft. Statistical methods do not practically demonstrate the high reliability needed. To close this gap, nondestructive test techniques and instrumentation for 1-W/1-A no-fire devices have been developed. Several lots of squibs have been evaluated using these techniques and this instrumentation in order to obtain data on the quality and normal behavior of each electroexplosive device without firing or degrading the unit. Performance data were obtained by initiating each electroexplosive

device with an impulsive waveform and sensing the initiation characteristics, sensitivity, and output.

M072 Initiation of Insensitive Explosives by Laser Energy

V. J. Menichelli and L. C. Yang

Technical Report 32-1557, June 1, 1972

Instantaneous longitudinal detonations have been observed in confined columns of pentaerythritol tetranitrate (PETN), cyclotrimethylene trinitramine (RDX), and tetryl when these materials were pulsed with light energy from a focused Q-switch ruby laser. The laser energy ranged from 0.5 to 4.2 J, with a pulse width of 25 ns. Enhancement of the ignition mechanism is hypothesized when a 100-nm (1000-Å) thick aluminum film is vacuum-deposited on the explosive side of the window. Upon irradiation from the laser, a shock is generated at the aluminum–explosive interface. Steady-state detonations can be reached in less than 0.5 μs, with less than 10% variation in detonation velocity for PETN and RDX.

M073 Detonation of Insensitive High Explosives by a Q-Switched Ruby Laser

L. C. Yang and V. J. Menichelli

Appl. Phys. Lett., Vol. 19, No. 11, pp. 473–475, December 1, 1971

For abstract, see Yang, L. C.

M074 Terminated Capacitor-Discharge Firing of Electroexplosive Devices

L. A. Rosenthal (Rutgers University) and V. J. Menichelli

IEEE Trans. Instr. Meas., Vol. IM-21, No. 2, pp. 177–180, May 1972

For abstract, see Rosenthal, L. A.

M075 Nondestructive Testing of Insensitive Electroexplosive Devices by Transient Techniques

L. A. Rosenthal (Rutgers University) and V. J. Menichelli

Mater. Eval., Vol. XXX, No. 1, pp. 13–19, January 1972

For abstract, see Rosenthal, L. A.

MEREDITH, R. E.

M076 Gravitational Effects on Electrochemical Batteries

R. E. Meredith (Oregon State University), G. L. Juvinall, and A. A. Uchiyama

Technical Report 32-1570, November 15, 1972

This report summarizes the existing work on gravitational effects on electrochemical batteries and makes recommendations for future activities in this field. Theoretical evaluations of the problem have met with only limited success; theories based upon a treatment of natural convection have fallen short of the mark, partly because the mass transfer involved in the power-producing electrochemical reactions in a battery is not completely due to convection, and partly because a battery is far removed from the idealized models necessarily employed in the development of the theory. The latter point is best illustrated by the fact that, although theory generally predicts that the limiting current density will vary with the 1/4 power of the acceleration constant, the experimental data falls in the range of a 1/3 to 1/5 power dependence because of differences in the way the cell is constructed.

The effects of sustained high-g environments on cycled silver–zinc and nickel–cadmium cells have been evaluated over four complete cycles in the region of 10 to 75 g. Although no effects on high current-discharge performances or on ampere-hour capacity were noted, severe zinc migration and sloughing of active material from the zinc electrode were observed. This latter effect constitutes real damage and, over a long period of time, would result in loss of capacity.

The work of Arcand, based upon smooth zinc electrodes, predicted a limiting current density of 7 mA/cm^2. However, the Mariner 7 battery easily provided a current density of 10.5 mA/cm^2 in deep space. Fundamental battery studies performed at zero g are necessary to resolve the conflict. To this end, experiments have been planned, and a breadboard model of an in-flight battery test unit has been designed and fabricated. It is recommended that a zero-g battery experiment be implemented. Both an orbiting-satellite and a sounding-rocket approach are being considered.

MEYER, R.

M077 DSN Progress Report for November–December 1971: Hydrogen Maser: Low Phase Noise, L-Band Frequency Multiplier

G. Lutes, J. MacConnell, and R. Meyer

Technical Report 32-1526, Vol. VII, pp. 81–83, February 15, 1972

For abstract, see Lutes, G.

M078 DSN Progress Report for May–June 1972: L-Band Frequency Multipliers: Phase Noise, Stability, and Group Delay

J. MacConnell and R. Meyer

Technical Report 32-1526, Vol. X, pp. 104–109, August 15, 1972

For abstract, see MacConnell, J.

MICCIO, J. A.

M079 DSN Progress Report for November–December 1971: DSN Traceability and Reporting Program: Micrographic Application

J. A. Miccio

Technical Report 32-1526, Vol. VII, pp. 185–189, February 15, 1972

Technology has advanced the development and utilization of higher and faster data rates for deep space satellite research; machine computation and analysis have been relied upon by investigators and analysts for a greater percentage of the data reduction. The investigator, analyst, and end user, however, still face a massive volume of output data. The longevity of spacecraft systems in high data transmission modes and the "one of a kind" nature of the data being returned increase the desire for extensive data acquisition and retention of scientific and engineering information. The result of increased volumes of data being processed with corresponding increases in magnetic tape and tab paper output poses cost and storage problems for the processing facility and the data analyst. An efficient and expeditious method for data reduction, retention, and retrieval is mandatory.

Micrographic technology, i.e., microfilm processes, microforms, and retrieval systems, combined with current computing techniques, affords the data user quick-look profiles and trend information in relatively short turnaround time, as well as accessibility to larger and more detailed data bases.

MICHEL, G.

M080 Fourier Spectroscopy With a One-Million-Point Transformation (Translation From the Original Published in the Nouvelle Revue d'Optique Appliquée, Vol. 1, pp. 3–22, 1970)

J. Connes (National Center for Scientific Research, Orsay, France), H. Delouis (National Center for Scientific Research, Orsay, France),
P. Connes (National Center for Scientific Research, Orsay, France), G. Guelachvili (National Center for Scientific Research, Orsay, France),
J.-P. Maillard (National Center for Scientific Research, Orsay, France), and G. Michel (National Center for Scientific Research, Orsay, France)

Technical Memorandum 33-525, March 15, 1972

For abstract, see Connes, J.

MINER, E.

M081 **Mariner 1969 Infrared Radiometer Results: Temperatures and Thermal Properties of the Martian Surface**

G. Neugebauer (California Institute of Technology),
G. Münch (California Institute of Technology),
H. Kieffer (University of California, Los Angeles),
S. C. Chase, Jr. (Santa Barbara Research Center),
and E. Miner

Astron. J., Vol. 76, No. 8, pp. 719–749,
October 1971

For abstract, see Neugebauer, G.

M082 **Infrared Radiometry Experiment on Mariner 9**

S. C. Chase, Jr. (Santa Barbara Research Center),
H. Hatzenbeler (Santa Barbara Research Center),
H. Kieffer (University of California, Los Angeles),
E. Miner, G. Münch (California Institute of
Technology), and G. Neugebauer (California
Institute of Technology)

Science, Vol. 175, No. 4019, pp. 308–309,
January 21, 1972

For abstract, see Chase, S. C., Jr.

MOACANIN, J.

M083 **Lifetime Estimates for Sterilizable Silver–Zinc Battery Separators**

E. F. Cuddihy, D. E. Walmsley, and J. Moacanin

JPL Quarterly Technical Review, Vol. 2, No. 1,
pp. 72–81, April 1972

For abstract, see Cuddihy, E. F.

M084 **Viscoelastic Behavior of Polymers Undergoing Crosslinking Reactions**

J. Moacanin and J. J. Aklonis (University of
Southern California)

J. Polym. Sci., Pt. C: Polym. Sym., No. 35,
pp. 71–76, 1971

A method was previously developed for predicting the viscoelastic response of polymers undergoing scission reactions. In this article, these results are now extended to include crosslinking reactions. As for scission, at any given time the character of the network chains is determined by the instantaneous crosslink density. For scis-

sion, all chains were assumed to carry the same stress; for crosslinking, however, the stress is distributed between the "new" and "old" chains. Equations for calculating the creep response of a system which experiences a step increase in crosslink density are derived.

MOLNAR, M. R.

M085 **Mariner 9 Ultraviolet Spectrometer Experiment: Stellar Observations**

C. F. Lillie (University of Colorado),
R. C. Bohlin (University of Colorado),
M. R. Molnar (University of Colorado),
C. A. Barth (University of Colorado), and
A. L. Lane

Science, Vol. 175, No. 4019, pp. 321–322,
January 21, 1972

For abstract, see Lillie, C. F.

MONDT, J. F.

M086 **Thermionic Reactor Electric Propulsion System Requirements**

J. F. Mondt, C. D. Sawyer, and
R. W. Schaupp (Ames Research Center)

Technical Memorandum 33-549, June 1, 1972

Mission analysis, system analysis, and mission engineering studies have been conducted to find a single nuclear–electric propulsion (NEP) system that would be applicable for a broad range of unmanned outer-planet missions. The NEP system studied uses an in-core nuclear thermionic reactor as the electric power source and mercury bombardment ion engines for propulsion. Many requirements imposed on the NEP system by the mission were determined in the process of trying to find a single NEP system for many missions. The NEP system requirements are preliminary in nature and subject to small changes with further iterations between these types of studies and the technology program. It was determined that other applications for in-core thermionic reactors must also be considered in determining specific reactor requirements. It is concluded that a single thermionic reactor NEP system could be useful for a broad range of unmanned outer-planet missions. The thermionic reactor NEP system should have: (1) a power level in the 70- to 120-kWe range, (2) a system specific weight of approximately 30 kg/kWe, and (3) a full power output capability of 20,000 hr.

MORELLI, F. A.

M087 **Surface Distribution of Microorganisms in Antarctic Dry-Valley Soils: A Martian Analog**

R. E. Cameron, H. P. Conrow, D. R. Gensel, G. H. Lacy, and F. A. Morelli

Antarctic J. U.S., Vol. VI, No. 5, pp. 211–213, September–October 1971

For abstract, see Cameron, R. E.

MORGAN, C. L.

M088 DSN Progress Report for January–February 1972: Integration of the DSN Sequence of Events Generator

C. L. Morgan

Technical Report 32-1526, Vol. VIII, pp. 125–126, April 15, 1972

This article reviews the concept, function, implementation, and operational status of the DSN sequence-of-events generator. The supporting software resides in an IBM 360/75 as a part of the real-time mission support software system. The program title is "Sequence-of-Events Generator."

MORRIS, G. A.

M089 Mars Radar Observations, a Preliminary Report

G. S. Downs, R. M. Goldstein, R. R. Green, and G. A. Morris

Science, Vol. 174, No. 4016, pp. 1324–1327, December 24, 1971

For abstract, see Downs, G. S.

MOSESMAN, M. M.

M090 Photolysis of CO_2 at 1849 Å

W. B. DeMore and M. M. Mosesman

J. Atmos. Sci., Vol. 28, No. 6, pp. 842–846, September 1971

For abstract, see DeMore, W. B.

MOYNIHAN, P. I.

M091 Attitude Propulsion Technology for TOPS

P. I. Moynihan

Technical Report 32-1560, November 1, 1972

This report summarizes the JPL Thermoelectric Outer Planet Spacecraft (TOPS) attitude-propulsion subsystem (APS) effort. It includes the tradeoff rationale that went into the selection of an anhydrous-hydrazine baseline system, followed by a discussion of the 0.22-N (0.05-lbf)

JPL-developed thruster and its integration into a portable, self-contained propulsion module that was designed, developed, and 'man-rated' to support the TOPS single-axis attitude control tests in the JPL Celestarium.

The results of a cold-start feasibility demonstration with a modified JPL thruster are presented. A description of three types of 0.44-N (0.1lbf) thrusters that were procured for in-house evaluation is included along with the results of the test program. This is followed by a description of the APS feed system components, their evaluations, and a discussion of an evaluation of elastomeric material for valve seat seals. The report concludes with a list of new-technology items which will be of value for application to future systems of this type.

M092 A Portable Hydrazine Attitude Propulsion Test System

P. I. Moynihan

Technical Memorandum 33-560, September 1, 1972

This report describes the portable hydrazine attitude-propulsion module that was designed and developed to support the attitude-control pitch axis simulation tests that were performed on an air-bearing table in JPL's Celestarium facility for the Thermoelectric Outer-Planet Spacecraft program. The propulsion module was a self-contained, liquid-hydrazine propulsion system from which the exhaust gases were generated within the catalyst bed of either of two nominal 0.22-N (0.05-lbf) opposing thrusters. The module, which was designed for convenient assembly onto and removal from an air-bearing table in the JPL Celestarium, was tested extensively to establish its operational safety. This test history and the very conservative design of the module enabled it to be "man-rated" for operation in the presence of personnel. The report briefly summarizes the system operations during air-bearing table tests, presents a detailed description of the propulsion module hardware, and discusses the system evolution.

M093 Minimum Impulse Tests of 0.45-N Liquid Hydrazine Catalytic Thrusters

P. I. Moynihan

JPL Quarterly Technical Review, Vol. 2, No. 1, pp. 107–112, April 1972

Many studies have identified the need for high-performance, low-total-impulse chemical thrusters for attitude-propulsion applications on spacecraft with limit cycle attitude control. Specifically, studies for outer-planet spacecraft have identified a need for thrusters with a steady-state thrust of 1.3×10^{-1} to 4.5×10^{-1} N (0.03 to 0.1 lbf) and a pulsed "impulse bit" of 4.5×10^{-4} to 4.5×10^{-3} N-s (10^{-4} to 10^{-3} lbf-s). No data on small cata-

lytic thrusters with this capability have heretofore been available. Therefore, in support of an attitude-control tradeoff study performed under the Thermoelectric Outer-Planet Spacecraft Project, an exploratory test series was conducted on three types of 0.45-N (0.1-lbf) liquid hydrazine thrusters to ascertain the minimum impulse bit capability for this class of engine. This article describes this test series and discusses the results. The testing was performed at 21 and 145°C (70 and 300°F) while maintaining nominal 0.45-N (0.1-lbf) upstream conditions. Valve on-times as low as 0.008 s were applied. Impulse bits as low as 1.0×10^{-3} and 2.6×10^{-3} N-s (2.3×10^{-4} and 5.7×10^{-4} lbf-s) were observed for thruster temperatures of 21 and 145°C (70 and 300°F), respectively.

M094   Small Rocket Exhaust Plume Data

J. E. Chirivella, P. I. Moynihan, and W. Simon

JPL Quarterly Technical Review, Vol. 2, No. 2, pp. 90–99, July 1972

For abstract, see Chirivella, J. E.

MUDGWAY, D. J.

M095   DSN Progress Report for January–February 1972: Viking Mission Support

D. J. Mudgway

Technical Report 32-1526, Vol. VIII, pp. 20–23, April 15, 1972

Until recently, the DSN configuration intended for support of the Viking 1975 mission included the Space Flight Operations Facility with its central processing system, mission support areas, and Simulation Center. In response to the NASA Headquarters directive of October 1, 1971, the Project/DSN interface was changed, deleting the Space Flight Operations Facility from the scope of DSN responsibility. As a consequence, many existing understandings between the DSN and the Project must now be renegotiated, with a resulting impact on schedules, documentation, and resources.

This article identifies areas where rework is necessary and describes progress toward defining the new DSN configuration for Viking and reestablishing a mutually acceptable interface between the project and the DSN.

M096   DSN Progress Report for May–June 1972: Viking Mission Support

D. J. Mudgway

Technical Report 32-1526, Vol. X, pp. 22–26, August 15, 1972

A previous article identified the probable impact of changes in the scope of the DSN to Flight Project interfaces for Viking. In this article the outcome of the changes is described in the areas of DSN configuration, interfaces, schedules, documentation, and organization in order to establish a background against which subsequent articles can report progress in each of these particular areas.

M097   DSN Progress Report for May–June 1972: Mariner Jupiter–Saturn 1977 Mission Support

D. J. Mudgway

Technical Report 32-1526, Vol. X, pp. 35–40, August 15, 1972

The Mariner Jupiter–Saturn 1977 Project has recently been formally established as a Flight Project. The mission calls for the launch of two Mariner-class spacecraft in 1977 to fly by Jupiter and Saturn. Flight times to Jupiter and Saturn are approximately 2 and 4 yr, respectively. The primary scientific objectives of the missions are to explore Jupiter, Saturn, and their satellites, and to investigate the nature of the interplanetary medium. Engineering objectives include the operation of a Mariner-class of spacecraft in space for periods of 4 yr, use of radioisotope thermoelectric generators as the primary power source, and a demonstration of communications and navigational accuracy out to 10 AU.

Support from the 26-m-diameter antenna subnet is required intermittently during the long cruise periods with 64-m-diameter antenna support covering the encounters. Navigation support will require S–X planetary ranging, S–X doppler, and differenced range versus integrated doppler and will be planned around complete "cycles" of data. The number of "cycles" per week will vary with the phases of the mission.

The Office of Computing and Information Systems organization will be responsible for the hardware, software, and simulation needed by the Mission Operations System to carry out the mission. This article provides an introduction to the mission requirements as presently understood.

M098   DSN Progress Report for July–August 1972: Viking Mission Support

D. J. Mudgway

Technical Report 32-1526, Vol. XI, pp. 19–22, October 15, 1972

The DSN support for Viking continues to move from the completion of the planning and negotiating phase into the implementation phase in accordance with established

schedules. Most documents reflecting this activity have been completed, and a major Project review of the ground data system design for Viking has been supported. A problem associated with the Viking requirement for simultaneous dual-carrier operation is being investigated.

M099 DSN Progress Report for September–October 1972: Viking Mission Support

D. J. Mudgway

Technical Report 32-1526, Vol. XII, pp. 14–18, December 15, 1972

DSN support for Viking continues to move forward into the implementation phase in accordance with new schedules developed to meet a new Viking requirement for advanced deep-space-station readiness dates. This article discusses network configurations for the DSN Tracking System, DSN/Viking interfaces, and schedule revisions and describes the continued investigation of the downlink interference effects caused by a dual-carrier environment at the Venus Deep Space Station (DSS 13).

MUELLER, R. L.

M100 Results of the 1970 Balloon Flight Solar Cell Standardization Program

R. F. Greenwood and R. L. Mueller

Technical Report 32-1575, December 1, 1972

For abstract, see Greenwood, R. F.

MUHLEMAN, D. O.

M101 Determination of Astrodynamic Constants and a Test of the General Relativistic Time Delay With S-Band Range and Doppler Data From Mariners 6 and 7

J. D. Anderson, P. B. Esposito, W. Martin, and D. O. Muhleman (California Institute of Technology)

Space Research XI, pp. 105–112, Akademie-Verlag, Berlin, 1971

For abstract, see Anderson, J. D.

MULDOON, W. J.

M102 Integration of a Breadboard Power Conditioner With a 20-cm Ion Thruster

T. D. Masek, T. W. Macie, E. N. Costogue, W. J. Muldoon (Hughes Aircraft Company), D. R. Garth (Hughes Aircraft Company), and G. C. Benson (Hughes Aircraft Company)

J. Spacecraft Rockets, Vol. 9, No. 2, pp. 71–78, February 1972

For abstract, see Masek, T. D.

MULHALL, B. D.

M103 DSN Progress Report for November–December 1971: Local and Transcontinental Mapping of Total Electron Content Measurements of the Earth's Ionosphere

K. W. Yip and B. D. Mulhall

Technical Report 32-1526, Vol. VII, pp. 61–67, February 15, 1972

For abstract, see Yip, K. W.

M104 DSN Progress Report for March–April 1972: Navigation Demonstrations With the Mariner Venus–Mercury 1973 Spacecraft Requiring X-Band Receiving Capability at a Second DSN Station

B. D. Mulhall

Technical Report 32-1526, Vol. IX, pp. 38–43, June 15, 1972

The opportunities to demonstrate two-station tracking with radio metric doppler and range data calibrated for charged particles by the X- and S-band technique during the Mariner Venus–Mercury 1973 mission are described together with the rationale for undertaking and experiments. The errors which corrupt two-station tracking for single and dual frequency operation are also described.

M105 DSN Progress Report for July–August 1972: An Evaluation of Charged Particle Calibration by a Two-Way Dual-Frequency Technique and Alternatives to This Technique

O. H. von Roos and B. D. Mulhall

Technical Report 32-1526, Vol. XI, pp. 42–52, October 15, 1972

For abstract, see von Roos, O. H.

M106 DSN Progress Report for September–October 1972: Determination of the Helios Spacecraft Attitude by Polarization Measurement

B. D. Mulhall

Technical Report 32-1526, Vol. XII, pp. 40–43,
December 15, 1972

This article describes the possibility of determining the
attitude or orientation of the Helios spacecraft by means
of polarization measurements of the spacecraft radio
signal. One principal error source is the Faraday rotation
of the S-band radio signal by Earth's ionosphere. If this
effect can be removed by independent measurements of
the ionosphere, then the orientation of the spacecraft in
two dimensions perpendicular to the spacecraft line-of-
sight can be determined to better than 0.5 deg.

MULLER, P. M.

M107 **3-D Multilateration: A Precision Geodetic
Measurement System**

P. R. Escobal, H. F. Fliegel, R. M. Jaffe,
P. M. Muller, K. M. Ong, O. H. von Roos, and
M. S. Shumate

JPL Quarterly Technical Review, Vol. 2, No. 3,
pp. 1–11, October 1972

For abstract, see Escobal, P. R.

M108 **A Surface-Layer Representation of the Lunar
Gravitational Field**

L. Wong (Aerospace Corporation),
G. Buechler (Aerospace Corporation),
W. Downs (Aerospace Corporation), W. L. Sjogren,
P. M. Muller, and P. Gottlieb

J. Geophys. Res., Vol. 76, No. 26, pp. 6220–6236,
September 10, 1971

For abstract, see Wong, L.

M109 **Apollo 15 Gravity Analysis From the S-Band
Transponder Experiment**

W. L. Sjogren, P. M. Muller, and
W. R. Wollenhaupt (Manned Spaceflight Center)

*Proceedings of the Conference on Lunar
Geophysics, Lunar Science Institute, Houston,
Texas, October 18–21, 1971*, pp. 411–418

For abstract, see Sjogren, W. L.

M110 **Lunar Gravity via Apollo 14 Doppler Radio Tracking**

W. L. Sjogren, P. Gottlieb, P. M. Muller, and
W. Wollenhaupt (Manned Spacecraft Center)

Science, Vol. 175, No. 4018, pp. 165–168,
January 14, 1972

For abstract, see Sjogren, W. L.

MÜNCH, G.

M111 **Mariner 1969 Infrared Radiometer Results:
Temperatures and Thermal Properties of the
Martian Surface**

G. Neugebauer (California Institute of Technology),
G. Münch (California Institute of Technology),
H. Kieffer (University of California, Los Angeles),
S. C. Chase, Jr. (Santa Barbara Research Center),
and E. Miner

Astron. J., Vol. 76, No. 8, pp. 719–749,
October 1971

For abstract, see Neugebauer, G.

M112 **Mariner 9 Science Experiments: Preliminary Results**

R. H. Steinbacher, A. J. Kliore, J. Lorell,
H. Hipsher (National Aeronautics and Space
Administration), C. A. Barth (University of
Colorado), H. Masursky (U.S. Geological Survey),
G. Münch (California Institute of Technology),
J. C. Pearl (Goddard Space Flight Center), and
B. A. Smith (New Mexico State University)

Science, Vol. 175, No. 4019, pp. 293–294,
January 21, 1972

For abstract, see Steinbacher, R. H.

M113 **Infrared Radiometry Experiment on Mariner 9**

S. C. Chase, Jr. (Santa Barbara Research Center),
H. Hatzenbeler (Santa Barbara Research Center),
H. Kieffer (University of California, Los Angeles),
E. Miner, G. Münch (California Institute of
Technology), and G. Neugebauer (California
Institute of Technology)

Science, Vol. 175, No. 4019, pp. 308–309,
January 21, 1972

For abstract, see Chase, S. C., Jr.

MYKKELTVEIT, J.

M114 **DSN Progress Report for March–April 1972: A Note
on Kerdock Codes**

J. Mykkeltveit (California Institute of Technology)

Technical Report 32-1526, Vol. IX, pp. 82–83,
June 15, 1972

The performance of an important class of low-rate non-
linear binary codes recently discovered by A. M. Kerdock
is superior to that of linear codes with the same parame-
ters. Before these codes can be put to practical use,
several questions must be answered. This article consid-
ers one of the questions. It shows that the nonlinear

Kerdock codes are systematic; i.e., they have distinguishable information and check positions.

M115 DSN Progress Report for September–October 1972: On the Weight Enumerators of Quadratic Residue Codes

J. Mykkeltveit (California Institute of Technology), C. Lam (California Institute of Technology), and R. J. McEliece

Technical Report 32-1526, Vol. XII, pp. 161–166, December 15, 1972

Binary quadratic-residue codes, some of which are currently being studied for use in the Mariner Jupiter–Saturn 1977 mission, are among the most powerful known block codes. They are, however, notoriously difficult to analyze. In this article, a method is developed for obtaining information about the weights of these codes by exploiting the fact that they are left invariant by the linear fractional group.

NAKAMURA, Y.

N001 Solid Propulsion Advanced Concepts

Y. Nakamura and J. I. Shafer

Technical Memorandum 33-534, May 1, 1972

In this study, the feasibility and application of a solid propulsion powered spacecraft concept to implement high-energy missions independent of multiplanetary swingby opportunities are assessed, and recommendations are offered for future work. An upper-stage, solid propulsion launch vehicle augmentation system was selected as the baseline configuration in view of the established program goals of low cost and high reliability.

During the study, a new high-mass-fraction solid motor staging design, the conesphere motor concept, was conceived, and its anticipated performance predictions further enhanced the candidacy of the solid propulsion baseline configuration. A class of missions of increasing scientific interest was identified, and the attendant launch energy thresholds for alternate approaches were determined. Spacecraft and propulsion system data that characterize mission performance capabilities were generated to serve as the basis for subsequent tradeoff studies. A cost-effectiveness model was used for the preliminary feasibility assessment to provide a meaningful comparative effectiveness measure of the various candidate designs. The results substantiated the feasibility of the powered spacecraft concept when used in conjunction with several intermediate-sized launch vehicles, as well as the existence of energy margins by which to exploit the attainment of extended mission capabilities. Additionally, in growth option applications, the employment

of advanced propulsion systems and alternate spacecraft approaches appears promising.

NANCE, H. E.

N002 DSN Progress Report for January–February 1972: DSN Tracking System: Operation With the Mutual Stations

W. D. Chaney and H. E. Nance

Technical Report 32-1526, Vol. VIII, pp. 5–7, April 15, 1972

For abstract, see Chaney, W. D.

NASH, D. B.

N003 Luminescence and Reflectance of Apollo 12 Samples

D. B. Nash and J. E. Conel

Proceedings of the Second Lunar Science Conference, Houston, Texas, January 11–14, 1971, Vol. 3, pp. 2235–2244, The M.I.T. Press, Cambridge, 1971

The objectives of the laboratory measurements reported in this article were to: (1) compare the luminescence and reflectance properties of Apollo 12 surface and core-sample material with those of the surface material of Apollo 11, (2) obtain a better estimate of the average luminescence characteristics of the lunar surface under solar irradiation, and (3) obtain additional spectral reflectance data on lunar samples for more accurate interpretation of telescopic observations of the lunar surface. It was found that luminescence, thermoluminescence, and spectral reflectance properties of samples from Oceanus Procellarum are qualitatively similar to those of Mare Tranquillitatis samples. Detailed differences are controlled by mineralogy; fines from Procellarum have higher plagioclase content relative to glass and opaques and higher pyroxene content relative to plagioclase than fines from Tranquillity. Luminescence properties and reflectance do not vary systematically with depth in the core. The variations observed are attributable to differences in relative abundances of mineral and glass phases and are not indicative of variations in particle size, radiation damage, or surface coatings on individual grains.

N004 Objectives and Requirements of Unmanned Rover Exploration of the Moon

D. B. Nash, J. E. Conel, and F. P. Fanale

The Moon, Vol. 3, No. 2, pp. 221–230,
August 1971

The scientific value of unmanned rovers for continued lunar exploration is considered in light of Apollo findings which suggest that the Moon's surface is more heterogeneous than expected. Major questions and investigations involving composition, internal structure, and thermal history are presented that form a scientific rationale for use of unmanned rovers in the post-Apollo period of lunar exploration. Visual, petrologic, chemical, and geophysical measurements that are essential for an unmanned rover traverse over previously unexplored lunar terrain are discussed. Unmanned rovers are well-suited for low-cost, low-risk preliminary reconnaissance where measurement of a few definitive parameters over a wide area is more important than obtaining a wide array of detailed results at a given site.

NEUGEBAUER, G.

**N005 Mariner 1969 Infrared Radiometer Results:
Temperatures and Thermal Properties of the
Martian Surface**

G. Neugebauer (California Institute of Technology),
G. Münch (California Institute of Technology),
H. Kieffer (University of California, Los Angeles),
S. C. Chase, Jr. (Santa Barbara Research Center),
and E. Miner

Astron. J., Vol. 76, No. 8, pp. 719–749,
October 1971

The reduced data of the Mariner 6 and 7 infrared radiometer experiments are presented, along with a discussion of the reduction and calibration procedures. Evidence is presented showing that the surface of Mars is strongly nonhomogeneous in its thermal properties, on scales ranging from those of the classical light and dark areas to the limit of resolution of the radiometers. On the sunlit side, the mean thermal inertia, for admissible bolometric albedos, is 0.006 $(cal\text{-}cm^{-2}\text{-}s^{-1/2}\text{-}°K^{-1})$. The dark areas Syrtis Major and Mare Tyrrhenum, observed at night, require thermal inertias as high as 0.010. The temperatures measured over the circular basin Hellas require a bolometric albedo of 0.40 and also a high thermal inertia. The temperature measured over the south polar cap, 148°K, provides evidence that the major constituent of the frost deposit is CO_2.

N006 Infrared Radiometry Experiment on Mariner 9

S. C. Chase, Jr. (Santa Barbara Research Center),
H. Hatzenbeler (Santa Barbara Research Center),
H. Kieffer (University of California, Los Angeles),
E. Miner, G. Münch (California Institute of
Technology), and G. Neugebauer (California
Institute of Technology)

Science, Vol. 175, No. 4019, pp. 308–309,
January 21, 1972

For abstract, see Chase, S. C., Jr.

NEUGEBAUER, M.

**N007 Dissipation Mechanisms in a Pair of Solar-Wind
Discontinuities**

T. W. J. Unti, G. Atkinson (Communications
Research Center), C.-S. Wu (University of
Maryland), and M. Neugebauer

J. Geophys. Res., Space Physics, Vol. 77, No. 13,
pp. 2250–2263, May 1, 1972

For abstract, see Unti, T. W. J.

NICKLE, N. L.

N008 Surveyer III Material Analysis Program

N. L. Nickle

*Proceedings of the Second Lunar Science
Conference, Houston, Texas, January 11–14, 1971*,
Vol. 3, pp. 2683–2697, The M.I.T. Press,
Cambridge, 1971

The Surveyor 3 components returned from the Moon by the Apollo 12 astronauts were released for scientific investigation by NASA on June 18, 1970. This article provides background information on return of the Surveyor 3 material and subsequent plans for analysis of the returned parts. Also discussed are the environmental conditions to which the returned material was subjected, exposure of the spacecraft and the returned parts to solar radiation, orientation of the spacecraft, results of investigations, and future plans for the remaining parts.

NICOLET, M.-A.

**N009 Thermal Noise in Space-Charge-Limited Hole
Current in Silicon**

A. Shumka, J. Golder, and M.-A. Nicolet

JPL Quarterly Technical Review, Vol. 2, No. 2,
pp. 72–76, July 1972

For abstract, see Shumka, A.

NISHIMURA, H. G.

**N010 DSN Progress Report for July–August 1972: Coaxial
Switch Evaluation**

H. G. Nishimura

Technical Report 32-1526, Vol. XI, pp. 135–139, October 15, 1972

Miniature coaxial transfer switches from various manufacturers were tested for the purpose of finding an acceptable replacement for the larger switch now used in the Deep Space Instrumentation Facility. The switches, which are planned for use in the S- through X-bands, were tested to determine both their mechanical and electrical properties. Two units were considered acceptable. These switches will reduce the size and cost of future microwave equipment and will meet increasing performance demands.

NISHIMURA, T.

N011 Spectral Factorization in Periodically Time-Varying Systems and Application to Navigation Problems

T. Nishimura

J. Spacecraft Rockets, Vol. 9, No. 7, pp. 540–546, July 1972

Spectral factorization is a powerful tool in deriving the steady-state solution of Kalman filtering equations. It is an algebraic, nonrecursive method and, therefore, economical in terms of computing cost when compared with the conventional iterative algorithm. In this paper the technique is extended to time-varying systems having periodic coefficient matrices for both discrete and continuous systems. The tracking of low-thrust spacecraft from an Earth-based station is used as an example and a sensitivity study is performed using a computer program incorporating the algorithm.

NOGUCHI, H.

N012 Reactions of N,N,N′,N′-Tetramethyl-α,ω-Diaminoalkanes With α,ω-Dihaloalkanes: I. 1-y Reactions

H. Noguchi and A. Rembaum

Macromolecules, Vol. 5, No. 3, pp. 253–260, May–June 1972

The reactions of *N,N,N′,N′*-tetramethyldiaminomethane with a number of α,ω-dihaloalkanes were investigated in dimethylformamide (DMF), DMF–methanol (1:1 by volume), and acetonitrile. The most important products of these reactions consisted of dimethylaminohaloalkanes, dimethylamine hydrohalides, cyclic and linear mono- and diammonium salts, as well as polyelectrolytes. The course of the reaction was influenced by the solvent. The reaction of tetramethyldiaminomethane with 1,4-dibromobutane yielded unexpectedly in DMF–methanol a linear diammonium compound containing two methoxy groups. A mechanism accounting for the reaction pro-

ducts is proposed and experimental evidence for the isolated compounds is presented.

N013 Reactions of N,N,N′,N′-Tetramethyl-α,ω-Diaminoalkanes With α,ω-Dihaloalkanes: II. x–y Reactions

A. Rembaum and H. Noguchi

Macromolecules, Vol. 5, No. 3, pp. 261–269, May–June 1972

For abstract, see Rembaum, A.

NOON, E. L.

N014 Nuclear Radiation Sources On-Board Outerplanet Spacecraft

E. L. Noon, G. H. Anno, and M. A. Dore

IEEE Trans. Nucl. Sci., Vol. NS-18, No. 5, pp. 50–57, October 1971

Radioisotope thermoelectric generators (RTGs) and radiation heater units (RHUs) are presently being used or considered for sources of electrical power and heat for the Apollo, Pioneer, and Viking Projects. Both RTGs and RHUs have considerable merit if proper precautions are taken to compensate for overall system response to the nuclear radiation sources.

This article summarizes the nuclear characteristics of plutonium fuel, which gives rise to the radiation from both RTGs and RHUs; gives Monte Carlo estimates of the neutron and gamma isodose profiles from a 2200-W(th) HELIPAK (General Electric Co. conceptual-model tradename) thermoelectric generator; and concludes with a presentation summary of shield thicknesses required for several sensitive radiation experiments due to combined RTG–RHU fields. This study is a part of a continuing program of analysis at JPL on the evaluation of RTG radiation fields on an outerplanet spacecraft.

NORMAN, R.

N015 Gain Calibration of a Horn Antenna Using Pattern Integration

A. C. Ludwig, J. Hardy, and R. Norman

Technical Report 32-1572, October 1, 1972

For abstract, see Ludwig, A. C.

NORRIS, D.

N016 DSN Progress Report for September–October 1972: Frequency Generation and Control: Atomic Hydrogen Dissociator

H. Erpenbach and D. Norris

Technical Report 32-1526, Vol. XII, pp. 56-58, December 15, 1972

For abstract, see Erpenbach, H.

NORTON, R. H.

N017 **Astronomical Infrared Spectroscopy With a Connes-Type Interferometer: III. Alpha Orionis, 2600-3450 cm^{-1}**

R. Beer, R. B. Hutchison, R. H. Norton, and D. L. Lambert (University of Texas)

Astrophys. J., Vol. 172, No. 1, Pt. 1, pp. 89-115, February 15, 1972

For abstract, see Beer, R.

N018 **Astronomical Infrared Spectroscopy With a Connes-Type Interferometer: I. Instrumental**

R. Beer, R. H. Norton, and C. H. Seaman

Rev. Sci. Instr., Vol. 42, No. 10, pp. 1393-1403, October 1971

For abstract, see Beer, R.

N019 **Jupiter: Observation of Deuterated Methane in the Atmosphere**

R. Beer, C. B. Farmer, R. H. Norton, J. V. Martonchik (University of Texas), and T. G. Barnes (University of Texas)

Science, Vol. 175, No. 4028, pp. 1360-1361, March 24, 1972

For abstract, see Beer, R.

O'HANDLEY, D. A.

0001 **Simultaneous Solution for the Masses of the Principal Planets From Analysis of Optical, Radar, and Radio Tracking Data**

J. H. Lieske, W. G. Melbourne, D. A. O'Handley, D. B. Holdridge, D. E. Johnson, and W. S. Sinclair

Celest. Mech., Vol. 4, No. 2, pp. 233-245, October 1971

For abstract, see Lieske, J. H.

0002 **Recent Developments in Digital Image Processing at the Image Processing Laboratory at the Jet Propulsion Laboratory**

D. A. O'Handley and W. B. Green

Proc. IEEE, Vol. 60, No. 7, pp. 821-828, July 1972

Image processing of spacecraft images has been carried on at JPL since 1964. The most recent advances in removal of geometric distortion and residual image effects along with various types of mapping projections are covered, and the recent applications of image processing to the areas of biomedicine, forensic sciences, and astronomy are discussed. These treatments are of a tutorial nature and should serve as a guide to more complete discussions on the subjects.

OAKLEY, E. C.

0003 **DSN Progress Report for January–February 1972: SOFTWARE: A General-Purpose External Function for PDP-11 BASIC**

E. C. Oakley

Technical Report 32-1526, Vol. VIII, pp. 80-88, April 15, 1972

This article describes a new tool to dramatically simplify the test and software development phases in computer-controllable subsystems for the DSN. This tool does not add to the endless computer language proliferation, but instead adds dimension to a well-established, high-level, moderately sophisticated language to enable simplified control of minicomputer peripherals. Some of its versatility is demonstrated by programs used to aid its own implementation in hardware exercisers.

OHTAKAY, H.

0004 **In-Flight Calibration of an Interplanetary Navigation Instrument**

T. C. Duxbury and H. Ohtakay

J. Spacecraft Rockets, Vol. 8, No. 10, pp. 1038-1042, October 1971

For abstract, see Duxbury, T. C.

OLIVER, R. E.

0005 **Furlable Spacecraft Antenna Development: An Interim Report**

R. E. Oliver and A. H. Wilson

Technical Memorandum 33-537, April 15, 1972

Activities at JPL directed toward the development of large furlable spacecraft antennas using conical main reflectors are described. Two basic antenna configurations which utilize conical main reflectors have been conceived at JPL and are under development. In the conical-Gregorian configuration each ray experiences two

reflections in traveling from the feed center to the aperture plane. In the Quadreflex configuration, each ray experiences four reflections, one at each of two subreflector surfaces and two at the main conical reflector surface.

The RF gain measurements obtained from the 1.83-m (6-ft) and 0.762-m (30-in.) models of the conical-Gregorian and Quadreflex concepts, respectively, were sufficiently encouraging to warrant further development of the concepts.

0006 Large Spacecraft Antennas: Conical Ring-Membrane Reflectors

R. E. Oliver, M. R. Trubert, and A. H. Wilson

JPL Quarterly Technical Review, Vol. 2, No. 2, pp. 42–47, July 1972

A 1.83-m(6-ft)-diameter, furlable, conical, Gregorian antenna based on a novel spoke-supported ring-membrane concept has been successfully demonstrated. Mechanical measurements of the conical reflecting surface, as well as RF gain measurements at Ku-band, show an rms surface deviation from the proper conical surface of 0.3 mm (0.012 in.), and a repeatability after multiple furling–unfurling cycles of ±0.05 mm (0.002 in.). Design features and performance characteristics of this antenna indicate that the spoke-supported ring-membrane concept is a promising approach for producing large, furlable, light-weight, conical reflectors for spacecraft high-gain antennas.

OLSON, R. L.

0007 A Re-evaluation of Material Effects on Microbial Release From Solids

D. M. Taylor, S. J. Fraser (The Boeing Company),
E. A. Gustan (The Boeing Company),
R. L. Olson (The Boeing Company), and
R. H. Green

Life Sciences and Space Research X, pp. 23–28, Akademie-Verlag, Berlin, 1972

For abstract, see Taylor, D. M.

ONDRASIK, V. J.

0008 DSN Progress Report for November–December 1971: Improved Navigation Capability Utilizing Two-Station Tracking Techniques for a Low-Declination Distant Spacecraft

K. H. Rourke and V. J. Ondrasik

Technical Report 32-1526, Vol. VII, pp. 51–60, February 15, 1972

For abstract, see Rourke, K. H.

0009 DSN Progress Report for January–February 1972: The Translation of the Tropospheric Zenith Range Effect From a Radiosonde Balloon Site to a Tracking Station

K. L. Thuleen and V. J. Ondrasik

Technical Report 32-1526, Vol. VIII, pp. 39–44, April 15, 1972

For abstract, see Thuleen, K. L.

0010 DSN Progress Report for May–June 1972: Preliminary Evaluation of Radio Data Orbit Determination Capabilities for the Saturn Portion of a Jupiter–Saturn–Pluto 1977 Mission

V. J. Ondrasik, C. E. Hildebrand, and G. A. Ransford

Technical Report 32-1526, Vol. X, pp. 59–75, August 15, 1972

This article investigates the navigation accuracies attainable with radio tracking of an outer-planets spacecraft in the vicinity of Saturn. Analysis of the results indicates that navigation-accuracy problems associated with low spacecraft declinations and with batch filtering of conventional radio data when unmodeled accelerations are acting on the spacecraft may be avoided by employing range and range-rate data taken simultaneously by two widely separated stations. With the availability of two-station simultaneous data, the uncertainty in Saturn's ephemeris becomes the error source which limits the accuracy of the pre-encounter navigation.

0011 DSN Progress Report for May–June 1972: Determining the Mass and Ephemeris of Saturn by Radio Tracking of a Jupiter–Saturn–Pluto 1977 Spacecraft

V. J. Ondrasik, C. E. Hildebrand, and G. A. Ransford

Technical Report 32-1526, Vol. X, pp. 76–81, August 15, 1972

This article presents preliminary estimates of the accuracies with which the mass and ephemeris of Saturn may be determined from radio tracking of an outer-planets spacecraft. It is shown that the determination of these parameters should employ radio metric data taken simultaneously from two stations. Indications are that the uncertainties in the mass and the ephemeris may be reduced by approximately three orders of magnitude for the mass and by a factor of two for the ephemeris.

0012 DSN Progress Report for July–August 1972: Topics in the Implementation and Application of Two-Station Tracking Data Types

K. H. Rourke and V. J. Ondrasik

Technical Report 32-1526, Vol. XI, pp. 62–70, October 15, 1972

For abstract, see Rourke, K. H.

0013 Application of New Radio Tracking Data Types to Critical Spacecraft Navigation Problems

V. J. Ondrasik and K. H. Rourke

JPL Quarterly Technical Review, Vol. 1, No. 4, pp. 116–132, January 1972

This article is concerned with newly envisioned Earth-based radio tracking data types involving simultaneous or near-simultaneous spacecraft tracking from widely separated tracking stations. These data types are conventional tracking instrumentation analogs of the very-long-baseline interferometry (VLBI) of radio astronomy—hence, the name quasi-VLBI. Quasi-VLBI promises to help alleviate two particularly troublesome problems encountered in interplanetary orbit determination: the zero declination and process noise problems. This article motivates quasi-VLBI with a preliminary analysis using simplified tracking data models. The results of accuracy analysis studies are then presented for a representative mission, Viking 1975. The results indicate that, contingent on projected, not overly optimistic future tracking system accuracy, quasi-VLBI can be expected to significantly improve navigation performance over that expected of conventional tracking data types.

ONG, K. M.

0014 3-D Multilateration: A Precision Geodetic Measurement System

P. R. Escobal, H. F. Fliegel, R. M. Jaffe,
P. M. Muller, K. M. Ong, O. H. von Roos, and
M. S. Shumate

JPL Quarterly Technical Review, Vol. 2, No. 3, pp. 1–11, October 1972

For abstract, see Escobal, P. R.

OTOSHI, T. Y.

0015 DSN Progress Report for May–June 1972: Error Analysis of Precision Calibrations of Perforated Plate Mesh Materials on a Tuned Reflectometer System

T. Y. Otoshi

Technical Report 32-1526, Vol. X, pp. 143–148, August 15, 1972

This article presents an error analysis of a waveguide technique for precision reflectivity-loss measurements of perforated-plate mesh materials useful for antenna surfaces, dichroic plates, or RF shields. It is shown that by use of a prescribed experimental procedure, the maximum reflectivity-loss measurement error due to imperfect system tuning can typically be kept to less than ±0.002 dB.

0016 DSN Progress Report for September–October 1972: RF Properties of the 64-m-Diameter Antenna Mesh Material as a Function of Frequency

T. Y. Otoshi

Technical Report 32-1526, Vol. XII, pp. 26–31, December 15, 1972

This article presents some accurate theoretical data on the RF properties of the perforated panels presently used as reflector surface material on the 64-m-diameter antenna. The properties are given for the frequency range of 1.0 to 30 GHz.

0017 A Precision Compact Rotary Vane Attenuator

T. Y. Otoshi and C. T. Stelzried

IEEE Trans. Microwave Theor. Techniq., Vol. MTT-19, No. 11, pp. 843–854, November 1971

The accurate attenuation range of many precision rotary vane attenuators is limited to about 40 dB because of a transmission error term not accounted for in the familiar $\cos^2$ attenuation law. This article presents a modified law that makes it possible to extend the useful dynamic attenuation range. The same modified law also makes it practical to reduce the length of the rotor section and, therefore, to develop compact rotary vane attenuators that are accurate over reduced dynamic attenuation ranges. The modified law requires the additional calibrations of the incremental attenuation and incremental phase change at the 90-deg vane angle setting.

To verify the modified law, a precision compact WR 112 rotary vane attenuator was fabricated and tested. The attenuator has a total dynamic attenuation range of about 30 dB and a rotor section length approximately one-third that of a conventional WR 112 attenuator. Application of the modified law resulted in good agreement between theoretical and measured incremental attenuations over the total dynamic attenuation range.

0018 A Study of Microwave Leakage Through Perforated Flat Plates

T. Y. Otoshi

IEEE Trans. Microwave Theor. Techniq.,
Vol. MTT-20, No. 3, pp. 235–236, March 1972

A simple formula useful for predicting leakage through a circular hole array in a metallic flat plate is presented. A correction is given for plate thickness. The formula is applicable to arrays having either a 60-deg (staggered) or 90-deg (square) hole pattern, but is restricted to the case of (1) an obliquely incident plane wave with the E field polarized normal to the plane of incidence, and (2) large transmission loss. When theoretical values were compared to experimental data obtained on test samples having transmission losses greater than 20 dB, the agreement between theory and experiment was typically better than 1 dB at S-band and 2 dB at X-band.

PACE, G. D.

P001 Scan Pointing Calibration for the Mariner Mars 1971 Spacecraft

W. F. Havens, G. I. Jaivin, G. D. Pace, and
R. A. Virzi

Technical Memorandum 33-556, August 1, 1972

For abstract, see Havens, W. F.

P002 Mariner Mars 1971 Scan Platform Pointing Calibration

G. D. Pace, G. I. Jaivin, and R. A. Virzi

JPL Quarterly Technical Review, Vol. 2, No. 1,
pp. 49–57, April 1972

Accurate calibration is required to meet the pointing accuracy requirements of science instruments mounted on a spacecraft scan platform. Calibration methods used on previous missions required excessive system-test time and did not achieve the desired accuracy. Therefore, a new technique was devised for the Mariner Mars 1971 mission wherein both ground and in-flight calibrations were performed. A more analytical approach was used for ground calibration, and in-flight calibration was performed using narrow-angle television pictures of stars. The results were outstanding, indicating the potential of this technique for future missions when imaging experiments are flown. The Mariner Mars 1971 calibration technique and results are summarized in this article.

PALLUCONI, F. D.

P003 Models for the Atmospheres of Jupiter and Saturn

N. Divine and F. D. Palluconi

JPL Quarterly Technical Review, Vol. 2, No. 2,
pp. 1–8, July 1972

For abstract, see Divine, N.

PALUKA, J. R.

P004 DSN Progress Report for January–February 1972: 100-kW X-Band Transmitter for FTS

J. R. Paluka

Technical Report 32-1526, Vol. VIII, pp. 98–102,
April 15, 1972

During the month of July 1971 a 100-kW X-band transmitter was installed on the Venus Deep Space Station 9-m antenna. This transmitter replaces the experimental 25-kW transmitter formerly used at this station to transmit timing signals via the Moon to five other tracking stations in the DSN. Primary results of this change are an improved signal-to-noise ratio, higher reliability, and a change from the experimental frequency of 8.450 GHz to the operational frequency of 7.1495 GHz.

PARTHASARATHY, S. P.

P005 An Anechoic Chamber Facility for Investigating Aerodynamic Noise

P. F. Massier and S. P. Parthasarathy

Technical Report 32-1564, September 15, 1972

For abstract, see Massier, P. F.

PAWLIK, E. V.

P006 Ion Thruster Performance Calibration

E. V. Pawlik, R. Goldstein, D. J. Fitzgerald, and
R. W. Adams

Preprint 72-475,
AIAA Ninth Electric Propulsion Conference,
Bethesda, Maryland, April 17–19, 1972

The calibration of a typical 20-cm-diameter ion thruster was examined to determine performance penalties that must be assessed in projecting measured performance into a space environment. Four specific areas were investigated. These include (1) double ion content of the beam, (2) back ingestion from the vacuum facility, (3) beam spreading, and (4) propellant flow rate measurements. The double ion content was measured and found to be as high as 5.5% at an arc voltage of 35 V. Back ingestion was observed to become significant above tank pressures of 6×10^{-6} torr. Beam spreading reduced effective thrust on the order of 2.5%.

PEARL, J. C.

P007 Mariner 9 Science Experiments: Preliminary Results

R. H. Steinbacher, A. J. Kliore, J. Lorell,
H. Hipsher (National Aeronautics and Space
Administration), C. A. Barth (University of
Colorado), H. Masursky (U.S. Geological Survey),
G. Münch (California Institute of Technology),
J. C. Pearl (Goddard Space Flight Center), and
B. A. Smith (New Mexico State University)

For abstract, see Steinbacher, R. H.

P008 Infrared Spectroscopy Experiment on the Mariner 9 Mission: Preliminary Results

R. A. Hanel (Goddard Space Flight Center),
B. J. Conrath (Goddard Space Flight Center),
W. A. Hovis (Goddard Space Flight Center),
V. G. Kunde (Goddard Space Flight Center),
P. D. Lowman (Goddard Space Flight Center),
J. C. Pearl (Goddard Space Flight Center),
C. Prabhakara (Goddard Space Flight Center),
B. Schlachman (Goddard Space Flight Center), and
G. V. Levin (Biospherics Incorporated)

For abstract, see Hanel, R. A.

PEELGREN, M. L.

P009 Completely Modular Thermionic Reactor Ion Propulsion System (TRIPS)

M. L. Peelgren, G. M. Kikin, and C. D. Sawyer

The nuclear-reactor-powered ion-propulsion system described is an advanced, completely modularized system which lends itself to development of prototype and/or flight type components without the need for complete system tests until late in the development program. This modularity is achieved in all of the subsystems and components of the electric propulsion system, including: (1) the thermionic fuel elements, (2) the heat-rejection subsystem (heat pipes), (3) the power-conditioning modules, and (4) the ion thrusters. Both flashlight- and external-fuel in-core thermionic reactors are considered as the power source.

The thermionic fuel elements would be useful over a range of reactor power levels. Electrically heated acceptance testing of fuel elements in their flight configuration is possible for the external-fuel case. Nuclear-heated testing by sampling methods could be used for acceptance testing of flashlight-fuel elements. The use of heat pipes for cooling the collectors and transporting heat to the radiator allows early prototype or flight configuration

of testing of a small module of the heat-rejection subsystem as opposed to full scale liquid-metal pumps and radiators in a large vacuum chamber. The power conditioner is arranged in modules with passive cooling which allows complete prototype testing. The ion engines are typically matched with one or more power-conditioner modules and are the same size for any power level propulsion system of interest.

PENG, T. J.

P010 Extensional Flow of Bulk Polymers

T. J. Peng

This article presents a study of the behavior of polyisobutylene under motion at a constant stretch history for both strip-biaxial extensional flow and simple extensional flow. Steady-state non-Newtonian viscosities were observed at various constant-stretch histories. Newtonian viscosities for both strip-biaxial and simple extensional flow were found to be in agreement with the classical theory. The results of this study provide an essential part of the experimental background necessary for the development of a new general stress–strain–time relation for uncrosslinked and lightly crosslinked polymers.

P011 Stored Energy Function of Rubberlike Materials Derived From Simple Tensile Data

T. J. Peng and R. F. Landel

This article develops an explicit formulation to obtain the stored energy function W from simple tension experiments alone, based on the Valanis–Landel separable, symmetric, stored-energy function

$$W(\lambda_1, \lambda_2, \lambda_3) = w(\lambda_1) + w(\lambda_2) + w(\lambda_3)$$

For a simple extension stress–strain law of the form $\lambda\sigma = E\epsilon$ the analytical formula of W in the limited range $1 < \lambda < 2.5$ is found to be

$$W = E\sum_{i=1}^{3} \left[\lambda_i - 1 - \ln\lambda_i - \frac{1}{6}(\ln\lambda_i)^2 \right.$$

$$\left. + \frac{1}{18}(\ln\lambda_i)^3 - \frac{1}{216}(\ln\lambda_i)^4 \right]$$

where the limitation originates with the stress–strain law. The expression is used to verify for validity of the Valanis–Landel postulation through prediction of the stress–strain behavior in multiaxial deformations.

PERKINS, G. S.

P012   A Mechanism for Three-Axis Control of an Ion Thruster Array

G. S. Perkins, K. G. Johnson, J. D. Ferrera, and T. D. Masek

J. Spacecraft Rockets, Vol. 9, No. 3, pp. 218–220, March 1972

The JPL solar–electric propulsion system technology hardware program (SEPST III) is directed toward developing the SEP technology required for several advanced missions. The SEP system has two principal functions: (1) to convert solar energy into spacecraft acceleration and (2) to provide control torques for spacecraft attitude control. The first function is performed by use of power conditioners, a thruster, a controller for power management and failure detection, and, if needed for reliability, a thruster power-conditioner switching matrix. The second function is performed by the thrust vector control (TVC) subsystem. This paper describes the mechanical portion of the TVC subsystem under development in the SEPST III program.

PERLMAN, M.

P013   An Organization of a Digital Subsystem for Generating Spacecraft Timing and Control Signals

M. Perlman

Technical Memorandum 33-539, May 15, 1972

A modulo-M counter (of clock pulses) is decomposed into parallel modulo-m_i counters, where each m_i is a prime power divisor of M. Each m_i is a cascade of α_i identical modulo-p_i counters, where

$$m_i = p_i{}^{\alpha_i}$$

The modulo-p_i counters are feedback shift registers which cycle through p_i distinct states. By this organization, every possible nontrivial data-frame subperiod (in terms of clock-pulse intervals) and delayed subperiod may be derived.

The number of clock pulses required to bring all (or a subset of all) modulo-p_i counters to a state or count designated for each counter is determined by the Chinese Remainder Theorem. This corresponds to the solution of simultaneous congruences over relatively prime moduli.

PETTY, S.

P014   DSN Progress Report for May–June 1972: Tracking and Ground Based Navigation: Performance of Hydrogen Maser Cavity Tuning Servo

S. Petty and C. Finnie

Technical Report 32-1526, Vol. X, pp. 113–115, August 15, 1972

An experimental automatic cavity tuner has been demonstrated with the atomic hydrogen-maser frequency standards developed by JPL. The ability of this tuner to prevent RF-cavity frequency drift in the maser is shown, and the methods used to modulate hydrogen transition line width in the maser during tuner operation are compared.

PHILLIPS, H. P.

P015   DSN Progress Report for September–October 1972: Hydrostatic Bearing Runner Leveling at Overseas 64-m-Diameter Antenna

H. P. Phillips

Technical Report 32-1526, Vol. XII, pp. 214–219, December 15, 1972

The hydrostatic-bearing runners on the DSN 64-m-diameter antennas must be set to flatness tolerances which represent a major field-alignment problem. A new method was successfully employed in setting the runners for the new 64-m-diameter antennas at the Ballima Deep Space Station (DSS 43) in Australia and the Robledo Deep Space Station (DSS 63) in Spain. The method, based on the use of an electronic level, is described in this article.

PHILLIPS, R. J.

P016   The Lunar Conductivity Profile and the Nonuniqueness of Electromagnetic Data Inversion

R. J. Phillips

Icarus, Vol. 17, No. 1, pp. 88–103, August 1972

This article presents a review of the theory for the electromagnetic functional used to date to determine the lunar conductivity profile from spectral analyses of lunar magnetometer data. The use of the spectral data in conjunction with the functional to find a least squares conductivity profile is examined from the point of view of the nonuniqueness of nonlinear estimation.

Of the models generated, those that best fit the data all have a conductivity peak at a depth of 240 km. However, all of these models are quite distinct elsewhere in the profile. It is shown how such models are dependent

on both the nature of the functional as well as the initial guess in the least squares procedure.

A correlation analysis shows that the only resolvable features from this type of model are a low conductivity crust, a high conductivity peak of limited radial extent, and a low conductivity zone beneath the peak. It is also concluded that the two-layer model of Kuckes (1971) is equally as valid as the peaked models, and the totality of "equally valid" models derived from the spectral data place no reasonable constraint on the electrical conductivity below a depth of 350 km.

PHILLIPS, W. M.

P017 Some Observations on Uranium Carbide Alloy/Tungsten Compatibility

W. M. Phillips

Technical Memorandum 33-547, May 15, 1972

Chemical compatibility tests between pure tungsten and thoriated tungsten were run at 1800°C for up to 3300 h with uranium carbide alloys. Alloying with zirconium carbide appeared to widen the homogeneity range of uranium carbide, making additional carbon available for reaction with the tungsten. Reaction layers were formed both by vapor phase reaction and by physical contact, producing UWC_2 and/or W_2C, depending upon the phases present in the starting fuel alloy. Formation of UWC_2 results in slow growth of the reaction layer with time, while W_2C formation results in rapid growth of the reaction layer, allowing equilibrium to be reached in less than 2500 h at 1800°C. The presence of a thermal gradient had no effect on the reactions observed nor did the presence of thoria in the tungsten clad.

PIMENTEL, G. C.

P018 Mariner Mars 1969 Infrared Spectrometer

K. C. Herr (University of California, Berkeley), P. B. Forney (University of California, Berkeley), and G. C. Pimentel (University of California, Berkeley)

Appl. Opt., Vol. 11, No. 3, pp. 493–501, March 1972

For abstract, see Herr, K. C.

PLAUNT, J. R.

P019 Adaptive Variable-Length Coding for Efficient Compression of Spacecraft Television Data

R. F. Rice and J. R. Plaunt

IEEE Trans. Commun., Vol. COM-19, No. 6, pp. 889–897, December 1971

For abstract, see Rice, R. F.

POSNER, E. C.

P020 DSN Progress Report for November–December 1971: Hiding and Covering in a Compact Metric Space

R. J. McEliece and E. C. Posner

Technical Report 32-1526, Vol. VII, pp. 101–105, February 15, 1972

For abstract, see McEliece, R. J.

P021 Hide and Seek, Data Storage, and Entropy

R. J. McEliece and E. C. Posner

Ann. Math. Statist., Vol. 42, No. 5, pp. 1706–1716, October 1971

For abstract, see McEliece, R. J.

P022 Epsilon Entropy and Data Compression

E. C. Posner and E. R. Rodemich

Ann. Math. Statist., Vol. 42, No. 6, pp. 2079–2125, December 1971

This article discusses efficient data transmission, or "data compression," from the standpoint of the theory of epsilon entropy. The notion of the entropy of a "data source" is defined. This quantity gives a precise measure of the amount of channel capacity necessary to describe a data source to within a given fidelity, epsilon, with probability 1, when each separate "experiment" must be transmitted without storage from experiment to experiment. Also defined is the absolute epsilon entropy of a source, which is the amount of capacity needed when storage of experiments is allowed before transmission. The absolute epsilon entropy is shown to be equal to Shannon's rate distortion function evaluated for zero distortion, when suitable identifications are made. The main result is that the absolute epsilon entropy and the epsilon entropy have ratio close to one if either is large. Thus, very little can be saved by storing the results of independent experiments before transmission.

POTTER, P. D.

P023 DSN Progress Report for January–February 1972: S- and X-Band Feed System

P. D. Potter

Technical Report 32-1526, Vol. VIII, pp. 53–60, April 15, 1972

To support the Mariner 1973 X-band experiment, it will be necessary to implement a dual-frequency microwave feed system for the Mars Deep Space Station 64-m antenna. This system must be capable of simultaneous low noise reception at S- and X-bands and high power transmission at S-band. To fulfill this requirement, a particularly attractive approach, the reflex feed system, is being implemented. The system makes simultaneous use of both an X-band feedcone and an S-band feedcone. By a system of two reflectors, one of which is dichroic, the effective S-band phase center is translated from its normal position in the S-band feedhorn to a new point which very nearly coincides with the X-band feedhorn phase center. Thus, during simultaneous S- and X-band operation, the antenna subreflector optics are aligned with the X-band feedcone position. This article describes the analytical techniques used to design and analyze the feed system, as well as preliminary results from scale model tests.

PO24   DSN Progress Report for March–April 1972: S- and X-Band RF Feed System

P. D. Potter

Technical Report 32-1526, Vol. IX, pp. 141–146, June 15, 1972

In support of the Mariner Venus–Mercury 1973 X-band experiment, it is necessary to implement a dual-frequency microwave feed system for the DSS 14 64-m-diameter antenna. To fulfill this requirement, a particularly attractive approach, the reflex feed system, is being implemented. The reflex feed configuration and the analytical techniques used for its analysis were described in a previous report. This article describes the calculated gain performance of the system at S-band and discusses the heating of the reflex-feed dichroic reflector caused by high-power S-band transmission.

PO25   DSN Progress Report for May–June 1972: Antenna Study: Performance Enhancement

P. D. Potter

Technical Report 32-1526, Vol. X, pp. 129–134, August 15, 1972

A study of possible Mars Deep Space Station (DSS 14) 64-m-diameter antenna gain improvement by utilizing existing dual-reflector shaping techniques has been previously published. That study was restricted to the case of axially-symmetric (unicone) initial 64-m-diameter antenna configuration. After installation of the asymmetrical tricone system, studies of shaping techniques were discontinued pending operational experience with the tricone system at S- and X-bands, and development of

new analytical tools for design and analysis of asymmetrical-shape reflector systems. The required analytical tools have been developed recently and are described in this article.

PO26   DSN Progress Report for May–June 1972: Network Engineering and Implementation: S- and X-Band Feed System

P. D. Potter

Technical Report 32-1526, Vol. X, pp. 135–142, August 15, 1972

In support of the Mariner Venus–Mercury 1973 X-band experiment, it is necessary to implement a dual-frequency microwave feed system for the Mars Deep Space Station (DSS 14) 64-meter-diameter antenna. To fulfill this requirement, a particularly attractive approach, the reflex feed system, is being implemented. The reflex feed configuration and its calculated aperture efficiency performance were described in a previous report. Additionally, calculated RF power dissipation data for the reflex feed were reported. In this article, two questions are analyzed: (1) the S-band effects of possible buckling of the dichroic flat plate caused by RF and solar heating, and (2) the effect of subreflector backscatter on the S-band focus characteristics of the antenna.

PO27   DSN Progress Report for September–October 1972: Improved RF Calibration Techniques—A Practical Technique for Accurate Determination of Microwave Surface Resistivity

R. C. Clauss and P. D. Potter

Technical Report 32-1526, Vol. XII, pp. 59–67, December 15, 1972

For abstract, see Clauss, R. C.

POULSON, P. L.

PO28   Operating Executive for the DSIF Tracking Subsystem Software

P. L. Poulson

JPL Quarterly Technical Review, Vol. 2, No. 1, pp. 135–142, April 1972

The advanced engineering model of the Deep Space Instrumentation Facility tracking subsystem is currently being developed. The subsystem will provide effective and reliable tracking and data acquisition support for the complex planetary and interplanetary spaceflight missions planned for the 1970 decade. The nucleus of the subsystem is a Honeywell H832 digital computer. This article describes the design and capabilities of the real-time operating executive software being developed for this subsystem.

PRABHAKARA, C.

**P029   Infrared Spectroscopy Experiment on the Mariner 9
Mission: Preliminary Results**

R. A. Hanel (Goddard Space Flight Center),
B. J. Conrath (Goddard Space Flight Center),
W. A. Hovis (Goddard Space Flight Center),
V. G. Kunde (Goddard Space Flight Center),
P. D. Lowman (Goddard Space Flight Center),
J. C. Pearl (Goddard Space Flight Center),
C. Prabhakara (Goddard Space Flight Center),
B. Schlachman (Goddard Space Flight Center), and
G. V. Levin (Biospherics Incorporated)

Science, Vol. 175, No. 4019, pp. 305–308,
January 21, 1972

For abstract, see Hanel, R. A.

PURDUE, R. E.

**P030   Tracking and Data System Support for the Pioneer
Project: Pioneers 6–9. Extended Missions: July 1,
1970–July 1, 1971**

A. J. Siegmeth, R. E. Purdue, and R. E. Ryan

Technical Memorandum 33-426, Vol. X,
August 15, 1972

For abstract, see Siegmeth, A. J.

QUADE, J. G.

**Q001   Microwave Emission From Geological Materials:
Observations of Interference Effects**

J. C. Blinn III, J. E. Conel, and
J. G. Quade (University of Nevada)

J. Geophys. Res., Vol. 77, No. 23, pp. 4366–4378,
August 10, 1972

For abstract, see Blinn, J. C., III

QUINN, R. B.

**Q002   DSN Progress Report for March–April 1972: Low
Noise Receivers: Microwave Maser Development**

R. C. Clauss and R. B. Quinn

Technical Report 32-1526, Vol. IX, pp. 128–136,
June 15, 1972

For abstract, see Clauss, R. C.

**Q003   DSN Progress Report for July–August 1972: Low
Noise Receivers: Microwave Maser Development**

R. C. Clauss, E. Wiebe, and R. B. Quinn

Technical Report 32-1526, Vol. XI, pp. 71–80,
October 15, 1972

For abstract, see Clauss, R. C.

RAKUNAS, R. R.

**R001   DSN Progress Report for March–April 1972: DSN
Command System Tests**

R. R. Rakunas and A. Schulze

Technical Report 32-1526, Vol. IX, pp. 15–17,
June 15, 1972

The DSN Command System is continually updated to
support successive flight projects. Tests are scheduled as
each new model of Space Flight Operations Facility/
Deep Space Instrumentation Facility Command System
software is delivered. The test philosophy and results for
the Mark III era are described.

RANSFORD, G. A.

**R002   DSN Progress Report for May–June 1972:
Preliminary Evaluation of Radio Data Orbit
Determination Capabilities for the Saturn Portion of
a Jupiter–Saturn–Pluto 1977 Mission**

V. J. Ondrasik, C. E. Hildebrand, and
G. A. Ransford

Technical Report 32-1526, Vol. X, pp. 59–75,
August 15, 1972

For abstract, see Ondrasik, V. J.

**R003   DSN Progress Report for May–June 1972:
Determining the Mass and Ephemeris of Saturn by
Radio Tracking of a Jupiter–Saturn–Pluto 1977
Spacecraft**

V. J. Ondrasik, C. E. Hildebrand, and
G. A. Ransford

Technical Report 32-1526, Vol. X, pp. 76–81,
August 15, 1972

For abstract, see Ondrasik, V. J.

RASOOL, S. I.

**R004   Mariner 9 S-Band Martian Occultation Experiment:
Initial Results on the Atmosphere and Topography
of Mars**

A. J. Kliore, D. L. Cain, G. Fjeldbo,
B. L. Seidel, and S. I. Rasool (National
Aeronautics and Space Administration)

Science, Vol. 175, No. 4019, pp. 313-317,
January 21, 1972

For abstract, see Kliore, A. J.

RATHBUN, T. W.

R005   DSN Progress Report for November–December
1971: High Voltage Control for 400-kW Transmitter

T. W. Rathbun

Technical Report 32-1526, Vol. VII, pp. 139-141,
February 15, 1972

This article describes a high-voltage control unit, whose
functions are to bring the high voltage to a required
level, provide voltage regulation, and reduce beam mod-
ulation. This unit, which has been installed in the 400-
kW transmitter subsystem at two deep space stations,
utilizes all solid-state devices mounted on printed circuit
boards. The motorized potentiometer is modularized for
ease of replacement. This feature and the printed-circuit-
board replacement capability necessitate a minimum of
maintenance by the operators, and repairs are made by
module replacement at the field level.

RAY, R. L.

R006   Long-Term Storage Test of a SYNCOM Solid
Rocket Motor

R. L. Ray

JPL Quarterly Technical Review, Vol. 2, No. 2,
pp. 77-82, July 1972

After 7.5 yr of storage at ambient temperature, a solid-
propellant apogee motor was tested successfully at the
Air Force Rocket Propulsion Laboratory. The perform-
ance of the motor had not deteriorated as a result of
prolonged storage. Tabular performance data and
graphic thrust and pressure variations are given.

RAZOUK, R.

R007   Surface Tension of Propellants

R. Razouk

JPL Quarterly Technical Review, Vol. 2, No. 1,
pp. 123-134, April 1972

The design and successful performance of the surface-
tension-type propellant management systems for space-
craft require knowledge of propellant surface tension and
contact angle values and of the behavior of these param-
eters under various conditions of temperature, pressure,

gravitational forces, and aging. The work reported in this
article is concerned with the measurement of surface
tension. An apparatus is described for determining the
surface tension of propellants by measuring the maxi-
mum bubble pressure using two capillaries of different
bores. The innovation is the use of a pressure transducer
coupled to a bridge supply and a strip chart recorder for
registering the development of the pressure difference as
the bubble is formed and released. This enables the
measurements to be made under controlled atmospheres
and the equipment to be remotely operated. Preliminary
experiments were done on propellant-grade hydrazine,
monomethylhydrazine, and purified hydrazine at temper-
atures between 275.4 and 353.2 K. Straight-line expres-
sions and logarithmic expressions reproduce equally well
the variation of surface tension with temperature. Con-
taminated hydrazine, pre-exposed to coupons of 6Al-4V
titanium alloy for long periods, gives slightly higher
values of surface tension.

REA, D. G.

R008   Topical Reviews: Composition of the Upper Clouds
of Venus

D. G. Rea

Rev. Geophys. Space Phys., Vol. 10, No. 1,
pp. 369-378, February 1972

Recent developments have shed new light on the compo-
sition of the upper Venus clouds. An analysis of the
Mariner 5 occultation data has led to improved tempera-
ture and pressure profiles. When these are combined
with transit data, it is concluded that there is an optically
thin cloud layer with a top at 81-km altitude where the
temperature and pressure are, respectively, 175°K and 3
mb. The inclusion of temperatures derived from the
near-infrared CO_2 bands leads to the postulate of a
second cloud deck with a top at 61-km altitude, where
the temperature is 260°K and the pressure is 240 mb.
Additional important constraints on cloud models are
imposed by the measured abundances of HCl and H_2O,
by the polarization data, and by the reflection and emis-
sion spectra. It is concluded that the leading candidate
for the uppermost clouds is liquid drops of HCl-H_2O,
that there is no recommended candidate for the second
cloud deck, and that H_2O ice is at most a minor compo-
nent of these cloud systems.

REASENBERG, R. D.

R009   Mariner 9 Celestial Mechanics Experiment: Gravity
Field and Pole Direction of Mars

J. Lorell, G. H. Born, E. J. Christensen,
J. F. Jordan, P. A. Laing, W. Martin,
W. L. Sjogren, I. I. Shapiro (Massachusetts
Institute of Technology),
R. D. Reasenberg (Massachusetts Institute of
Technology), and G. L. Slater (Massachusetts
Institute of Technology)

Science, Vol. 175, No. 4019, pp. 317–320,
January 21, 1972

For abstract, see Lorell, J.

REEDY, G. K.

**R010 Determination of Solid-Propellant Transient
Regression Rates Using a Microwave Doppler Shift
Technique**

L. D. Strand, A. L. Schultz, and G. K. Reedy

Technical Report 32-1569, October 15, 1972

For abstract, see Strand, L. D.

REICHLEY, P. E.

R011 Second Decrease in the Period of the Vela Pulsar

P. E. Reichley and G. S. Downs

Nature Phys. Sci., Vol. 234, No. 46, p. 48,
November 15, 1971

This article discusses a second discontinuity in period of
the Vela Pulsar which occurred between August 21 and
September 4, 1971. A preliminary analysis of the data
shows that the period decreased by 179 ns and that the
rate of change of period increased. A definitive analysis
of the discontinuity will have to await more data because
of the normally irregular behavior of the period.

REID, M. S.

**R012 DSN Progress Report for January–February 1972:
Improved RF Calibration Techniques: System
Operating Noise Temperature Calibrations**

M. S. Reid

Technical Report 32-1526, Vol. VIII, pp. 61–67,
April 15, 1972

System operating noise temperatures and other calibra-
tion data of the S-band research operational cone at the
Venus Deep Space Station and the tricone system at the
Mars Deep Space Station are reported for the period
October 1, 1971 through January 31, 1972. During this
reporting period, the tricone system consisted of the
polarization diversity S-band (PDS) cone, the S-band
megawatt transmit (SMT) cone, and the multifrequency

X- and K-band (MXK) cone. S-band calibration data for
various configuration modes of the PDS and SMT cones
as well as X-band calibration data for the MXK cone are
reported.

**R013 DSN Progress Report for May–June 1972: Tracking
and Ground Based Navigation: A Description of the
Weather Project**

M. S. Reid

Technical Report 32-1526, Vol. X, pp. 116–122,
August 15, 1972

The Weather Project forms part of an overall Radio
Systems Development Project which seeks to optimize
the spacecraft-to-ground communications link. In order
to meet the future requirements of the planetary explora-
tion program, a study of weather-dependent characteris-
tics of X- and K-band propagation through the atmo-
sphere is imperative. The objective of the Weather Pro-
ject is, therefore, the statistical prediction of the per-
formance of the DSN at X-band, and in the future at
K-band.

This article discusses the general approach of the
Weather Project, the measurements, the calibrations, the
equipment, and the methods. Problems encountered are
also discussed as well as the proposed future work.

**R014 DSN Progress Report for May–June 1972: Improved
RF Calibration Techniques: System Operating Noise
Temperature Calibrations**

M. S. Reid

Technical Report 32-1526, Vol. X, pp. 123–128,
August 15, 1972

System operating noise temperatures and other calibra-
tion data of the S-band radar operational cone at the
Venus Deep Space Station (DSS 13) and the tricone
system at the Mars Deep Space Station (DSS 14) are
reported for the period February 1 through May 31,
1972. During this reporting period the tricone system
consisted of the polarization-diversity S-band (PDS) cone,
the S-band megawatt transmit (SMT) cone and the multi-
frequency X- and K-band (MXK) cone. S-band calibration
data for various configuration modes of the PDS and
SMT cones are reported as well as X-band calibration
data for the MXK cone.

**R015 DSN Progress Report for July–August 1972:
Preliminary Analysis of the Microwave Weather**

M. S. Reid and R. W. D. Booth

Technical Report 32-1526, Vol. XI, pp. 111–120,
October 15, 1972

The Weather Project forms part of an overall Radio
Systems Development Project which seeks to optimize

the spacecraft-to-ground communications link. Statistical correlations of weather and communications capability at X- and K-bands are needed to provide practical predictions of link performance. Thus the objective of the Weather Project is the statistical prediction of the performance of the DSN at X-band and, in the future, at K-band. A previous article discussed the general approach of the Weather Project, the measurements, calibrations, equipment, and methods. Problems encountered were also discussed as well as proposed future work.

This article reports on a preliminary analysis of the Weather Project data for calendar year 1971. These results are presented in tabular form. Cumulative frequency distributions of percentages of excess system temperature are tabulated as a function of time (whole year and quarterly periods) and of antenna elevation angle (four elevation ranges and all elevation angles). Averages, standard deviations, and confidence limits are tabulated, and the experimental results are compared with the data from a theoretical study based on estimated and observed cloud-cover effects.

R016 DSN Progress Report for September–October 1972: An Analysis of System Performance Under the Severe Weather Conditions at Goldstone, December 1971

M. S. Reid

Technical Report 32-1526, Vol. XII, pp. 32–34, December 15, 1972

Adverse weather conditions, unusual for the area in their severity, were experienced at Goldstone Deep Space Communications Complex in California in December 1971. This article summarizes an analysis of the system performance under these conditions and reports subsequent conclusions. The results of a brief study of cloud-cover characteristics in the southwestern United States to a distance of several hundred miles from Goldstone are also presented.

R017 DSN Progress Report for September–October 1972: Improved RF Calibration Techniques: System Operating Noise Temperature Calibrations

M. S. Reid

Technical Report 32-1526, Vol. XII, pp. 83–87, December 15, 1972

This article reports the system operating-noise-temperature performance and other calibration data of the low-noise research cones at the Goldstone Deep Space Communications Complex for June 1, 1972 through September 30, 1972. The performance of the following cones is presented for this reporting period: the S-band radar operational cone at the Venus Deep Space Station (DSS 13), the S-band megawatt transmit cone at the Mars

Deep Space Station (DSS 14), and the polarization diversity S-band cone at DSS 14. In addition to the above S-band calibration data, elevation profile measurements were made at fixed azimuth at 8415 MHz on the multi-frequency X- and K-band cone.

REIER, M.

R018 The Response of Covered Silicon Detectors to Monoenergetic Gamma Rays

M. Reier

Technical Memorandum 33-524, January 15, 1972

Measurements have been made of the efficiency in detecting gamma rays of 0.3-, 3-, and 5-mm silicon detectors covered with different absorbers. Calibrated sources covering the range from 279 keV to 2.75 MeV were used. The need for the absorbers to obtain meaningful results and their contribution to the response of the detectors at electron biases from 50 to 200 keV are discussed in detail. It is shown that the results are virtually independent of the atomic number of the absorber. In addition, the role of the absorber in increasing the efficiency with increasing photon energy for low bias settings is demonstrated for the 0.3-mm crystal. Qualitative explanations are given for the shapes of all curves of efficiency versus energy at each bias.

R019 The Response of Covered Silicon Detectors to Monoenergetic Gamma Rays

M. Reier

Nucl. Sci. Eng., Vol. 47, No. 4, pp. 409–414, April 1972

Measurements have been made of the efficiency in detecting gamma rays of a 0.3-mm-, 3-mm-, and 5-mm-thick silicon detector covered with different absorbers. Calibrated sources over the range from 279 keV to 2.75 MeV were used. The need for the absorbers to obtain meaningful results and their contribution to the response of the detectors at electron biases from 50 to 200 keV are discussed in detail. It is shown that the results are virtually independent of the atomic number of the absorber. In addition, the role of the absorber in increasing the efficiency with increasing photon energy for low bias settings is demonstrated for the 0.3-mm crystal. Qualitative explanations are given for the shapes of all curves of efficiency versus energy at each bias.

REMBAUM, A.

R020 Superconductivity in the Alkali Metal Intercalates of Molybdenum Disulphide

R. B. Somoano, V. Hadek, and A. Rembaum

JPL Quarterly Technical Review, Vol. 2, No. 2, pp. 83–89, July 1972

For abstract, see Somoano, R. B.

R021 Solution Properties of Novel Polyelectrolytes

D. Casson and A. Rembaum

Macromolecules, Vol. 5, No. 1, pp. 75–81, January–February 1972

For abstract, see Casson, D.

R022 Reactions of N,N,N′,N′-Tetramethyl-α,ω-Diaminoalkanes With α,ω-Dihaloalkanes: I. 1-y Reactions

H. Noguchi and A. Rembaum

Macromolecules, Vol. 5, No. 3, pp. 253–260, May–June 1972

For abstract, see Noguchi, H.

R023 Reactions of N,N,N′,N′-Tetramethyl-α,ω-Diaminoalkanes With α,ω-Dihaloalkanes: II. x-y Reactions

A. Rembaum and H. Noguchi

Macromolecules, Vol. 5, No. 3, pp. 261–269, May–June 1972

The reactions of $N,N,N′,N′$-tetramethyl-1,2-diaminoethane, -1,3-diaminopropane, -1,4-diaminobutane, and -1,6-diaminohexane with a number of α,ω-dibromoalkanes were investigated in solution. The main products of these reactions consisted of cyclic diammonium compounds (1:1 addition), linear diammonium compounds (1:2 addition), and ionene polymers (polyaddition). The conditions under which these products are formed as well as the information described in Part I permit one to conclude that the reactions of tetramethyldiaminoethane with dibromobutane and of tetramethyldiaminopropane with dibromopropane yield ionene polymers with the highest known density of positive charges in a polymer backbone. The reaction of tetramethyldiaminobutane with dibromomethane in dimethylformamide–methanol (1:1 by volume) yielded unexpectedly tetramethyldiaminobutane dihydrobromide, indicating participation of methanol in the reaction. Elucidation of these results as well as experimental evidence for the isolated products is presented.

RENNELS, D. A.

R024 The STAR (Self-Testing and Repairing) Computer: An Investigation of the Theory and Practice of Fault-Tolerant Computer Design

A. Avižienis, G. C. Gilley, F. P. Mathur, D. A. Rennels, J. A. Rohr, and D. K. Rubin

IEEE Trans. Computers, Vol. C-20, No. 11, pp. 1312–1321, November 1971

For abstract, see Avižienis, A.

RENZETTI, N. A.

R025 DSN Progress Report for November–December 1971: DSN Functions and Facilities

N. A. Renzetti

Technical Report 32-1526, Vol. VII, pp. 1–4, February 15, 1972

The Deep Space Network (DSN), established by the NASA Office of Tracking and Data Acquisition and under the system management and technical direction of JPL, is designed for two-way communications with unmanned spacecraft traveling approximately 16,000 km (10,000 mi) from Earth to planetary distances. The objectives, functions, and organization of the DSN are summarized, and its three facilities—the Deep Space Instrumentation Facility, the Ground Communications Facility, and the Space Flight Operations Facility—are described.

R026 DSN Progress Report for January–February 1972: DSN Functions and Facilities

N. A. Renzetti

Technical Report 32-1526, Vol. VIII, pp. 1–4, April 15, 1972

The Deep Space Network (DSN), established by the NASA Office of Tracking and Data Acquisition and under the system management and technical direction of JPL, is designed for two-way communications with unmanned spacecraft traveling approximately 16,000 km (10,000 mi) from Earth to planetary distances. The objectives, functions, and organization of the DSN are summarized, and its three facilities—the Deep Space Instrumentation Facility, the Ground Communications Facility, and the Space Flight Operations Facility—are described.

R027 DSN Progress Report for March–April 1972: DSN Functions and Facilities

N. A. Renzetti

Technical Report 32-1526, Vol. IX, pp. 1–4, June 15, 1972

The DSN, established by the NASA Office of Tracking and Data Acquisition and under the system management and technical direction of JPL, is designed for two-way communications with unmanned spacecraft traveling ap-

proximately 16,000 km (10,000 mi) from Earth to planetary distances. The objectives, functions, and organization of the DSN are summarized, and its three facilities—the Deep Space Instrumentation Facility, the Ground Communications Facility, and the Space Flight Operations Facility—are described.

R028   DSN Progress Report for May–June 1972: DSN Functions and Facilities

N. A. Renzetti

Technical Report 32-1526, Vol. X, pp. 1-4, August 15, 1972

The Deep Space Network (DSN), established by the NASA Office of Tracking and Data Acquisition and under the system management and technical direction of JPL, is designed for two-way communications with unmanned spacecraft traveling approximately 16,000 km (10,000 mi) from Earth to planetary distances. The objectives, functions, and organization of the DSN are summarized, and its three facilities—the Deep Space Instrumentation Facility, the Ground Communications Facility, and the Space Flight Operations Facility—are described.

R029   DSN Progress Report for July–August 1972: DSN Functions and Facilities

N. A. Renzetti

Technical Report 32-1526, Vol. XI, pp. 1-4, October 15, 1972

The Deep Space Network (DSN), established by the NASA Office of Tracking and Data Acquisition and under the system management and technical direction of JPL, is designed for two-way communications with unmanned spacecraft traveling approximately 16,000 km (10,000 mi) from Earth to planetary distances. The objectives, functions, and organization of the DSN are summarized, and the Deep Space Instrumentation Facility, the Ground Communications Facility, and the Network Control System are described.

R030   DSN Progress Report for September–October 1972: DSN Functions and Facilities

N. A. Renzetti

Technical Report 32-1526, Vol. XII, pp. 1-4, December 15, 1972

The Deep Space Network (DSN), established by the NASA Office of Tracking and Data Acquisition and under the system management and technical direction of JPL, is designed for two-way communications with unmanned spacecraft traveling approximately 16,000 km (10,000 mi) from Earth to planetary distances. The objectives, functions, and organization of the DSN are sum-

marized, and the Deep Space Instrumentation Facility, the Ground Communications Facility, and the Network Control System are described.

R031   Tracking and Data System Final Report for the Mariner Mars 1971 Project

N. A. Renzetti

Technical Memorandum 33-523, Vol. I, March 15, 1972

The Tracking and Data System support for the Mariner Mars 1971 Project was planned and implemented in close cooperation with the project's Mission Operations and Spacecraft Systems. The configuration of each Deep Space Network system supporting the project is described.

Also described are new features of the Tracking and Data System for this project, such as the new Deep Space Network command system, the high-rate telemetry system, the 4800-bit/s modem high-speed data lines from all deep space stations to the JPL Space Flight Operations Facility and the Goddard Space Flight Center, and the 50,000-bit/s wideband data lines from the Mars Deep Space Station to the Space Flight Operations Facility.

The Tracking and Data System performed prelaunch training and testing and provided support for the Mariner Mars 1971/Mission Operations System training and testing. The facilities of the Air Force Eastern Test Range, the Deep Space Network Compatibility Test Station at Cape Kennedy, and Manned Space Flight Network stations provided flight support coverage at launch and during the near-Earth phase. The Deep Space Network provided the deep-space phase support from the launch date, May 30, 1971, through the first trajectory correction maneuver on June 4, 1971, the end of the period covered in this volume.

Analysis of the support performance shows that all tracking and telemetry data received on Earth were acquired, processed, and delivered to the project. All commands were transmitted successfully.

REY, R. D.

R032   DSN Progress Report for November–December 1971: Automatic Angle Tracking: Angle Error Analysis and Tests

R. D. Rey

Technical Report 32-1526, Vol. VII, pp. 207-212, February 15, 1972

Tests are being developed to measure the angle errors of the 26-m-diameter antenna stations. Analysis is performed in order to define performance requirements.

Receiver degradation due to the mean and variance of the angle error is determined using an approximation of the antenna gain pattern. The equation for the angle error variance is determined. Measured data were compared with the theoretical results and were found to agree well.

RHEIN, R. A.

R033 **New Polymer Systems: Chain Extension By Dianhydrides**

R. A. Rhein and J. D. Ingham

JPL Quarterly Technical Review, Vol. 1, No. 4, pp. 97–103, January 1972

New highly stable polymers are required for materials applications on future long-term planetary missions. This article presents the results of a systematic investigation on the use of anhydrides to prepare stable elastomeric materials using mild reaction conditions. The three anhydrides investigated were found to provide effective chain extension of hydroxy-terminated poly(alkylene oxides) and poly(butadienes). These were tetrahydrofuran tetracarboxylic dianhydride, pyromellitic dianhydride, and benzophenone tetracarboxylic dianhydride. The most effective catalyst investigated was ferric acetylacetonate, which resulted in chain extension at 333 K (60°C). A novel feature of these anhydride reactants is that they are difunctional as anhydrides, but tetrafunctional if conditions are selected that lead to reaction of all carboxyl groups. Therefore, chain extension can be effected and then followed by crosslinking via the residual carboxyl groups.

RHO, J. H.

R034 **Direct Fluorometric Determination of Urea in Urine**

J. H. Rho

Clinical Chem., Vol. 18, No. 5, pp. 476–478, 1972

In this quantitative fluorometric method, diacetylmonoxime is used for the determination of the urea. The products of the reaction of urea with diacetylmonoxime in acid solution exhibit two fluorescence maxima, at 410 and 525 nm. The intensity of the 525-nm maximum is linear over a wide range of urea concentration and the reaction is shown to be practically specific for urinary urea.

R035 **Absence of Porphyrins in an Apollo 12 Lunar Surface Sample**

J. H. Rho, A. J. Bauman, T. F. Yen (University of Southern California), and J. Bonner (California Institute of Technology)

Proceedings of the Second Lunar Science Conference, Houston, Texas, January 11–14, 1971, Vol. 2, pp. 1875–1877, The M.I.T. Press, Cambridge, 1971

As described in this article, no porphyrins were found in 15 g of the Apollo 12 lunar fines from the Ocean of Storms under the conditions in which porphyrins would have been detected had they been present in amounts as small as 10^{-14} mole. An instrumental artifact at 600, 630, and 680 nm that resembled porphyrin peaks was observed in the control sample in which no porphyrins were present. This was produced by the interaction of grating anomalies with light scattering materials and was associated with a definite plane of polarization. When the data from the grating monochromator were corrected, or when prism monochromator data were used, no fluorescence attributable to the presence of porphyrins was found.

However, in the organic phase of the lunar sample extract, species which fluoresced at 365 to 380 nm when activated at 300 nm were found to be present. The corresponding aqueous phase of the sample extract also contained a material which exhibits a fluorescence maximum at 415 nm. All fluorescence attributable to organic materials in the lunar sample was also found in the Lunar Receiving Laboratory sand blank in equivalent amounts.

RICE, R. F.

R036 **Adaptive Variable-Length Coding for Efficient Compression of Spacecraft Television Data**

R. F. Rice and J. R. Plaunt

IEEE Trans. Commun., Vol. COM-19, No. 6, pp. 889–897, December 1971

An adaptive variable-length coding system is presented. Although developed primarily for the proposed Grand Tour missions, many features of this system clearly indicate a much wider applicability.

Using sample-to-sample prediction, the coding system produces output rates within 0.25 bit/picture element (pixel) of the one-dimensional difference entropy for entropy values ranging from 0–8 bits/pixel. This is accomplished without the necessity of storing any code words. Performance improvements of 0.5 bit/pixel can be simply achieved by utilizing previous line correlation.

A basic compressor, using concatenated codes, adapts to rapid changes in source statistics by automatically selecting one of three codes to use for each block of 21 pixels. The system adapts to less frequent, but more dramatic, changes in source statistics by adjusting the mode in which the basic compressor operates on a line-to-line basis. Furthermore, the compression system is indepen-

dent of the quantization requirements of the pulse-code modulation system.

RICHARDS, J. H.

R037 **A Simple Electrostatic Model for the Chromatographic Behavior of the Primary Dithizonates**

A. J. Bauman and J. H. Richards

Separ. Sci., Vol. 6, No. 5, pp. 715–725, October 1971

For abstract, see Bauman, A. J.

RIEBLING, R. W.

R038 **Experimental Evaluation of High-Thrust, Throttleable, Monopropellant Hydrazine Reactors**

R. W. Riebling and G. W. Kruger

Technical Report 32-1551, March 1, 1972

Throttleable monopropellant hydrazine catalytic reactors of a size applicable to a planetary landing vehicle have been designed, fabricated, and tested. An experimental evaluation of two 2670-N (600-lbf) reactor designs has been conducted. The steady-state and dynamic characteristics of the thruster/valve combinations have been determined. The results of the testing, including the engine characteristic velocity, smoothness of combustion, insensitivity to heat sterilization, and response during various simulated duty cycles, are presented and discussed. No problems of a fundamental nature were encountered as a result of rapid dynamic throttling of these large hydrazine reactors.

RINDERLE, E. A.

R039 **DSN Progress Report for November–December 1971: A Comparison of Cowell's Method and a Variation-of-Parameters Method for the Computation of Precision Satellite Orbits: Addendum 1**

S. S. Dallas and E. A. Rinderle

Technical Report 32-1526, Vol. VII, pp. 32–36, February 15, 1972

For abstract, see Dallas, S. S.

R040 **DSN Progress Report for July–August 1972: A Comparison of Cowell's Method and a Variation-of-Parameters Method for the Computation of Precision Satellite Orbits: Phase Three Results**

S. S. Dallas and E. A. Rinderle

Technical Report 32-1526, Vol. XI, pp. 30–35, October 15, 1972

For abstract, see Dallas, S. S.

ROBINSON, E. Y.

R041 **A Basic Model for Acoustic Emission From Fiber-Reinforced Material**

E. Y. Robinson

Technical Memorandum 33-564, September 1, 1972

Acoustic emission from fiber-reinforced composites can often be conveniently interpreted by use of normalized coordinates in graphical data display. Many aspects of the shape of the acoustic-emission pattern are invariant with the signal-amplification ratio, and the use of normalized coordinates allows simultaneous comparison of acoustic-emission pattern shapes from different experiments. In this paper, the first order model of acoustic emission from fiber composites, based on filament breaking rates, is cast into a normalized form useful for correlating experimental data. The general features of the normalized model are shown and compare favorably with available data.

R042 **A Brief Survey of Carbon–Carbon Refractory Composites at the Jet Propulsion Laboratory**

E. Y. Robinson

Technical Memorandum 33-579, December 1, 1972

Refractory composites of carbon–carbon material are being considered for application in: (a) rocket-motor nozzles and skirts, (b) a unique integrated propulsion structure, and (c) planetary-atmosphere-entry shells. The first application is intended for radiation-cooled nozzles and skirts which, with presently available materials, can meet operational requirements of deep space missions at substantially lower weights. The second application requires very high structural performance as well as refractory capability, and is feasible only if high-strength graphite filaments are efficiently incorporated into a carbon-matrix composite. The third application is comparable in many respects to Earth-entry aeroshells and heat shields; however, planetary atmospheres may pose new gas-dynamic and corrosion problems. Furthermore, the entry shell is likely to be an integral structural element which is not jettisoned, and to which critical hard-point attachment must be made. This memorandum describes technical developments and plans in each of these areas.

R043 **Estimating Weibull Parameters for Materials**

E. Y. Robinson

Technical Memorandum 33-580,
December 15, 1972

This memorandum deals with the statistical analysis of strength and fracture of materials in general with application to fiber composites. The "weakest link" model is considered in a fairly general form, and the resulting equations are demonstrated by using a Weibull distribution for flaws. This distribution appears naturally in a variety of problems, and therefore additional attention is devoted to analysis and statistical estimation connected with this distribution. Special working charts are included to facilitate interpretation of observed data and estimation of parameters. Implications of the size effect are considered for various kinds of flaw distributions.

The memorandum describes failure and damage in a fiber-reinforced system. Some useful graphs are included for predicting the strength of such a system. Recent data on organic-fiber (PRD 49) composite material is analyzed by the Weibull distribution with the methods presented here. This memorandum should serve as a useful handbook for data characterization and statistical fracture analysis.

R044   **On the Elastic Properties of Fiber Composite Laminates With Statistically Dispersed Ply Orientation**

E. Y. Robinson

JPL Quarterly Technical Review, Vol. 2, No. 2, pp. 48–60, July 1972

Structural application of advanced composite filamentary materials requires lamination of the basic orthotropic plies into "angle-ply" laminates. The resulting elastic and strength properties depend on the pattern of orientation and are influenced by inevitable errors and inaccuracy in placement of the angle plies. Misorientation results also from irregular displacements following processing at elevated temperatures.

This article reviews the effect of orientation dispersion on laminate elastic properties. The conventional constitutive relations are recast in a homologous form to account for orientation dispersion by addition of a single parameter. Graphical results are presented to show the behavior of the most important advanced composite materials. These results are useful for estimating effects of manufacturing inaccuracy and for design of partially-oriented reinforced structures.

RODEMICH, E. R.

R045   **Epsilon Entropy and Data Compression**

E. C. Posner and E. R. Rodemich

Ann. Math. Statist., Vol. 42, No. 6, pp. 2079–2125, December 1971

For abstract, see Posner, E. C.

ROHR, J. A.

R046   **The STAR (Self-Testing and Repairing) Computer: An Investigation of the Theory and Practice of Fault-Tolerant Computer Design**

A. Aviženis, G. C. Gilley, F. P. Mathur, D. A. Rennels, J. A. Rohr, and D. K. Rubin

IEEE Trans. Computers, Vol. C-20, No. 11, pp. 1312–1321, November 1971

For abstract, see Aviženis, A.

ROSCHKE, E. J.

R047   **Partially Ionized Gas Flow and Heat Transfer in the Separation, Reattachment, and Redevelopment Regions Downstream of an Abrupt Circular Channel Expansion**

L. H. Back, P. F. Massier, and E. J. Roschke

Trans. ASME, Ser. C: J. Heat Transf., Vol. 94, No. 1, pp. 119–127, February 1972

For abstract, see Back, L. H.

R048   **Partially Ionized Gas Flow and Heat Transfer in the Separation, Reattachment, and Redevelopment Regions Downstream of an Abrupt Circular Channel Expansion**

L. H. Back, P. F. Massier, and E. J. Roschke

Trans. ASME, Ser. C: J. Heat Transf., Vol. 94, No. 1, pp. 119–127, February 1972

For abstract, see Back, L. H.

R049   **Experimental Investigation of Heat Transfer From Partially Ionized Argon With an Applied Transverse Magnetic Field**

E. J. Roschke

Trans. ASME, Ser. C: J. Heat Transf., Vol. 94, No. 2, pp. 174–180, May 1972

Wall heat transfer measurements were obtained for laminar flow of partially ionized argon flowing within the conducting walls of a square channel, with and without an applied transverse magnetic field. Tests were conducted for subsonic flows and for flows which were supersonic before a magnetic field was applied. Increases in Stanton number by a factor of as much as six were observed at field strengths approaching 10 kG as com-

pared to values at zero magnetic field. These large increases in heat transfer are believed to have been due to (1) a small amount of joule heating augmented or accompanied by (2) magnetically induced ionization. Heat transfer and flow data were used to estimate effective values of the joule heating parameter, Hall coefficient, and current density. The experimental data have been compared to theoretical predictions for several limiting cases.

ROSENTHAL, L. A.

R050 Electrothermal Follow Display Apparatus for Electroexplosive Device Testing

L. A. Rosenthal (Rutgers University) and
V. J. Menichelli

Technical Report 32-1554, March 15, 1972

By employing a self-balancing bridge, it is possible to ascertain the electrothermal and nonlinear behavior of an electroexplosive device. A sinusoidal current is passed through the device that provides a signal in the form of a unique Lissajous display. This display can be qualitatively evaluated, and abnormal units can be readily detected. This technique for evaluating electroexplosive devices is described in this report.

R051 Fault Determinations in Electroexplosive Devices by Nondestructive Techniques

V. J. Menichelli and L. A. Rosenthal (Rutgers University)

Technical Report 32-1553, March 15, 1972

For abstract, see Menichelli, V. J.

R052 Terminated Capacitor-Discharge Firing of Electroexplosive Devices

L. A. Rosenthal (Rutgers University) and
V. J. Menichelli

IEEE Trans. Instr. Meas., Vol. IM-21, No. 2, pp. 177–180, May 1972

By terminating the discharge of energy into an insensitive electroexplosive device, firing-energy parameters can be determined. A simple capacitor-discharge system providing exponential pulses terminated at an adjustable width is described. Basic theory and application to testing are discussed.

R053 Nondestructive Testing of Insensitive Electroexplosive Devices by Transient Techniques

L. A. Rosenthal (Rutgers University) and
V. J. Menichelli

Mater. Eval., Vol. XXX, No. 1, pp. 13–19, January 1972

By pulsing an electroexplosive device with a safe level constant current and examining the resistance variation of the bridgewire, it is possible to explore the electrothermal behavior of the bridgewire-explosive interface. The bridgewire, acting as a resistance thermometer, provides a signal which describes the average wire temperature and the heat sinking to the explosive and enclosure. This article describes equipment and observations specific to nondestructive testing of 1-W/1-A no fire devices.

ROSS, R. G., JR.

R054 Summary Report on the Development, Design and Test of a 66-W/kg (30-W/lb) Roll-Up Solar Array

W. A. Hasbach and R. G. Ross, Jr.

Technical Report 32-1562, September 15, 1972

For abstract, see Hasbach, W. A.

R055 An Algorithm for Synthesizing Mass and Stiffness Matrices From Experimental Vibration Modes

R. G. Ross, Jr.

JPL Quarterly Technical Review, Vol. 2, No. 3, pp. 12–21, October 1972

It is sometimes desirable to derive a dynamic model of highly complex structures from experimental vibration data. This article presents an algorithm for synthesizing the mass and stiffness matrices from experimentally derived modal data in a way that preserves the physical significance of the individual mass and stiffness elements. The mass and stiffness matrices are derived for a rollup-solar-array example, and are then used to define the modal response of a modified array.

ROURKE, K. H.

R056 DSN Progress Report for November–December 1971: Improved Navigation Capability Utilizing Two-Station Tracking Techniques for a Low-Declination Distant Spacecraft

K. H. Rourke and V. J. Ondrasik

Technical Report 32-1526, Vol. VII, pp. 51–60, February 15, 1972

This article presents the results of an uncompromised accuracy analysis study investigating the advantages of using two-station simultaneous tracking (quasi very long baseline interferometry) techniques to determine the far-approach orbit of a distant spacecraft at a low declination angle. The analysis is restricted to batch filtering

techniques, but includes the effects of unmodeled spacecraft accelerations. By properly processing the simultaneous doppler and simultaneous range data, the errors resulting from the low-declination geometry are reduced by a factor of two to four, and the errors resulting from unmodeled spacecraft accelerations are reduced by two orders of magnitude.

R057 DSN Progress Report for July–August 1972: Topics in the Implementation and Application of Two-Station Tracking Data Types

K. H. Rourke and V. J. Ondrasik

Technical Report 32-1526, Vol. XI, pp. 62–70, October 15, 1972

Two proposed two-station-tracking data-processing techniques, direct data filtering and differenced data filtering, are analyzed using advanced orbit-determination filtering methods. Both techniques are shown to perform comparably, yet direct filtering methods prove to be more sensitive to error-model assumptions. Two-station tracking data are shown to be potentially superior to conventional tracking data in determining deep space station locations.

R058 Application of New Radio Tracking Data Types to Critical Spacecraft Navigation Problems

V. J. Ondrasik and K. H. Rourke

JPL Quarterly Technical Review, Vol. 1, No. 4, pp. 116–132, January 1972

For abstract, see Ondrasik, V. J.

ROWE, W. M.

R059 Stress Analysis and Design of Silicon Solar Cell Arrays and Related Material Properties

A. M. Salama, W. M. Rowe, and R. K. Yasui

Technical Report 32-1552, March 1, 1972

For abstract, see Salama, A. M.

RUBIN, D. K.

R060 The STAR (Self-Testing and Repairing) Computer: An Investigation of the Theory and Practice of Fault-Tolerant Computer Design

A. Avižienis, G. C. Gilley, F. P. Mathur, D. A. Rennels, J. A. Rohr, and D. K. Rubin

IEEE Trans. Computers, Vol. C-20, No. 11, pp. 1312–1321, November 1971

For abstract, see Avižienis, A.

RUPE, J. H.

R061 Liquid-Phase Mixing of Bipropellant Doublets

F. W. Hoehn, J. H. Rupe, and J. G. Sotter

Technical Report 32-1546, February 15, 1972

For abstract, see Hoehn, F. W.

R062 Effect on Supersonic Jet Noise of Nozzle Plenum Pressure Fluctuations

R. Kushida and J. H. Rupe

AIAA J., Vol. 10, No. 7, pp. 946–948, July 1972

For abstract, see Kushida, R.

RUSSELL, R. K.

R063 DSN Progress Report for January–February 1972: On Modeling Continuous Accelerations as Piecewise Constant Functions

R. K. Russell and D. W. Curkendall

Technical Report 32-1526, Vol. VIII, pp. 45–52, April 15, 1972

Random, non-gravitational forces acting on the spacecraft in an unpredictable manner have long been identified as a major limitation in using DSN radio data to deduce the state of the spacecraft and predict its subsequent motion. An important aspect of properly handling the non-gravitational forces is determining when their presence affects the data to an extent and in a manner that cannot be modeled accurately within the limitations of the batch filtering orbit determination procedures. This is relevant in its own right but is also important in regard to the proper configuration of the operational sequential filters.

The design of these filters is such that the data is segregated into a series of batches. Between batches, stochastic elements are assumed to enter, and any or all of the parameters subject to solution can change at that time. Within any one batch, however, every parameter is assumed constant, and, within that batch, the data is treated exactly as it is treated in the classical least squares problem. In the limit as batch size reduces to a single data point, this machinery becomes identical to the point sequential filter widely discussed in the literature. To reduce the computational complexity of the operational sequential filters, however, it is desirable to keep the batch sizes as large as possible. Determining this bound in the presence of what is viewed as a continuously varying force model becomes the focus of this article.

RYAN, R. E.

R064 Tracking and Data System Support for the Pioneer Project: Pioneers 6–9. Extended Missions: July 1, 1970–July 1, 1971

A. J. Siegmeth, R. E. Purdue, and R. E. Ryan

Technical Memorandum 33-426, Vol. X, August 15, 1972

For abstract, see Siegmeth, A. J.

SALAMA, A. M.

S001 Stress Analysis and Design of Silicon Solar Cell Arrays and Related Material Properties

A. M. Salama, W. M. Rowe, and R. K. Yasui

Technical Report 32-1552, March 1, 1972

Mechanical failures that may arise in components of composite solar cell arrays in a thermal environment can be avoided by properly selecting compatible material for the components and introducing certain geometric changes in a proposed design. This report provides the solar cell array designer with a rational systematic approach. A prerequisite to this approach is the characterization of material properties at different temperatures. Significant data were obtained for the thermal behavior of the silicon solar cell material and adhesives. Upon determining the mechanical and thermal material properties of the components of the solar cell array, utilizing a finite-element idealization for predicting the stress fields in the components, and employing the von Mises failure criterion, potential failure areas in various design configurations in a given thermal environment can be identified. Guidelines and means to optimize a given design are illustrated by two examples.

SATO, T.

S002 Transformation of Received Signal Polarization Angle to the Plane of the Ecliptic

C. T. Stelzried, T. Sato, and A. Abreu

J. Spacecraft Rockets, Vol. 9, No. 2, pp. 69–70, February 1972

For abstract, see Stelzried, C. T.

SAVAGE, J. E.

S003 DSN Progress Report for July–August 1972: Reducing the Complexity of Calculating Syndromes for Error-Correcting Codes

L. H. Harper and J. E. Savage

Technical Report 32-1526, Vol. XI, pp. 89–91, October 15, 1972

For abstract, see Harper, L. H.

SAWYER, C. D.

S004 Closed-Loop Dynamics of In-Core Thermionic Reactor Systems

C. D. Sawyer and J. E. Boudreau

Technical Memorandum 33-546, May 15, 1972

Using a point model of an in-core thermionic converter, alternative schemes for providing closed-loop reactor control were investigated. It was found that schemes based on variable-gain power regulation buffers which use the reactor current as the control variable provide complete protection from thermionic burnout and also provide a virtually constant voltage to the user. A side benefit is that the emitter-temperature transients are small; even for a complete electric load drop, the emitter temperature transient is less than 100°K. The current-regulation scheme was selected for further study with a distributed-parameter model which was developed to account for variations in thermionic and heat transfer properties along the length of a cylindrical converter. It was found that, even though the emitter-temperature range is about 200°K along the converter length, the dynamic properties are unchanged when using the current-control scheme.

S005 Thermionic Reactor Electric Propulsion System Requirements

J. F. Mondt, C. D. Sawyer, and R. W. Schaupp (Ames Research Center)

Technical Memorandum 33-549, June 1, 1972

For abstract, see Mondt, J. F.

S006 Completely Modular Thermionic Reactor Ion Propulsion System (TRIPS)

M. L. Peelgren, G. M. Kikin, and C. D. Sawyer

Technical Memorandum 33-550, May 15, 1972

For abstract, see Peelgren, M. L.

SCHAUPP, R. W.

S007 Thermionic Reactor Electric Propulsion System Requirements

J. F. Mondt, C. D. Sawyer, and R. W. Schaupp (Ames Research Center)

Technical Memorandum 33-549, June 1, 1972

For abstract, see Mondt, J. F.

SCHLACHMAN, B.

S008   Infrared Spectroscopy Experiment on the Mariner 9 Mission: Preliminary Results

R. A. Hanel (Goddard Space Flight Center),
B. J. Conrath (Goddard Space Flight Center),
W. A. Hovis (Goddard Space Flight Center),
V. G. Kunde (Goddard Space Flight Center),
P. D. Lowman (Goddard Space Flight Center),
J. C. Pearl (Goddard Space Flight Center),
C. Prabhakara (Goddard Space Flight Center),
B. Schlachman (Goddard Space Flight Center), and
G. V. Levin (Biospherics Incorporated)

Science, Vol. 175, No. 4019, pp. 305–308,
January 21, 1972

For abstract, see Hanel, R. A.

SCHMIT, D. D.

S009   Mariner 9 Propulsion Subsystem Performance During Interplanetary Cruise and Mars Orbit Insertion

M. J. Cork, R. L. French, C. J. Leising, and
D. D. Schmit

JPL Quarterly Technical Review, Vol. 2, No. 1,
pp. 113–122, April 1972

For abstract, see Cork, M. J.

SCHORN, R. A. J.

S010   High Dispersion Spectroscopic Studies of Mars: V. A Search for Oxygen in the Atmosphere of Mars

J. S. Margolis, R. A. J. Schorn, and
L. D. G. Young

Icarus, Vol. 15, No. 2, pp. 197–203, October 1971

For abstract, see Margolis, J. S.

SCHULTZ, A. L.

S011   Determination of Solid-Propellant Transient Regression Rates Using a Microwave Doppler Shift Technique

L. D. Strand, A. L. Schultz, and G. K. Reedy

Technical Report 32-1569, October 15, 1972

For abstract, see Strand, L. D.

SCHULZE, A.

S012   DSN Progress Report for March–April 1972: DSN Command System Tests

R. R. Rakunas and A. Schulze

Technical Report 32-1526, Vol. IX, pp. 15–17,
June 15, 1972

For abstract, see Rakunas, R. R.

SCHURMEIER, H. M.

S013   The 1969 Mariner View of Mars

H. M. Schurmeier

Proceedings of the Twenty-First International Astronautical Congress, Constance, Germany, October 4–10, 1970, pp. 193–210,
North-Holland Publishing Co., Amsterdam, 1971

The second step in the U.S. program to explore Mars by spacecraft was completed by the Mariner mission in 1969. This article presents a brief summary of that mission, highlighting the planetary encounter and discussing the various scientific experiments. The scientific results analyzed to date are also summarized.

SEAMAN, C. H.

S014   Astronomical Infrared Spectroscopy With a Connes-Type Interferometer: I. Instrumental

R. Beer, R. H. Norton, and C. H. Seaman

Rev. Sci. Instr., Vol. 42, No. 10, pp. 1393–1403,
October 1971

For abstract, see Beer, R.

SEELEY, L. N.

S015   Mariner Mars 1971 Television Picture Catalog: Sequence Design and Picture Coverage

P. E. Koskela, M. R. Helton, L. N. Seeley, and
S. J. Zawacki

Technical Memorandum 33-585, Vol. II,
December 15, 1972

For abstract, see Koskela, P. E.

SEIDEL, B. L.

S016   DSN Progress Report for September–October 1972: Improved RF Calibration Techniques: Commercial Precision IF Attenuator Evaluation

C. T. Stelzried, B. L. Seidel, M. Franco, and
D. Acheson

Technical Report 32-1526, Vol. XII, pp. 74–82,
December 15, 1972

For abstract, see Stelzried, C. T.

S017 Bistatic Radar Measurements of the Surface of Mars With Mariner 1969

G. Fjeldbo, A. J. Kliore, and B. L. Seidel

Icarus, Vol. 16, No. 3, pp. 502–508, June 1972

For abstract, see Fjeldbo, G.

S018 Mariner 9 S-Band Martian Occultation Experiment: Initial Results on the Atmosphere and Topography of Mars

A. J. Kliore, D. L. Cain, G. Fjeldbo,
B. L. Seidel, and S. I. Rasool (National
Aeronautics and Space Administration)

Science, Vol. 175, No. 4019, pp. 313–317,
January 21, 1972

For abstract, see Kliore, A. J.

S019 Summary of Mariner 6 and 7 Radio Occultation Results on the Atmosphere of Mars

A. J. Kliore, G. Fjeldbo, and B. L. Seidel

Space Research XI, pp. 165–175, Akademie-Verlag,
Berlin, 1971

For abstract, see Kliore, A. J.

SHAFER, J. I.

S020 Initiation System for Low Thrust Motor Igniter

L. D. Strand, D. P. Davis, and J. I. Shafer

Technical Memorandum 33-520, January 1, 1972

For abstract, see Strand, L. D.

S021 Solid-Propellant Motors for High-Incremental-Velocity Low-Acceleration Maneuvers in Space

J. I. Shafer

Technical Memorandum 33-528, March 1, 1972

Recent advancements in motor technology offer promise
of extending the applicability of solid-propellant rockets
into a regime of high-performance long-burning tasks
beyond the capability of existing motors. Successful
static test firings have demonstrated the feasibility of: (1)
utilizing fully case-bonded end-burning propellant
charges without mechanical stress relief, (2) using an all-

carbon radiative nozzle markedly lighter than the flight-
weight ablative nozzle it replaces, and (3) producing low
spacecraft acceleration rates during the thrust transient
through a controlled-flow igniter that promotes opera-
tion beyond the L^* combustion limit. It remains now to
show that a 350-kg-sized motor, with all features inte-
grated, performs reliably and produces the predicted
motor performance, a mass fraction of 0.92 with a vac-
uum specific impulse of 2840 N/kg.

S022 Solid Propulsion Advanced Concepts

Y. Nakamura and J. I. Shafer

Technical Memorandum 33-534, May 1, 1972

For abstract, see Nakamura, Y.

SHAPIRO, I. I.

S023 Mariner 9 Celestial Mechanics Experiment: Gravity Field and Pole Direction of Mars

J. Lorell, G. H. Born, E. J. Christensen,
J. F. Jordan, P. A. Laing, W. Martin,
W. L. Sjogren, I. I. Shapiro (Massachusetts
Institute of Technology),
R. D. Reasenberg (Massachusetts Institute of
Technology), and G. L. Slater (Massachusetts
Institute of Technology)

Science, Vol. 175, No. 4019, pp. 317–320,
January 21, 1972

For abstract, see Lorell, J.

SHIMADA, K.

S024 Out-of-Core Evaluations of Uranium Nitride-Fueled Converters

K. Shimada

Technical Memorandum 33-545, May 1, 1972

Two uranium–nitride-fueled converters were tested para-
metrically for their initial characterization and are cur-
rently being life-tested out of core. In this memorandum,
the test method being employed for the parametric and
diagnostic measurements during the life tests and the test
results are presented. One converter, with a rhenium
emitter, had an initial output power density of 6.9
W/cm^2 at the blackbody emitter temperature, T_E, of
1900°K. The power density remained unchanged for the
first 1000 h of the life test at $T_E = 1900$°K but it
degraded nearly 50% during the following 1000 h. The
electrode work function measurements indicated that the
uranium fuel was diffusing out of the emitter clad of
0.635-mm thickness. The other converter, with a tung-
sten emitter, had an initial output power density of 2.2

W/cm^2 at T_E = 1900°K. The power density increased exponentially to 3.6 W/cm^2 during the 3500 h of the life test. The rate of improvement increased thereafter and the power density was 3.9 W/cm^2 at 4300 h. The power density suddenly degraded within 20 h to practically zero output at 4735 h.

S025 Probe Measurements of Cesium Plasma in a Simulated Thermionic Energy Converter

K. Shimada

Technical Memorandum 33-551, May 15, 1972

Cesium-filled thermionic energy converters are being considered as candidate electrical energy sources in future spacecraft requiring tens to hundreds of kilowatts of electric power. The high operating temperatures necessary for a large specific power and high efficiency inevitably impose stringent constraints on the converter fabrication to achieve the desired reliability of the power system. The converter physics for reducing operating temperatures and cesium plasma losses are being studied to achieve high reliability without sacrificing the power performance of the converters. Various cesium parameters that affect the converter performance are: (1) electron temperatures, (2) plasma ion densities, and (3) electric potential profiles. These were investigated using a Langmuir probe in a simulated converter. The parameters were measured in different cesium discharge modes.

SHINOZUKA, M.

S026 On the First Excursion Probability in Stationary Narrow-Band Random Vibration

J.-N. Yang and M. Shinozuka (Columbia University)

Trans. ASME, Ser. E: J. Appl. Mech., Vol. 38, No. 4, pp. 1017-1022, December 1971

For abstract, see Yang, J.-N.

SHIRLEY, D. L.

S027 Mariner Venus–Mercury 1973 Encounter Strategy

D. L. Shirley

AIAA Preprint 72-942, AIAA (American Institute of Aeronautics and Astronautics)/AAS (American Astronautical Society) Astrodynamics Conference, Palo Alto, California, September 11-12, 1972

This paper describes the selection of launch and arrival conditions and Venus and Mercury encounter aiming zones to maximize the science return from the Mariner Venus–Mercury mission. A single Mariner spacecraft will be launched in November 1973, fly by Venus in early

February 1974, and encounter Mercury (the primary target) in late March 1974. Mercury aiming points will provide: (a) Sun and Earth occultation, (b) 1000-km periapsis altitude, and (c) return to Mercury after 176 days (two Mercury years). The selected Mercury arrival dates allow high-contrast television imaging. Aiming points at Venus allow gravity assist to Mercury and also permit Earth occultation.

SHOEMAKE, G. R.

S028 Rare Gases of the Atmosphere: Gas Chromatography Using a Thermal Conductivity Detector and a Palladium Transmodulator

J. E. Lovelock, P. G. Simmonds, and G. R. Shoemake

Anal. Chem., Vol. 43, No. 14, pp. 1958-1961, December 1971

For abstract, see Lovelock, J. E.

SHUMATE, M. S.

S029 3-D Multilateration: A Precision Geodetic Measurement System

P. R. Escobal, H. F. Fliegel, R. M. Jaffe, P. M. Muller, K. M. Ong, O. H. von Roos, and M. S. Shumate

JPL Quarterly Technical Review, Vol. 2, No. 3, pp. 1-11, October 1972

For abstract, see Escobal, P. R.

SHUMKA, A.

S030 Thermal Noise in Space-Charge-Limited Hole Current in Silicon

A. Shumka, J. Golder, and M.-A. Nicolet

JPL Quarterly Technical Review, Vol. 2, No. 2, pp. 72-76, July 1972

Present theories on noise in single-carrier space-charge-limited currents in solids have not been quantitatively substantiated by experimental evidence. To obtain such experimental verification, the noise in specially fabricated silicon structures is being measured and analyzed. The first results of this verification effort are reported in this article.

SIEGMETH, A. J.

S031 DSN Progress Report for November–December 1971: Pioneer Mission Support

A. J. Siegmeth

Technical Report 32-1526, Vol. VII, pp. 5-16,
February 15, 1972

The Pioneer F and G missions are planned to extend the exploration of the solar system toward the outer planets. The major objectives will be the first penetration of the asteroid belt and a Jupiter flyby. Since Jupiter missions require new types of solar orbits, some adaptations of the tracking and data acquisition capabilities and resources are necessary to meet effectively the requirements of these new challenges. The Pioneer F and G mission characteristics and the near-Earth and deep-space phase support plans are delineated in this article.

**S032   DSN Progress Report for January-February 1972:
Pioneer Mission Support**

A. J. Siegmeth

Technical Report 32-1526, Vol. VIII, pp. 8-15,
April 15, 1972

The previous articles on the Jupiter-bound Pioneer F and G mission support delineated the mission description and the functional planning activities of the Tracking and Data System. Beginning with the current article, an account will be given of the actual management organization and engineering planning activities which were essential to assure effective scientific data return and spacecraft control.

**S033   DSN Progress Report for March-April 1972:
Pioneer Mission Support**

A. J. Siegmeth

Technical Report 32-1526, Vol. IX, pp. 18-32,
June 15, 1972

This article reviews the status of the second-generation Pioneer missions, Pioneers 6, 7, 8, and 9; and the pre-launch and launch support of Pioneer 10, which is the first member of the third generation, whose destinations are Jupiter and beyond. This mission was identified in previous reports as Pioneer F: it was renamed Pioneer 10 after its successful launch. The planning activities for the second mission of the third generation, Pioneer G, and a summary on the fourth-generation Pioneers planned for the exploration of Venus are also presented.

**S034   DSN Progress Report for May-June 1972: Pioneer
6-9 Mission Support**

A. J. Siegmeth

Technical Report 32-1526, Vol. X, pp. 10-13,
August 15, 1972

To meet the specific scientific objectives of the Pioneer 10 and G missions, the importance of the simultaneous

support of the still-active Pioneers 6-9 has increased. The Pioneer Project requires tracks during the radial- and spiral-type configurations of the Pioneer 8, 9, and 10 missions. Fields and particles data acquired by DSN will make possible the measurement of distribution gradients. This article gives a description of the radial and spiral configurations and opportunities and the support requirements.

**S035   DSN Progress Report for May-June 1972: Pioneer
10 and G Mission Support**

A. J. Siegmeth

Technical Report 32-1526, Vol. X, pp. 27-34,
August 15, 1972

The DSN has already furnished more than four months of continuous data acquisition and command support for Pioneer 10, launched on March 3, 1972. After the description of the new DSN/Flight Project interface, a brief review of the qualitative and quantitative performance of the DSN's data recovery support is presented.

**S036   DSN Progress Report for May-June 1972: Pioneer
Venus Mission Support**

A. J. Siegmeth

Technical Report 32-1526, Vol. X, pp. 49-51,
August 15, 1972

The DSN has advanced capabilities which can be used for spaceflight missions to Venus. This article summarizes a presentation given to the Pioneer Venus study team on the ranging and S/X-band systems, which can enhance the navigational accuracy of deep-space missions.

**S037   DSN Progress Report for July-August 1972:
Pioneers 6-9 Mission Support**

A. J. Siegmeth

Technical Report 32-1526, Vol. XI, pp. 12-13,
October 15, 1972

During July and August 1972, the DSN supported a radial experiment requiring simultaneous signals of Pioneers 9 and 10. The Pioneer principal investigators plan to establish the distribution of fields and particle gradients. The DSN demonstrated a Mark III-system-type station software which can transmit Pioneers 6,7,8, and 9 telemetry data by high-speed data lines.

**S038   DSN Progress Report for July-August 1972:
Pioneers 10 and G Mission Support**

A. J. Siegmeth

Technical Report 32-1526, Vol. XI, pp. 14–18,
October 15, 1972

The DSN has already completed 6 months of continuous telemetry data acquisition, command, and radio metric tracking support for Pioneer 10, which was launched on March 4, 1972. The Pioneer 10 spacecraft, on the way to the giant planet Jupiter, crossed the orbit of Mars during the first part of May and entered the asteroid belt in the middle of July 1972. This article presents a summary of extended-mission support capabilities.

S039   DSN Progress Report for July–August 1972: Pioneer Venus Mission Support

A. J. Siegmeth

Technical Report 32-1526, Vol. XI, pp. 23–25,
October 15, 1972

This article presents a summary of the history of the Pioneer Venus missions, as well as the characteristics of the 1976/1977 probe missions. The Pioneer Project is investigating a preliminary plan to develop a cooperative agreement on the Venus Orbiter mission with the European Space Research Organization.

S040   Tracking and Data System Support for the Pioneer Project: Pioneers 6–9. Extended Missions: July 1, 1970–July 1, 1971

A. J. Siegmeth, R. E. Purdue, and R. E. Ryan

Technical Memorandum 33-426, Vol. X,
August 15, 1972

The Tracking and Data System supported the deep space phases of the Pioneer 6, 7, 8, and 9 missions, with two spacecraft in an inward trajectory and two spacecraft in an outward trajectory from the Earth in heliocentric orbits. During the period of this report, scientific instruments aboard each of the spacecraft continued to register information relating to interplanetary particles and fields, and radio metric data generated by the network continued to improve our knowledge of the celestial mechanics of the solar system. In addition to network support activity detail, network performance and special support activities are covered.

SILVER, R. H.

S041   A Study of the Frictional and Stick–Slip Behavior of Magnetic Recording Tapes

S. H. Kalfayan, R. H. Silver, and J. K. Hoffman

Technical Report 32-1548, April 1, 1972

For abstract, see Kalfayan, S. H.

S042   Studies on the Frictional Behavior of Magnetic Recording Tapes

S. H. Kalfayan, R. H. Silver, and J. K. Hoffman

JPL Quarterly Technical Review, Vol. 2, No. 1,
pp. 100–106, April 1972

For abstract, see Kalfayan, S. H.

S043   Long-Term Aging of Elastomers: Chemorheology of Viton B Fluorocarbon Elastomer

S. H. Kalfayan, R. H. Silver, A. A. Mazzeo, and
S. T. Liu

JPL Quarterly Technical Review, Vol. 2, No. 3,
pp. 32–39, October 1972

For abstract, see Kalfayan, S. H.

SIMKO, G. J.

S044   Dry-Heat Resistance of Bacillus Subtilis Var. Niger Spores on Mated Surfaces

G. J. Simko, J. D. Devlin, and M. D. Wardle

Appl. Microbiol., Vol. 22, No. 4, pp. 491–495,
October 1971

Bacillus subtilis var. *niger* spores were placed on the surfaces of test coupons manufactured from typical spacecraft materials (stainless steel, magnesium, titanium, and aluminum). These coupons were then juxtaposed at the inoculated surfaces and subjected to test pressures of 0, 1000, 5000, and 10,000 psi. Tests were conducted in ambient, nitrogen, and helium atmospheres. While under the test pressure condition, the spores were exposed to 125°C for intervals of 5, 10, 20, 50, or 80 min, with survivor data being subjected to a linear regression analysis that calculated decimal reduction times. Differences in the dry-heat resistance of the test organism resulting from pressure, atmosphere, and material were observed.

SIMMONDS, P. G.

S045   Rare Gases of the Atmosphere: Gas Chromatography Using a Thermal Conductivity Detector and a Palladium Transmodulator

J. E. Lovelock, P. G. Simmonds, and
G. R. Shoemake

Anal. Chem., Vol. 43, No. 14, pp. 1958–1961,
December 1971

For abstract, see Lovelock, J. E.

S046   Novel Type of Hydrogenator

P. G. Simmonds and C. F. Smith

Anal. Chem., Vol. 44, No. 8, pp. 1548–1550,
July 1972

This article describes the investigation of a palladium–silver tube as a catalytic reactor for the vapor phase hydrogenation of unsaturated carbon–carbon bonds in a variety of organic compounds. The device is simple to construct from an appropriate length of palladium–silver tubing and may be used for both continuous and batch hydrogenations. Furthermore, in contrast to other hydrogenation techniques, the palladium-tube device does not cause hydrogenolysis of sensitive aldehyde groups.

SIMON, H. S.

S047   DSN Progress Report for March–April 1972:
Mariner Mars 1971/Pioneer 10 Multi-Mission Level Modeling Runs Using the SFOF Mark IIIA Central Processing System Model

H. S. Simon

Technical Report 32-1526, Vol. IX, pp. 162–176,
June 15, 1972

Simulation models are currently being used for Space Flight Operations Facility (SFOF) development at JPL. This article documents the results of a series of modeling runs made during January and February 1972. The model contained a majority of the SFOF Mark IIIA central processing system capabilities required to support simultaneously the orbital phase of the Mariner Mars 1971 mission and the early cruise phase of the Pioneer 10 mission.

SIMON, M. K.

S048   On the Selection of an Optimum Design Point for Phase-Coherent Receivers Employing Band-Pass Limiters

M. K. Simon

JPL Quarterly Technical Review, Vol. 1, No. 4,
pp. 69–77, January 1972

In the design of phase-coherent receivers employing band-pass limiters, it is customary to specify system performance relative to its value at a fixed design point. For a given design point, an optimum tradeoff can be found between the power allocated to the carrier and the sideband signals. This article describes an attempt to further improve the performance of such coherent carrier systems by optimizing the design point based upon a given practical optimizing criterion. The single-channel system is treated in detail, and a brief discussion is given on how to extend the technique to a two-channel system.

S049   On the Selection of an Optimum Design Point for Phase-Coherent Receivers Employing Bandpass Limiters

M. K. Simon

IEEE Trans. Commun., Vol. COM-20, No. 2,
pp. 210–214, April 1972

In the design of phase-coherent receivers employing bandpass limiters, it is customary to specify system performance relative to its value at a fixed design point. For a given design point, it is well known that an optimum tradeoff can be found between the power allocated to the carrier and sideband signals. This paper describes an attempt to further improve the performance of such coherent carrier systems by optimizing the design point based upon a given practical optimization criterion. The single-channel system is treated in detail and a brief discussion is given on how to extend the optimization technique to a two-channel system.

S050   On the Selection of a Sampling Filter Bandwidth for a Digital Data Detector

M. K. Simon

IEEE Trans. Commun., Vol. COM-20, No. 3,
pp. 438–441, June 1972

This article discusses the problem of selecting the low-pass sampling bandwidth for a digital mechanization of a matched-filter bit-synchronizer combination. In particular, if digital data at a rate R bits/s plus gaussian noise is passed through a filter of bandwidth KR and then sampled at the Nyquist rate, i.e., $2KR$, then how small can K be without paying an appreciable penalty in the signal-to-noise ratio performance of the data detector?

S051   Carrier Synchronization and Detection of Polyphase Signals

W. C. Lindsey (University of Southern California)
and M. K. Simon

IEEE Trans. Commun., Vol. COM-20, No. 3,
pp. 441–454, June 1972

For abstract, see Lindsey, W. C.

SIMON, W.

S052   Plume Backscatter Measurements Using Quartz Crystal Microbalances in JPL Molsink (Molecular Sink)

W. Simon

Technical Memorandum 33-540, May 15, 1972

Recent tests in the JPL Molsink facility have provided the first quantitative evidence of gas flows in the far

upstream region of small nozzles with large boundary layer flow. Gas-mass fluxes were measured using quartz-crystal microbalances. Both nitrogen and carbon dioxide were used as test gases. Gas deposition rates on the order of 100 monolayers per min were detected 13 in. upstream from the nozzle exit plane. It is significant to note that the crystals detected gases considerably beyond the Prandtl–Meyer turning angle. Tests are being continued using improved cryogenic, quartz-crystal systems and additional types of gases. The data from these tests will be essential in the formulation of scaling laws and analytical prediction methods for viscous plume behavior.

S053 Nozzle Exhaust Plume Backscatter Experiment Using the JPL Molsink Facility

W. Simon

JPL Quarterly Technical Review, Vol. 1, No. 4, pp. 89–96, January 1972

The flow field of gases and scattered particulates in the forward direction from a rocket nozzle is not presently predictable on a quantitative basis. Qualitative tests have been made with water injected through the nozzle wall and the droplet trajectories observed photographically. These tests were conducted for nozzles where the boundary layer is a significant portion of the flow. The tests indicated that both gases and particulate matter will be found in the region outside of the plume boundaries that can be calculated using current analytical techniques. A test program is being conducted in the JPL Molsink facility to measure the distribution of exhaust gases from small nozzles using an electron beam/photomultiplier system and a matrix of quartz crystal microbalances. Analysis of data from these tests, using nitrogen, will result in a better understanding of the backscattering flow field. Calibration tests of the Molsink, using simulated hydrazine exhaust product gas mixtures, have also been conducted, and future tests with small hydrazine thrusters are being considered. The test program and results of the pumping calibration tests with hydrazine (simulated hydrazine exhaust products) are reported.

S054 Small Rocket Exhaust Plume Data

J. E. Chirivella, P. I. Moynihan, and W. Simon

JPL Quarterly Technical Review, Vol. 2, No. 2, pp. 90–99, July 1972

For abstract, see Chirivella, J. E.

SINCLAIR, W. S.

S055 Simultaneous Solution for the Masses of the Principal Planets From Analysis of Optical, Radar, and Radio Tracking Data

J. H. Lieske, W. G. Melbourne, D. A. O'Handley, D. B. Holdridge, D. E. Johnson, and W. S. Sinclair

Celest. Mech., Vol. 4, No. 2, pp. 233–245, October 1971

For abstract, see Lieske, J. H.

SJOGREN, W. L.

S056 A Surface-Layer Representation of the Lunar Gravitational Field

L. Wong (Aerospace Corporation), G. Buechler (Aerospace Corporation), W. Downs (Aerospace Corporation), W. L. Sjogren, P. M. Muller, and P. Gottlieb

J. Geophys. Res., Vol. 76, No. 26, pp. 6220–6236, September 10, 1971

For abstract, see Wong, L.

S057 Lunar Gravity Estimate: Independent Confirmation

W. L. Sjogren

J. Geophys. Res., Vol. 76, No. 29, pp. 7021–7026, October 10, 1971

Reduction of 2½ days of Lunar Orbiter 4 radio tracking data has provided an independent estimate of the low-degree spherical harmonic coefficients in the lunar potential model. The estimate is in good agreement with previous results and confirms that the Moon is essentially homogeneous. These doppler data, never incorporated in other gravity estimates, were obtained at relatively high spacecraft altitudes (2700–6000 km). These high-altitude data allowed the model to fit to the noise level of 1 mm/s unlike previous results, where systematic residuals of tens of millimeters per second occurred, owing to local gravity anomalies detectable at low spacecraft altitudes (≈ 100 km).

S058 Apollo 15 Gravity Analysis From the S-Band Transponder Experiment

W. L. Sjogren, P. M. Muller, and W. R. Wollenhaupt (Manned Spaceflight Center)

Proceedings of the Conference on Lunar Geophysics, Lunar Science Institute, Houston, Texas, October 18–21, 1971, pp. 411–418

The S-band transponder experiment used precision doppler tracking data of the command and service module, the lunar module and the subsatellite to provide detailed information about the near-side lunar gravity field. No special instruments are required other than the existing S-band transponder used for real-time navigation. The data consists of variations in the spacecraft speed as

measured by the Earth-based radio tracking system, which has a resolution of 0.65 mm/s.

Initial data reduction, which has been concentrated on the low altitude ($\approx$20 km) command and service module data, provides new detailed gravity profiles of the Serenitatis and Crisium mascons. The results are in good agreement with Apollo 14 analysis and strongly suggest that the mascons are near-surface features with a mass distribution per unit area of approximately 800 kg/cm^2. The Apennines reveal themselves as a local gravity high of 85 mgal and Marius Hill likewise have a gravity high of 62 mgal.

The subsatellite data is too sparse at present to definitely determine new gravity-anomaly locations. The spacecraft is functioning well and a dense data block is being obtained, which will provide a new gravity map from ±95° longitude to ±30° latitude. Since periapsis altitudes are relatively close to predicted altitudes, it seems fairly safe at this point to believe the subsatellite lifetime will be at least one yr.

S059 Lunar Gravity via Apollo 14 Doppler Radio Tracking

W. L. Sjogren, P. Gottlieb, P. M. Muller, and
W. Wollenhaupt (Manned Spacecraft Center)

Science, Vol. 175, No. 4018, pp. 165–168,
January 14, 1972

Gravity measurements at high resolution were obtained over a 100-km band from 70 to –70 deg of longitude during the orbits of low periapsis altitude (approximately 16 km). The line-of-sight accelerations are plotted on Aeronautical Chart and Information Center mercator charts (scale 1:1,000,000) as contours at 10-mgal intervals. Direct correlations between gravity variations and surface features are easily determined. Theophilus, Hipparchus, and Ptolemaeus are negative features, whereas Mare Nectaris is a large positive region. The acceleration profiles over Mare Nectaris are suggestive of a broad disk near the surface rather than a deeply buried spherical body. These data are in good agreement with the short arc of Apollo 12 lunar module descent data.

S060 Mariner 9 Celestial Mechanics Experiment: Gravity Field and Pole Direction of Mars

J. Lorell, G. H. Born, E. J. Christensen,
J. F. Jordan, P. A. Laing, W. Martin,
W. L. Sjogren, I. I. Shapiro (Massachusetts
Institute of Technology),
R. D. Reasenberg (Massachusetts Institute of
Technology), and G. L. Slater (Massachusetts
Institute of Technology)

Science, Vol. 175, No. 4019, pp. 317–320,
January 21, 1972

For abstract, see Lorell, J.

SLADE, M. A.

S061 DSN Progress Report for September–October 1972: Very Long Baseline Interferometry (VLBI) Possibilities for Lunar Study

M. A. Slade, P. F. MacDoran, and J. B. Thomas

Technical Report 32-1526, Vol. XII, pp. 35–39,
December 15, 1972

The availability of several channels for transmissions from the lunar surface and lunar-orbiting vehicles presents opportunities for demonstrating the utility of radio-interferometric tracking. The expected accuracy of such very-long-baseline-interferometry (VLBI) tracking is expected to be equivalent to 50 cm (transverse to the line of sight) at the moon's distance, affording significant opportunities for studies of lunar dynamics and selenodesy. In addition to direct applicability to lunar study, VLBI tracking of these several lunar-based signals provides an opportunity to evaluate simultaneous multiprobe tracking techniques which could significantly enhance the Viking 1975 and Pioneer Venus 1977 missions, where multiprobe tracking is imperative.

SLATER, G. L.

S062 Mariner 9 Celestial Mechanics Experiment: Gravity Field and Pole Direction of Mars

J. Lorell, G. H. Born, E. J. Christensen,
J. F. Jordan, P. A. Laing, W. Martin,
W. L. Sjogren, I. I. Shapiro (Massachusetts
Institute of Technology),
R. D. Reasenberg (Massachusetts Institute of
Technology), and G. L. Slater (Massachusetts
Institute of Technology)

Science, Vol. 175, No. 4019, pp. 317–320,
January 21, 1972

For abstract, see Lorell, J.

SLAUGHTER, D. W.

S063 DSN Progress Report for November–December 1971: Hi-Rel Integrated Circuit Packaging Development

D. W. Slaughter

Technical Report 32-1526, Vol. VII, pp. 113–123,
February 15, 1972

Standardized modular hardware for the packaging of Deep Space Instrumentation Facility integrated circuit logic systems is described. The status of development is reported, and a schedule is given for the production of station-quality hardware.

SLEKYS, A.

S064 DSN Progress Report for March–April 1972: Predetection Recording and Dropouts

A. Slekys

Technical Report 32-1526, Vol. IX, pp. 115–118, June 15, 1972

Predetection recording of spacecraft telemetry data allows possible future analysis of data records in the event of failures of transmitted signals. Dropouts occurring in the playback process necessarily cause loss of information and, more importantly, loss of time synchronization with the remaining data. The object of this study is to show that, with proper digital handling of a timing signal initially recorded along with telemetry data, using a device incorporating a proposed digital dropout detector, time synchronization can be maintained throughout dropouts of lengths less than 100 ms, within some small probability of error. Uses extend to recording of planetary-entry low-rate and very-long-baseline interferometry data and, in particular, to planetary radio-occultation information, which is already recorded with a timing signal on the same tape track.

SMITH, B. A.

S065 Mariner 9 Science Experiments: Preliminary Results

R. H. Steinbacher, A. J. Kliore, J. Lorell, H. Hipsher (National Aeronautics and Space Administration), C. A. Barth (University of Colorado), H. Masursky (U.S. Geological Survey), G. Münch (California Institute of Technology), J. C. Pearl (Goddard Space Flight Center), and B. A. Smith (New Mexico State University)

Science, Vol. 175, No. 4019, pp. 293–294, January 21, 1972

For abstract, see Steinbacher, R. H.

SMITH, C. F.

S066 Novel Type of Hydrogenator

P. G. Simmonds and C. F. Smith

Anal. Chem., Vol. 44, No. 8, pp. 1548–1550, July 1972

For abstract, see Simmonds, P. G.

SMITH, J. G.

S067 Bias and Spread in Extreme Value Theory Measurements of Probability of Error

J. G. Smith

JPL Quarterly Technical Review, Vol. 1, No. 4, pp. 58–68, January 1972

Performance tests of communication systems characterized by low bit rates and high data reliability requirements frequently utilize classical extreme value theory (EVT) to avoid the excessive test times required by bit error rate (BER) tests. If the underlying noise is gaussian or perturbed gaussian, EVT will produce results either biased or with excessive spread if an insufficient number of test samples are used. This article examines EVT to explain the cause of the bias and spread, gives experimental verification, and points out procedures that minimize these effects. Even under these conditions, however, EVT test results are not particularly more significant than BER test results.

SMITH, R. H.

S068 DSN Progress Report for March–April 1972: 10-W S-Band Amplifier

R. H. Smith

Technical Report 32-1526, Vol. IX, pp. 196–200, June 15, 1972

A more powerful S-band amplifier was needed to drive the high-power transmitters of the DSN. Two types of 10-W solid-state amplifiers with 23-dB gain, operating at 2115 MHz for the DSN 400-kW transmitter and 2388 MHz for the 450-kW research-and-development transmitter, were developed.

S069 DSN Progress Report for September–October 1972: Dual Carrier

R. H. Smith

Technical Report 32-1526, Vol. XII, pp. 200–204, December 15, 1972

Two simultaneous (dual) uplink carriers from a single DSN 64-m-diameter antenna site are required to support the Viking 1975 project. A prototype dual-carrier exciter has been built and tested. The dual-carrier exciter amplifies and combines two standard DSN exciter signals, which are used to drive a high-power klystron operating in a linear mode (10% of normal power). The measured intermodulation products were at least 20 dB below the carrier's power.

SOHA, J. M.

S070 An Orthographic Photomap of the South Pole of Mars From Mariners 6 and 7

A. R. Gillespie and J. M. Soha

Icarus, Vol. 16, No. 3, pp. 522–527, June 1972

For abstract, see Gillespie, A. R.

SOMOANO, R. B.

S071 Superconductivity in the Alkali Metal Intercalates of Molybdenum Disulphide

R. B. Somoano, V. Hadek, and A. Rembaum

JPL Quarterly Technical Review, Vol. 2, No. 2, pp. 83–89, July 1972

The complete series of alkali metals, lithium through cesium, has been intercalated into molybdenum disulphide, using both the liquid-ammonia and vapor techniques. All the intercalates, with the exception of lithium, yielded full superconducting transitions with onset temperatures of 6 K for A_xMoS_2 $(A_x = $ K,Rb,Cs$)$ and 4 K for B_xMoS_2 $(B_x = $ Li,Na$)$. The superconducting transition for lithium was incomplete down to 1.5 K. Stoichiometries and unit-cell parameters have been determined for the intercalation compounds. Both rhombohedral and hexagonal polymorphs of MoS_2 have been intercalated and found to exhibit the same superconductivity behavior. The nature of the extraneous superconducting transition of some intercalated samples on exposure to air was elucidated.

SOTTER, J. G.

S072 Liquid-Phase Mixing of Bipropellant Doublets

F. W. Hoehn, J. H. Rupe, and J. G. Sotter

Technical Report 32-1546, February 15, 1972

For abstract, see Hoehn, F. W.

SRIDHAR, R.

S073 Analytical Methods for Performance Evaluation of Nonlinear Filters

A. K. Bejczy and R. Sridhar (University of California, Los Angeles)

J. Math. Anal. Appl., Vol. 36, No. 3, pp. 477–505, December 1971

For abstract, see Bejczy, A. K.

S074 Approximate Nonlinear Filters and Deterministic Filter Gains

A. K. Bejczy and R. Sridhar (University of California, Los Angeles)

Trans. ASME, Ser. G: J. Dynam. Sys., Meas., Contr., Vol. 94, No. 1, pp. 57–63, March 1972

For abstract, see Bejczy, A. K.

STEARNS, J. W.

S075 Elements of Cost Comparison for Planetary Missions With Advanced Propulsion

J. W. Stearns

Technical Memorandum 33-553, July 1, 1972

Cost and performance comparisons are made between chemical propulsion and nuclear–electric propulsion for planetary missions to Jupiter and beyond. Nuclear rocket comparisons are made for performance only. Titan, Saturn, and Space Shuttle launches, utilizing advanced propulsion upper stages, are evaluated. Appendixes include a performance analysis of multiple Shuttle launches with assembly in Earth orbit and a discussion of nonrecurring costs.

STEIN, C. K.

S076 DSN Progress Report for May–June 1972: DSN System Testing: A Critical Review of the Pioneer 10 Test Program

C. K. Stein

Technical Report 32-1526, Vol. X, pp. 207–209, August 15, 1972

The Pioneer 10 test program was unique since the majority of DSN testing was conducted during the Mariner 9 encounter and orbiting. The importance of both programs to the NASA effort required special emphasis to assure that successful programs can be supported simultaneously. This critique lists the major problems encountered and the solutions used for a successful Pioneer 10 launch, while fully supporting all Mariner Mars 1971 requirements.

STEINBACHER, R. H.

S077 Mariner 9 Science Experiments: Preliminary Results

R. H. Steinbacher, A. J. Kliore, J. Lorell, H. Hipsher (National Aeronautics and Space Administration), C. A. Barth (University of Colorado), H. Masursky (U.S. Geological Survey), G. Münch (California Institute of Technology), J. C. Pearl (Goddard Space Flight Center), and B. A. Smith (New Mexico State University)

To form the science payload for the Mariner 9 spacecraft, NASA selected six experiments: television, infrared spectroscopy, infrared radiometry, ultraviolet spectrometer, S-band occultation, and celestial mechanics. This article presents a brief summary of results from these experiments, obtained during the first 30 days after orbit insertion.

STELZRIED, C. T.

S078 DSN Progress Report for September–October 1972: Improved RF Calibration Techniques: Commercial Precision IF Attenuator Evaluation

C. T. Stelzried, B. L. Seidel, M. Franco, and D. Acheson

The intermediate frequency (IF) attenuator normally used for system-noise temperature calibrations is the largest single contributor to measurement inaccuracy. Various IF attenuators have been evaluated and calibrated using a National Bureau of Standards IF precision standard. This article describes the measurement techniques used and presents measurement results. It is noted that there is a wide spread in accuracy among various manufacturers and also in the same model type from a particular manufacturer. Excessive use appears to be an important factor in accuracy degradation.

S079 Jupiter: New Evidence of Long-Term Variations of Its Decimeter Flux Density

M. J. Klein, S. Gulkis, and C. T. Stelzried

For abstract, see Klein, M. J.

S080 A Precision Compact Rotary Vane Attenuator

T. Y. Otoshi and C. T. Stelzried

For abstract, see Otoshi, T. Y.

S081 Transformation of Received Signal Polarization Angle to the Plane of the Ecliptic

C. T. Stelzried, T. Sato, and A. Abreu

The solar occultation of the Pioneer 6 spacecraft in November 1968 provided the first opportunity to measure the polarization rotation of a continuous-wave signal in the solar corona. The received signal polarization angle measured with the JPL 64-m Mars Deep Space Station azimuth–elevation mount antenna was transformed to the plane of the ecliptic. The derivation of the equations required for this transformation is presented.

S082 Operating Noise-Temperature Calibrations of Low-Noise Receiving Systems

C. T. Stelzried

A technique has been developed for calibrating the operating noise-temperature of low-noise Earth station receiving systems. The technique, which consists of switching the maser input between the antenna and a microwave ambient termination, has been used on several antenna/cone configurations for the JPL/NASA Deep Space Communications System. Extensive operational measurement data are presented for the period July 1966 to March 1968. The details of the calibration technique, error analysis, and programming are presented. For a receiving system with 30-K total operating noise temperature, the total probable error (dispersion and bias) is approximately 0.30 K.

STEWART, A. I.

S083 Mariner 9 Ultraviolet Spectrometer Experiment: Initial Results

C. A. Barth (University of Colorado),
C. W. Hord (University of Colorado),
A. I. Stewart (University of Colorado), and
A. L. Lane

For abstract, see Barth, C. A.

STICKFORD, G. H., JR.

S084 Detailed Measurements of the Hβ Line Shape in a Transient Plasma Using a Fiber Optics Slit System

G. H. Stickford, Jr.

Preprint 72-106,
AIAA Tenth Aerospace Sciences Meeting,
San Diego, California, January 17–19, 1972

Through the use of fiber optics, a series of very narrow slits have been constructed and placed at the exit plane of a spectrograph. Plasma radiation which is dispersed by the spectrograph is incident on the slits and is transmitted to separate phototubes via the quartz fibers. With this technique, time resolved measurements of the spectral shape of the hydrogen $H\beta$ line have been made and used to determine the electron density of a transient plasma. Data obtained in a shock tube indicated that the thermodynamic conditions behind the reflected shock in a mixture of 20% H_2 and 80% He, at incident shock speeds of 12 to 14 km/s and pressures of 66.6 to 133.3 N/m^2 (0.5 to 1.0 mm Hg), correspond to theoretically predicted conditions. Immediately behind the incident shock at speeds of 17 to 24 km/s the data indicate that the plasma reached equilibrium and then demonstrated a drop in intensity which has been attributed to radiative cooling.

S085 Total Radiative Intensity Calculations for 100% H_2 and 87% H_2–13% He

G. H. Stickford, Jr.

J. Quant. Spectrosc. Radiat. Transfer, Vol. 12, No. 4, pp. 525–529, April 1972

Isothermal radiative intensity calculations for 100% H_2 and 87% H_2–13% He are presented for temperatures of 10,000–25,000°K, density ratios of 10^{-4}–10^{-1}, and path lengths of 1.0–30.0 cm. The actual spectral details of the absorption coefficient were computed for 16,000 points from 240 to 30,000 Å by summing the various line and continuum radiative processes at each point. This method should result in a very accurate calculation of radiative emission, including an accurate accounting for re-absorption due to overlapping lines.

STINNETT, W. G.

S086 DSN Progress Report for May–June 1972: DSN Command System Performance Evaluation

W. G. Stinnett

Technical Report 32-1526, Vol. X, pp. 213–216, August 15, 1972

This article presents a general performance description of the DSN Command System as configured for support of the Mariner Mars 1971 and Pioneer 10 missions. Included are statistics related to system reliability and availability. A comparison of command activity is presented for previous Mariner- and Pioneer-type missions.

STIRN, R. J.

S087 Junction Characteristics of Silicon Solar Cells: Nonilluminated Case

R. J. Stirn

Technical Memorandum 33-557, Pt. I, August 15, 1972

This report presents precise values of the reverse saturation currents in 2- and 10-Ω-cm silicon solar cells and magnitudes of the diffusion and recombination components. The recombination current as well as leakage current due to shunting are shown to be nonuniform across the cell. The diffusion lengths calculated from the diffusion current components agree well with diffusion lengths measured independently in similar material. Models are presented demonstrating the effect of recombination and shunting currents on the dark current–voltage characteristics of solar cells.

S088 Comment on "Temperature Dependence of Hole Velocity in p GaAs"

R. J. Stirn

J. Appl. Phys., Vol. 43, No. 5, pp. 2484–2485, May 1972

A comparison of magnetoresistance mobility values and their temperature dependence with theoretical values of the conductivity mobility was made in a recent publication. In this article, reasons are discussed as to why such a comparison is unwarranted, particularly when multiple-carrier conduction is present.

STIVER, R. A.

S089 DSN Progress Report for November–December 1971: Mark IIIA IBM Computer Configuration Expansion

R. A. Stiver

Technical Report 32-1526, Vol. VII, pp. 126–130, February 15, 1972

In order to meet Pioneer Project requirements while continuing to support the Mariner Mars 1971 mission, it has been necessary to expand the Space Flight Operations Facility computer configuration. This expansion has been implemented in the following areas: high-speed data input/output interface, display control and switching, subchannel extension and user device switching, and magnetic tape drives. Expansion was accomplished with minimum impact on operating system design.

STRAND, L. D.

S090 Determination of Solid-Propellant Transient Regression Rates Using a Microwave Doppler Shift Technique

L. D. Strand, A. L. Schultz, and G. K. Reedy

Technical Report 32-1569, October 15, 1972

A microwave doppler-shift system, with increased resolution over earlier microwave techniques, was developed for the purpose of measuring the regression rates of solid propellants during rapid pressure transients (10^4–10^5 N/cm^2-s). A continuous microwave beam is transmitted to the base of a burning propellant sample cast in a metal waveguide tube. A portion of the wave is reflected from the regressing propellant-flame-zone interface. The phase-angle difference between the incident and reflected signals and its time differential are continuously measured using a high-resolution microwave network analyzer and related instrumentation. The apparent propellant regression rate is directly proportional to this latter differential measurement.

Experiments were conducted to verify the (1) spatial and time resolution of the system, (2) effect of propellant surface irregularities and compressibility on the measurements, and (3) accuracy of the system for quasi-steady-state regression-rate measurements. The microwave system was also used in two different transient combustion experiments: in a rapid-depressurization bomb, and in the high-frequency acoustic pressure environment of a T-burner. Polyether-polyurethane, hydroxy-terminated polybutadiene, and carboxyl-terminated polybutadiene/ammonium perchlorate composite propellants were tested.

In the rapid-depressurization tests the measured apparent regression rates generally fell near or below the steady-state rate at the corresponding pressure and exhibited oscillations in tests near the critical depressurization rates for extinguishment. The results seem to reinforce the description of rapid-depressurization extinction presented by Steinz and Selzer. Comparisons with the only other known transient data, that of Yin and Hermance, yielded both points of agreement and disagreement.

Unreasonably high oscillatory regression rates were obtained in the T-burner experiments. A set of parametric calculations were carried out, the results of which predict that flame-ionization effects could be of sufficient magnitude to account for these high-response results.

A direct comparison of the analytical predictions and experimental results yielded the conclusion that flame-ionization effects probably produced some errors in the absolute values, but not the general characteristics, of the rapid-depressurization regression-rate measurements.

S091 Initiation System for Low Thrust Motor Igniter

L. D. Strand, D. P. Davis, and J. I. Shafer

Technical Memorandum 33-520, January 1, 1972

A test program was carried out to demonstrate an igniter motor initiation system utilizing the bimetallic material Pyrofuze (trademark of Pyrofuze Corporation) for a solid-propellant rocket with controlled low rate of thrust buildup. The program consisted of a series of vacuum ignition tests using a slab burning window motor that simulated the principal initial ballistic parameters of the full-scale igniter motor. A Pyrofuze/pyrotechnic igniter system was demonstrated that uses a relatively low electrical current level for initiation and that eliminates the necessity of a pyrotechnic squib, with its accompanying accidental firing hazards and the typical basket of pyrotechnic pellets. The Pyrofuze ignition system does require an initial constraining of the igniter motor nozzle flow, and, at the low initiating electrical current level, the ignition delay time of this system was found to be quite sensitive to factors affecting the local heat generation or loss rates.

S092 Dynamic Measurement of Bulk Modulus of Dielectric Materials Using a Microwave Phase Shift Technique

B. J. Barker and L. D. Strand

Technical Memorandum 33-577, November 15, 1972

For abstract, see Barker, B. J.

SWANSON, J.

S093 Accelerated Life Testing of Spacecraft Subsystems

D. Wiksten and J. Swanson

Technical Memorandum 33-575, November 1, 1972

For abstract, see Wiksten, D.

SWARD, A.

S094 Measurement of the Power Spectral Density of Phase of the Hydrogen Maser

A. Sward

JPL Quarterly Technical Review, Vol. 1, No. 4, pp. 30–33, January 1972

Hydrogen masers are being developed by JPL to satisfy the needs of the Deep Space Network for improved frequency standards in order to achieve better timing accuracies, reduced doppler residuals, and lower phase noise in the tracking system. Performance data for the JPL hydrogen masers are given in two forms: time-domain performance, useful for analyzing time-keeping systems and doppler systems; and frequency-domain per-

formance, useful for analyzing tracking systems. Particular attention is given to frequency-domain performance, as obtained from both time-domain measurements and direct measurements.

SZEJN, R. M.

S095 Theoretical Determination of Cesiated Work Functions

R. M. Szejn

Technical Memorandum 33-565,
September 15, 1972

A computer program based on the theoretical work of Gyftopoulos, Steiner, and Levine on bimetallic systems and using a modified version of Wilkins' SIMCON subroutine SURFAS has been written for the UNIVAC 1108 computer. This program, WFGSL, accepts the operating conditions and the physical parameters pertinent to the substrate and adsorbate and outputs the field-free work function, electron current (Richardson equation), ion current (Saha equation), and fractional substrate coverage by the adsorbate. This memorandum presents a brief description of the theory together with a program description and listing. An application of the program to a bimetallic system of cesium (adsorbate) and rhenium (substrate) is also described.

TAHERZADEH, M.

T001 Neutron Radiation Characteristics of Plutonium Dioxide Fuel

M. Taherzadeh

Technical Report 32-1555, June 1, 1972

The major sources of neutrons from plutonium-dioxide nuclear fuel are considered in detail. These sources include spontaneous fission of several Pu isotopes, (α,n) reactions with low Z impurities in the fuel, and (α,n) reactions with ^{18}O. For spontaneous fission neutrons, a neutron emission rate of $(1.95 \pm 0.07) \times 10^3$ n/s/g PuO_2 is obtained.

The neutron yield from (α,n) reactions with oxygen is calculated by integrating the reaction rate equation over all α-particle energies and all center-of-mass angles. The results indicate a neutron emission rate of $(1.14 \pm 0.26) \times 10^4$ n/s/g PuO_2.

The neutron yield from (α,n) reactions with low Z impurities in the fuel is presented in tabular form for one part per million of each impurity. The total neutron yield due to the combined effects of all the impurities depends upon the fractional weight concentration of each impurity. The total neutron flux emitted from a particular fuel

geometry is estimated by adding the neutron yield due to the induced fission to that of the other neutron sources.

T002 Neutron Radiation Characteristics of Plutonium Dioxide Fuel

M. Taherzadeh

Technical Report 32-1555, Rev. 1,
December 1, 1972

This report considers in detail the major sources of neutrons from plutonium-dioxide nuclear fuel. These sources include spontaneous fission of several of the Pu isotopes, (α,n) reactions with low-Z impurities in the fuel, and (α,n) reactions with oxygen 18. For spontaneous fission neutrons, a value of $(1.95 \pm 0.07) \times 10^3$ n/s/g PuO_2 is obtained. The neutron yield from (α,n) reactions with oxygen is calculated by integrating the reaction-rate equation over all α-particle energies and all center-of-mass angles. The results indicate a neutron emission rate of $(1.42 \pm 0.32) \times 10^4$ n/s/g PuO_2.

The neutron yield from (α,n) reactions with low-Z impurities in the fuel is presented in tabular form for one part per million of each impurity. The total neutron yield due to the combined effects of all the impurities depends upon the fractional weight concentration of each impurity. The total neutron flux emitted from a particular fuel geometry is estimated by adding the neutron yield due to the induced fission to that of the other neutron sources.

T003 The Response of a 0.03-cm Silicon Detector to a Mixed Neutron and Gamma Field as a Function of Shield Material and Thickness

M. Taherzadeh

JPL Quarterly Technical Review, Vol. 2, No. 2, pp. 25–41, July 1972

The neutron and gamma radiation from a multi-hundred-watt radioisotope thermoelectric generator was used to evaluate the total response of a shielded 0.3-mm silicon detector. The generator employs a 2200-W(th) PuO_2 heat source concept known as the Helipak. The total integrated neutron and gamma ray fluxes at 100 cm away from the source along the radial direction were 1.67 × 10^3 n/cm²/s and 1.49 × 10^4 γ/cm²/s, respectively. Experimental values of the response function of the shielded silicon detector were used to determine the total counting rates due to photons at bias energies ranging from 50 to 200 keV. For neutrons, analytically computed response functions were used to determine the total counting rates at the same bias energies.

It was found that for an aluminum shield the neutrons are not significant, regardless of the thickness of the shield. However, the magnitude of the total counting rate due to neutrons increases with increased atomic number of the shield and becomes comparable to the

counting rate due to photons for a platinum-shield thickness of 5 cm.

T004 Neutron Radiation Characteristics of Plutonium Dioxide Fuel

M. Taherzadeh and P. J. Gingo (Akron State University)

Nucl. Technol., Vol. 15, No. 3, pp. 396–410, September 1972

The major sources of neutrons from plutonium-dioxide nuclear fuel are considered in detail. These sources include spontaneous fission of several of the plutonium isotopes, (α,n) reactions with low Z impurities in the fuel, and (α,n) reactions with oxygen 18. For spontaneous fission neutrons a value of $(1.95 \pm 0.07) \times 10^3$ n/s/g PuO_2 is used.

The neutron yield from (α,n) reactions with oxygen is calculated by integrating the reaction rate equation over all alpha-particle energies and all center-of-mass angles. The results indicate a neutron emission rate of $(1.14 \pm 0.26) \times 10^4$ n/s/g PuO_2.

The neutron yield from (α,n) reactions with low Z impurities in the fuel is presented in tabular form for 1 part per million of each impurity. The total neutron yield due to the combined effects of all the impurities depends on the fractional weight concentration of each impurity. The total neutron flux emitted from a particular fuel geometry is estimated by adding the neutron yield due to the induced fission to that of the other neutron sources.

TAUSWORTHE, R. C.

T005 Convergence of Oscillator Spectral Estimators for Counted-Frequency Measurements

R. C. Tausworthe

IEEE Trans. Commun., Vol. COM-20, No. 2, pp. 214–217, April 1972

A common intermediary connecting frequency-noise calibration or testing of an oscillator to useful applications is the spectral density of the frequency-deviating process. In attempting to turn test data into predicts of performance characteristics, one is naturally led to estimation of statistical values by sample-mean and sample-variance techniques. However, sample means and sample variances themselves are statistical quantities that do not necessarily converge (in the mean-square sense) to actual ensemble-average means and variances, except perhaps for excessively large sample sizes. This is especially true for the flicker noise component of oscillators. This article shows, for the various types of noises found in oscillators, how sample averages converge (or do not converge) to their statistical counterparts. The convergence rate is

shown to be the same for all oscillators of a given spectral type.

T006 Simplified Formula for Mean Cycle-Slip Time of Phase-Locked Loops With Steady-State Phase Error

R. C. Tausworthe

IEEE Trans. Commun., Vol. COM-20, No. 3, pp. 331–337, June 1972

Previous work has shown that the mean time from lock to a slipped cycle of a phase-locked loop is given by a certain double integral. Accurate numerical evaluation of this formula for the second-order loop has proved extremely vexing because the difference between exponentially large quantities is involved. This article simplifies the general formula to avert this problem, provides a useful approximation to a needed conditional expectation, and produces an asymptotic formula for the mean slip time that is moderately accurate even at low loop signal-to-noise ratios (less than 7 dB) and small steady-state phase errors (less than 0.3 rad). The approximations extend to higher order loops as well.

TAYLOR, D. M.

T007 A Re-evaluation of Material Effects on Microbial Release From Solids

D. M. Taylor, S. J. Fraser (The Boeing Company), E. A. Gustan (The Boeing Company), R. L. Olson (The Boeing Company), and R. H. Green

Life Sciences and Space Research X, pp. 23–28, Akademie-Verlag, Berlin, 1972

A previous report concerned with the percentage of microbial release from the interior of solid materials after hard impact, raised questions about the possibility that dissimilar materials might have different release properties. Therefore additional studies were conducted to obtain information on the release of micro-organisms from different solid materials impacted onto two types of surfaces. The combined study was performed by inoculating 10^4 *Bacillus subtilis* var. *niger* spores into Eccobond and methyl methacrylate. These materials were then machined into projectiles and fired from guns into stainless steel plates or sand at velocities ranging from 168 to 1554 m-s^{-1}. Bacteriological examination of the fractured particles was conducted to establish the number of viable spores released from the interior of the projectiles.

Analysis of the results from two solid materials, two impact surfaces and four velocities showed that the number of micro-organisms released is less than 1% in all cases. However, statistical evaluation of all data demonstrates a significant difference in percentage microbial

release between materials. Since significant differences were observed between materials, broad extrapolations of percentage release data should be avoided until release characteristics of different classes of spacecraft solid materials have been determined.

TAYLOR, F. J.

T008   Telecommunications System Design for the Mariner Mars 1971 Spacecraft

F. J. Taylor and G. W. Garrison

Technical Memorandum 33-535, May 1, 1972

The configuration of the Mariner Mars 1971 spacecraft telecommunications system is detailed, with particular attention to modifications performed to accommodate the orbital mission. This memorandum describes the analysis and planning prior to launch. Results of major analyses and tests are summarized.

TAYLOR, F. W.

T009   Temperature Sounding Experiments for the Jovian Planets

F. W. Taylor

J. Atmos. Sci., Vol. 29, No. 5, pp. 950–958, July 1972

The possibilities for vertical temperature sounding experiments by medium-resolution measurements of outgoing radiance are examined for non-scattering models of Jupiter, Saturn, Uranus, and Neptune. It is shown that for Jupiter the widest vertical coverage of the atmosphere results from five or six channels placed in the ν_4 band of methane at 7.5 μm, but energy constraints render this experiment marginal at Saturn and useless at Uranus and Neptune. For the outermost planets, the best experiment is three or four channels located in the long-wavelength half of the pressure-induced S(O) line of hydrogen in the range 25–40 μm with which a limited vertical range of about two scale heights can be covered. Some results of inversion of synthetic data are presented in each case, and the likely effect of clouds on the measurements is discussed.

T010   Methods and Approximations for the Computation of Transmission Profiles in the ν_4 Band of Methane in the Atmosphere of Jupiter

F. W. Taylor

J. Quant. Spectrosc. Radiat. Transfer, Vol. 12, No. 7, pp. 1151–1156, July 1972

This article discusses the validity of certain band models and scaling approximations for computing transmissions

in the ν_4 band of methane along inhomogeneous paths in the atmosphere of Jupiter. It is shown that Goody's random band model approximates the results of a rigorous numerical line-by-line calculation of the transmission profile of a Jovian model atmosphere.

T011   The Infrared Spectrum of Jupiter: Structure and Radiative Properties of the Clouds

F. W. Taylor and G. E. Hunt

Proceedings of the Conference on Atmospheric Radiation, Fort Collins, Colorado, August 7–9, 1972, pp. 100–102

The interpretation of ground-based observations of Jupiter in terms of the composition and structure of the atmosphere is greatly complicated by clouds and haze which appear to extensively cover the planet. Most observers and theoreticians have attempted to take account of absorption and scattering by clouds in their calculations by simple modeling, but it has been usual to ignore the horizontal and vertical inhomogeneous which are apparently present in the cloud structure. This is a serious shortcoming in models which are used to plan experiments to be carried by spacecraft, when high spatial resolution will be available.

No useful way to approximate the radiative transfer properties of the Jovian clouds at thermal infrared wavelengths has been proposed, except for the dangerous expedient of neglecting cloud effects entirely. As a result, thermal equilibrium models of the planet and temperature structure and composition determinations based on emission measurements will be in error by some unknown amount.

This paper describes a model for the Jovian clouds which is inhomogeneous both vertically and laterally and presents radiative transfer calculations which include cloud effects to show that the model can account for the available observations at all wavelengths.

TEXTOR, G. P.

T012   DSN Progress Report for March–April 1972: Mariner Mars 1971 Mission Support

G. P. Textor

Technical Report 32-1526, Vol. IX, pp. 35–37, June 15, 1972

On Feburary 12, 1972, Mariner 9 completed its 180th revolution about the planet Mars and its 90th day of scientific data gathering from orbit. This marked the end of the nominal mission, which was to obtain data from orbit for a minimum of 90 days, and marked the beginning of the extended mission. This article presents the

objectives, constraints, profile, and present DSN coverage plan for the Mariner Mars 1971 extended mission.

T013 DSN Progress Report for May–June 1972: Mariner Mars 1971 Mission Support

G. P. Textor

Technical Report 32-1526, Vol. X, pp. 20–21, August 15, 1972

The Mariner Mars 1971 Extended Mission utilizes the Mars Deep Space Station (DSS 14), the 64-m-diameter antenna station at Goldstone, California, for acquiring telemetry and radio metric data. The 26-m-diameter antenna stations at Madrid, Spain and Goldstone, California, however, are playing an important part maximizing the quantity and quality of the data received at DSS 14. This article describes the role of the 26-m-diameter antenna stations presently engaged in the Mariner Mars 1971 Extended Mission.

T014 Tracking and Data System Support for the Mariner Mars 1971 Mission: First Trajectory Correction Maneuver Through Orbit Insertion

G. P. Textor, L. B. Kelly, and M. Kelly

Technical Memorandum 33-523, Vol. II, June 15, 1972

This document describes the Tracking and Data System (TDS) activities in support of the Mariner Mars 1971 Project from the first trajectory correction maneuver on June 4, 1971, through cruise and orbit insertion on November 14, 1971. Included are presentations of the changes and updates to the TDS requirements, plan, and configuration plus detailed information on TDS flight support performance evaluation and pre-orbital testing and training during this report period.

With the loss of Mariner 8 at launch, a few changes to the Mariner Mars 1971 requirements, plan, and configuration were necessitated. Mariner 9 is now assuming the mission plan of Mariner 8, including the TV mapping cycles and a 12-hr orbital period.

A second trajectory correction maneuver was not required because of the accuracy of the first maneuver. All testing and training for orbital operations were completed satisfactorily and on schedule. The orbit insertion was accomplished with excellent results.

THOMAS, J. B.

T015 DSN Progress Report for November–December 1971: An Analysis of Long Baseline Radio Interferometry

J. B. Thomas

Technical Report 32-1526, Vol. VII, pp. 37–50, February 15, 1972

The VLBI (very long baseline interferometer) cross-correlation procedure is analyzed for both a natural point source and a completely incoherent extended source. The analysis is based on a plane wave description of a radio signal that consists of stationary random noise. A formulation of the time delay is developed on the basis of plane wave phase. A brief discussion is devoted to small time delay corrections that are generated by relativistic differences in clock rates in the various coordinate frames. The correlation analysis, which includes electronic factors such as amplitude and phase modulation and the heterodyne process, leads to expressions for fringe amplitude and fringe phase. It is shown that the cross-correlation function for an extended source is identical to the point-source expression if one adjusts the fringe amplitude to include the transform of the brightness distribution. Examples of diurnal paths in the u–v plane are presented for various baselines and source locations. Finally, delay and delay rate measurement accuracy is briefly discussed.

T016 DSN Progress Report for January–February 1972: An Analysis of Long Baseline Radio Interferometry, Part II

J. B. Thomas

Technical Report 32-1526, Vol. VIII, pp. 29–38, April 15, 1972

This article continues the analysis of the cross-correlation procedure used in long baseline radio interferometry begun in Technical Report 32-1526, Vol. VII, pp. 37–50. It is assumed that the radio signal is generated by a very distant, completely incoherent, extended source. For both digital and analog recording systems, the normalized cross-correlation function is derived in terms of noise temperature, fringe visibility, and bandpass overlap. For very strong point sources and accurate model delays, it is shown that the digital cross-correlation function becomes a sawtooth time function whose extrema and zero crossings agree with the sinusoidal cross-correlation function produced by an analog system. For weak sources, such as those common to most very long baseline interferometry measurements, the digital cross-correlation function is identical to the normalized analog cross-correlation function, except for a loss of $2/\pi$ in amplitude.

General signal/noise (SNR) expressions are derived for both the digital and the analog cross-correlation functions. For a very strong point source, the SNR in a digital system can be infinitely better than that in an analog system at time points of maximum correlation. However, at points of weak correlation, the digital SNR is $2/\pi$ smaller than the analog value. In the case of small correlated amplitude, the digital system produces an

SNR that is uniformly $2/\pi$ worse than the analog system ratio.

T017 DSN Progress Report for September–October 1972: Very Long Baseline Interferometry (VLBI) Possibilities for Lunar Study

M. A. Slade, P. F. MacDoran, and J. B. Thomas

Technical Report 32-1526, Vol. XII, pp. 35–39, December 15, 1972

For abstract, see Slade, M. A.

THOMAS, J. R.

T018 Mariner Venus–Mercury 1973 Mission Solar Proton Environment: Fluence and Dose

J. R. Thomas (The Boeing Company)

JPL Quarterly Technical Review, Vol. 2, No. 1, pp. 12–28, April 1972

The solar proton environment for the Mariner Venus–Mercury 1973 mission may be the most severe yet encountered in space missions, because the trajectory by Mercury will bring the spacecraft significantly closer to the Sun than any previous spacecraft. This study presents a derivation of proton fluence over the duration of the mission in terms of a relatively constant low-energy component, the solar wind, and a probabilistic high-energy component from discrete solar events. An updated correlation of yearly energetic proton fluence with yearly average Sunspot number is presented. This correlation and Sunspot cycle forecasts for the period of the mission (late-1973 through early-1975) form the basis for the high-energy proton fluence estimates with various confidence levels. Uncertainties in the probability estimates and in calculation of the scaling with distance from the Sun are discussed. Selection of a particular 95-percentile model as the design constraint is recommended, along with reasons for not using the worst-case model. Interior fluences are calculated and expressed in terms expected to be useful for spacecraft design.

THOMPSON, A. R.

T019 The Distribution of Linear Polarization in Cassiopeia A at Wavelengths of 9.8 and 11.1 cm

G. S. Downs and A. R. Thompson (Stanford University)

Astron. J., Vol. 77, No. 2, pp. 120–133, March 1972

For abstract, see Downs, G. S.

THOMPSON, T. W.

T020 Map of Lunar Radar Reflectivity at 7.5-m Wavelength

T. W. Thompson (Cornell–Sydney University Astronomy Center)

Icarus, Vol. 13, No. 3, pp. 363–370, November 1970

The radar reflectivity of a substantial portion of the Earth-visible lunar surface has been mapped at a wavelength of 7.5 m. This mapping—the first to use interferometric techniques in lunar observations—demonstrated that delay-doppler mapping of the Moon is possible at wavelengths of several meters. In the map that was obtained, the maria at a given angle of incidence had echo powers approximately half of those of highlands at the same angle of incidence. Also, an enhancement associated with the lunar crater Tycho was observed.

THULEEN, K. L.

T021 DSN Progress Report for January–February 1972: The Translation of the Tropospheric Zenith Range Effect From a Radiosonde Balloon Site to a Tracking Station

K. L. Thuleen and V. J. Ondrasik

Technical Report 32-1526, Vol. VIII, pp. 39–44, April 15, 1972

The temporal behavior of the wet tropospheric zenith range effect, $\Delta\rho_z(w)$, over the radiosonde balloon sites at Edwards Air Force Base and Yucca Flats, Nevada, is compared. The $\Delta\rho_z(w)$ over the balloon site may be translated to a nearby tracking station for use in performing tropospheric navigational error analysis studies and for developing models, incorporating seasonal variations, to be used for the tropospheric calibration of radio metric data. The daily variations in $\Delta\rho_z(w)$ appear to prohibit the use of radiosonde balloon data for the daily calibration of radio metric data.

TIMOR, U.

T022 DSN Progress Report for May–June 1972: Frame Synchronization in Time-Multiplexed PCM Telemetry With Variable Frame Length

U. Timor

Technical Report 32-1526, Vol. X, pp. 96–103, August 15, 1972

This article presents new methods of parallel and serial synchronization for time-multiplexed phase-coherent telemetry signals. In the parallel case, i.e., when the synchronization code is transmitted on a separate channel,

M synchronization codes are generated by concatenating a common pseudonoise-like sequence of short length with words from a self-synchronizing code. The frame synchronizer can lock on any of the *M* codes, which is particularly useful when frames of different lengths have to be transmitted. In the serial case, that is, when each frame starts with an identical synchronization code, false synchronization due to replicas of the code randomly generated by the data is completely eliminated by transferring the synchronization code to the quadrature channel, while the data are transmitted on the in-phase channel.

T023 Interplex—An Efficient Multichannel PSK/PM Telemetry System

S. Butman and U. Timor

IEEE Trans. Commun., Vol. COM-20, No. 3, pp. 415–419, June 1972

For abstract, see Butman, S.

T024 Equivalence of Time-Multiplexed and Frequency-Multiplexed Signals in Digital Communications

U. Timor

IEEE Trans. Commun., Vol. COM-20, No. 3, pp. 435–438, June 1972

In comparing different techniques for multiplexing N binary data signals into a single channel, time-division multiplexing (TDM) is known to have a theoretic efficiency of 100% (neglecting sync power) and thus seems to outperform frequency-division multiplexing (FDM) systems. By considering more general FDM systems, it will be shown that both TDM and FDM are equivalent and have an efficiency of 100%. The difference between the systems is in the multiplexing and demultiplexing subsystems, but not in the performance or in the generated waveforms.

TOTH, R. A.

T025 Global Studies of Atmospheric Pollutants and Trace Constituents

R. A. Toth (California Institute of Technology) and C. B. Farmer (California Institute of Technology)

AIAA Preprint 71-1109, ACS (American Chemical Society)/AIAA (American Institute of Aeronautics and Astronautics)/EPA (Environmental Protection Agency)/IEEE (Institute of Electrical and Electronic Engineers)/ISA (Instrument Society of America)/NASA (National Aeronautics and Space Administration)/NOAA (National Oceanographic and Atmospheric Administration) Joint Conference on Sensing of Environmental Pollutants, Palo Alto, California, November 8–10, 1971

A high-speed, high-resolution, Fourier interferometer operating in the 1- to 5-μ spectral region can best meet the needs for remotely detecting and monitoring various molecular species in the atmosphere. An operational breadboard version of the instrument exists. Spectra obtained from ground sites in the Los Angeles area demonstrate the presence of several gases in the atmosphere. Spectra in the 2.1- and 2.3-μ regions are presented, from which relative abundances of carbon dioxide and carbon monoxide are derived. Ground-based operations and aircraft flights with the present instrument verify the potential operational capacity for a satellite instrument. A discussion is presented on the use of the instrument from a spacecraft.

T026 Line Strengths of N$_2$O in the 2.9 Micron Region

R. A. Toth

J. Molec. Spectrosc., Vol. 40, No. 3, pp. 588–604, December 1971

The line strengths of the bands 10^01–00^00, 02^01–00^00, and 11^11–01^10 of N_2O have been measured with low sample pressures and high resolution (0.031–0.33 cm^{-1}). The data are analyzed to determine the band strengths and dipole moment matrix elements. At 300°K the strengths of the two Σ–Σ bands in order of increasing frequency are 1.77 and 36.9 cm^{-2}-atm^{-1}. The band strength of the π–π band is 4.25 cm^{-2}-atm^{-1} at 300°K. Five lines of the band 06^00–00^00 and two lines of the 06^0–00^00 bands have been observed in the spectrum of the 10^01–00^00 band. The strengths and frequencies of these lines have been measured. These results are used in conjunction with perturbation theory to determine the Fermi interaction term W. Molecular constants and the band strength of the 06^00–00^00 band are obtained from W and the data. The band strength of the 06^00–00^00 band is 0.0092 cm^{-2}-atm^{-1} at 300°K.

T027 Self-Broadened and N$_2$ Broadened Linewidths of N$_2$O

R. A. Toth

J. Molec. Spectrosc., Vol. 40, No. 3, pp. 605–615, December 1971

The self and N_2-broadened linewidths of N_2O have been measured directly in the 10^01-00^00 and 02^01-00^00 bands of N_2O at 297°K with a resolution of 0.03 cm^{-1}. The experimental results are compared with linewidths calculated from Anderson's impact theory as amplified by Tsao and Curnutte. The agreement between experiment and theory is good for both types of broadening. Best-fit values for the quadrupole moments and hard-sphere diameters of N_2O and N_2 are listed and compared with previous values. The best-fit values were used to calculate the N_2O + N_2 linewidths at temperatures of 180, 220, and 260°K.

TRUBERT, M. R.

T028 Large Spacecraft Antennas: Conical Ring-Membrane Reflectors

R. E. Oliver, M. R. Trubert, and A. H. Wilson

JPL Quarterly Technical Review, Vol. 2, No. 2, pp. 42–47, July 1972

For abstract, see Oliver, R. E.

TSAY, F.-D.

T029 Ferromagnetic Resonance of Lunar Samples

F.-D. Tsay (California Institute of Technology), S. I. Chan (California Institute of Technology), and S. L. Manatt

Geochim. Cosmochim. Acta, Vol. 35, No. 9, pp. 865–875, September 1971

Evidence is presented to show that the electron-spin-resonance spectra observed for a selection of Apollo 11 lunar samples arise from the ferromagnetic centers consisting of metallic Fe. A model study to simulate the polycrystalline spectra has been carried out, from which it was possible to ascertain with some degree of certainty the size and shape of the ferromagnetic centers as well as the metallic iron content. Some variations in the metallic Fe content have been noted in these samples, e.g., between rocks and fine soil.

T030 Electron Paramagnetic Resonance of Radiation Damage in a Lunar Rock

F.-D. Tsay, S. I. Chan, and S. L. Manatt

Nature Phys. Sci., Vol. 237, No. 77, pp. 121–122, June 19, 1972

Although lunar material has been exposed to radiations from indigenous radioactive atoms, solar wind protons, and cosmic ray particles for a very long time, no electron paramagnetic resonance (EPR) signals attributable to natural radiation damage had been observed in the returned Apollo 11 and 12 samples. This article presents evidence of radiation-induced EPR signals in one of the lunar samples examined.

T031 Magnetic Resonance Studies of Apollo 11 and Apollo 12 Samples

F.-D. Tsay (California Institute of Technology), S. I. Chan (California Institute of Technology), and S. L. Manatt

Proceedings of the Second Lunar Science Conference, Houston, Texas, January 11–14, 1971, Vol. 3, pp. 2515–2528, The M.I.T. Press, Cambridge, 1971

This article describes the electron-spin-resonance (ESR) studies at both X-band (9.5 GHz) and K-band (34.8 GHz) frequencies that have been carried out on a selection of Apollo 11 and Apollo 12 lunar samples. On the basis that no significant temperature dependence of the absorption intensity is noted, together with the result that the signal intensity is at least three orders of magnitude greater than that expected for possible paramagnetism, the broad, asymmetric resonance signal centered at $g = 2.09 \pm 0.03$ has been assigned to ferromagnetic centers. A model study to simulate the polycrystalline spectra using computer simulation techniques has been carried out, from which it was possible to ascertain with some degree of certainty the size and shape of the ferromagnetic centers and to ascertain that the ferromagnetism is due to metallic Fe particles. Metallic Fe contents have been measured for all lunar samples studied, and these range in concentration from 0.001 to 0.50 wt%. These results suggest an apparent correlation between the metallic Fe contents and the geological and surface exposure ages of the samples.

Weak paramagnetic resonances attributable to octahedrally coordinated Mn^{2+} ions have also been observed in some samples in which the metallic Fe content is either low or partially removed. From the g value (2.002 $\pm$ 0.002) and the nuclear hyperfine coupling constant (-95.0 $\pm$ 2.0 gauss), it appears that these resonances originate from $Mn(H_2O)_6^{2+}$. No ESR signals ascribable to free electrons and/or holes, which would be indicative of radiation damage, or Ti^{3+} have been detected in these samples.

UCHIYAMA, A. A.

U001 Gravitational Effects on Electrochemical Batteries

R. E. Meredith (Oregon State University), G. L. Juvinall, and A. A. Uchiyama

Technical Report 32-1570, November 15, 1972

For abstract, see Meredith, R. E.

UNTI, T. W. J.

U002 Dissipation Mechanisms in a Pair of Solar-Wind Discontinuities

T. W. J. Unti, G. Atkinson (Communications Research Center), C.-S. Wu (University of Maryland), and M. Neugebauer

J. Geophys. Res., Space Physics, Vol. 77, No. 13, pp. 2250–2263, May 1, 1972

A pair of sharp, closely-spaced discontinuities in the solar wind was recorded by the high time resolution instruments aboard OGO 5 on March 14, 1968. There is plasma turbulence within the double structure, and there appear to be small-amplitude hydromagnetic waves radiating from the discontinuities. The generation of the plasma turbulence is discussed in terms of magnetic drift waves. Although it seems probable that the surfaces are tangential discontinuities, arguments are also advanced that the double structure may represent the Petschek mechanism in which rapid field-line merging occurs between standing waves.

VAN DER CAPELLEN, A. G.

V001 Development of a 20-W Solid-State S-Band Power Amplifier

A. G. van der Capellen

JPL Quarterly Technical Review, Vol. 1, No. 4, pp. 43–48, January 1972

As an alternative to the use of traveling-wave-tube amplifiers in spacecraft with long-life mission requirements, JPL is developing a solid-state 20-W S-band power amplifier. Traveling-wave-tube amplifiers have limited reliability because of the relative short life of the cathode and the complexity of the power supply. A solid-state amplifier with an output of 20 W at 2295 MHz, a dc/RF efficiency of 38%, and a gain of 27 dB has been developed. This article describes the physical and electrical performance of the solid-state amplifier.

VIRZI, R. A.

V002 Scan Pointing Calibration for the Mariner Mars 1971 Spacecraft

W. F. Havens, G. I. Jaivin, G. D. Pace, and R. A. Virzi

Technical Memorandum 33-556, August 1, 1972

For abstract, see Havens, W. F.

V003 Mariner Mars 1971 Scan Platform Pointing Calibration

G. D. Pace, G. I. Jaivin, and R. A. Virzi

JPL Quarterly Technical Review, Vol. 2, No. 1, pp. 49–57, April 1972

For abstract, see Pace, G. D.

VOLKOFF, J. J.

V004 DSN Progress Report for March–April 1972: Photon Noise Generation of Cathode-Ray Tube Display Systems

J. J. Volkoff

Technical Report 32-1526, Vol. IX, pp. 152–161, June 15, 1972

The mean-square fluctuation components associated with the various luminous fluxes of ambient and generated light emitted from a cathode-ray tube (CRT) system are derived and combined to represent the photon-noise component. A rationale for the criteria required for the discernment of noisy shades of gray as displayed by CRT systems is developed. The criteria are applied to an actual CRT system and are verified with experimental results.

VON ROOS, O. H.

V005 DSN Progress Report for July–August 1972: An Evaluation of Charged Particle Calibration by a Two-Way Dual-Frequency Technique and Alternatives to This Technique

O. H. von Roos and B. D. Mulhall

Technical Report 32-1526, Vol. XI, pp. 42–52, October 15, 1972

This article discusses the accuracy of the three charged-particle calibration methods—differenced range versus integrated doppler, Faraday rotation, and dual frequency—as they apply to the various tracking modes, e.g., one-station tracking, two-station tracking, spacecraft very-long-baseline interferometry. It is found that many calibration schemes are deficient at small Sun–Earth–probe angles (SEPs). Observations of the Sun during its active period between 1967 and 1969 have been used to obtain quantitative information on range degradation at small SEPs. Likewise, range errors at small SEPs during a quiet Sun period (in this case the 1964–1965 solar minimum) have also been computed with the result that, even at times of a comparatively inactive Sun, range errors engendered by plasma clouds are still troublesome inasmuch as they prevent range measurement with an accuracy of less than 1 m.

V006 DSN Progress Report for July–August 1972: Derivation of a General Expression for Ionospheric Range Corrections Valid for Arbitrary Solar Zenith Angles, Azimuths, Elevation Angles and Station Locations

O. H. von Roos and K. W. Yip

Technical Report 32-1526, Vol. XI, pp. 53–61, October 15, 1972

A general expression is derived for the electron-density profile as a function of latitude and longitude for that part of the Earth which is in direct sunlight including dawn and dusk. This expression allows one to determine by standard means the range correction for arbitrary ray-path directions. It is also shown that the naive application of the Chapman ionosphere entails range-correction errors which for low elevation angles (<20 deg) and large solar zenith angles (>40 deg) cannot be tolerated. Numerical calculations are displayed showing the dependence of the range correction on the pertinent parameters.

V007 3-D Multilateration: A Precision Geodetic Measurement System

P. R. Escobal, H. F. Fliegel, R. M. Jaffe, P. M. Muller, K. M. Ong, O. H. von Roos, and M. S. Shumate

JPL Quarterly Technical Review, Vol. 2, No. 3, pp. 1–11, October 1972

For abstract, see Escobal, P. R.

V008 Method for the Solution of Electromagnetic Scattering Problems for Inhomogeneous Dielectrics as a Power Series in the Ratio (Dimension of Scatterer)/Wavelength

O. H. von Roos

J. Appl. Phys., Vol. 42, No. 11, pp. 4197–4201, October 1971

In this article, the definitive work of Stevenson for the Rayleigh series expansion of electromagnetic scattering from homogeneous scatterers is extended to inhomogeneous scatterers. Furthermore, it is shown that a determination of the strength of the multipoles induced by the incident radiation is sufficient to determine the far field and, therefore, the scattering cross section, without relying on an awkward expansion and subsequent matching of far and near fields. The calculations are thus enormously simplified.

WALMSLEY, D. E.

W001 Lifetime Estimates for Sterilizable Silver–Zinc Battery Separators

E. F. Cuddihy, D. E. Walmsley, and J. Moacanin

JPL Quarterly Technical Review, Vol. 2, No. 1, pp. 72–81, April 1972

For abstract, see Cuddihy, E. F.

WANG, J. T.

W002 Cold-Welding Test Environment

J. T. Wang

Technical Report 32-1547, February 1, 1972

Spacecraft designers concerned with the development of excessive friction or cold-welding in mechanisms with moving parts operating in space vacuum for an extended period should consider cold-weld qualification tests. To establish requirements for effective test programs, a flight test was conducted, and the results were compared with ground test data from various facilities. Sixteen typical spacecraft material couples were mounted on an experimental research satellite (ERS-20), where a motor intermittently drove the spherical moving specimens across the faces of the flat fixed specimens in an oscillating motion. Friction coefficients were measured over a period of 14-mo orbital time. Surface-to-surface sliding was found to be the controlling factor of generating friction in a vacuum environment. Friction appears to be independent of passive vacuum exposure time.

Prelaunch and postlaunch tests identical to the flight test were performed in a TRW oil-diffusion-pumped ultrahigh vacuum (1.33×10^{-6} N/m^2) chamber. Only 50% of the resultant data agreed with the flight data due to pump oil contamination. Subsequently, identical ground tests were run in the JPL Molsink, a unique ultrahigh vacuum facility, and a TRW ion-pumped vacuum chamber. The agreement (90%) between data from these tests and the flight data established the adequacy of these test environments and facilities.

WARDLE, M. D.

W003 Dry-Heat Resistance of Bacillus Subtilis Var. Niger Spores on Mated Surfaces

G. J. Simko, J. D. Devlin, and M. D. Wardle

Appl. Microbiol., Vol. 22, No. 4, pp. 491–495, October 1971

For abstract, see Simko, G. J.

WEETALL, H. H.

W004 Studies of Antigen–Antibody Interaction on Some Specific Solid Adsorbents Derived From Cellulose

N. Weliky and H. H. Weetall

Immunochemistry, Vol. 9, No. 10, pp. 967–978, October 1972

For abstract, see Weliky, N.

WELCH, L. R.

W005 DSN Progress Report for May–June 1972: A Minimization Algorithm for a Class of Functions

L. R. Welch

Technical Report 32-1526, Vol. X, pp. 110-112, August 15, 1972

Let N be a positive integer and $A_0, \cdots, A_N$ be non-negative numbers with at least one positive. Define

$$G(x) = \frac{N}{x} + \sum_{k=0}^{N} A_k x^k$$

The problem is to compute $z > 0$ with

$$G(z) = \min_{x>0} G(x)$$

This article gives a simple algorithm requiring $[(3/2)(\ln N/\ln 2)] + 8$ evaluations of a polynomial of degree $N + 1$ and 6 evaluations of its derivative. This algorithm is required to optimize the DSN resource allocation process.

WELIKY, N.

W006 Studies of Antigen–Antibody Interaction on Some Specific Solid Adsorbents Derived From Cellulose

N. Weliky and H. H. Weetall

Immunochemistry, Vol. 9, No. 10, pp. 967–978, October 1972

Studies of the dissociation of complexes using specific insoluble complexing agents under specified conditions can yield information concerning the nature of the specific interactions contributing to complex formation. For the case of the interaction of specific antibody with antigen conjugates, data is obtained concerning heterogeneity of apparent equilibrium constants and the influence of antigen and immunoadsorbent structure on protein interaction and antigen–antibody dissociation. Such information can be useful for predicting conditions for antiserum purification or antibody recovery.

For the case of the cellulose adsorbents chosen, it was found that (1) the adsorbent may contribute strongly to the interaction of ionizable haptens with antibody, with a pH dependency typical of acid catalyzed reactions, (2)

immunoadsorbent properties can be modified through physical and chemical structural changes, (3) the dissociation of antibody from the haptenic and protein immunoadsorbents showed no significant discontinuities in the acid range, and (4) antibodies to those haptens chosen which do not ionize in the acid range, do not dissociate appreciably from the immunoadsorbent in the acid range but do at sufficiently high pH.

WELLS, R. A.

W007 DSN Progress Report for November–December 1971: High-Rate Telemetry Preprocessor for the SFOF 360/75 Computers

R. A. Wells

Technical Report 32-1526, Vol. VII, pp. 109–112, February 15, 1972

The concluding phase has been reached for an advanced development task to determine the feasibility of implementing a computer-based system to preprocess digitally encoded block-formatted video data at serial rates up to 250 kbits/s. A software model has been completed showing that under typical mission conditions the Space Flight Operations Facility (SFOF) 360/75 primary computer would be virtually preempted by raw video data at this rate. A high-rate telemetry preprocessor or some similar concept would relieve the primary computer in the central processing system of the severe loading that could result from injecting unpreprocessed video information directly into the SFOF 360/75 serial input channels in a real-time or near-real-time environment. A recommendation is made that the technique of video preprocessing be pursued in order to meet the known objectives of future missions.

WHANG, M. M.

W008 DSN Progress Report for May–June 1972: The Use of an Interplex Modulation Technique for the Mariner Venus–Mercury 1973 Mission

M. M. Whang

Technical Report 32-1526, Vol. X, pp. 157–160, August 15, 1972

The use of interplex modulation for the Mariner Venus–Mercury 1973 mission necessitates modification of the station ground equipment to effect compatibility. The Simulation Conversion Assembly (SCA) is to be modified to provide a source for generation of simulated telemetry data, using interplex, for system testing, training, and software development. Implementation of the SCA hardware modifications, together with a discussion of the simulation test modes, is presented.

WICK, M. R.

W009 DSN Progress Report for January–February 1972: DSN Programmed Oscillator Development

M. R. Wick

Technical Report 32-1526, Vol. VIII, pp. 115–124, April 15, 1972

This article describes the development of a programmed oscillator utilizing a Dana Laboratory Digiphase synthesizer Model 7010-S-179. A brief description of the synthesizer characteristics and the technique for digital control is given. With this synthesizer, the programmed oscillator has the capability of being controlled at rates and ranges required for tracking outer-planet probes while providing the resolution and stability required for narrow-loop bandwidth receivers.

W010 DSN Progress Report for May–June 1972: Programmed Oscillator Development

H. Donnelly and M. R. Wick

Technical Report 32-1526, Vol. X, pp. 180–185, August 15, 1972

For abstract, see Donnelly, H.

WIEBE, E.

W011 DSN Progress Report for July–August 1972: Low Noise Receivers: Microwave Maser Development

R. C. Clauss, E. Wiebe, and R. B. Quinn

Technical Report 32-1526, Vol. XI, pp. 71–80, October 15, 1972

For abstract, see Clauss, R. C.

WIGGINS, C. P.

W012 DSN Progress Report for September–October 1972: X-Band Radar Development

C. P. Wiggins

Technical Report 32-1526, Vol. XII, pp. 19–21, December 15, 1972

A high-power X-band radar is under development for use on the 64-m-diameter antenna at the Mars Deep Space Station (DSS 14). The 400-kW transmitter will operate at 8.495 GHz. Ground testing of portions of the transmitter will start in early 1973.

WIKSTEN, D.

W013 Accelerated Life Testing of Spacecraft Subsystems

D. Wiksten and J. Swanson

Technical Memorandum 33-575, November 1, 1972

This memorandum presents the results of a study performed to establish the rationale and requirements for conducting accelerated life tests on electronic subsystems of spacecraft. A method for applying data on the reliability and temperature sensitivity of the parts contained in a subsystem to the selection of accelerated life-test parameters is described. Additional considerations affecting the formulation of test requirements are identified, and practical limitations of accelerated aging are described.

WILLIAMS, H. E.

W014 Analysis of a Laterally Loaded Ring With a Hinged Cross Section

H. E. Williams (Harvey Mudd College)

AIAA Preprint 72-355, AIAA (American Institute of Aeronautics and Astronautics)/ASME (American Society of Mechanical Engineers)/SAE (Society of Automotive Engineers) Thirteenth Structures, Structural Dynamics, and Materials Conference, San Antonio, Texas, April 10–12, 1972

A ring assembly constructed by lacing together three elements into a basic channel cross section is analyzed. The ring is supported at three equidistant points and loaded by a uniform distribution of radial and transverse loads. Bulkheads may be introduced at discrete cross sections to prevent distortion. The purpose of this analysis is to determine the behavior of the deflection as the number and location of the bulkheads and the degree of rigidity of the supports are varied.

The method of analysis is an application of the Principle of Virtual Work within the framework of small displacement theory. Numerical results are presented for the geometrical parameters of a model. An important result is the observation that bulkheads have virtually no effect on the deflections of the web.

WILLIAMS, W. F.

W015 Reduction of Near-In Sidelobes Using Phase Reversal Aperture Rings

W. F. Williams

JPL Quarterly Technical Review, Vol. 1, No. 4, pp. 34–42, January 1972

Spacecraft antennas having high gain and extremely low sidelobes will be needed for communications satellites. Low sidelobe performance is needed to isolate beams of multibeam systems using the same carrier frequency (frequency re-use). Because of a limited allowable spectrum for transmission, frequency re-use may be necessary. A

technique for reducing near-in lobes by cancellation is described. This technique takes a small portion of the radiation from the antenna aperture and generates the near-in lobes, which are then fed out-of-phase relative to the main signal. Results of sample cases indicate that the first three lobes can be nearly eliminated at a 40% reduction in aperture efficiency.

WILSON, A. H.

W016 Furlable Spacecraft Antenna Development: An Interim Report

R. E. Oliver and A. H. Wilson

Technical Memorandum 33-537, April 15, 1972

For abstract, see Oliver, R. E.

W017 Large Spacecraft Antennas: Conical Ring-Membrane Reflectors

R. E. Oliver, M. R. Trubert, and A. H. Wilson

JPL Quarterly Technical Review, Vol. 2, No. 2, pp. 42–47, July 1972

For abstract, see Oliver, R. E.

WILSON, L.

W018 An ESCA Study of Lunar and Terrestrial Materials

W. T. Huntress, Jr., and L. Wilson (Varian Associates)

Earth Planet. Sci. Lett., Vol. 15, pp. 59–64, May 1972

For abstract, see Huntress, W. T., Jr.

WINKELSTEIN, R.

W019 DSN Progress Report for November–December 1971: Spectral Estimate Variance Reduction by Averaging Fast-Fourier Transform Spectra of Overlapped Time Series Data

R. Winkelstein

Technical Report 32-1526, Vol. VII, pp. 74–80, February 15, 1972

An analysis is made of the variance of the spectral estimates calculated in the DSN by two methods, namely the correlation method and the Fast Fourier Transform (FFT) method. It is shown that the FFT method using consecutive sequences of data samples produces the same variance as the correlation method. However, a reduction of over 20% in variance can be obtained by using the FFT method with overlapped sequences of

data. A relationship is derived giving the variance reduction as a function of the amount of data sequence overlap.

W020 DSN Progress Report for September–October 1972: Complex Mixer Error Analysis

R. Winkelstein

Technical Report 32-1526, Vol. XII, pp. 47–50, December 15, 1972

The complex mixer is composed of two channels. One channel contains the signal mixed with the sine of the reference frequency and the other contains the signal mixed with the cosine of the reference frequency. Errors unique to this system are gain and phase shifts of one channel with respect to the other. When the power spectrum of the mixer's output, considered a complex quantity, is calculated, these errors produce an unwanted image response to each signal component in the true spectrum. This analysis was carried out to ensure that hardware specifications were sufficient to limit these image responses to tolerable levels. Calculations for various gain and phase errors show that image responses in the power spectrum for prototype hardware will be limited to less than 1% of the true signal components.

W021 Precision Signal Power Measurement

R. Winkelstein

JPL Quarterly Technical Review, Vol. 2, No. 2, pp. 18–24, July 1972

Accurate estimation of signal power is an important DSN consideration. Ultimately, spacecraft power and weight is saved if no reserve transmitter power is needed to compensate for inaccurate measurements. Spectral measurement of the received signal has proved to be an effective method of estimating signal power over a wide dynamic range. Furthermore, on-line spectral measurements provide an important diagnostic tool for examining spacecraft anomalies. Prototype equipment installed at the DSN 64-m-diameter antenna site, the Mars Deep Space Station of the Goldstone Deep Space Communications Complex, has been successfully used to make measurements of carrier power and sideband symmetry of telemetry signals received from the Mariner Mars 1971 spacecraft.

WINN, F. B.

W022 DSN Progress Report for November–December 1971: Tropospheric Refraction Calibrations and Their Significance on Radio-Metric Doppler Reductions

F. B. Winn

Technical Report 32-1526, Vol. VII, pp. 68–73,
February 15, 1972

This article describes the tropospheric refraction algorithm used in the Mariner Mars 1971 tracking data reductions and orbit determination effort; this algorithm differs from models used to support past missions and performs two times better than the stated mission requirement. Although single-pass reductions of doppler tracking data are extremely influenced by tropospheric refraction models, fits to doppler acquired over large time periods, weeks or months, are influenced only slightly, in that the tropospheric refraction corruption of the doppler observables simply is left in the after-the-fit observed minus computed residuals.

WINSTEIN, S.

W023 **Carbon-to-Metal Chlorine Exchange: IV. Mercuric Salt Promoted Acetolysis of exo-Norbornyl Chloride**

J. P. Hardy, A. F. Diaz, and S. Winstein

J. Am. Chem. Soc., Vol. 94, No. 7,
pp. 2363–2370, April 5, 1972

For abstract, see Hardy, J. P.

WOLLENHAUPT, W.

W024 **Lunar Gravity via Apollo 14 Doppler Radio Tracking**

W. L. Sjogren, P. Gottlieb, P. M. Muller, and W. Wollenhaupt (Manned Spacecraft Center)

Science, Vol. 175, No. 4018, pp. 165–168,
January 14, 1972

For abstract, see Sjogren, W. L.

WOLLENHAUPT, W. R.

W025 **Apollo 15 Gravity Analysis From the S-Band Transponder Experiment**

W. L. Sjogren, P. M. Muller, and
W. R. Wollenhaupt (Manned Spaceflight Center)

Proceedings of the Conference on Lunar Geophysics, Lunar Science Institute, Houston, Texas, October 18–21, 1971, pp. 411–418

For abstract, see Sjogren, W. L.

WONG, L.

W026 **A Surface-Layer Representation of the Lunar Gravitational Field**

L. Wong (Aerospace Corporation),
G. Buechler (Aerospace Corporation),
W. Downs (Aerospace Corporation), W. L. Sjogren,
P. M. Muller, and P. Gottlieb

J. Geophys. Res., Vol. 76, No. 26, pp. 6220–6236,
September 10, 1971

A surface-layer representation of the lunar gravitational field has been derived dynamically from the analysis of doppler observations on both polar and equatorial lunar orbiters. The force model contained 600 discrete masses located on the mean lunar surface between the approximate boundaries of ±60-deg latitude and ±95-deg longitude. The derived major mascons were generally in agreement with a model based on polar orbits alone. A technique for combining the discrete mass gravitational field for the front side with a spherical harmonics expansion for the back side is described. Harmonic analysis of the resultant field shows that the higher end of the power spectrum roughly follows the decay rule predicted by W. M. Kaula in 1963.

WONG, S. K.

W027 **Geocentric Gravitational Constant Determined From Mariner 9 Radio Tracking Data**

P. B. Esposito and S. K. Wong

Preprint of paper presented at International Symposium on Earth Gravity Models and Related Problems (Sponsored by the American Geophysical Union, NASA), St. Louis, Missouri, August 16–18, 1972

For abstract, see Esposito, P. B.

WU, C.-S.

W028 **Dissipation Mechanisms in a Pair of Solar-Wind Discontinuities**

T. W. J. Unti, G. Atkinson (Communications Research Center), C.-S. Wu (University of Maryland), and M. Neugebauer

J. Geophys. Res., Space Physics, Vol. 77, No. 13, pp. 2250–2263, May 1, 1972

For abstract, see Unti, T. W. J.

WU, F.

W029 **Raman Scattering Cross Section for N_2O_4**

C. J. Chen and F. Wu (State University of New York, Buffalo)

Appl. Phys. Lett., Vol. 19, No. 11, pp. 452–453, December 1, 1971

For abstract, see Chen, C. J.

YAMAKAWA, K. A.

Y001   Radiation Effects on Three Low-Power Microcircuits

K. A. Yamakawa

Technical Memorandum 33-576, November 15, 1972

This memorandum gives the results of irradiating several low-power circuit elements with cobalt-60 gamma radiation, low-energy (1.5-MeV) and high-energy (28- to 85-MeV) electrons, and neutrons. The bipolar circuits used were an SE480Q NAND gate and a micropower frequency divider used in electronic wristwatches that is designated ICB-9002. The metal-oxide-semiconductor device used was a dual p-channel metal-oxide semiconductor–field-effect transistor designated 2N4067.

YANG, J.-N.

Y002   Nonstationary Envelope Process and First Excursion Probability

J.-N. Yang

JPL Quarterly Technical Review, Vol. 1, No. 4, pp. 1–12, January 1972

A definition of the envelope of nonstationary random processes is proposed. The establishment of the envelope definition makes it possible to simulate the nonstationary random envelope directly. The envelope statistics, such as the density function, the joint density function, the moment function, and the level crossing rate, relevant to the analyses of the catastrophic failure, fatigue, and crack propagation of structures, are derived. Applications of the envelope statistics to the prediction of structural reliability under random loadings are demonstrated in detail.

Y003   Simulation of Random Envelope Processes

J.-N. Yang

J. Sound Vibr., Vol. 21, No. 1, pp. 73–85, March 1972

Efficient and practical methods of simulating stationary and nonstationary random envelope processes are presented. The stationary envelope processes are simulated by using the fast Fourier transform while the nonstationary envelope processes are simulated as the square root of the sum of a series of cosine functions and a series of sine functions with random phase angles. Typical applications of the envelope simulation are the simulations of

peaks and troughs which play an important role in the analyses of the first excursion probability, fatigue and crack propagation. In particular, applications to the crack propagation under random loadings are demonstrated in detail.

Y004   Statistical Distribution of Spacecraft Maximum Structural Response

J.-N. Yang

J. Spacecraft Rockets, Vol. 9, No. 1, pp. 57–59, January 1972

This article presents a direct statistical analysis of spacecraft maximum response under conditions of nonstationary random excitations resulting from booster engine shutdown and describes the resultant spacecraft structural reliability. It is found that the Gumbel Type I asymptotic distribution of maximum values provides a reasonably good statistical model for spacecraft maximum responses. This approach makes it possible to perform the reliability-based optimum design of spacecraft structures.

Y005   On the First Excursion Probability in Stationary Narrow-Band Random Vibration

J.-N. Yang and M. Shinozuka (Columbia University)

Trans. ASME, Ser. E: J. Appl. Mech., Vol. 38, No. 4, pp. 1017–1022, December 1971

Dealing with a stationary narrow-band gaussian process $X(t)$ with mean zero, this paper derives a number of approximate solutions on the basis of the point-process approach. In particular, upper and lower bounds sharper than those presently available are established, an approximation based on the Markov point process is obtained, and the clump size approach is also used for approximation. These approximations are checked against the results of semisimulations performed elsewhere. Some remarks are also made on the use of the principle of maximum entropy.

YANG, L. C.

Y006   Initiation of Insensitive Explosives by Laser Energy

V. J. Menichelli and L. C. Yang

Technical Report 32-1557, June 1, 1972

For abstract, see Menichelli, V. J.

Y007   Detonation of Insensitive High Explosives by a Q-Switched Ruby Laser

L. C. Yang and V. J. Menichelli

Appl. Phys. Lett., Vol. 19, No. 11, pp. 473–475, December 1, 1971

Immediate longitudinal detonations have been observed in confined small-diameter columns of PETN, RDX, and tetryl by using a focused Q-switched ruby laser. The energy ranged from 0.8 to 4.0 J in a pulse width of 25 ns. A 1000-Å-thick aluminum film deposited on a glass window was used to generate a shock wave at the window-explosive interface when irradiated by the laser. In some cases steady-state detonations were reached in less than 1/2 μs with less than 10% variation in the detonation velocity.

YANKURA, G.

Y008 Survey of Materials for Hydrazine Propulsion Systems in Multicycle Extended Life Applications

C. D. Coulbert and G. Yankura

Technical Memorandum 33-561, September 15, 1972

For abstract, see Coulbert, C. D.

YASUI, R. K.

Y009 Stress Analysis and Design of Silicon Solar Cell Arrays and Related Material Properties

A. M. Salama, W. M. Rowe, and R. K. Yasui

Technical Report 32-1552, March 1, 1972

For abstract, see Salama, A. M.

Y010 Solar Cell Contact Pull Strength as a Function of Pull-Test Temperature

R. K. Yasui and P. A. Berman

Technical Report 32-1563, September 1, 1972

Four types of solar-cell contacts were given pull-strength tests at temperatures between –173 and + 165°C. Contacts tested were (1) solder-coated titanium–silver contacts on n–p cells, (2) palladium-containing titanium–silver contacts on n–p cells, (3) titanium–silver contacts on 0.2-mm-thick n–p cells, and (4) solder-coated electroless-nickel-plated contacts on p–n cells. Maximum pull strength was demonstrated at temperatures significantly below the air mass zero cell equilibrium temperature of + 60°C. At the lowest temperatures, the chief failure mechanism was silicon fracture along crystallographic planes; at the highest temperatures, it was loss of solder strength. At intermediate temperatures, many failure mechanisms operated. Pull-strength tests give a good indication of the suitability of solar-cell contact systems for space use, and the tests reported here were the first to be carried out under simulated spaceflight temperatures.

Procedures used to maximize the validity of the results are described in detail.

YEN, T. F.

Y011 Absence of Porphyrins in an Apollo 12 Lunar Surface Sample

J. H. Rho, A. J. Bauman, T. F. Yen (University of Southern California), and J. Bonner (California Institute of Technology)

Proceedings of the Second Lunar Science Conference, Houston, Texas, January 11–14, 1971, Vol. 2, pp. 1875–1877, The M.I.T. Press, Cambridge, 1971

For abstract, see Rho, J. H.

YIP, K. W.

Y012 DSN Progress Report for November–December 1971: Local and Transcontinental Mapping of Total Electron Content Measurements of the Earth's Ionosphere

K. W. Yip and B. D. Mulhall

Technical Report 32-1526, Vol. VII, pp. 61–67, February 15, 1972

The interchangeability of total electron content data for the purpose of ionospheric calibration of deep space radio metric data, both locally and across the North American Continent, is demonstrated. Comparisons were made between calibrations produced from Faraday rotation data recorded at Stanford and Goldstone in California and at Hamilton in Massachusetts for simulated missions to Mars. The results, in terms of equivalent station location errors, are shown. The averages of the differences between the tracking station spin radius errors are below 1 m with standard deviations of about 1 m for both data sources. The averages of the differences of ionospheric effect on longitude changes are also less than 1 m with uncertainties of 2–3 m. Transcontinental mapping of Faraday rotation measurements is concluded to be a competitive calibration scheme with local mapping. However, because of the large scatter in the longitude changes, the improvement in this coordinate using the electron data from another station is at best marginal.

The geomagnetic latitude factor used in the mapping is also investigated. This factor is found essential to the mapping procedure.

Y013 DSN Progress Report for July–August 1972: Derivation of a General Expression for Ionospheric Range Corrections Valid for Arbitrary Solar Zenith Angles, Azimuths, Elevation Angles and Station Locations

O. H. von Roos and K. W. Yip

Technical Report 32-1526, Vol. XI, pp. 53–61,
October 15, 1972

For abstract, see von Roos, O. H.

YOKOYAMA, H.

Y014   Isolation and Characterization of Keto-Carotenoids From the Neutral Extract of Algal Mat Communities of a Desert Soil

A. J. Bauman, H. G. Boettger, A. M. Kelly,
R. E. Cameron, and H. Yokoyama (U.S.
Department of Agriculture)

Eur. J. Biochem., Vol. 22, No. 2, pp. 287–293,
September 1971

For abstract, see Bauman, A. J.

YOST, E.

Y015   Apollo 12 Multispectral Photography Experiment

A. F. H. Goetz, F. C. Billingsley,
J. W. Head (Bellcomm, Inc.),
T. B. McCord (Massachusetts Institute of
Technology), and E. Yost (Long Island University)

*Proceedings of the Second Lunar Science
Conference, Houston, Texas, January 11–14, 1971,*
Vol. 3, pp. 2301–2310, The M.I.T. Press, 1971

For abstract, see Goetz, A. F. H.

YOUNG, A. T.

Y016   Observing Venus Near the Sun

A. T. Young and L. D. G. Young

Sky Telesc., Vol. 43, No. 3, pp. 140–144,
March 1972

Daytime astronomical observing is very difficult within a few degrees of the Sun. If any direct sunlight falls inside the telescope tube or on the objective, it can ruin the seeing and image contrast. This article discusses the problems, special requirements, hints, and optimum conditions for near-Sun observation of Venus.

YOUNG, L. D. G.

Y017   Comments on Accurate Formula for Gaseous Transmittance in the Infrared

L. D. G. Young

Appl. Opt., Vol. 11, No. 1, pp. 202–203,
January 1972

This article discusses the accuracy of data previously published for gaseous transmittance in the infrared. The choice of input data, rather than the method of calculation, is questioned.

Y018   High Dispersion Spectroscopic Studies of Mars: V. A Search for Oxygen in the Atmosphere of Mars

J. S. Margolis, R. A. J. Schorn, and
L. D. G. Young

Icarus, Vol. 15, No. 2, pp. 197–203, October 1971

For abstract, see Margolis, J. S.

Y019   Relative Intensity Calculations for Nitrous Oxide

L. D. G. Young

J. Quant. Spectrosc. Radiat. Transfer, Vol. 12,
No. 3, pp. 307–322, March 1972

A tabulation of calculated rotational line intensities, relative to the integrated intensity of a vibration–rotation band, is given for Σ–Σ, Π–Σ, Σ–Π, Π–Π, and Δ–Π transitions of $^{14}N^{16}O_2$. These calculations were made for a temperature of 250°K (typical for the Earth's atmosphere) and for 300°K (representative of laboratory conditions). A summary of band-intensity measurements is also given.

Y020   Observing Venus Near the Sun

A. T. Young and L. D. G. Young

Sky Telesc., Vol. 43, No. 3, pp. 140–144,
March 1972

For abstract, see Young, A. T.

YOUNGER, H. C.

Y021   DSN Progress Report for September–October 1972: DSS Receiving System Saturation at High Signal Levels

H. C. Younger

Technical Report 32-1526, Vol. XII, pp. 220–225,
December 15, 1972

A loss of telemetry data from the Lunar Module occurred at the Mars Deep Space Station (DSS 14) during the Apollo 16 mission. This was caused by saturation of the first mixer in the DSS 14 receiving system by a very strong Command Module signal. Tests have been conducted to determine the saturation characteristics of the major components of the deep space station receiving system. The problem will be avoided during the Apollo 17 mission by using a lower-gain maser as prime maser,

and by adding a pad following the high-gain backup maser.

ZANTESON, R. A.

Z001 DSN Progress Report for May–June 1972: Improvements to Angle Data System Autocollimators

R. A. Zanteson

Technical Report 32-1526, Vol. X, pp. 191–193, August 15, 1972

The Angle Data System of the 64-m-diameter antenna utilizes two-axis autocollimators as the optical link between the precision instrument mount and the intermediate reference optical assembly. The accuracy, resolution, and stability of these instruments directly affects the pointing accuracy of the antennas. With an accuracy and resolution of better than one arc second, great care must be taken in each phase of the design and construction.

ZAWACKI, S. J.

Z002 Mariner Mars 1971 Television Picture Catalog: Sequence Design and Picture Coverage

P. E. Koskela, M. R. Helton, L. N. Seeley, and S. J. Zawacki

Technical Memorandum 33-585, Vol. II, December 15, 1972

For abstract, see Koskela, P. E.

ZOHAR, S.

Z003 DSN Progress Report for March–April 1972: New Hardware Realizations of Non-Recursive Digital Filters

S. Zohar

Technical Report 32-1526, Vol. IX, pp. 65–81, June 15, 1972

Analysis of the bit-level operations involved in the convolution realizing a non-recursive digital filter leads to hardware designs of digital filters based on the operation of counting. Two distinct designs are outlined: The first is capable of very high speed, but is rather expensive. The second is quite slow, but has the advantages of low cost and high flexibility. The basic designs considered utilize fixed-point representation for the data and filter coefficients. Variants which allow floating-point representation of the coefficients are also described.

ZUNDEL, E. F.

Z004 DSN Progress Report for July–August 1972: High-Reliability Microcircuit Procurement in the DSN

E. F. Zundel

Technical Report 32-1526, Vol. XI, pp. 121–123, October 15, 1972

This article discusses the implementation of microelectronic circuits in the DSN together with utilization of an equivalent MIL-STD-883 Class B device, screening tests to be used, and screening philosophy relative to failure-mechanism patterns. The expected costs and the advantages of standardization of device types to increase quantity buys are also discussed.

ZWEBEN, C.

Z005 Development of Boron Epoxy Rocket Motor Chambers

W. M. Jensen, A. C. Knoell, and C. Zweben (Materials Sciences Corporation)

Proceedings of the Twenty-Seventh Annual Technical Conference of the Reinforced Plastics/Composites Institute, Washington, D.C., February 8–11, 1972, sponsored by the Society of the Plastics Industry, Inc., Sect. 17-C, pp. 1–10

For abstract, see Jensen, W. M.

Subject Index

Subject Categories

Subjects

Subject	Entry
self-broadened and N_2 broadened linewidths of N_2O	T027
antigen–antibody interaction on specific solid adsorbents derived from cellulose	W006

Comets
proposed solar–electric spacecraft mission to Comet Encke	G003
	G004
structure of comets	L067

Computer Applications and Equipment
efficient implementation of a multichannel high-speed correlator	A011
ultrareliable self-testing and repairing computer	A021
cost and effectiveness of arithmetic error codes applied to digital-systems design	A022
computer-generated color-image display of Apollo lunar color-separation photographs	B040
computer display and entry panel	B057
information equipment and operations used by DSN Tracking System with Mutual stations (combined DSN and Spaceflight Tracking and Data Network equipment)	C025
firmware for ranging demodulator assembly	C041
occultation recording assembly	D007
Thermoelectric Outer-Planet Spacecraft (TOPS) centralized data-handling system for use on Grand Tour mission	E001
new crowbar logic unit for 400-kW transmitter	F014
bright-field electron microscope with heavy/light atom-discrimination using computer	F028
solar–electric spacecraft on-board computer	G003
computer image-processing techniques used to make orthographic photomap of Martian south pole from Mariner Mars 1969 photographs	G012
post-detection subcarrier recording equipment for analog-recording playback	H005
installation of SDS 930 computer at Mars Deep Space Station (DSS 14)	J002
use of interactive graphics with NASA structural analysis system (NASTRAN)	K006
computer program for evaluation of computers	K020
minicomputer use and software	L013
multicomputer communications system	L017
Deep Space Instrumentation Facility Tracking and Monitor and Control Subsystem prototype implementation	L042
DSN data-decoder assembly implementation for support of Pioneer F mission	M016
computer fault-diagnosis algorithms	M039

Subject	Entry
reliability modeling and analysis of ultrareliable fault-tolerant digital systems	M042
JPL digital image-processing development	O002
hardware for Deep Space Instrumentation Facility tracking subsystem	P028
computer equipment used in support of Pioneer Project	S033
software for Space Flight Operations Facility central processing system multi-mission modeling	S047
Mariner Mars 1971/Pioneer 10 multi-mission-level modeling runs using Space Flight Operations Facility central processing system model	S047
Space Flight Operations Facility Mark IIIA IBM computer configuration expansion	S089
high-rate telemetry preprocessor	W007
DSN programmed-oscillator–computer interface	W009

Computer Programs
programs used by DSN Monitor System	A007
software for self-testing and repairing computer	A021
program for analytical modeling of spacecraft propulsion subsystem	C055
assembly programs for Sigma 5 computer	E010
	K019
programs for prediction of Mariner 9 propulsion subsystem performance	E016
user's manual for VISCEL, a general-purpose program for analysis of linear viscoelastic structures	G041
program manual for VISCEL, a general-purpose program for analysis of linear viscoelastic structures	G042
program for solution of eigenvalue problems by Sturm sequence method	G044
algorithm and subroutines for sequential estimation	H008
programs for generating telemetry predicts	H013
program for automated analysis of astronomical spectra	H065
program for spacecraft-maneuver turns	J012
use of COMTANK program in development of boron epoxy rocket motor chambers	J014
program for evaluation of computers	K020
minicomputer use and software	L013
least-squares process of MEDIA program for computing differenced-range-versus-integrated-doppler calibration polynomials	L019
software for implementing improved condensation methods in eigenvalue problems	L033

Subject	Entry

Subject	Entry

Subject	Entry

Teflon coating of storage sphere for hydrogen-maser frequency standard E011

development of boron epoxy rocket motor chambers J014

long-term aging of elastomers K003

vibration and buckling analysis of composite plates and shells M056

viscoelastic behavior of polymers undergoing crosslinking reactions M084

extensional flow of bulk polymers P010

stored-energy function of rubberlike materials derived from experimental tensile data P011

use of anhydrides to make stable elastomeric materials to be used as solid-propellant binders R033

model for acoustic emission from fiber-reinforced material R041

JPL carbon–carbon refractory composites R042

estimation of Weibull parameters for structural fiber-composite materials R043

elastic properties of fiber composite laminates with statistically dispersed ply orientations R044

Mathematical Sciences

cost and effectiveness of arithmetic error codes applied to digital-systems design A022

analysis and numerical calculations for very high temperature laminar flow of gas through entrance region of cooled tube B002

Griesmer bound for word length in linear code B021

weights of irreducible cyclic codes B022

combinatorial packing problem B023

estimation and control scheme for propulsive landing of nonlifting spacecraft B028

analytical methods for performance evaluation of nonlinear filters B029

approximate nonlinear filters and deterministic filter gains B030

decoding of Golay code B032

analysis of effects of Pioneer 10 antenna polarization and spacecraft rotation on radio metric data B033

power-series evaluation of transition and covariance matrices B039

partial-step algorithm for nonlinear estimation problem B046

analysis of cross-flow blowing of a two-dimensional stationary arc B052

expressions for characteristics of third-order phase-locked loops B058

Markov chain technique for determining acquisition behavior of digital tracking loop C018

error probability of a wide-band FSK receiver in presence of multipath fading C019

general relaxation method for inverse solution of full radiative transfer equation C021

Mariner Mars 1969 failure-rate computations C029

formal solution for field and radiation patterns of a dipole antenna in space–time periodic media E005

electromagnetic wave propagation and wave-vector diagram in space–time periodic media E006

matrix representation of Fourier interferometer F034

general analytical method for polarization effects in fourier spectroscopy F035

analysis of orientation of nonspherical particles on solid surfaces G002

mathematical model of solar light pressure used to compute forces acting on Mariner 9 spacecraft G011

dynamic response analysis of geometrically nonlinear structures subjected to high impact G043

solution of eigenvalue problems by Sturm sequence method G044

computational algorithm for sequential estimation H008

reduction in complexity of calculating syndromes for error-correcting codes H012

approximations for use in one-dimensional line radiative-transfer problems H014

analysis of new mechanization of a first-order all-digital phase-locked loop H041

maximum likelihood method for deep space station clock synchronization using long-baseline interferometry H062

efficient generation of statistically good pseudonoise by linearly interconnected shift registers H063

analysis of effect of noisy carrier reference on sequential decoding L016

process for computing least-squares polynomial approximation of data points in which optimum degree of polynomial is automatically determined L019

correlated sampling with application to carrier estimation accuracy L024

RF carrier power estimation L025

analysis of signal-to-noise ratio estimator L026, L027

exact closed-form expression for power spectrum of biphase-modulated squarewave carrier L028

Subject	Entry
algorithm for optimum frame sync acquisition for biorthogonally coded telemetry	L031
improved condensation methods for eigenvalue problems in structural engineering	L033
equations of motion for rigid bodies in tree topology	L039
analysis of automatic steering of vehicle on roadway	L041
carrier synchronization and detection of polyphase signals	L043
derivation of global lunar gravity field from tracking data	L049
computer fault-diagnosis algorithms	M039
reliability modeling and analysis of ultrareliable fault-tolerant digital systems	M042
hiding and covering in a compact metric space	M050
improved method for calculating weights modulo 8 in a binary cyclic code	M052
hide and seek, data storage, and entropy	M054
vibration and buckling analysis of composite plates and shells	M056
systematic nonlinear Kerdock codes	M114
weight enumerators of quadratic residue codes	M115
spectral factorization in periodically time-varying systems and application to navigational tracking problems	N011
error analysis of precision calibrations of RF properties of perforated plates	O015
organization of digital subsystem for generating spacecraft timing and control signals	P013
epsilon entropy and data compression	P022
analysis of asymmetrical antenna reflectors	P025
analysis of automatic angle-tracking errors in 26-m antennas	R032
estimation of Weibull parameters for structural fiber-composite materials	R043
algorithm for synthesizing mass and stiffness matrices from experimental vibration modes	R055
analysis of radio metric data processing techniques	R057
modeling of continuous accelerations as piecewise constant functions in tracking problems	R063
selection of optimum design point for phase-coherent receivers using bandpass limiters	S048 S049
selection of sampling filter bandwidth for digital data detector	S050
bias and spread in extreme-value-theory measurements of probability of error	S067

Subject	Entry
calculation of effects of radiation on scientific instruments	T003
convergence of oscillator spectral estimators for counted-frequency measurements	T005
simplified formula for mean cycle-slip time of phase-locked loops with steady-state phase error	T006
methods and approximations for computation of transmission profiles in ν_4 band of methane in atmosphere of Jupiter	T010
analysis of long-baseline radio interferometry	T015 T016
synchronization methods for time-multiplexed phase-coherent telemetry	T022
equivalence of time-multiplexed and frequency-multiplexed signals in digital communications	T024
derivation of general expression for ionospheric range corrections	V006
method for solution of electromagnetic scattering problems for inhomogeneous dielectrics as a power series in the dimension-of-scatterer/wavelength ratio	V008
minimization algorithm for a class of functions	W005
analysis of laterally loaded ring with hinged cross section	W014
spectral estimate variance reduction by averaging fast-Fourier transform spectra of overlapped time series data	W019
error analysis for complex mixer	W020
structural reliability in terms of nonstationary envelope process and first-excursion probability	Y002
simulation of random envelope processes	Y003
statistical distribution of spacecraft maximum structural response	Y004
first excursion probability in stationary narrow-band random vibration	Y005

Mechanics

Subject	Entry
dynamic response analysis of geometrically nonlinear structures subjected to high impact	G043
solution of eigenvalue problems by Sturm sequence method	G044
large-deformation modal-coordinates for nonrigid-vehicle dynamics	L039
algorithm for synthesizing mass and stiffness matrices from experimental vibration modes	R055
structural reliability in terms of nonstationary envelope process and first-excursion probability	Y002
simulation of random envelope processes	Y003

Subject	Entry

statistical distribution of spacecraft maximum
structural response Y004

first excursion probability in stationary narrow-
band random vibration....................................... Y005

Mechanisms

solar–electric spacecraft mechanisms.................G003
G004

mechanism for three-axis control of ion-thruster
array... P012

high-vacuum space-simulation tests of friction
and cold welding in mechanisms....................W002

Meteors

science results of Apollo missions..................... B056

comparison of primordial rare-gas
concentrations in normal chondrites with
inferred values for bulk Earth material....................... F001

adsorption of rare gases on Allende meteorite............... F002

Optics

infrared Connes-type interferometer................... B026

computer-generated color-image display of
Apollo lunar color-separation photographs.................. B040

Raman-scattering cross section for N_2O_4.........................C030

Viking orbiter experiment for detection and
mapping of water vapor in Martian
atmosphere F008

matrix representation of Fourier interferometer............. F034

polarization effects in Fourier spectroscopy.................... F035

rational approximation for Voigt line profile H016

Mariner Mars 1969 infrared spectrometer......................H024

Stark-effect modulation of CO_2 laser by NH_2D............. J019

apparatus for measuring nonequilibrium
ionization in hydrogen–helium mixtures....................... L022

design of conical-gregorian antennas................................. L060

laboratory simulation of diffuse reflectivity from
a cloudy planetary atmosphere.............................M018

Martian optical characteristics from Mariner
Mars 1971 data M022

measurements of $H\beta$ line shape in transient
plasma using fiber-optics slit system............................. S084

photon-noise generation of cathode-ray-tube
display systems... V004

techniques for terrestrial observation of objects
near the Sun Y016

accurate formula for gaseous transmittance in
infrared... Y017

improvements to antenna-angle data-system
autocollimators... Z001

Orbits and Trajectories

basic parameters for low-thrust mission and
system analysis... B009

partial-step algorithm for nonlinear estimation
problem used in determining orbits............................. B046

comparison of Cowell's method and a
variation-of-parameters method for
computation of precision satellite orbits.....................D001
D002

aiming strategies for quarantined multi-planet
missions D022

Pioneer 10 maneuver strategy............................. F031

solar–electric spacecraft low-thrust navigation.................G003
G004

Mariner Venus–Mercury 1973 midcourse-
velocity requirements and delivery accuracy...............M060

relation of trajectories to solid-propulsion
options...N001

spectral factorization in periodically time-
varying systems and application to
navigational tracking problems...................................N011

preliminary evaluation of radio-data orbit-
determination capabilities required for
vicinity of Saturn...O010

modeling of continuous accelerations as
piecewise constant functions in tracking
problems R063

Mariner Venus–Mercury 1973 encounter
strategy... S027

Packaging and Cabling

miniature biotelemeter design C015

solar–electric spacecraft packaging and cabling.............G003
G004

dual-in-line package microcircuit card and card
cage assembly H025

cabling for ion-thruster array P012

high-reliability integrated-circuit packaging.................... S063

DSN programmed oscillator packaging.........................W009

Particle Physics

analysis of cross-flow blowing of a two-
dimensional stationary arc............................... B052

equilibrium theory of close-packed liquids.....................C012

approximate scheme for numerical calculation
of dielectric function of electron gas...........................C013

quantum crystals in the single-particle picture...............C014

Cerenkov and transition radiation in space–time
periodic media... E007

bright-field electron microscope with heavy/
light atom-discrimination using computer...................F028

Subject	Entry
measurements of Jupiter RF radiation	K018
results of Mars radio-occultation experiment by Mariner Mars 1969 spacecraft	K024
improved sensitivity in gas chromatography using a thermal-conductivity detector and a palladium transmodulator	L057
laboratory simulation of diffuse reflectivity from a cloudy planetary atmosphere	M018
high-resolution spectra of Mars	M019
mechanism for equatorial acceleration of Jupiter	M043
laboratory simulation of absorption spectra in cloudy atmospheres	M046
composition of upper clouds of Venus	R008
Mariner Mars 1969 science results	S013
temperature-sounding experiments for outer-planet spacecraft	T009
methods and approximations for computation of transmission profiles in ν_4 band of methane in atmosphere of Jupiter	T010
model for clouds of Jupiter	T011

Planetary Exploration, Advanced

Subject	Entry
study of Jupiter trapped-radiation belts as future spacecraft environment	B024
Antarctic soil microbial and ecological investigations in preparation for Mars surface exploration	C002
	C004
	H046
nonequilibrium ionization measurements in hydrogen–helium mixtures in simulation of Jupiter atmospheric-entry conditions	L022
cost comparisons for planetary missions with advanced propulsion systems	S075
temperature-sounding experiments for outer-planet spacecraft	T009
DSN programmed oscillator for tracking outer-planet spacecraft	W009

Planetary Interiors

Subject	Entry
relative masses of Earth, Moon, and Mars determined from Mariner Mars 1969 tracking data	A009
simultaneous solution for masses and ephemerides of the principal planets from analysis of optical, radar, and radio tracking data	L038
Mariner Mars 1971 determination of Mars gravity field	L056
	M022

Planetary Motion

Subject	Entry
radar observations of Mercury	G019
simultaneous solution for masses and ephemerides of the principal planets from analysis of optical, radar, and radio tracking data	L038
Mariner 9 determination of Mars pole direction	L056
proposed determination of mass and ephemeris of Saturn by radio tracking	O011

Planetary Quarantine

Subject	Entry
aiming strategies for quarantined multi-planet missions	D022
effect of temperature on survival of microorganisms in deep space vacuum	H002
Antarctic soil microbial and ecological investigations: implied non-survival of Earth organisms in Martian environment	H046
microbiological sampling of returned Surveyor 3 cabling	K025
dry-heat resistance of *Bacillus subtilis* var. *niger* spores on mated surfaces	S044
release of microbes by materials after impact	T007

Planetary Surfaces

Subject	Entry
Mariner Mars 1971 science results	B014
	C028
	H007
	K023
	K030
	M022
	M037
	S077
Antarctic soil microbial and ecological investigations in preparation for Mars surface exploration	C002
	C004
	H046
Earth-based radar observations of Mars	D019
Mariner Mars 1969 science results	F019
	N005
	S013
orthographic photomap of Martian south pole	G012
radar observations of Mercury	G019
Viking lander carbon-assimilation experiment for detection of possible life on Mars	H045

Plasma Physics

Subject	Entry
noise effects of spacecraft ion beam on antenna radio signal	A014
partially ionized gas flow and heat transfer downstream from circular channel expansion	B005
	B006

| Subject | Entry | Subject | Entry |

| Subject | Entry | Subject | Entry |

liquid-phase mixing of bipropellant doublets H031

techniques for selection of spacecraft auxiliary
propulsion...H037

international auxiliary-propulsion development................H038

Thermoelectric Outer-Planet Spacecraft (TOPS)
trajectory-correction propulsion subsystem....................L052

portable hydrazine attitude-propulsion test
system...M092

minimum impulse tests of small liquid-
hydrazine catalytic thrusters for spacecraft
attitude control..M093

measurement of surface tension of liquid
propellants R007

experimental evaluation of high-thrust,
throttleable, monopropellant hydrazine rocket
engines.. R038

JPL carbon–carbon refractory composites for use
in rocket engines... R042

JPL Molsink used to study nozzle exhaust-
plume backscatter S053

cost comparisons for planetary missions with
advanced propulsion systems S075

Propulsion, Solid

dynamic measurement of bulk modulus of
dielectric materials such as solid propellants
using a microwave phase-shift technique..................... B010

detonation of explosives by laser......................................H015
M072

techniques for selection of spacecraft auxiliary
propulsion...H037

international auxiliary-propulsion development................H038

development of boron epoxy rocket motor
chambers.. J014

solid-propulsion advanced concepts..................................N001

long-term-storage test of solid-propellant rocket
motor.. R006

use of anhydrides to make stable elastomeric
materials to be used as solid-propellant
binders.. R033

JPL carbon–carbon refractory composites for
use in rocket engines... R042

high-incremental-velocity low-acceleration solid-
propellant rocket engines S021

cost comparisons for planetary missions with
advanced propulsion systems S075

determination of solid-propellant transient-
regression rates using microwave doppler-shift
technique.. S090

initiation system for low-thrust solid-propellant
rocket-motor igniter... S091

Pyrotechnics

nondestructive testing of electroexplosive
devices..M070
M071
R050
R053

ignition of insensitive explosives by laser.......................M072
Y007

terminated capacitor-discharge firing of
electroexplosive devices R052

initiation system for low-thrust solid-propellant
rocket-motor igniter.. S091

Quality Assurance and Reliability

cycle-life studies of heat-sterilized silver-oxide–
zinc batteries... A017

ultrareliable self-testing and repairing computer........... A021

magnetic tape recorder for long operating life
in space... B007

fabrication of dependable lithium-doped solar
cells.. B038

Mariner Mars 1969 failure-rate computations..................C029

analysis of failure of polyester drive belt of
Mariner Mars 1971 spacecraft tape recorder..............C061

solar–electric spacecraft redundant systems G004

tests of spacecraft radio amplifier tubes..........................H052

investigation of gold embrittlement in
connector solder joints... L011

reliability modeling and analysis of ultrareliable
fault-tolerant digital systems M042

nondestructive testing of electroexplosive
devices..M071
R053

high-reliability integrated-circuit packaging..................... S063

statistics of DSN Command System reliability................ S086

high-vacuum space-simulation tests of friction
and cold welding in mechanisms...................................W002

accelerated life testing of spacecraft electronic
subsystems..W013

study of radiation effects on low-power
microcircuits... Y001

structural reliability in terms of nonstationary
envelope process and first-excursion
probability Y002

solar-cell contact pull strength as function of
pull-test temperature Y010

DSN high-reliability microcircuit procurement............... Z004

Radar

lunar subsurface exploration with coherent
radar B060

Apollo lunar bistatic-radar experiments...........................C026

Subject	Entry
Earth-based radar observations of Mars	D019
Mariner 6 and 7 bistatic radar measurements of Martian surface	F019
radar observations of Mercury	G019
DSN planetary radar experiments	G027
	J004
	J005
	J006
lunar-radar clock synchronization	H026
simultaneous solution for masses and ephemerides of the principal planets from analysis of optical, radar, and radio tracking data	L038
combined radar–radiometer with variable polarization	M024
map of lunar radar reflectivity at 7.5-m wavelength	T020
X-band radar development	W012

Radio Astronomy

Subject	Entry
distribution of linear polarization in Cassiopeia A at 9.8 and 11.1 cm	D017
DSN radio science support	G027
	J001
	J002
	J004
	J005
	J006
	L044
	L045
	L046
	L047
thermal component of radio emission from the major planets	G039
measurements of Jupiter RF radiation	K018
Mariner 9 S-band occultation of Mars	K023
	K024
simultaneous solution for masses and ephemerides of the principal planets from analysis of optical, radar, and radio tracking data	L038
second decrease in period of Vela pulsar	R011
transformation of received-signal polarization angle to plane of ecliptic	S081
analysis of long-baseline radio interferometry	T015
	T016

Relativity

Subject	Entry
general relativity results from Mariner Mars 1969 radio metric data	A009
	S013

Subject	Entry
electromagnetic wave propagation and wave-vector diagram in space–time periodic media	E006
Cerenkov and transition radiation in space–time periodic media	E007

Safety Engineering

Subject	Entry
RF-level pocket monitor	J005
microwave radiation protective suit	K017
Deep Space Instrumentation Facility fire-protection studies	K031
ignition of insensitive explosives by laser	M072
	Y007
error analysis of precision calibrations of RF properties of perforated plates	O015
microwave leakage through perforated flat plates	O016
	O018

Scientific Instruments

Subject	Entry
infrared Connes-type interferometer	B026
new Fourier spectroscope with million-point transformation ability	C046
instruments for planned infrared investigations of outer planets during Grand Tour mission	F006
Viking orbiter experiment for detection and mapping of water vapor in Martian atmosphere	F008
development and testing of Mariner Mars 1971 ultraviolet spectrometer	F010
bright-field electron microscope with heavy/light atom-discrimination using computer	F028
solid-state detector for analysis of X-rays excited in silicate rocks by alpha-particle bombardment	F029
matrix representation of Fourier interferometer	F034
Mariner Mars 1969 infrared spectrometer	H024
Viking lander carbon-assimilation experiment for detection of possible life on Mars	H045
effects of electrons and protons on scientific instruments	J015
combined radar–radiometer with variable polarization	M024
Mariner Mars 1971 spacecraft scan platform pointing calibration	P002
response of covered silicon detectors to monoenergetic gamma rays	R018
	R019
effects of radioisotope thermoelectric generator radiation on scientific instruments	T003

Subject	Entry	Subject	Entry

Subject	Entry
DSN telemetry-predicts generation and distribution	H013
DSN support of Apollo Project	H017
analysis of new mechanization of a first-order all-digital phase-locked loop	H041
DSN Telemetry System tests	K014
DSN support of Mariner Mars 1971 Project	L002
	L042
	R031
	T012
	T013
	T014
optimum buffer management strategy for sequential decoding	L014
comparison of maximum-likelihood and sequential decoding of variable-length short-constraint-length convolutional codes	L015
analysis of effect of noisy carrier reference on sequential decoding	L016
flexible high-speed sequential-decoding machine	L018
algorithm for optimum frame sync acquisition for biorthogonally coded telemetry	L031
use of interplex modulation in multichannel telemetry	L032
carrier synchronization and detection of polyphase signals	L043
improved method for calculating weights modulo 8 in a binary cyclic code	M052
DSN support of Viking Project	M095
	M096
	M098
	M099
DSN support of Mariner Jupiter–Saturn 1977 Project	M097
weight enumerators of quadratic residue codes	M115
DSN support of Pioneer Project	S031
	S032
	S033
	S034
	S035
	S036
	S037
	S038
	S039
	S040
selection of optimum design point for phase-coherent receivers using bandpass limiters	S049
selection of sampling filter bandwidth for digital data detector	S050
predetection recording of spacecraft telemetry data	S064

Subject	Entry
extreme-value-theory measurements of probability of error in digital communications systems	S067
DSN Command System performance evaluation	S086
simplified formula for mean cycle-slip time of phase-locked loops with steady-state phase error	T006
Mariner Mars 1971 telecommunications subsystem design	T008
synchronization methods for time-multiplexed phase-coherent telemetry	T022
equivalence of time-multiplexed and frequency-multiplexed signals in digital communications	T024
simulation conversion assembly for simulated interplex telemetry	W008
alterations to DSN masers to prevent saturation	Y021
loss of telemetry data during Apollo 16 mission due to saturation of DSN system component	Y021

Temperature Control

Subject	Entry
solar–electric spacecraft temperature control	G003
	G004
temperature control for modular thermionic-reactor-powered ion-propulsion system	P009
temperature control of in-core thermionic-reactor systems	S004

Test Facilities and Equipment

Subject	Entry
equipment for measuring turbulent boundary layer and heat transfer along a convergent-divergent nozzle	B004
apparatus for measuring partially ionized gas flow and heat transfer downstream from circular channel expansion	B005
gas flow test apparatus	B006
test equipment for dynamic measurement of bulk modulus of dielectric materials using a microwave phase-shift technique	B010
laser apparatus to test Raman-scattering cross section for N_2O_4	C030
Molsink vacuum facility used to study small rocket exhaust plumes	C033
test waveguide for determination of microwave surface resistivity	C038
apparatus for stability evaluation of rocket engine	C039
solid-state detector for analysis of X-rays excited in silicate rocks by alpha-particle bombardment	F029
apparatus to determine effect of temperature on survival of microorganisms in deep space vacuum	H002

Publication Index

Technical Reports

DSN Progress Reports for November 1971–October 1972
(Technical Report 32-1526, Vols. VII–XII)

DSN Progress Reports for November 1971–October 1972
(Technical Report 32-1526, Vols. VII–XII) (contd)

JPL Technical Section	Entry
331 Communications Systems Research (contd)	L015
	L016
	L017
	L031
	L065
	L066
	M004
	M050
	M052
	M114
	M115
	S064
	T022
	W005
	W019
	W020
	Z003
332 DSIF Engineering	D016
	G001
	H036
	J022
	K005
	K006
	K031
	L033
	L034
	L035
	L036
	L048
	L062
	M057
	M058
	P015
	Z001
333 Communications Elements Research	B016
	B017
	C036
	C037
	C038
	E011
	E012
	O015
	O016
	P014
	P023
	P024

JPL Technical Section	Entry
333 Communications Elements Research (contd)	P025
	P026
	R012
	R013
	R014
	R015
	R016
	R017
	S078
335 R. F. Systems Development	B017
	B058
	B061
	C041
	C059
	D014
	F014
	F015
	F026
	G026
	G027
	J001
	J002
	J004
	J005
	J006
	J016
	L020
	L029
	M002
	N010
	O003
	P004
	R005
	S068
	S069
	W009
	W012
337 DSIF Operations	B011
	C026
	C067
	L024
	L025
	L026
	L027
	M063
	R032

JPL Technical Section	Entry	JPL Technical Section	Entry
918 SFOF/GCF Development (contd)	V004	918 SFOF/GCF Development (contd)	W007

Technical Memorandums

Number	Entry	Number	Entry
33-426, Vol. X	S040	33-546	S004
33-466, Vol. I, Rev. 1	G041	33-547	P017
33-466, Vol. II	G042	33-549	M086
33-520	S091	33-550	P009
33-521	C045	33-551	S025
33-522	A016	33-552	C010
33-523, Vol. I	R031	33-553	S075
33-523, Vol. II	T014	33-554	G037
33-524	R018	33-555	H038
33-525	C046	33-556	H020
33-528	S021	33-557, Pt. I	S087
33-531	C034	33-558	J012
33-532	H042	33-560	M092
33-533	L011	33-561	C057
33-534	N001	33-563	L021
33-535	T008	33-564	R041
33-536	B047	33-565	S095
33-537	O005	33-566	M038
33-538	H014	33-567	M039
33-539	P013	33-568	M040
33-540	S052	33-569	F010
33-541	M017	33-570	M024
33-542	L019	33-571	E002
33-543	J015	33-573	H051
33-544	A018	33-574	E016
33-545	S024	33-575	W013

Technical Memorandums (contd)

JPL Quarterly Technical Review, Vol. 1, No. 4–Vol. 2, No. 3

Open Literature Reporting

Publication	Entry
ACS/AIAA/EPA/IEEE/ISA/NASA/NOAA Joint Conference on Sensing of Environmental Pollutants, Palo Alto, California, November 8-10, 1971	
AIAA Preprint 71-1109	T025
Advan. Astronaut. Sci.	
Vol. 29, No. I, pp. 203-222	G039
Vol. 29, No. I, pp. 589-599	F006
Vol. 29, No. II, pp. 367-376	E001
Advances in X-Ray Analysis	
Vol. 15, pp. 388-406	F029
AIAA Guidance, Control and Flight Mechanics Conference, Hempstead, New York, August 16-18, 1971	
Preprint 71-903	B028
AIAA J.	
Vol. 9, No. 10, pp. 2096-2098	M068
Vol. 9, No. 10, pp. 2107-2109	B001
Vol. 10, No. 1, pp. 80-86	B052
Vol. 10, No. 5, pp. 675-679	B046
Vol. 10, No. 7, pp. 946-948	K034
AIAA Ninth Electric Propulsion Conference, Bethesda, Maryland, April 17-19, 1972	
Preprint 72-426	B009
Preprint 72-475	P006
AIAA/AAS Astrodynamics Conference, Palo Alto, California, September 11-12, 1972	
AIAA Preprint 72-942	S027
AIAA/ASME/SAE Thirteenth Structures, Structural Dynamics, and Materials Conference, San Antonio, Texas, April 10-12, 1972	
AIAA Preprint 72-355	W014
AIAA Tenth Aerospace Sciences Meeting, San Diego, California, January 17-19, 1972	
Preprint 72-106	S084

Publication	Entry
Am. Ind. Hygiene Assoc. J.	
Vol. 32, No. 11, pp. 771-774	K017
Anal. Chem.	
Vol. 43, No. 14, pp. 1958-1961	L057
Vol. 44, No. 8, pp. 1497-1499	H010
Vol. 44, No. 8, pp. 1548-1550	S046
Ann. Math. Statist.	
Vol. 42, No. 5, pp. 1706-1716	M054
Vol. 42, No. 6, pp. 2079-2125	P022
Antarctic J. U.S.	
Vol. VI, No. 5, pp. 211-213	C002
Appl. Microbiol.	
Vol. 22, No. 4, pp. 491-495	S044
Appl. Opt.	
Vol. 10, No. 12, pp. 2711-2716	F034
Vol. 11, No. 1, pp. 160-173	F035
Vol. 11, No. 1, pp. 202-203	Y017
Vol. 11, No. 3, pp. 493-501	H024
Vol. 11, No. 5, pp. 1212-1216	M018
Appl. Phys. Lett.	
Vol. 19, No. 11, pp. 452-453	C030
Vol. 19, No. 11, pp. 473-475	Y007
Vol. 19, No. 12, pp. 503-506	J019
Astron. J.	
Vol. 76, No. 8, pp. 711-718	H065
Vol. 76, No. 8, pp. 719-749	N005
Vol. 76, No. 10, pp. 1152-1154	G019
Vol. 77, No. 2, pp. 120-133	D017
Astrophys. J.	
Vol. 170, No. 3, Pt. 1, pp. 551-555	H066
Vol. 172, No. 1, Pt. 1, pp. 89-115	B025
Vol. 176, No. 2, Pt. 2, pp. L85-L88	K018

Open Literature Reporting (contd)

Publication	Entry	Publication	Entry

Astrophys. Space Sci.

Vol. 15, No. 2, pp. 175–184.............................L067

Biophys. J.

Vol. 12, No. 5, pp. 484–511............................F028

Celest. Mech.

Vol. 4, No. 2, pp. 233–245.............................L038

Chem. Phys. Lett.

Vol. 12, No. 2, p. 403.................................G008

Clinical Chem.

Vol. 18, No. 5, pp. 476–478............................R034

Comput. J.

Vol. 14, No. 3, pp. 285–290............................H008

Earth Planet. Sci. Lett.

Vol. 11, No. 5, pp. 362–368............................F001

Vol. 15, pp. 59–64....................................H059

Eur. J. Biochem.

Vol. 22, No. 2, pp. 287–293............................B018

Geochim. Cosmochim. Acta

Vol. 35, No. 9, pp. 865–875............................T029

Vol. 36, No. 3, pp. 319–328............................F002

Icarus

Vol. 13, No. 3, pp. 363–370............................T020

Vol. 15, No. 2, pp. 190–196............................F007

Vol. 15, No. 2, pp. 197–203............................M019

Vol. 15, No. 2, pp. 279–303............................F003

Vol. 16, No. 1, pp. 34–46.............................F008

Vol. 16, No. 1, pp. 147–152............................H045

Vol. 16, No. 3, pp. 502–508............................F019

Vol. 16, No. 3, pp. 552–527............................G012

Vol. 17, No. 1, pp. 88–103............................P016

IEEE Trans. Aerosp. Electron. Sys.

Vol. AES-7, No. 6, pp. 1147–1150.......................H043

IEEE Trans. Anten. Prop.

Vol. AP-20, No. 2, pp. 146–152.........................L060

Vol. AP-20, No. 3, pp. 280–287.........................E005

Vol. AP-20, No. 4, pp. 534–536.........................E006

IEEE Trans. Automat. Contr.

Vol. AC-17, No. 2, pp. 228–232.........................B039

IEEE Trans. Commun.,

Vol. COM-19, No. 5, pp. 699–707........................C019

IEEE Trans. Commun.

Vol. COM-19, No. 5, pp. 813–820........................L018

Vol. COM-19, No. 6, pp. 889–897........................R036

Vol. COM-20, No. 2, pp. 119–131........................H041

Vol. COM-20, No. 2, pp. 210–214........................S049

Vol. COM-20, No. 2, pp. 214–217........................T005

Vol. COM-20, No. 3, pp. 331–337........................T006

Vol. COM-20, No. 3, pp. 415–419........................B065

Vol. COM-20, No. 3, pp. 435–438........................T024

Vol. COM-20, No. 3, pp. 438–441........................S050

Vol. COM-20, No. 3, pp. 441–454........................L043

IEEE Trans. Computers

Vol. C-20, No. 11, pp. 1312–1321.......................A021

Vol. C-20, No. 11, pp. 1322–1331.......................A022

Vol. C-20, No. 11, pp. 1376–1382.......................M042

IEEE Trans. Inform. Theor.

Vol. IT-18, No. 1, pp. 214–215.........................C020

IEEE Trans. Instr. Meas.

Vol. IM-21, No. 2, pp. 177–180.........................R052

IEEE Trans. Magnetics

Vol. MAG-7, No. 3, pp. 517–520.........................B007

IEEE Trans. Microwave Theor. Techniq.

Vol. MTT-19, No. 11, pp. 843–854.......................O017

Vol. MTT-20, No. 3, pp. 235–236........................O018

Open Literature Reporting (contd)

Publication	Entry
IEEE Trans. Nucl. Sci.	
Vol. NS-18, No. 5, pp. 50–57	N014
Immunochemistry	
Vol. 9, No. 10, pp. 967–978	W006
Inform. Control	
Vol. 20, No. 2, pp. 158–175	B022
International Symposium on Earth Gravity Models and Related Problems, St. Louis, Missouri, August 16–18, 1972	
Preprint	E014
Int. J. Heat Mass Transfer	
Vol. 15, No. 5, pp. 1001–1021	B002
Int. J. Numer. Methods Eng.	
Vol. 4, No. 2, pp. 163–174	G043
Vol. 4, No. 3, pp. 379–404	G044
J. Am. Chem. Soc.	
Vol. 94, No. 7, pp. 2363–2370	H011
Vol. 94, No. 12, pp. 4255–4261	B054
J. Appl. Phys.	
Vol. 42, No. 11, pp. 4197–4201	V008
Vol. 43, No. 4, pp. 1764–1767	L037
Vol. 43, No. 5, pp. 2484–2485	S088
Vol. 43, No. 7, pp. 3064–3067	P011
Vol. 43, No. 9, pp. 3719–3723	E007
J. Appl. Polym. Sci.	
Vol. 15, No. 12, pp. 3101–3108	C062
J. Atmos. Sci.	
Vol. 28, No. 6, pp. 842–846	D010
Vol. 29, No. 4, pp. 741–747	C021
Vol. 29, No. 5, pp. 950–958	T009
Vol. 29, No. 5, pp. 1007–1008	M043
J. Chem. Phys.	
Vol. 55, No. 11, pp. 5227–5232	C012

Publication	Entry
Vol. 55, No. 11, pp. 5413–5414	H060
Vol. 56, No. 10, pp. 5111–5120	H061
Vol. 57, No. 4, p. 1814	G007
J. Colloid Interface Sci.	
Vol. 37, No. 2, pp. 403–409	G002
J. Compos. Mater.	
Vol. 5, pp. 529–532	M056
J. Geophys. Res.	
Vol. 76, No. 26, pp. 6220–6236	W026
Vol. 76, No. 29, pp. 7021–7026	S057
Vol. 77, No. 23, pp. 4366–4378	B044
J. Geophys. Res., Space Physics	
Vol. 77, No. 13, pp. 2250–2263	U002
J. Math. Anal. Appl.	
Vol. 36, No. 3, pp. 477–505	B029
J. Molec. Spectrosc.	
Vol. 40, No. 3, pp. 588–604	T026
Vol. 40, No. 3, pp. 605–615	T027
J. Opt. Soc. Am.	
Vol. 62, No. 6, pp. 827–828	H016
J. Polym. Sci., Pt. C: Polym. Sym.	
No. 35, pp. 71–76	M084
J. Quant. Spectrosc. Radiat. Transfer	
Vol. 12, No. 3, pp. 307–322	Y019
Vol. 12, No. 3, pp. 387–404	H054
Vol. 12, No. 3, pp. 405–419	H055
Vol. 12, No. 4, pp. 525–529	S085
Vol. 12, No. 4, pp. 751–757	M020
Vol. 12, No. 6, pp. 1023–1028	H056
Vol. 12, No. 7, pp. 1151–1156	T010
J. Sound Vibr.	
Vol. 21, No. 1, pp. 73–85	Y003

Open Literature Reporting (contd)

Publication	Entry	Publication	Entry

J. Spacecraft Rockets

Vol. 8, No. 10, pp. 1038–1042 ....D021

Vol. 9, No. 1, pp. 57–59 ....Y004

Vol. 9, No. 2, pp. 69–70 ....S081

Vol. 9, No. 2, pp. 71–78 ....M029

Vol. 9, No. 3, pp. 218–220 ....P012

Vol. 9, No. 6, pp. 420–427 ....B003

Vol. 9, No. 7, pp. 540–546 ....N011

Life Sciences and Space Research X

pp. 23–28 ....T007

Macromolecules

Vol. 5, No. 1, pp. 75–81 ....C017

Vol. 5, No. 3, pp. 253–260 ....N012

Vol. 5, No. 3, pp. 261–269 ....R023

Mater. Eval.

Vol. XXX, No. 1, pp. 13–19 ....R053

Mechanical Behavior of Materials: Proceedings of the 1971 International Conference on Mechanical Behavior of Materials

pp. 496–507 ....L008

Microwave J.

Vol. 14, No. 6, pp. 41–46, 48 ....S082

Nature

Vol. 234, No. 5329, pp. 402–403 ....J007

Nature Phys. Sci.

Vol. 233, No. 40, pp. 102–103 ....M046

Vol. 234, No. 46, p. 48 ....R011

Vol. 237, No. 77, pp. 121–122 ....T030

Nucl. Instr. Methods

Vol. 98, No. 1, pp. 183–184 ....H003

Nucl. Sci. Eng.

Vol. 47, No. 4, pp. 409–414 ....R019

Nucl. Technol.

Vol. 15, No. 3, pp. 396–410 ....T004

Photogr. Sci. Eng.

Vol. 16, No. 1, pp. 51–57 ....B040

Phycologia

Vol. 11, No. 2, pp. 133–139 ....C004

Phys. Rev., Pt. B: Solid State

Vol. 5, No. 1, pp. 238–240 ....C013

Vol. 6, No. 4, pp. 1081–1090 ....C014

Proceedings of the Conference on Atmospheric Radiation, Fort Collins, Colorado, August 7–9, 1972

pp. 100–102 ....T011

Proceedings of the Conference on Lunar Geophysics, Lunar Science Institute, Houston, Texas, October 18–21, 1971

pp. 411–418 ....S058

Proceedings of the Second Lunar Science Conference, Houston, Texas, January 11–14, 1971

Vol. 2, pp. 1875–1877 ....R035

Vol. 3, pp. 2235–2244 ....N003

Vol. 3, pp. 2301–2310 ....G016

Vol. 3, pp. 2515–2528 ....T031

Vol. 3, pp. 2683–2697 ....N008

Vol. 3, pp. 2715–2719 ....K025

Vol. 3, pp. 2735–2742 ....C016

Proceedings of the Twenty-First International Congress, Constance, Germany, October 4–10, 1970

pp. 193–210 ....S013

Proceedings of the Twenty-Seventh Annual Technical Conference of the Reinforced Plastics/Composites Institute, Washington, D.C., February 8–11, 1972

Sect. 17-C, pp. 1–10 ....J014

Open Literature Reporting (contd)

Publication	Entry
Proc. IEEE	
Vol. 60, No. 5, pp. 552–557	H026
Vol. 60, No. 7, pp. 821–828	O002
Progr. Astronaut. Aeronaut.	
Vol. 25, pp. 19–41	H052
Rev. Geophys. Space Phys.	
Vol. 10, No. 1, pp. 369–378	R008
Rev. Sci. Instr.	
Vol. 42, No. 10, pp. 1393–1403	B026
Science	
Vol. 173, No. 4001, pp. 1017–1020	L049
Vol. 174, No. 4016, pp. 1324–1327	D019
Vol. 175, No. 4018, pp. 165–168	S059
Vol. 175, No. 4019, pp. 293–294	S077
Vol. 175, No. 4019, pp. 294–305	M037
Vol. 175, No. 4019, pp. 305–308	H007
Vol. 175, No. 4019, pp. 308–309	C028
Vol. 175, No. 4019, pp. 309–312	B014
Vol. 175, No. 4019, pp. 313–317	K023
Vol. 175, No. 4019, pp. 317–320	L056
Vol. 175, No. 4019, pp. 321–322	L040
Vol. 175, No. 4028, pp. 1360–1361	B027
Vol. 176, No. 4032, pp. 242–245	H046
Separ. Sci.	
Vol. 6, No. 5, pp. 715–725	B020

Publication	Entry
SIAM/AMS Book Series	
Vol. IV, pp. 97–108	B023
Sky Telesc.	
Vol. 43, No. 3, pp. 140–144	Y016
Space Life Sci.	
Vol. 3, No. 2, pp. 108–117	H002
Space Research XI	
pp. 31–49	J008
pp. 105–112	A009
pp. 165–175	K024
Tetrahedron	
Vol. 27, No. 4, pp. 689–700	C031
Vol. 27, No. 4, pp. 701–709	C032
The Moon	
Vol. 3, No. 2, pp. 221–230	N004
Vol. 3, No. 3, pp. 337–345	J009
Vol. 4, pp. 113–127	B060
Trans. ASME, Ser. C: J. Heat Transf.	
Vol. 93, No. 4, pp. 397–407	B004
Vol. 94, No. 1, pp. 119–127	B005
Vol. 94, No. 1, pp. 119–127	B006
Vol. 94, No. 2, pp. 174–180	R049
Trans. ASME, Ser. E: J. Appl. Mech.	
Vol. 38, No. 4, pp. 1017–1022	Y005
Trans. ASME, Ser. G: J. Dynam. Sys., Meas., Contr.	
Vol. 94, No. 1, pp. 57–63	B030